Remarks

Reconsideration of this Application is respectfully requested.

Upon entry of the foregoing amendment, claims 1, 34-39, 41-44, 46, and 52-54 are pending in the application, with claims 1, 34, 36-37, and 52 being the independent claims. Claims 2-33, 40, 50, and 51 were previously sought to be canceled without prejudice to or disclaimer of the subject matter therein. Claims 45 and 47-49 are herewith sought to be canceled without prejudice to or disclaimer of the subject matter therein. Applicants reserve the right to pursue any of the canceled subject matter in related applications. Claims 1, 34, 36-37, 44, and 52 are sought to be amended. These changes are believed to introduce no new matter, and their entry is respectfully requested.

The specification at the bridging paragraph of pages 5-6 has been amended to correct obvious grammatical errors. Support for the amendment is found, *inter alia*, in the specification as originally filed in the original bridging paragraph at pages 5-6.

The specification at page 34, lines 3-26, has been amended to correct obvious typographical errors. Support for the amendment is found, *inter alia*, in the specification as originally filed at page 34, lines 3-26.

Support for the amendments to claims 1, 34, 36-37, and 52 is found, *inter alia*, in the specification as originally filed at page 3, lines 13-24; page 3, lines 25-30; pages 3-4, bridging paragraph; pages 5-6, bridging paragraph; page 8, lines 28-33; pages 14-15, bridging paragraph; page 15, lines 3-15; page 3, line 10; page 5, lines 14-23; page 18, lines 10-15; page 19, lines 25-31; and pages 19-20, bridging paragraph.

Support for the amendment to claim 37 is found, *inter alia*, in the specification as originally filed at page 4, lines 19-34; page 5, lines 5-9; and page 16, lines 7-17.

Claim 44 has been amended to correct an obvious spelling error.

Based on the above amendment and the following remarks, Applicants respectfully request that the Examiner reconsider all outstanding objections and rejections and that they be withdrawn.

I. Claim Rejections under 35 U.S.C. § 112, First Paragraph, Written Description

Claims 34-36, 39, 41-42, 44-49, and 52-53 were rejected under 35 U.S.C. § 112, first paragraph, as allegedly failing to comply with the written description requirement. Applicants respectfully traverse the rejection.

Based on Applicants' previous claim limitation reciting "an agent that reduces uptake" and a qualification made in Applicants' Specification stating "[w]hile not wishing to be bound by theory," the Examiner asserts lack of written description, alleging that "Applicant doesn't understand why or how the mechanism work[s]...." Office Action at pages 3-4; Office Action at page 4, fourth paragraph under "Response to Argument-written description;" and bridging paragraph of the Specification at pages 2-3. Purely in the interest of furthering prosecution and not as an admission that the Examiner's assertions are correct, Applicants have amended the claims to recite "an agent that reduces Kupffer cell function."

Applicants' Specification teaches a clear cause and effect relationship between reducing Kupffer cell function and increasing the levels of a therapeutic gene product in a subject. *See*, e.g., Example 5. Furthermore, while Applicants' Specification discloses

that Kupffer cell function may be reduced by mechanisms including lowering Kupffer cell levels and/or reducing Kupffer cell uptake of the viral vector, the claims do not recite or require a specific mechanism by which an agent reduces Kupffer cell function. Specification at page 3, lines 8-9; page 3, line 27, to page 4, line 3; and page 5, line 32, to page 6, line 2. Because of the latter, Applicants are under no requirement to demonstrate a specific mechanism underlying the claimed effect.

No burden exists under the written description requirement to demonstrate "why or how" an invention works when no specific mechanism is claimed. In fact, it is well-settled that an Applicant need not understand why or how an invention works as long as the disclosure indicates how to achieve the *claimed* result. *Newman v. Quigg*, 877 F.2d 1575, 1581, 11 USPQ2d 1340, 1345 (Fed. Cir. 1989)("...it is not a requirement of patentability that an inventor correctly set forth, or even know, how or why the invention works..."); *Diamond Rubber Co. v. Consolidated Rubber Co.,* 220 U.S. 428, 435-436, 31 S. Ct. 444, 447-48, 55 L.Ed. 527 (1911)("It is certainly not necessary that [a patentee] understand or be able to state the scientific principles underlying his invention..."); M.P.E.P. § 2138.05, citing *Parker v. Frilette*, 462 F.2d 544, 547, 174 USPQ 321, 324 (CCPA 1972)("[a]n inventor need not understand precisely why his invention works in order to achieve an actual reduction to practice."). *See also*, Utility Examination Guidelines, 66 Fed. Reg. 1092, 1095-1096 (Jan. 5, 2001)(Response to Comment 15, discussing satisfaction of the written description requirement and reciting the above-quoted statement from *Newman v. Quigg*).

As stated in *Newman*, what is required is that a disclosure teaches "how to achieve the claimed result, even if the theory of operation is not correctly explained or

even understood." *Id.* at 1581, 11 USPQ2d at 1345. Applicants' claims recite the reduction of Kupffer cell function, *e.g.*, "an agent that reduces Kupffer cell function" in independent claims 1, 34, 36, 37, and 52, and do not require a specific mechanism through which reduction is achieved. Because Applicants' claims do not recite a specific mechanism, Applicants are under no requirement to demonstrate how or why reduction of Kupffer cell function occurs or to demonstrate how or why such reduction leads to the claimed increase in levels of a therapeutic gene product. Applicants' disclosure teaches the methodology required for increasing the level of a therapeutic gene product by administration of an agent that reduces Kupffer cell function. As such, Applicants teach "how to achieve the claimed result," thereby satisfying the written description requirement.

In asserting alleged lack of description for viral vectors, viral particles, and viral nucleic acids other than adenovirus and alleged lack of description for particulate matter, the Examiner states that "...mere description, without any linked cause and effect, does not provide possession beyond...the use of adenoviruses to increase the transformation of more adenovirus encoding a transgene." Office Action at page 4. The latter statement is without legal or factual basis under a correct application of the written description requirement. An analysis of whether Applicants' Specification fulfills the written description requirement for "agents" must be based upon whether the Specification provides "sufficiently detailed, relevant identifying characteristics which provide evidence that applicant was in possession of the claimed invention." *See* M.P.E.P. § 2163.II.3. Applicants' disclosure clearly demonstrates possession of viral and particulate matter agents and their use in the claimed methods and compositions to reduce Kupffer

cell function such that one of ordinary skill in the art could identify members of the class 'agents.' For example, the Specification discloses virally-derived agents such as viral vectors, viral particles, and viral nucleic acids. Specification at page 3, lines 13-26; page 4, lines 4-11; and page 15, lines 6-15. Applicants' Specification also discloses agents as "particulate matter," describing in detail the characteristics of the agents encompassed by the term. *See, e.g.,* Specification at page 15, lines 16-33. Such agents, being well-known and understood, do not require further elaboration. *See Capon v. Eshhar*, 418 F.3d 1349, 1358 (Fed. Cir. 2005); described in more detail in the previous Office Action Reply at pages 13-14. Further, Applicants' Specification specifically describes the use of agents in the claimed methods and compositions. *See, e.g.,* the Specification at pages 2-7, and page 14, line 33, to page 17, line 9. In view of the latter, there is a clear association of the claimed methods with the described agents: an agent as defined can be used to increase the expression of a therapeutic gene product by practicing the claimed methods and compositions.

In view of the reasons set forth above, Applicants respectfully request that the Examiner reconsider and withdraw the written description rejection.

II. Claim Rejections under 35 U.S.C. § 112, First Paragraph, Enablement

Claims 1, 38-49, and 52-53 were stated as being rejected under 35 U.S.C. § 112, first paragraph, as allegedly failing to comply with the enablement requirement. Applicants note that claim 40 was recognized by the Examiner as being cancelled and that claim 54 depends from claim 1 and is presumably rejected as well. As such, Applicants' Reply assumes that the claims at issue are claims 1, 38-39, 41-49, and 52-54.

Applicants respectfully request clarification if this assumption is incorrect. Applicants respectfully traverse the rejection.

In the Office Action at page 5, concerning claims 1, 38-39, 41-46, and 52-53 and presumably claim 54, the Examiner recognizes enablement for "a method for increasing the level of a therapeutic gene product in the liver of a subject" by a method comprising administering "a first adenoviral vector comprising a heterologous transgene encoding" a "therapeutic transgene product, operably linked to expression control elements for expression in hepatocytes" and an agent in the form of a second adenoviral vector not comprising the transgene that is administered prior to or concurrently with the first adenoviral vector, with the second adenoviral vector administered "intravenously, intraperitoneally, or directly to the liver." *Id.* The Examiner recognizes that any route of administration of adenoviral vector expressing a therapeutic gene product is enabled. *Id.* at page 6. The Examiner also recognizes enablement when the agent is "a liposome encapsulated cytotoxic agent" and is administered under the same conditions that the Examiner recognizes as enabling when the agent is a second adenoviral vector. *Id.* at pages 5-6. The Examiner further recognizes enablement for "a pharmaceutical composition comprising an adenovirus encoding a therapeutic gene product encoding a therapeutic transgene operably linked to expression control elements for expression in liver cells, a second adenovirus not encoding such transgene, and a pharmaceutically-acceptable carrier." *Id.* at page 6. Presumably the Examiner also recognizes enablement for an identical pharmaceutical composition when the agent is "a liposome encapsulated cytotoxic agent."

The Examiner alleges lack of enablement for:

(a) uptake by Kupffer cells of viral agents other than adenoviral agents [Office Action at page 9 in view of recognized enablement at page 5],

(b) use of any viral vector to transform liver cells other than an adenoviral vector [Office Action at page 6 in view of recognized enablement at page 5],

(c) increasing the expression of the therapeutic product in any tissue other than liver [Office Action at page 6],

(d) use of any non-viral agent other than known liposomally-encapsulated cytotoxic agents [Office Action at page 6 in view of recognized enablement at page 5 and comments at pages 7].

(e) using any route for administering an agent other than intravenous administration, intraperitoneal administration, or direct administration to the liver [Office Action at page 6 in view of recognized enablement at page 5], and

(f) reducing toxicity associated with expression of a transgene-encoded gene product [Office Action at page 12].

The Examiner at page 6 of the Office Action also alleges non-enablement for "any viral vector for modulating Kupffer cell function." Since the prior claims were directed to reduction of Kupffer cell uptake and the Examiner's comments are based on the latter, Applicants address the rejection under (a). *Id.* Similarly, the Examiner asserts "administration of any viral nucleic acid" as an alleged basis for non-enablement at page 6 of the Office Action; Applicants understand the latter to correspond to the rejections addressed in (a)-(c).

(a) Uptake by Kupffer cells of any viral vector other than adenoviral vector

The Examiner asserts that uptake of any virus other than adenovirus is allegedly not enabled due to lack of a "well-recognized genera of viral vectors that...exhibit 'uptake' by Kupffer cells." Office Action at page 9, second paragraph. The Examiner also alleges that it would require undue experimentation to determine viruses beyond adenoviruses that would be taken up by Kupffer cells. *Id.* Applicants respectfully traverse the rejection.

While the claims as amended only require that the 'agent' reduce Kupffer cell function, thereby leading to increased levels of a therapeutic gene product encoded by a viral vector, Applicants assert that one of ordinary skill would understand that numerous viruses are capable of being taken up by Kupffer cells and that Kupffer cells were recognized to possess a generic capacity to uptake viruses and nucleic acid. For example, Laurent *et al.* show that a ^{35}S-labeled plasmid DNA molecule associated with poly-L-lysine or poly-D-lysine is predominantly taken up by Kupffer cells following intravenous injection. *FEBS Letters 443*: 61-65, 63-64 and Fig. 6 (1999), attached herewith as exhibit A. As noted in the previous Reply, Kupffer cells were also known to uptake Dengue virus (a flavivirus). Marianneau *et al.*, *J. Virol. 73*(6): 5201-5206 (1999); previous Reply at page 23. As shown by Rubin *et al.*, Kupffer cells were known to uptake reoviruses as well frog virus 3 (a ranavirus of the iridoviridae family). *J. Virol. 61*(10): 3222-3226 (1987), attached herewith as exhibit B. Further, Rubin *et al.* showed that reduction of Kupffer cell function by agents such as silica dioxide and carrageenan reduces the ability of Kupffer cells to uptake virus. *Id.* at page 3223, Results section "Agents that affect macrophages influence virus transport." Experiments performed by

Selgrade and Osborn indicated that murine cytomegalovirus (MCMV), a member of the herpes virus family, is taken up by liver macrophages of the reticuloendothelial system. *Infection and Immunity 10*(6): 1383-1390 (1974), attached herewith as exhibit C; *see* Fahimi, *J. of Cell Biol. 47*:247-263 (1970), submitted with the previous Reply, describing hepatic reticuloendothelial cells as Kupffer cells. Selgrade and Osborn showed that reduction of macrophage function by silica (known be selectively toxic to macrophages, including Kupffer cells) resulted in 4 to 20-fold higher levels of virus in liver extracts compared to the liver extracts of mice not receiving silica. *Id.* at 1385-1386, "Effects of silica treatment o[n] MCMV infection." Brunner *et al.* demonstrated that Kupffer cells phagocytize viruses such as vesicular stomatitis virus (a rhabdovirus) and Newcastle disease virus (a paramyxovirus) and noted that intravenous injection of tobacco mosaic virus (a tobamovirus) was known to lead to concentration of the virus in Kupffer cells. *J. Immunol. 85*: 99-105 (1960), attached herewith as exhibit D (further noting that "[i]n view of their size and colloidal characteristics, virus particles might be expected to be efficiently cleared from the blood by the liver Kupffer cells." *Id.* at 99, first column, last paragraph). Brunner *et al.* showed that reduction of Kupffer cell function using thorium dioxide, known to block phagocytic function, prevented Kupffer cell uptake of Newcastle disease virus. *Id.* at page 102, second column, second sentence, and page 104, first column, 3rd sentence from bottom. Additionally, van Til *et al.*, using Applicants' claimed methods, have examined Kupffer cell uptake of lentivirus. *Molecular Therapy* 11(1): 26-34 (2005), attached herewith as exhibit E. van Til *et al.* showed that reduction of Kupffer cell function by gandolinium chloride blocked phagocytic uptake of lentiviral vector by Kupffer cells as a result of reduced Kupffer cell

levels. *Id.* at page 29, first column, first paragraph. Reduced Kupffer cell function in the latter experiment resulted in increased expression of transgene from the administered lentiviral vector, as taught by Applicants. *Id.* The preceding shows that Kupffer cells uptake a diverse array of viruses, including dsRNA viruses, (+) sense RNA viruses, (-) sense RNA viruses, dsDNA viruses, and retroviruses. *See* the NCBI Taxonomy Browser for Viruses at http://www.ncbi.nlm.nih.gov/Taxonomy/Browser/wwwtax.cgi?name=Viruses, last accessed July 30, 2006 for preceding classifications. Furthermore, the preceding shows that reduction of Kupffer cell function can reduce uptake of a diverse array of viruses. Given the latter, it was recognized that Kupffer cells possess a generic capacity for uptake of viruses and that reduction of Kupffer cell function reduces the latter capacity.

"The test for enablement is whether one reasonably skilled in the art could make or use the invention from the disclosures in the patent coupled with information known in the art without undue experimentation." *United States v. Techtronics, Inc.*, 857 F.2d 778, 785, 8 USPQ2d 1217, 1223 (Fed. Cir. 1988). Based on knowledge in the art regarding the uptake capacity of Kupffer cells and based on knowledge that Kupffer cells were known to uptake a wide range of viruses, there is no indication that Kupffer cells are limited in the types of viruses capable of being taken up. *See, e.g.*, Specification at page 15, lines 6-22; Fahimi, H.D, *J. Cell Biol.* 47(1): 247-262, 242 (1970); Marianneau *et al.*, *J. Virol. 73(6)*: 5201-5206 (1999)(describing phagocytic and endocytic uptake as noted in the previous Reply at page 23); and references cited above. Further, Applicants' Specification clearly teaches how to make and use the claimed subject matter comprising viral vector agents, allowing one of ordinary skill in the art to practice the claimed

methods using a viral vector agent and thereby achieving increased levels of a therapeutic product. As such, Applicants claims are enabled as to viral vectors and viral vector agents.

Moreover, it would be apparent to one of ordinary skill in the art that increased levels of therapeutic product can be obtained by practicing Applicants' claimed methods regardless of whether an administered viral vector agent comprises a therapeutic transgene. As such, Applicants have amended claims 1, 34, 36, and 52 to encompass administration of viral vector agents encoding a therapeutic transgene except under circumstances where the agent is administered concurrently with a viral vector encoding a therapeutic transgene. For concurrent administration, Applicants' claims recite the limitation that the agent is not identical to the viral vector comprising a therapeutic transgene.

(b) Use of any viral vector to transform liver cells other than adenoviral vector

The Examiner alleges non-enablement for the transformation of liver cells by non-adenoviral vectors. Office Action at page 6 in view of recognized enablement at page 5. Applicants respectfully traverse the rejection.

Applicants note that the claims are directed, *inter alia*, to "increasing the level of a therapeutic gene product in a subject." The claims are not limited to transformation of liver cells, nor do the claims require that liver cells be transformed for transformation to be increased in another tissue. Despite transformation of liver cells not being required, Applicants note that the references above demonstrate myriad viruses which are capable of transforming liver cells. For example, Marianneau *et al.* noted that Dengue viral

antigens can be detected in hepatocytes. *J. Virol. 73(6)*: 5201-5206, 5201, first paragraph (1999). As noted in Selgrade and Osborn, mice receiving silica to lower Kupffer cell levels demonstrated a 4 to 20-fold higher titer of the herpes virus family member murine cytomegalovirus in liver extracts. *Infection and Immunity 10*(6): 1383-1390, 1386, first column (1974). Additionally, using Applicants' claimed methods, van Til *et al.* showed that lentiviral vectors transform hepatocytes. *Molecular Therapy* 11(1): 26-34, 31-32 (2005). Further, it was well-recognized in the art at the time of Applicants' filing date that vectors could be targeted to specific organs and that therapeutic transgenes could be selectively expressed in particular tissues utilizing methods of targeted delivery and targeted expression available to one of ordinary skill in the art. *See, e.g.*, Dachs *et al.*, *Oncology Research 9*:313-325 (1997), attached herewith as exhibit F. Thus, while the claims are not limited as such, based on the knowledge that transgenes or viral proteins encoded by non-adenoviral vectors can be expressed in liver cells and based on available methods of targeted delivery and expression, one of ordinary skill in the art would be able to utilize Applicants' claimed methods for increasing expression of therapeutic products in liver cells using non-adenoviral vectors.

(c) Increasing the expression of the therapeutic product in any tissue other than liver

The Examiner alleges non-enablement for transformation and increased expression in any tissue other than liver. Office Action at pages 6-8 in view of recognized enablement at page 5. In particular, the Examiner asserts that macrophages in other tissues would allegedly "be reasonably predicted to act to sequester adenoviral

vectors" "regardless of whether the Kupffer cells are depleted or inactivated." Office Action at page 8. Applicants respectfully traverse the rejection.

In terms of adenoviral vectors, it was known that despite uptake of adenoviral vectors by liver tissue, expression could be achieved in other tissues by increasing the dose of administered vector. *See*, van Beusechem *et al.*, *Gene Therapy 7*: 1940-1946, 1946 (2000), attached herewith as exhibit G, noting that:

> *In vivo* delivery of adenoviral vectors yields efficient transduction of cells that may not be a target for the therapy, most notably liver cells. Because of this vector sequestration by non-target cells, high vector doses are needed for effective gene delivery into target cells.

Id. at 1940, first paragraph. Based on the latter, one of ordinary skill in the art would understand that even though a vector dose may pass through the liver and may transduce hepatocytes, adjusting the size of the vector dose allows transduction of other tissues. It would be apparent that an increase in the total amount of available vector would allow for delivery to target cells based on knowledge in the art that increased dosages allow for viral vectors to bypass the liver and to be delivered to non-liver target tissues. van Beusechem *et al.* at page 1940. Similarly, following reduction of Kupffer cell function by an agent, one of skill would understand that, if necessary, the dose of adenoviral vector could be modified to achieve effective delivery and expression in other tissues regardless of whether or not macrophages are present in those tissues. *See,* Specification at page 16, line 25 to page 17, line 3; page 21, lines 26-35; and Examples. Even if macrophages were present in a non-liver target tissue, the macrophage population would be more limited in its uptake capacity as compared with Kupffer cells, the latter being "the largest group of fixed macrophages in mammalian organism[s]." Fahimi, H.D., *J. Cell Biol. 47*(1): 247-262, 242 (1970). As such, following reduction of Kupffer cell

function by an agent, it would be routine for one of ordinary skill to modify the dose of administered vector encoding the therapeutic transgene to allow for effective delivery to non-liver target tissues. Further, one of skill would understand that the therapeutic nucleic acid could be operably linked to a tissue-specific, cell-specific, or condition-specific promoter to allow for expression in a target tissue such that an increase in available vector would lead to a concomitant increase in expression. Dachs *et al.*, *Oncology Research* 9:313-325 (1997).

Similarly, one of ordinary skill in the art would be able to practice Applicants' invention with only routine experimentation by selecting among non-adenoviral vectors for transformation and expression in a desired target tissue. By reducing Kupffer cell function, non-adenoviral vectors that would otherwise be taken up by Kupffer cells would be available in increased numbers for delivery to and expression in target tissues. Because Applicants' claims do not require transformation of liver cells, and because it was understood that viral vector passing through the liver could be effectively targeted to other tissues by adjusting dosage, it would be understood that a non-adenoviral vector could be targeted or delivered to non-liver tissues and that adjusted availability of vector would lead to increased expression as described above. Similarly, one of ordinary skill could also modify the amounts of vector reaching non-liver tissues by utilizing methodologies known in the art for targeting delivery and expression of viral vectors. Dachs *et al.*, *Oncology Research* 9:313-325 (1997). As such, it would be apparent to one of ordinary skill, based on Applicants' teachings, that reduction of Kupffer cell function by an agent would allow for increased expression of a therapeutic gene product from a non-adenoviral vector in non-liver tissues.

(d) Use of any non-viral agent other than known liposomally-encapsulated cytotoxic agents

The Examiner asserts that "liposome-encapsulated cytotoxic agents" are enabled but only those known in the art and only those that are liposomally-encapsulated. Office Action at page 7. *See, e.g.*, Specification at page 15, lines 6-22. Applicants respectfully assert that the Examiner's restriction of enablement to known liposomally-encapsulated cytotoxic compounds for reduction of Kupffer cell function is overly narrow.

Applicants note that Lieber *et al.*, *J. Virol. 71(11)*: 8798-8807, 8804 (1997) shows that use of gadolinium chloride selectively eliminates Kupffer cells. The latter compound is not liposomally-encapsulated. Similarly, Kolb-Bachofen describes the use of silica particles to reduce Kupffer cell levels. *J. Clin. Invest.*, *90*: 1819-1824 (1992), attached herewith as exhibit H; *see also*, Selgrade and Osborn, *Infection and Immunity 10*(6): 1383-1390 (1974). Rubin *et al.* further describes that carrageenan can decrease the ability of Kupffer cells to uptake particulate substances. *J. Virol. 61*(10): 3222-3226, 3223 (second paragraph of the Results section)(1987). Brunner *et al.* describes the use of thorium dioxide to block phagocytosis by Kupffer cells. *J. Immunol. 85*: 99-105, 10154 (1960). Zenilman, *et al.* also describe use of the ricin A-chain to lower Kupffer cell levels. *J. Surg. Res. 45*: 82-89 (1988), attached herewith as exhibit I. It was also known that glycine and methyl palmitate suppress Kupffer cell function. *See* Cai *et al.*, *Toxicology 210*: 197-204, 198(first paragraph), 201(first paragraph of discussion)(2005), attached herewith as exhibit J; Rentsch *et al.*, *Transplant International* 18: 1079-1089 (2005), attached herewith as exhibit K; and references therein. As such, non-viral agents

known to reduce Kupffer cell function include agents that are not liposomally encapsulated.

Applicants further assert that it would be routine for one of skill in the art to determine substances capable of reducing Kupffer cell function, such that the Examiner's limitation to *known* substances unduly restricts the scope of Applicants' claimed invention. For example, one of ordinary skill in the art would be able to utilize techniques described in the above-noted references as well as generally practiced *in vitro* and *in vivo* studies as known in the art to determine the effect of a compound on Kupffer cell function without undue experimentation. Using the latter techniques, one of ordinary skill in the art could readily determine the effects of a particular substance on Kupffer cell function. Moreover, one of ordinary skill would comprehend that any newly discovered substance shown to reduce Kupffer cell function could be utilized within Applicants' methodology to achieve the claimed effect.

Regarding alleged non-enablement of particulate matter agents other than adenoviral vector, Applicants note that a variety of non-vector agents have been shown to reduce Kupffer cell function, including silica and carragenan. Further, non-adenoviral vectors were known to be taken up by Kupffer cells as described above. In view of Applicants' teachings that administration of a viral vector agent reduces Kupffer cell function and that a particulate matter agent can be about the same diameter as the viral vector encoding the therapeutic product, one of ordinary skill in the art would understand that particulate matter agents other than adenovirus can be utilized within Applicants' claimed methods to increase the expression of a therapeutic product by reducing Kupffer

cell function. *See* Specification, *e.g.* Examples 1, 3 and 5; page 4, lines 11-18; and page 15, lines 16-33.

(e) Using any route for administering an agent other than intravenous administration, intraperitoneal administration, or direct administration to the liver

The Examiner recognizes that Applicants' claims are enabled for any route of administration of an adenoviral vector comprising a therapeutic nucleic acid. Office Action at page 10. However, the Examiner asserts that the claims allegedly lack enablement for administration of an agent by any route other than intraperitoneal, intravenous, or direct administration to the liver. Office Action at pages 10-11. Purely in the interests of furthering prosecution and not as an admission that the Examiner's assertions are correct, Applicants have amended the claims to recite administration of an agent by a route selected from the group consisting of direct administration to the liver, intravenous administration, or intraperitoneal administration.

(f) Reducing toxicity associated with expression of a transgene-encoded gene product

The Examiner maintains the enablement rejection of claims 47-49 in the present Office Action. Purely in the interests of furthering prosecution and not as an admission that the Examiner's assertions are correct, Applicants have canceled claims 47-49, reserving the right to pursue the subject matter of these claims in related applications.

In view of the reasons set forth above, Applicants respectfully request that the Examiner reconsider and withdraw the enablement rejection.

III. Claim Rejections under 35 U.S.C. § 103

Claims 37, 39, 41-42, and 44-46 were rejected under 35 U.S.C. § 103(a) as allegedly being unpatentable over U.S. Patent No. 6,025,195 (Sandig *et al.*) and Wolff *et al.*, *J. Virol. 71*(1): 624-629 (1997). Applicants respectfully traverse the rejection.

To establish a *prima facie* case of obviousness under 35 U.S.C. § 103, an Examiner must demonstrate that: (1) an Applicant's claimed invention could have been attained by either a modification of the primary reference or a combination of references based on some motivation or suggestion in the prior art, (2) there would be a reasonable expectation of success associated with the motivation or suggestion, and (3) the reference(s) teach all the claim limitations. *See* M.P.E.P. § 2142, citing *In re Vaeck*, 947 F.2d 488, 20 USPQ2d 1438 (Fed. Cir. 1991).

Purely in the interests of furthering prosecution and not as an admission that the Examiner's assertions are correct, Applicants have amended claim 37 to state that the particulate agent is administered "less than 2 days prior to" administration of a viral vector comprising a therapeutic nucleic acid encoding a therapeutic gene product. Sandig *et al.* discusses adenoviral vectors for liver-specific gene therapy. *Id.* As noted by the Examiner, Sandig *et al.* does not teach the administration of an agent to decrease the uptake of a viral vector comprising a therapeutic nucleic acid such that expression of a therapeutic product is increased. Office Action at page 15. Wolff *et al.* discusses administration of liposomal clodronate two days prior to administration of an adenoviral vector in order to deplete Kupffer cells. *Id.* at page 624, "In vivo studies." As recognized by the Examiner, Wolff *et al.* does not teach the administration of a particulate agent less than 2 days prior to administration of a viral vector comprising a

therapeutic nucleic acid encoding a therapeutic gene product. Office Action at pages 15-16, bridging paragraph. As such, Wolff *et al.* in combination with Sandig *et al.* fails to teach each and every limitation of Applicants' claims and thus can not serve to establish a *prima facie* case of obviousness under 35 U.S.C. § 103.

In view of the reasons set forth above, Applicants respectfully request that the Examiner reconsider and withdraw the obviousness rejection.

Conclusion

All of the stated grounds of objection and rejection have been properly traversed, accommodated, or rendered moot. Applicants therefore respectfully request that the Examiner reconsider all presently outstanding objections and rejections and that they be withdrawn. Applicants believe that a full and complete reply has been made to the outstanding Office Action and, as such, the present application is in condition for allowance. If the Examiner believes, for any reason, that personal communication will expedite prosecution of this application, the Examiner is invited to telephone the undersigned at the number provided.

Prompt and favorable consideration of this Amendment and Reply is respectfully requested.

Respectfully submitted,

STERNE, KESSLER, GOLDSTEIN & FOX P.L.L.C.

Elizabeth J. Haanes, Ph.D.
Attorney for Applicants
Registration No. 42,613

Date: August 4, 2006

1100 New York Avenue, N.W.
Washington, D.C. 20005-3934
(202) 371-2600

520904_10.DOC

FEBS 21420 FEBS Letters 443 (1999) 61–65

Uptake by rat liver and intracellular fate of plasmid DNA complexed with poly-L-lysine or poly-D-lysine

Nathanael Laurent, Simone Wattiaux-De Coninck, Eugenie Mihaylova, Ekaterina Leontieva, Marie-Thérèse Warnier-Pirotte, Robert Wattiaux*, Michel Jadot

Laboratoire de Chimie Physiologique, Facultés Universitaires Notre-Dame de la Paix, 61, rue de Bruxelles, B-5000 Namur, Belgium

Received 27 November 1998

Abstract **Efficiency of transfection is probably dependent on the rate of intracellular degradation of plasmid DNA. When a non-viral vector is used, it is not known to what extent the plasmid DNA catabolism is subordinated to the catabolism of the vector. In the work reported here, the problem was approached by following the intracellular fate in rat liver, of plasmid [^{35}S]DNA complexed with a cationic peptide poly-L-lysine that can be hydrolyzed by cellular peptidases or with its stereoisomer, poly-D-lysine, that cannot be split by these enzymes. Complexes of DNA with poly-L-lysine and poly-D-lysine are taken up to the same extent by the liver, mainly by Kupffer cells, but the intracellular degradation of nucleic acid molecules is markedly quicker when poly-L-lysine is injected. The association of DNA with the polycations inhibits DNA hydrolysis in vitro by purified lysosomes but similarly for poly-L-lysine and poly-D-lysine. The intracellular journey followed by [^{35}S]DNA complexed with poly-L- or poly-D-lysine was investigated using differential and isopycnic centrifugation. Results indicate that [^{35}S]DNA is transferred more slowly to lysosomes, the main site of intracellular degradation of endocytosed macromolecules, when it is given as a complex with poly-D-lysine than with poly-L-lysine. They suggest that the digestion of the vector in a prelysosomal compartment is required to allow endocytosed plasmid DNA to rapidly reach lysosomes. Such a phenomenon could explain why injected plasmid DNA is more stable in vivo when it is associated with poly-D-lysine.**

Key words: Lysosome; Cationic peptide; Transfection; Non-viral vector

1. Introduction

Efficiency of transfection is probably dependent on the rate of intracellular degradation of plasmid DNA. When nucleic acid molecules are complexed with a vector such as a cationic peptide (polylysine, polyarginine) or a cationic lipid, they are taken up by endocytosis [1] and therefore are mostly degraded in lysosomes, the main site of endocytosed macromolecule hydrolysis [2]. Two factors will chiefly influence the rate of plasmid DNA degradation: the rate with which nucleic acid molecules are delivered to lysosomes after having been picked up by the cells and the susceptibility of these molecules to lysosomal nucleases. Cationic compounds could affect these factors by making nucleic acids more resistant to nucleases, as has been shown in vitro [3], and by delaying their transfer to lysosomes [4,5]. How the type of cationic compound influences the intracellular degradation of plasmid DNA is poorly documented. Particularly, it is not known to what extent the plasmid DNA catabolism is dependent on the catabolism of the vector when a non-viral vector is used. The problem was approached in the work presented here, by following the intracellular fate in rat liver of plasmid [^{35}S]DNA complexed with a cationic peptide poly-L-lysine that can be hydrolyzed by cellular peptidases, or with its stereoisomer poly-D-lysine that cannot been split by these enzymes. Our results show that in vivo, the rate of DNA degradation is markedly lower when the plasmid was complexed with poly-D-lysine than when it was associated with poly-L-lysine. Analysis of intracellular distribution of radioactivity by centrifugation indicates that DNA is transferred more slowly to lysosomes when it is given as a complex with poly-D-lysine than with poly-L-lysine. Such a phenomenon could explain why plasmid DNA is more stable in vivo when it is associated with poly-D-lysine.

2. Materials and methods

Experiments were performed with male Wistar rats weighing 300–350 g. Labeled DNA was obtained by nick translation of pGL3 control vector (Promega, Madison, USA) with [^{35}S]dATP. Labeling was performed with a kit from Amersham (Buckinghamshire, UK), according to the protocol provided by the manufacturer, except that a 10-fold excess of template was used and that the reaction was supplemented with 10 units of DNA polymerase I (Boehringer, Mannheim, Germany). Such a procedure makes it possible to obtain a labeled full length DNA as shown by agarose gel electrophoresis. For injection, 1 μg of [^{35}S]DNA was mixed with 5 μg of poly-L- or poly-D-lysine (75–150 kDa, Sigma) in a volume of 25 μl; after 10 min, 0.6 ml of 0.15 M NaCl was added. We found that the sedimentation profile after centrifugation in 0.15 M NaCl is the same for the two complexes obtained in these conditions. We also checked that complexes with poly-L-lysine are totally dissociated after treatment with trypsin whereas complexes with poly-D-lysine are stable in the presence of the proteolytic enzyme.

Rats were injected intravenously and killed at various times after injection. The liver was perfused with cold 0.15 M NaCl, removed and homogenized in ice-cold 0.25 M sucrose. The homogenate was fractionated by differential centrifugation as described by de Duve et al. [6], giving a nuclear fraction N, a heavy mitochondrial fraction M, a light mitochondrial fraction L, a microsomal fraction P and a soluble fraction S. Isopycnic centrifugation of the total mitochondrial fraction (M+L) was performed according to Beaufay et al. [7], at 240 000 × *g* in a VTI65 Beckman rotor for 180 min. The sucrose gradient extended from 1.09 to 1.35 g/ml. Arylsulfatase was measured by the method of Bowers et al. [8] and proteins according to Lowry et al. [9]. Degradation of [^{35}S]DNA after its uptake was assessed by measuring the acid-soluble radioactivity in 5% perchloric acid. Purification of rat liver lysosomes was achieved by the method of Wattiaux et al. [10]. Separation of liver cells (hepatocytes, endothelial cells and Kupffer cells) was performed by the method of Seglen [11].

*Corresponding author. Fax: (32) (81) 724272.
E-mail: robert.wattiaux@fundp.ac.be

PII: S0014-5793(98)01677-9

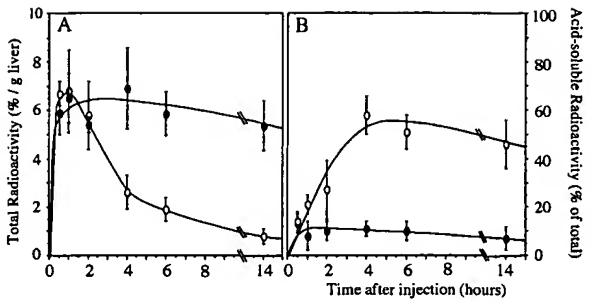

Fig. 1. Uptake of [^{35}S]DNA by rat liver. Radioactivity was measured in homogenates of rat liver at increasing times after injection of [^{35}S]DNA associated with poly-L-lysine (open circle) or poly-D-lysine (closed circle). A: Total radioactivity. The values are given as percentages of the injected dose/g liver. B: Acid-soluble radioactivity. The values are given as percentages of the total radioactivity. Means of at least three animals with S.D. are presented.

3. Results

3.1. Uptake of [^{35}S]DNA by rat liver

As illustrated in Fig. 1A, the complexes of DNA with poly-L-lysine and poly-D-lysine are taken up by the liver to the same extent, the maximal amount being reached after 30–60 min. Radioactivity originating from poly-D-lysine remains constant and mostly acid-precipitable (Fig. 1B) for many hours. In contrast, 60 min after poly-L-lysine injection, the liver radioactivity decreases and becomes more and more acid-soluble. Thus, apparently, the rate of plasmid DNA degradation is higher when the nucleic acid molecules are taken up as a complex with poly-L-lysine than when they are associated with poly-D-lysine.

3.2. Degradation of [^{35}S]DNA by purified lysosomes

The main intracellular destination of an endocytosed macromolecule is the lysosomes where these compounds are subjected to degradation by hydrolases present in these organelles [2]. We have measured the rate of hydrolysis by purified rat liver lysosomes of plasmid [^{35}S]DNA, naked or complexed with poly-L- or poly-D-lysine (Fig. 2). The association of DNA with the polypeptides inhibits DNA hydrolysis by lysosomal nucleases but similarly for the two polymers. This indicates that the difference of DNA stability in vivo, depending on the fact that poly-L- or poly-D-lysine is used, probably does not originate from a difference of resistance to hydrolysis of the molecule by lysosomal nucleases.

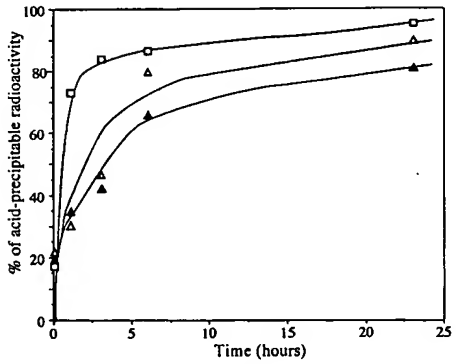

Fig. 2. Degradation of [^{35}S]DNA by purified lysosomes. 1 μg of [^{35}S]DNA was incubated for increasing times at 37°C in a medium containing 0.05 M acetate buffer pH 5 and purified rat liver lysosomes (25 μg protein), in a volume of 1 ml. The reaction was stopped by addition of the same volume of 10% perchloric acid. The precipitate was discarded by centrifugation and the radioactivity measured in the supernatant. Acid-soluble radioactivity is given as a percentage of the total radioactivity present in the incubation medium. Open square: naked [^{35}S]DNA; open triangle: [^{35}S]DNA complexed with poly-L-lysine; closed triangle: [^{35}S]DNA complexed with poly-D-lysine.

3.3. Intracellular journey of [^{35}S]DNA

The intracellular journey followed by plasmid [^{35}S]DNA complexed with poly-L- or poly-D-lysine was investigated by centrifugation methods. First, liver homogenates from rats were analyzed by differential centrifugation according to de Duve et al. [6], the animals being killed 1, 4 or 14 h after injection. Results are presented in Fig. 3 according to the method of de Duve et al. [6], shaded areas indicate the proportion of acid-soluble radioactivity. One hour after poly-L-lysine injection, the largest part of radioactivity, mostly acid-precipitable, is recovered in the heavy mitochondrial fraction M. Later, the distribution profile of radioactivity becomes similar to that of lysosomal enzymes (exemplified by arylsulfatase distribution) except that a relatively high amount of radioactivity (totally acid-soluble) is present in the unsedimentable S fraction. A significant proportion of radioactivity found in the mitochondrial fractions M and L is acid-soluble. One hour after poly-D-lysine injection, the radioactivity distribution does not differ from that observed after poly-L-lysine

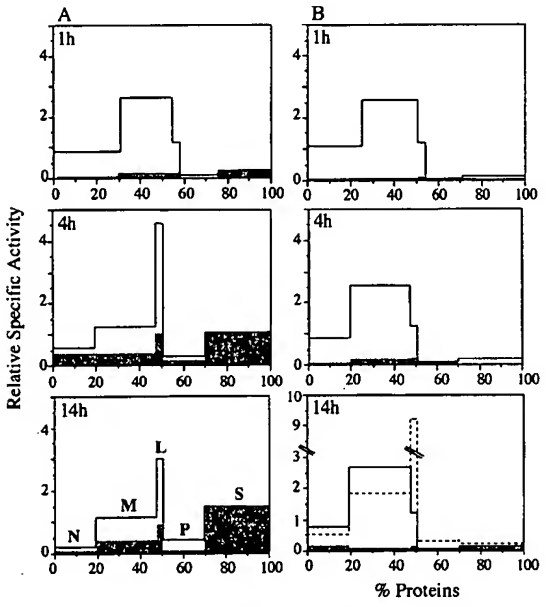

Fig. 3. Distribution of radioactivity after differential centrifugation. The radioactivity distributions were obtained with livers of rats killed at increasing times after injection of [^{35}S]DNA associated with poly-L-lysine (A) or poly-D-lysine (B). Ordinate: relative specific radioactivity of fractions (percentage of total recovered radioactivity/percentage of total recovered proteins); abscissa: relative protein content of fractions (cumulatively from left to right). N, nuclear fraction; M, heavy mitochondrial fraction; L, light mitochondrial fraction; P, microsomal fraction; S soluble fraction. Shaded areas represent the percentage of acid-soluble radioactivity found in the fractions. In broken line, a representative distribution of arylsulfatase.

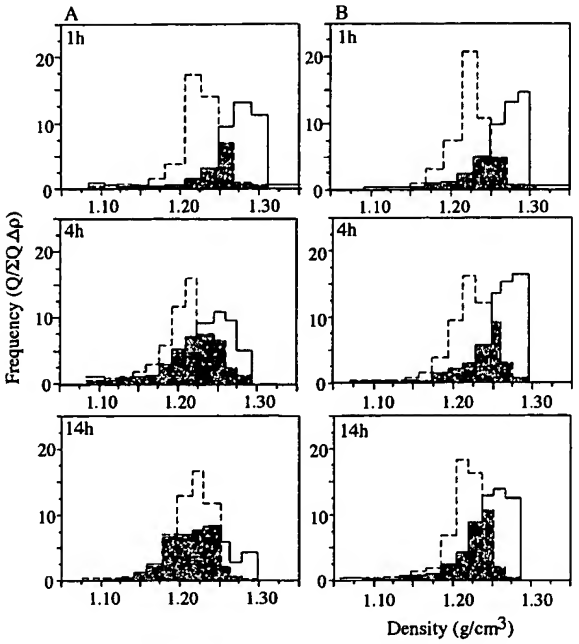

Fig. 4. Density distribution histograms of radioactivity (continuous line) and arylsulfatase (broken line) after isopycnic centrifugation of a total mitochondrial fraction (M+L) in a sucrose gradient. The particle preparations were isolated at increasing times after injection of [^{35}S]DNA associated with poly-L-lysine (A) or poly-D-lysine (B). Centrifugations were performed at 240 000×g in a VTI 65 Beckman rotor for 180 min. The sucrose density gradient extended from 1.09 to 1.30 g/cm^3 density. Ordinate: frequency $Q/\Sigma Q.\Delta\rho$ where Q represents the activity found in the fraction, ΣQ the total activity recovered in the sum of the fractions and $\Delta\rho$ the increment of density from top to bottom of the fraction.

injection but remains unchanged even after 14 h; moreover, at any time, radioactivity is almost totally acid-precipitable.

To more clearly characterize the radioactivity bearing structures that are mainly present in the M and L fractions, granule preparations corresponding to the sum of these fractions were analyzed by isopycnic centrifugation in a sucrose gradient. Results are given in Fig. 4. One hour after poly-L-lysine or poly-D-lysine injection, radioactivity is located in organelles the distribution of which exhibits only a limited overlap (shaded areas) with that of arylsulfatase, marker of lysosomes. These structures are mainly recovered in high density regions of the gradient. Four hours after injection of poly-L-lysine, the radioactivity distribution curve is shifted towards lower density regions and markedly overlaps the distribution curve of the lysosomal enzyme; this phenomenon is still more evident after 14 h. When poly-D-lysine was injected, radioactivity remains located to a large extent in high density regions of the gradient, even after 14 h.

3.4. Effect of Triton WR 1339

Differential and isopycnic centrifugation results strongly suggest that the transfer of radioactivity to lysosomes is more rapid when [^{35}S]DNA is complexed with poly-L-lysine. An interesting method to assess the lysosomal location of a compound is to specifically change the density of lysosomes by injecting the animal with a substance that accumulates in these organelles because it cannot be digested by lysosomal hydrolases. As a result, the distribution profile of lysosomal enzyme in a density gradient is shifted towards lower or higher densities [11]. If a substance (an endocytosed molecule for example), is associated with lysosomes, its distribution profile will be similarly affected [12]. Triton WR 1339, a non-ionic detergent of low density, is particularly suitable for this purpose: it is endocytosed by the liver and, being resistant to digestion by lysosomal hydrolases, it accumulates in these organelles and decreases their density [13]. Fig. 5 illustrates the effect of Triton WR 1339 treatment on the distribution of radioactivity at increasing times after poly-L-lysine or poly-D-lysine injection and on the distribution of arylsulfatase. As expected, lysosomal hydrolase distribution curve is strikingly shifted towards low density regions. One hour after injection of poly-L-lysine or poly-D-lysine, the major part of radioactivity remains well separated from arylsulfatase, as is also seen in normal rats (see Fig. 4), and is slightly affected by Triton WR 1339 treatment. Four hours after poly-L-lysine injection, a large proportion of radioactivity is recovered in low density zones like arylsulfatase and has been subjected to the same shift of distribution as the lysosomal enzyme by Triton WR 1339. The distribution shift caused by Triton WR 1339 is less pronounced for radioactivity originating from poly-D-lysine indicating a slower transfer of labeled molecules to lysosomes.

3.5. Distribution of [^{35}S]DNA in liver cells

Three main cell types are present in the liver: hepatocytes, endothelial cells and Kupffer cells. We investigated whether the cellular location of plasmid DNA taken up by the liver depended on the cationic compound with which it was associated. As illustrated in Fig. 6, most of the radioactivity found in the liver 1 h after poly-L-lysine or poly-D-lysine injection is

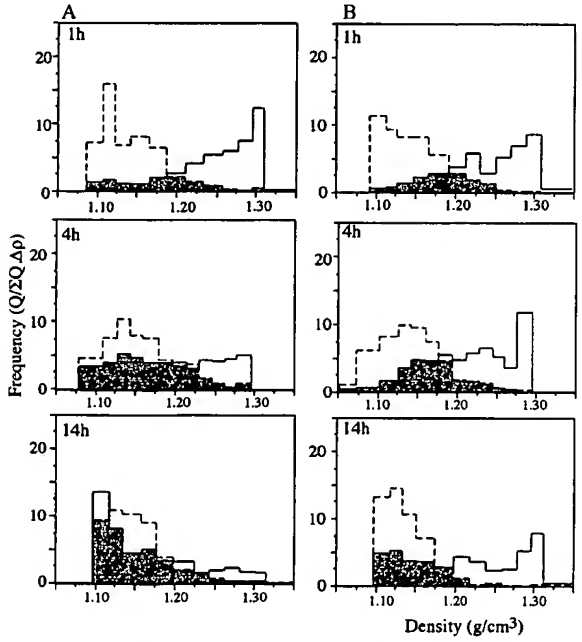

Fig. 5. Density distribution histograms of radioactivity (continuous line) and arylsulfatase (broken line) after isopycnic centrifugation of a total mitochondrial fraction (M+L) in a sucrose gradient. Effect of Triton WR 1339. Experiments were performed as described in the legend of Fig. 4 with rats intravenously injected with Triton WR 1339 (170 mg in 1 cm^3 of saline) 4 days before injection of [^{35}S]DNA associated with poly-L-lysine (A) or poly-D-lysine (B).

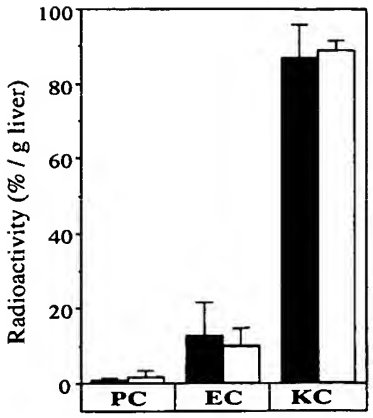

Fig. 6. Distribution of radioactivity in rat liver cells. The radioactivity distributions were obtained with livers of rats killed 1 h after injection of [^{35}S]DNA associated with poly-L-lysine (open bar) or poly-D-lysine (closed bar). Values are given as percentages of total liver radioactivity. Means of at least three animals with S.D. are presented. PC, parenchymal cells; EC, endothelial cells; KC, Kupffer cells.

located in non-parenchymal cells, to a large extent in Kupffer cells. No significant differences were observed between the two complexes. Hence, the differences we observed between the fates of poly-L-lysine and poly-D-lysine do not arise from a difference of cellular location in the liver.

4. Discussion

Our results show that the intracellular degradation of a plasmid DNA injected as a complex with a cationic vector poly-L-lysine or poly-D-lysine is markedly more rapid when the vector is poly-L-lysine. The two polycations have the same molecular weight and the same charge. They give rise to complexes with plasmid DNA exhibiting the same size, as shown by their sedimentation properties in a centrifugal field, that are taken up to the same extent by sinusoidal cells of the liver. In fact, the main and probably the only difference between the two molecules that we have to consider here is that poly-L-lysine is metabolizable while poly-D-lysine is not. How such a difference can influence the intracellular degradation of plasmid DNA was investigated here.

The lysosomes are the main site of hydrolysis of plasmid DNA when it is endocytosed as a complex with a cationic vector. As has been shown previously, cationic lipids delay the transfer of plasmid DNA to lysosomes [4,5]. The same is true for polylysine. Indeed, according to our centrifugation results, 1 h after injection of the labeled complexes, most of the radioactivity originating from poly-L-lysine or poly-D-lysine is located in non-lysosomal structures and is acid-precipitable, whereas at this time it is already present in lysosomes when naked [^{35}S]DNA was injected [4]. However, later it is clear that transfer to lysosomes takes place but at a rate that is lower when the polycation is poly-D-lysine. Four hours after poly-L-lysine injection, most of the radioactivity recovered in the mitochondrial fractions is distributed like lysosomes in differential and isopycnic centrifugation. Moreover, the fact that a large amount of radioactivity is present in the non-sedimentable fraction of the homogenate and is acid-soluble indicates that part of the plasmid DNA has already been hydrolyzed, probably by lysosomal nucleases, the digestion products having diffused in the cytosol. Radioactivity distributions observed after poly-D-lysine injection indicate that a longer time is required to clearly identify the association of a significant proportion of the radioactivity with lysosomes. One can roughly estimate the percentage of radioactivity present in lysosomes by measuring its distribution area that overlaps the distribution curve of arylsulfatase. Such calculations show that 4 h after injection of the complexes 70–80% of radioactivity sedimenting in the mitochondrial fractions are located in lysosomes when the vector is poly-L-lysine and about 45% when the vector is poly-D-lysine. It is to be noted that results are the same whether the rats are injected with Triton WR 1339 or not.

To explain why cationic lipids delay the transfer of plasmid DNA to lysosomes, we have proposed that, due to their size, DNA-cationic lipid complexes are taken up mostly by a process similar to phagocytosis [5] and that degradation of the complexes would be required to allow phagosomes to hand over their content to lysosomes [5], the delivery of phagocytic particles to lysosomes depending on their size [14]. The same hypothesis can be proposed to explain that polylysine delays the transfer of DNA to lysosomes.

Why is there a difference between poly-L- and poly-D-lysine? We think that it is because poly-L-lysine is degradable and poly-D-lysine is not. The presence of cathepsins in endosomes and the possible fusion of these organelles with phagosomes have been described [15–17]. Therefore, after internalization, DNA-polylysine complexes can be exposed to the peptidolytic action of these enzymes which are efficient on poly-L-lysine but not on poly-D-lysine. Hydrolysis of poly-L-lysine would dissociate the complexes, reducing their size and even releasing free DNA inside a prelysosomal compartment. As a result the transfer of nucleic acid molecules to lysosomes would take place but with a certain delay. Another consequence of poly-L-lysine hydrolysis in a prelysosomal compartment is that plasmid DNA released from the complex would be more easily digested by nucleases when it arrives in lysosomes. Such a process would not be possible with poly-D-lysine, which cannot be split by cathepsins.

Acknowledgements: N.L. is the recipient of a fellowship from the F.R.I.A. This work was supported by the Fonds de la Recherche Scientifique Médicale (Contract 3.45.16.97).

References

[1] Zhou, H. and Huang, L. (1994) Biochim. Biophys. Acta 1189, 195–203.
[2] de Duve, C. and Wattiaux, R. (1966) Annu. Rev. Physiol. 28, 435–492.
[3] Capacioli, S., Di Pasquale, G., Mini, E., Mazzei, T. and Quattrone, A. (1993) Biochem. Biophys. Res. Commun. 197, 818–825.
[4] Wattiaux, R., Jadot, J., Dubois, F., Misquith, S. and Wattiaux-De Coninck, S. (1995) Biochem. Biophys. Res. Commun. 213, 81–87.
[5] Wattiaux, R., Jadot, M., Laurent, N., Dubois, F. and Wattiaux-De Coninck, S. (1996) Biochem. Biophys. Res. Commun. 227, 448–454.
[6] de Duve, C., Pressman, B.C., Gianetto, R., Wattiaux, R. and Appelmans, F. (1955) Biochem. J. 60, 604–617.
[7] Beaufay, H., Jacques, P., Baudhuin, P., Sellinger, O.Z., Berthet, J. and de Duve, C. (1964) Biochem. J. 92, 184–205.
[8] Bowers, W.E., Finkenstaedt, J.T. and de Duve, C. (1967) J. Cell Biol. 32, 325–337.
[9] Lowry, O.H., Rosebrough, N.J., Farr, A.L. and Randall, R.J. (1951) J. Biol. Chem. 193, 265–275.

[10] Wattiaux, R., Wattiaux-De Coninck, S., Ronveaux-Dupal, M.F. and Dubois, F. (1978) J. Cell Biol. 78, 349–367.
[11] Seglen, P.O. (1976) Methods Cell Biol. 13, 29–83.
[12] Wattiaux, R. (1976) Prog. Surf. Membr. Sci. 10, 1–25.
[13] Wattiaux, R., Wibo, M. and Baudhuin, P. (1963) Ciba Found. Symp. Lysosomes, pp. 176–200.
[14] de Chastelier, C. and Thilo, L. (1997) Eur. J. Cell Biol. 74, 49–62.
[15] Berg, T., Gjoen, T. and Bakke, O. (1995) Biochem. J. 307, 313–326.
[16] Pitt, A., Mayorga, L.S. and Sthal, P.D. (1992) J. Biol. Chem. 267, 126–132.
[17] de Chastelier, C., Lang, Th. and Thilo, L. (1995) Eur. J. Cell Biol. 68, 167–182.

JOURNAL OF VIROLOGY, Oct. 1987, p. 3222–3226
0022-538X/87/103222-05$02.00/0

Vol. 61, No. 10

Transport of Infectious Reovirus into Bile: Class II Major Histocompatibility Antigen-Bearing Cells Determine Reovirus Transport

DONALD H. RUBIN,[1]* TERESA COSTELLO,[1] CAM L. WITZLEBEN,[2] AND MARK I. GREENE[3]

Departments of Medicine and Research, Veterans Administration Medical Center, and Department of Microbiology,[1] and Division of Immunology, Department of Pathology and Laboratory Medicine,[3] University of Pennsylvania, and Department of Pathology, Children's Hospital of Philadelphia,[2] Philadelphia, Pennsylvania 19104*

Received 2 April 1987/Accepted 9 July 1987

We have previously demonstrated that mammalian reovirus type 1 enters the bile and gut lumen after systemic administration. In the present study, we showed that Kupffer cell uptake is essential for the transport of reovirus into the bile. Furthermore, class II major histocompatibility antigen (I-A)-bearing cells are a major determinant for the transit of reovirus from the hepatic environment, as well as from the intestine, during the course of systemic infection. These findings may provide an approach to the control of viral pathogens that cause systemic disease by selective utilization or modification of I-A-bearing cells.

We have used a reovirus model to gain an understanding of how viruses that produce systemic disease reenter the intestinal lumen for subsequent transmission. Previous investigations with reovirus type 1 strain Lang (type 1/L) have demonstrated that infectious virions are actively secreted or transported into both the lumen of the intestine and the biliary tract (20). Reovirus type 1/L can be recovered from bile within 30 min after the development of viremia and after reaching a plateau level at 3 h remains at a constant level in the bile until h 26 (20). However, the cellular pathway for the entry of virus into bile has not been elucidated.

Several previous studies have demonstrated that pathogenic organisms and particulate antigens are rapidly removed from the blood by tissue-fixed macrophages. Frog virus 3 and reovirus type 3 are both known to specifically infect tissue-fixed macrophages (Kupffer cells) in the liver (4, 14, 15). In addition, the Kupffer cell selectively transports immunoglobulin A (IgA) molecules from systemic circulation and presents them to hepatocytes for rapid secretion into the bile (12, 18). We postulate that reovirus type 1/L may be transported in a manner similar to that of IgA. This transport mechanism might further preserve reovirus integrity, as measured by infectivity. The studies described here were aimed at further clarification of the mechanisms involved in passage of reovirus type 1/L from the blood into the bile.

MATERIALS AND METHODS

Mice. Adult female A/J mice (Jackson Laboratory, Bar Harbor, Maine), 8 to 12 weeks old, were fed a house diet ad libitum (Purina, St. Louis, Mo.). There was no evidence of a systemic humoral immune response to reovirus by enzyme-linked immunosorbent assay in any mouse used for these experiments (22).

Virus. Reovirus type 1/L and reassortant clone 31 were a generous gift from B. N. Fields, Harvard Medical School, Boston, Mass. The characteristics of reovirus type 1 have been previously described (3). Clone 31 is derived from a genetic cross of reovirus type 1/L and reovirus type 3 strain Dearing. It contains all the outer capsid encoded polypeptides (μ1c, σ1, σ3, and λ2) from reovirus type 1. For mouse inoculation, a stock of reovirus that was passed twice in L cells was purified by substituting ultrasonic disruption (Ultrasonic 250; Branson Sonic Power Co., Danbury, Conn.) for cell homogenization in a modification of published techniques (6). The particle-to-PFU ratio was approximately 100:1 for purified virus stocks used in these experiments (24).

Mouse inoculation and monoclonal antibodies. Groups of 8- to 12-week-old A/J and ABY mice were inoculated intravenously with a total volume of 0.2 ml of 10^{10} PFU of reovirus 1/L or clone 31 suspended in sterile saline containing gelatin after cannulation of the gallbladder and ligation of the common bile duct as previously described (20). Groups of mice were treated for the 4 days preceding virus inoculation with, per day, 100 μg of IgG2a anti-I-A^k monoclonal antibody (10.3.6 hybridoma-derived monoclonal anti-I-A antibody IgG2a.k, specific for I-$A^{k,s,f,r,z}$ or 100 μg of IgG2a monoclonal antibody to an irrelevant antigen (UPC10 IgG2a.k, specific for β-2,6-linked fructosan [Sigma Chemical Co., St. Louis, Mo.]). An additional group of A/J mice were not treated with antibody before inoculation with reovirus.

Titration of virus from mouse fluids. Bile was collected for virus titration in aliquots hourly. Blood was collected at the conclusion of the experiment. Specimens of blood and bile were measured and then diluted 1 to 5 with saline-gelatin and stored at −70°C until titers were determined. Specimens of intestinal fluids were collected and assayed as previously described (19). Briefly, mice were killed 4 h after virus inoculation, and the small intestine, from the gastroduodenal junction to the ileocecal valve, was removed and divided into proximal, middle, and distal segments approximating the duodenum, jejunum, and ileum. The large intestine, consisting of the cecum and colon, was assayed for virus. The lumen of each bowel segment was washed with 1 ml of saline-gelatin, which was then collected into sample vials. All samples of intestinal contents were frozen and thawed three times. The samples were disrupted by ultrasound

* Corresponding author.

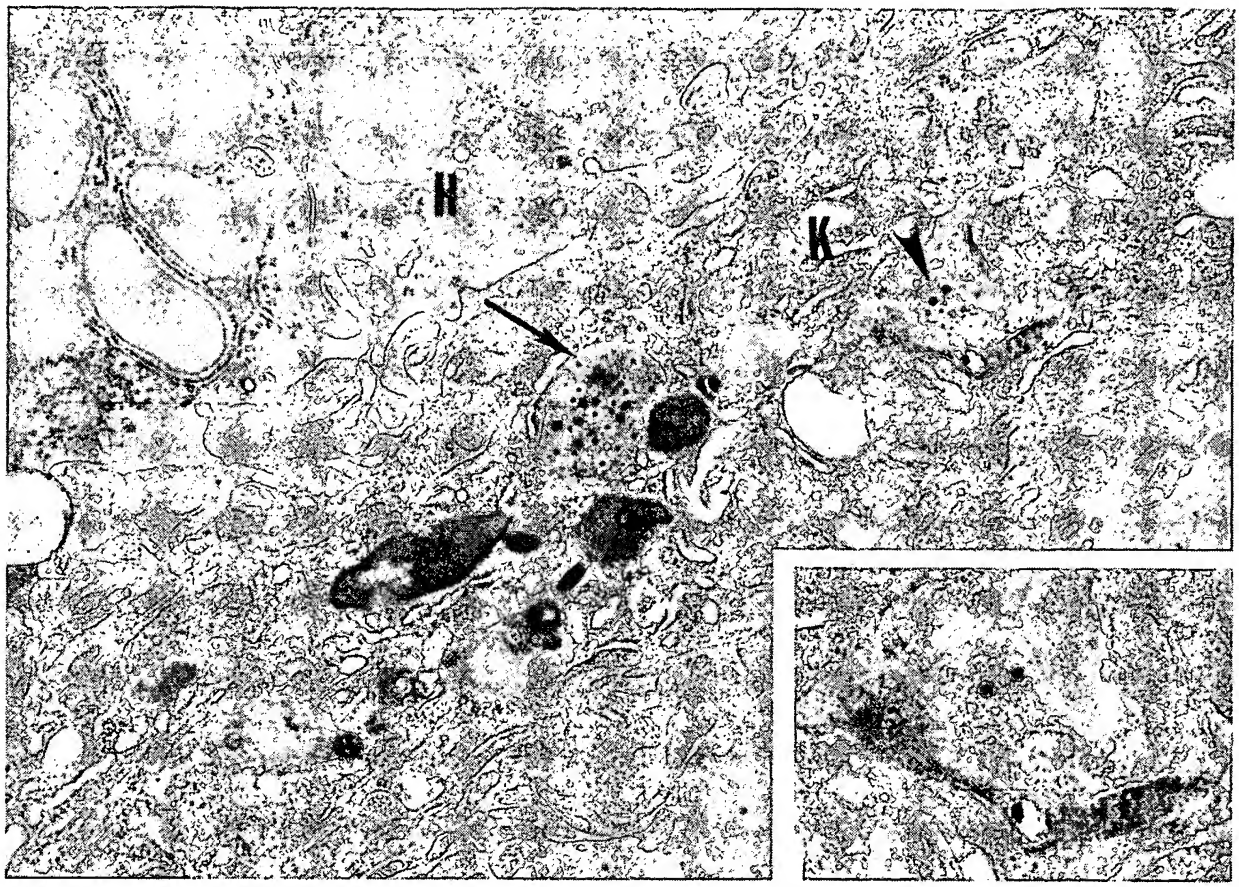

FIG. 1. Reovirus type 1/L in Kupffer cells. A/J mice (8 to 12 weeks old) were inoculated via the tail vein with 10^{10} PFU of reovirus and killed 2 h later. The liver was fixed for electron microscopic examination. Shown is a Kupffer cell (K) adjacent to a hepatocyte (H). Within the Kupffer cells are a number of lysosomes, one of which (arrow) contains a number of virus particles. Some virus particles also lie free within the cytoplasm (arrowhead). A higher magnification of these particles are shown in the inset. Magnification, ×18,000; inset magnification, ×37,700.

(Branson Ultrasonic 250) and then assayed on L-cell monolayers in 12-well cluster plates (Costar, Cambridge, Mass.) (21).

Collection of bile. Mice were anesthetized with pentobarbital sodium and then the common bile duct was ligated at the site of insertion into the duodenum. The gallbladder was freed from its supporting ligaments and cannulated with PE-10 tubing (Clay Adams, Parsippany, N.J.). After gallbladder cannulation, the mice were hydrated by subcutaneous inoculation of 0.5 ml each of 0.145 M NaCl and 5% glucose in water. The mice were then placed under a grow light (75 W) at 30 cm for the duration of each experiment. For all experiments, the hourly output of bile averaged 50 to 100 μl in virus-inoculated mice that had received various antibody treatments and was not statistically different from the volume of bile collected from noninfected controls.

Electron microscopy of liver sections. Animals were killed by cervical dislocation. Fragments of liver were immediately cut into 1-mm cubes and fixed in 2.5% phosphate-buffered glutaraldehyde. The tissue was postfixed in osmium, dehydrated in a series of alcohols, and embedded in Epon 812. The sections were cut and stained with uranyl acetate and lead nitrate and examined in a Phillips 301 electron microscope.

RESULTS

Visualization of reovirus. To determine whether Kupffer cells may be involved in reovirus type 1/L entry into the bile, transmission electron microscopy was used to locate virus particles in the liver. Adult A/J mice were inoculated with 10^{10} PFU of reovirus type 1/L intravenously and killed 2 h later. Reovirus type 1/L was found within the lysosomes of Kupffer cells, as well as in a free form within the cytoplasm (Fig. 1). While virus was not visualized in endothelial cells, hepatocytes, or biliary duct epithelium 2 h after inoculation, it was visualized in hepatocytes 48 h after inoculation (data not shown).

Agents that affect macrophages influence virus transport. Silica dioxide and the highly anionic derivative of seaweed, carrageenan, both act upon Kupffer cells and decrease their ability to take up particulate substances (2). Mice given 3 mg of silica dioxide intraperitoneally 18 h before virus challenge were found to have a 1,000-fold decrease in virus secreted into the bile at 3 h (steady-state conditions). Mice pretreated with 1 mg of carrageenan intravenously 18 h before virus inoculation had undetectable levels of virus in the bile 3 h after inoculation. In addition, in the carrageenan-treated mice, the quantity of reovirus present in the blood was

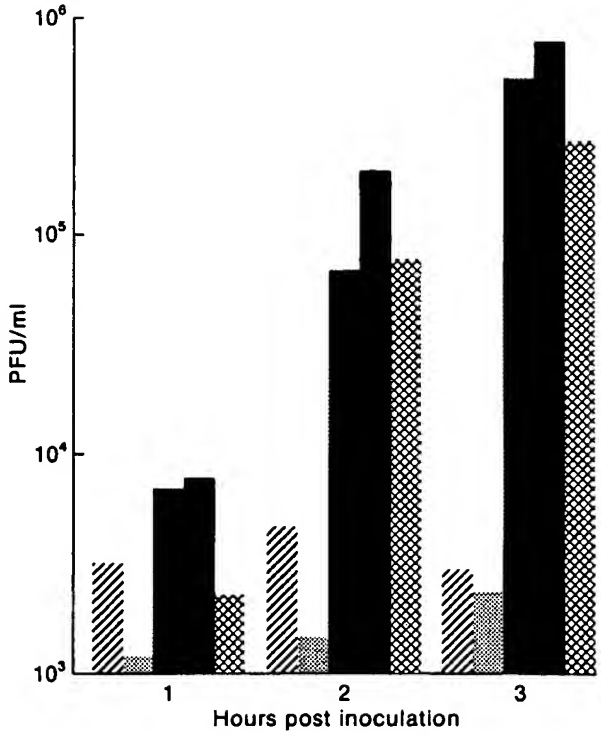

FIG. 2. Decrease of infectious reovirus type 1/L in the bile of A/J (I-A^k) mice by anti-I-A^k antibody treatment. Groups of mice were inoculated intravenously with irrelevant (control) monoclonal antibody, anti-I-A^k antibody, or neither antibody. A/J mice received clone 31 reovirus and control immunoglobulin monoclonal antibody (■) or anti-I-A^k immunoglobulin (▨). Reovirus type 1 was given to ABY (■) and A/J (▩) mice treated with anti-I-A^k immunoglobulin or to non-antibody-treated A/J mice (▩). Titers in sera obtained at the termination of the experiments were similar in all groups. The results shown are the means for two to four mice.

approximately 10-fold higher than in control mice (data not shown).

Anti-I-A antibody affects reovirus passage in vivo. Activated macrophages have been shown to express class II major histocompatibility antigens. It is known that these cells have accessory cell functions, such as antigen presentation to thymus-derived lymphocytes to initiate immune responses (1). It has been previously demonstrated that 40 to 60% of liver Kupffer cells are I-A positive (18). We examined the role of this subset of Kupffer cells in the transport of virus. To interfere with I-A-positive Kupffer cells, mice were administered a highly purified IgG2a anti-I-A^k monoclonal antibody (10.3.6) (25). The same preparation of anti-I-A antibody was simultaneously shown to be effective in the functional inactivation of splenic antigen-presenting cells expressing I-A antigens in vivo in a well-defined antigenic system (25; A. M. Carroll and M. I. Greene, Immunology, in press). A/J (*H-2*^{a} [I-A^k]) mice were inoculated with either the anti-I-A^k antibody or an irrelevant IgG2a monoclonal antibody before virus challenge. In addition, BALB/c (*H-2*^{d}) or ABY (*H-2*^{b}) mice congenic with A/J mice were inoculated with the same batches of anti-I-A^k antibody. As determined by electron microscopic analysis, anti-I-A^k treatment did not eliminate cells which are morphologically defined as Kupffer cells from the sinusoids of A/J mice and virus particles were visible within these cells at 2 h (data not shown). Moreover, the titer of virus recoverable from blood taken 4 h after virus inoculation (4.2×10^4 PFU/ml) from anti-I-A^k antibody-treated mice was similar to that at 4 h in control A/J mice (6.5×10^4 PFU/ml). However, A/J mice inoculated with the anti-I-A^k monoclonal antibody had at least a 300-fold decrease in the quantity of infectious virus in bile at 3 h after inoculation compared with that in A/J control mice (1.8×10^3 and 5.5×10^5 PFU/ml, respectively). ABY or A/J mice that received control IgG2a had no discernible change in virus concentration in the bile compared with that in control A/J mice (Fig. 2). Additional control BALB/c (*H-2*^{d}) mice that received irrelevant IgG2a or anti-I-A^k antibody had titers of virus recoverable from bile that were similar to each other, but the absolute titer of virus in the bile at 3 h in BALB/c mice was somewhat less than that in control A/J mice (data not shown).

The quantity of infectious reovirus particles in the bile does not account for all the infectious virus found within the lumen of the bowel 4 h after intravenous inoculation (18). The contribution of I-A-bearing cells to the presence of virus in the intestinal lumen was analyzed (Fig. 3). It was found that after pretreatment with anti-I-A^k monoclonal antibody, but not with control immunoglobulin monoclonal antibody,

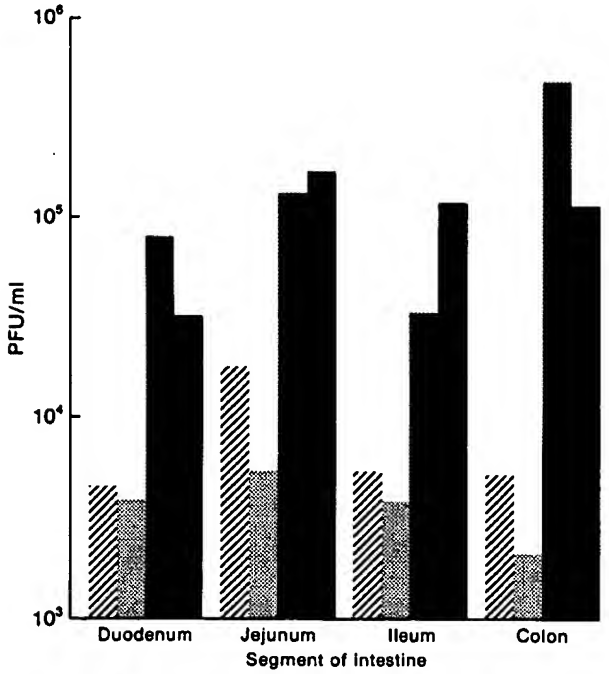

FIG. 3. Decrease of infectious reovirus type 1/L in the gut lumen of A/J mice by anti-I-A^k antibody treatment. Groups of A/J mice were inoculated with either control monoclonal antibody or anti-I-A^k antibody intravenously. A/J mice received clone 31 reovirus and control immunoglobulin monoclonal antibody (■) or anti-I-A^k immunoglobulin (▨). Reovirus type 1 was given to ABY (■) or A/J (▩) mice treated with anti-I-A^k antibody after ligation of the common bile duct. Four hours later, the mice were killed, and the intestines were removed and divided into segments corresponding to the duodenum, jejunum, ileum, and colon. The lumen was flushed with phosphate-buffered saline (pH 7.4), and the virus titers in the liquid contents obtained were determined on L-cell monolayers as described in Materials and Methods (21). The results shown are the means for two to four mice.

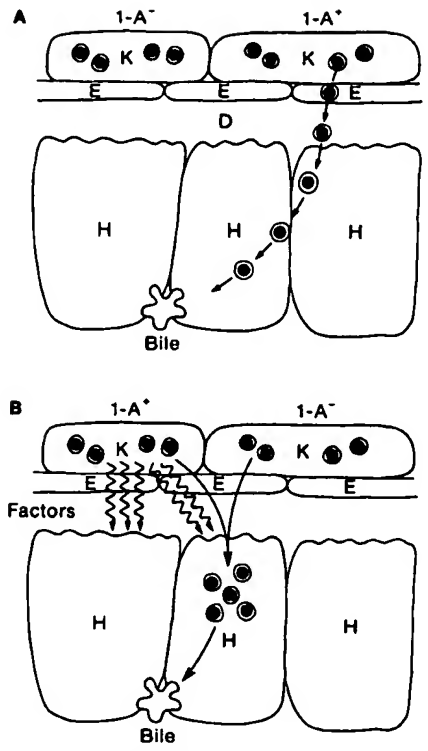

FIG. 4. Roles I-A antigen-bearing cells may play in secretion of reovirus type 1/L. (A) The I-A antigen-bearing Kupffer cell (K) directly interacts with reovirus and serves as the conduit for passage of the virus into the space of Disse (D) for presentation of the virus to hepatocytes (H) and passage to the bile. The endothelial cells (E) do not concentrate virus or participate in the passage of virus. (B) Soluble factors from I-A antigen-bearing cells induced by reovirus uptake affect the transport of reovirus through a second cell (i.e., a hepatocyte).

there was an absolute decrease in the entry of infectious virus into all segments of the bowel (84 to 99.9% decrease depending upon the bowel segment examined; Fig. 3).

DISCUSSION

In this study we extended our observation that reovirus type 1 is transported into the bile of mice (20). We examined several strains of mice (A/J, ABY, and BALB/c) and found that infectious reovirus type 1 was recoverable from the bile of all strains. However, BALB/c mice tended to a have a lower quantity of infectious virus in both the bile and the lumen of the intestine (data not shown) than did other strains. These data suggest that host genetic factors may influence viral transport to the mucosal surface.

The electron microscopic studies demonstrated that reovirus resides selectively within the Kupffer cells 2 h after intravenous virus inoculation and indicated that Kupffer cells concentrate and sequester reovirus type 1/L from the systemic circulation. This finding is supported by our results that indicate increased titers of virus in the blood of mice with impaired macrophage ingestion compared with titers in nontreated controls. Moreover, the dramatic effect of silica dioxide and carrageenan in limiting the appearance of infectious reovirus in the bile strongly suggests that Kupffer cell uptake is also involved in the early steps of transport of reovirus from the blood into the bile.

Kupffer cells were not eliminated by anti-I-A^k monoclonal antibody treatment, as determined by direct electron microscopic visualization of treated liver cells. Similarly, anti-I-A^k antibody does not inhibit the phagocytic activity of I-A-negative macrophages (M. I. Greene, unpublished results). Therefore, when mice were treated with anti-I-A^k antibody, which effectively inactivates I-A-bearing cells, no decrease in the amount of infectious virus was observed in the blood compared with that in controls. However, the anti-I-A^k antibody treatment had a significant effect on decreasing the transport or passage of virus into the bile. Since Kupffer cells are the predominant I-A-bearing cells in the liver, the results obtained with anti-I-A^k antibody treatment reflect an influence on these cells. Moreover, treatment with anti-I-A^k antibody also affected the release of virus into the lumen of the intestine. Therefore, I-A-bearing cells are associated in some manner in the transport of infectious virus into the lumen of the bowel and into the bile. Thus, these experiments defined an unexpected and novel pathway for the elimination of infectious virus from the host.

I-A gene expression is regulated and is inducible during infection in various tissues (9–11). Our findings strongly suggest that I-A-bearing cells are capable of affecting the transport of macromolecular complexes such as viruses onto the mucosal surface. Our observations should be considered in conjunction with studies that show that lactation is correlated with the induction of I-A antigens on secretory breast epithelial cells (7). The expression of I-A antigens may therefore be a marker for a secretory or transport function of a broad set of cells. We hypothesize that I-A antigen-bearing cells affect transport of reovirus by one of two routes: (i) I-A antigen-bearing cells are the conduit for the passage of reovirus from the systemic circulation into hepatocytes for secretion and therefore are directly responsible for transport of reovirus (Fig. 4A) or (ii) soluble factors from I-A antigen-bearing cells induced by virus uptake influence the capacity of a second cell, i.e., a hepatocyte, to secrete virus (Fig. 4B). Whether the I-A antigen-bearing cell regulates secretion and transport (16) or is a marker for an activated cell which expresses an increased capacity to sequester and then secrete or permit passage of virus is under investigation.

The results suggest that I-A-bearing cells may influence the fate of infectious reovirus. It is conceivable that I-A-positive Kupffer cells and other I-A-bearing cells in the gut mucosa may be relevant to many aspects of gut-associated immune responses as well as viral pathogenesis. The delivery of substances to the mucosal surface via the activity of I-A-positive cells may result in (i) the elimination of antigens, (ii) the presentation of antigens in mucosally associated lymphoid tissues (8, 13, 26), or (iii) the transmission of pathogens to a new host via body secretions. Based upon these findings, the treatment of certain viral diseases may be directed toward the regulation of the expression of I-A genes. It is under investigation whether such treatment affects the transport of human immunodeficiency virus, a virus that persists in macrophages, into the nervous system or onto the mucosal surfaces (5, 23).

ACKNOWLEDGMENTS

We thank S. Weiss, F. Gonzalez-Scarano, J. Cebra, and S. London for critical review of the manuscript and Edward Cahill for expert technical assistance.

D.H.R. was supported by a Career Development Award from the Veterans Administration Medical Center and a Veterans Administration research grant. M.I.G. was supported by Public Health

Service grants from the National Institutes of Health and the National Cancer Institute and grants from the American Cancer Society and CTR.

LITERATURE CITED

1. **Benacerraf, B.** 1981. Role of MHC gene products in immune regulation. Science **212**:1229–1238.
2. **Djeu, J. T., J. A. Heinbaugh, W. D. Vierira, H. T. Holden, and R. B. Heberman.** 1979. The effect of immunopharmacological agents on mouse natural cell-mediated cytotoxicity and on its augmentation by poly I:C. Immunopharmacology **1**:231–244.
3. **Fields, B. N., and M. I. Greene.** 1981. Genetic and molecular mechanism of viral pathogenesis: implication for prevention and treatment. Nature (London) **300**:602–607.
4. **Gut, J. P., S. Schmitt, A. Bingen, M. Anton, and A. Kirn.** 1982. Protective effect of colectomy in frog virus 3 hepatitis in rats: possible role of endotoxin. J. Infect. Dis. **146**:594–605.
5. **Ho, D. D., T. R. Rota, R. T. Schooley, J. C. Kaplan, J. D. Allan, J. E. Groopman, L. Resnick, D. Felsenstein, C. A. Andrews, and M. S. Hirsch.** 1985. Isolation of HTLV-III from cerebrospinal fluid and neural tissues of patients with neurologic syndromes related to the acquired immunodeficiency syndrome. N. Engl. J. Med. **313**:1493–1497.
6. **Joklik, W.** 1972. Studies on the effect of chymotrypsin on reoviruses. Virology **49**:700–710.
7. **Klareskog, L., F. Urban, and P. A. Peterson.** 1980. Hormonal regulation of the expression of Ia antigens on mammary gland epithelium. Eur. J. Immunol. **10**:958–963.
8. **London, S. L., D. H. Rubin, and J. J. Cebra.** 1987. Gut mucosal immunization with reovirus serotype 1/L stimulates viral specific cytotoxic T cell precursors as well as IgA memory cells in Peyer's patches. J. Exp. Med. **165**:830–847.
9. **Massa, P. T., R. Dorries, and V. ter Meulen.** 1986. Viral particles induce Ia antigen expression on astrocytes. Nature (London) **320**:543–546.
10. **Mayrhofer, C., C. W. Pugh, and A. N. Barclay.** 1983. Distribution, ontogeny and origin in the rat of Ia-positive cells with dendritic morphology and of Ia antigen in epithelium, with special reference to intestine. Eur. J. Immunol. **13**:112–122.
11. **Mayrhofer, C., and M. A. Schon-Hegrad.** 1983. Ia antigens in rat kidney, with special reference to their expression in tubular epithelium. J. Exp. Med. **157**:2097–2109.
12. **Mullock, B. M., R. H. Hinton, M. Dobrota, J. Peppard, and E. Orlans.** 1979. Endocytic vesicles in liver carry polymeric IgA from serum to bile. Biochim. Biophys. Acta **587**:381–391.
13. **Owen, R. L.** 1982. Macrophage function in Peyer's patch epithelium. Adv. Exp. Med. Biol. **149**:507–513.
14. **Papadimetriou, J. M.** 1965. Electron micrographic features of acute murine reovirus hepatitis. Am. J. Pathol. **47**:565–585.
15. **Papadimetriou, J. M.** 1968. The biliary tract in acute murine reovirus 3 infection: light and electron microscopic study. Am. J. Pathol. **52**:595–611.
16. **Peterson, T. C., and K. W. Renton.** 1986. Kupffer cell factor mediated depression of hepatic parenchymal cell cytochrome P-450. Biochem. Pharmacol. **35**:1491–1497.
17. **Renston, R. H., A. L. Jones, W. D. Christiansen, G. T. Dradek, and B. J. Underdown.** 1980. Evidence for a vesicular transport mechanism in hepatocytes for biliary secretion of immunoglobulin A. Science **208**:1276–1278.
18. **Richman, L. K., R. J. Klingenstein, J. A. Richman, W. Strober, and J. A. Berzofsky.** 1979. Characterization of the cell serving accessory function in antigen-specific T cell proliferation. J. Immunol. **123**:2602–2609.
19. **Rubin, D. H., M. A. Eaton, and A. O. Anderson.** 1986. Reovirus infection in adult mice: the virus hemagglutinin determines the site of intestinal disease. Microb. Pathogen. **1**:79–87.
20. **Rubin, D. H., M. A. Eaton, and T. Costello.** 1986. Reovirus type 1 is secreted into the bile. J. Virol. **60**:726–728.
21. **Rubin, D. H., M. J. Kornstein, and A. O. Anderson.** 1985. Reovirus serotype 1 intestinal infection: a novel replicative cycle with ileal disease. J. Virol. **53**:391–398.
22. **Rubin, D. H., A. Plotkin, and A. O. Anderson.** 1983. Potentiation of the secretory IgA response by oral and enteric administration of CP 20961. Ann. N.Y. Acad. Sci. **409**:866–870.
23. **Sei, Y., R. J. Petrella, P. Tsang, J. G. Bekesi, and M. M. Yokoyama.** 1986. Monocytes in AIDS. N. Engl. J. Med. **315**: 1611–1612.
24. **Smith, R. E., H. J. Zweerink, and W. K. Joklik.** 1969. Polypeptide components of virion, top component and cores of reovirus type 3. Virology **39**:791–810.
25. **Steinner, L. R., R. T. Rosenbaum, S. Srivam, and H. O. McDevitt.** 1981. In vivo effects of antibodies to immune response gene products: prevention of experimental allergic encephalitis. Proc. Natl. Acad. Sci. USA **78**:7111–7114.
26. **Wolf, J. L., D. H. Rubin, R. Finberg, R. S. Kauffman, A. H. Sharpe, J. S. Trier, and B. N. Fields.** 1981. Intestinal M cells: a pathway for entry of reovirus into the host. Science **212**: 471–472.

INFECTION AND IMMUNITY, Dec. 1974, p. 1383-1390

Vol. 10, No. 6
Printed in U.S.A.

Role of Macrophages in Resistance to Murine Cytomegalovirus

MARYJANE K. SELGRADE[1] AND JUNE E. OSBORN

Department of Medical Microbiology, University of Wisconsin Medical School, Madison, Wisconsin 53706

Received for publication 18 July 1974

The role of macrophages in protecting mice from murine cytomegalovirus (MCMV) was studied in Swiss, CBA/J, and C57BL/6J mice. CBA/J mice were more resistant to virus than were C57BL/6J mice at all ages tested. Prior treatment of adult Swiss mice with 60 mg of silica, a dose selectively toxic to macrophages, increased mortality due to MCMV infection. Transfer of syngeneic adult macrophages to suckling mice significantly increased their resistance to subsequent MCMV infection. Transfer of syngeneic, nonimmune adult lymphocytes to suckling mice also had a lesser but significant protective effect against subsequent MCMV challenge. In vitro infection of adult CBA/J and C57BL/6J macrophages with virulent and attenuated MCMV resulted in productive infection in only a small percentage of cells and recovery of very little virus from the extracellular fluid. Infection of CBA macrophages was no less productive than C57BL/6J nor was infection with virulent virus more productive than with attenuated virus. Histological examination of the livers of MCMV-infected CBA/J and C57BL/6J mice suggested that divergent cellular immune responses to infection might account for differences in susceptibility. It is postulated that the macrophage may facilitate the inductive phase of cellular immunity, one possible explanation for its demonstrated importance in host defenses against MCMV.

Numerous studies have demonstrated the importance of the "macrophage" in host defenses against a variety of viral infections (3, 5-7, 17, 23). (As in most of the literature, the term "macrophage" is used throughout this paper to refer to that population of mononuclear leukocytes which adhere to glass. This terminology is adopted for the sake of simplicity and is not intended to suggest that macrophages are the only cells present in this population, nor that they are solely responsible for the activities observed.) In the case of herpes simplex virus (HSV), a picture of macrophage function has developed based on studies of suckling mice, which develop lethal encephalitis due to infection, and of adult mice, which are resistant to infection. It appears that macrophage maturation is a contributing factor in this age-dependent resistance, since transfer of syngeneic adult macrophages to suckling mice protected them (6), whereas impairment of macrophage activity in adult mice with silica or antimacrophage serum allowed lethal infection to occur (23). Also, macrophages from suckling mice supported growth and spread of HSV in vitro whereas macrophages from adult mice did not (7), suggesting that the ability of HSV to multiply in and spread from suckling macrophages results in lethal infection and that changes occur during macrophage maturation that prevent HSV multiplication, thus protecting the animal from lethal infection.

Murine cytomegalovirus (MCMV), another member of the *Herpesvirus* family, is similar to HSV in that suckling mice are much more susceptible to infection than are adults (9). Since reticuloendothelial organs are the site of maximal involvement in the early stages of virulent, but not of attenuated, MCMV infection (15), and virulent MCMV has been shown to suppress clearance of Newcastle disease virus from the blood stream (12), it seemed reasonable to test the possibility that the macrophage is also an important host defense mechanism in MCMV infection. Therefore, in the present experiments, the influence of macrophages on the course of MCMV infection was studied in vivo, both in suckling mice pretreated with syngeneic adult macrophages and in adult mice pretreated with silica. In addition, in vitro infection of macrophages from two strains of mice—a resistant strain (CBA/J) and a susceptible strain (C57BL/6J)—was studied to deter-

[1] Present address: Department of Bacteriology, School of Medicine, University of North Carolina, Chapel Hill, N.C. 27514.

mine whether variations in the ability of macrophages to support viral replication might account for differences in the susceptibility of these two strains as well as the differences between virulent and attenuated MCMV.

(This paper is taken from a thesis presented by M.K.S. to the Department of Medical Microbiology, University of Wisconsin, in partial fulfillment of the requirements for the Ph.D. degree.)

MATERIALS AND METHODS

Mice. Outbred Swiss mice were obtained from ARS Sprague-Dawley (Madison, Wis.). Swiss mice (free of known viral pathogens) used to generate virus pools were obtained from National Laboratory Animal Co. (Creve Coeur, Mo.). CBA/J and C57BL/6J (referred to subsequently as CBA and C57BL) inbred strains of mice and (CBA/J × C57BL/6J)F_1 hybrid mice were obtained from Jackson Laboratory (Bar Harbor, Me.).

Viruses. MCMV of the Smith strain maintained by mouse passage was used in these studies. Pools of virulent and attenuated MCMV (the latter passaged nine times in tissue culture) were prepared as previously described, with the exception that virus-containing materials were stored in medium which contained 10% dimethylsulfoxide (Me_2SO) as stabilizer instead of sorbitol (14).

To obtain a pool of mouse-adapted HSV, an HF strain which had been passed an undetermined number of times in Vero cells was passed four times in primary mouse embryo cell culture (MECC). After each passage virus was harvested by freezing and thawing infected cells three times. The resultant pool of HSV was stored in small samples at −70 C.

Media and reagents. MECC were grown in medium 199 containing 10% calf serum, 5% lactoalbumin hydrolysate, and 0.06% sodium bicarbonate ($NaHCO_3$). Cells were maintained in medium containing 5% calf serum and 0.15% $NaHCO_3$.

Adherent peritoneal exudate cells (APEC) were harvested in Eagle minimal essential medium containing 20% fetal calf serum and 1 mmol of glutamine per liter. APEC were maintained in the same medium, to which 0.15% $NaHCO_3$ was added. Splenocytes were cultured in medium 199 containing 5% fetal calf serum and 0.06% $NaHCO_3$. Maintenance medium containing 0.8% tragacanth (10) was used for overlay. All media contained 200 U of penicillin and 200 μg of streptomycin per ml.

For fixation of cells, a solution of ethanol-acetic acid-formaldehyde (6:2:1) was used; crystal violet staining facilitated viral plaque visualization on fixed monolayers.

Silica was prepared by mixing 1.5 g of silica powder (325 mesh, Sargent-Welch Co.) in 400 ml of saline. The solution was allowed to settle for 15 min, and supernatant fluid was decanted and centrifuged for 15 min at 1500 rpm. The pellet was then resuspended in a small volume of saline, sterilized, put through a membrane filter (Millipore Corp.) of known weight, and adjusted to a concentration of 60 mg/ml with sterile saline. Particle size was approximately 2 μm by microscopic examination.

Neutral red staining of peritoneal exudate cells. Peritoneal exudate suspension was placed on slides coated with neutral red dye, covered with a cover glass, and incubated for 15 to 20 min at 37 C. Monocytes were distinguished microscopically from other cells with criteria described by Sabin (19); in particular, the cytoplasm of the macrophage was filled with fine, uniform particles that stained darker than neutrophilic granules, whereas lymphocytes in general had a clear cytoplasm.

Tissue culture. Primary and secondary MECC were prepared as previously described (14). To obtain APEC ("macrophages"), mice were sacrificed, the skin over the abdomen was removed, and 4 ml of medium was injected into the intact peritoneal cavity. The abdomen was massaged gently, and 3 ml of fluid was removed through a 20-gauge needle into a syringe. This fluid contained approximately 10^6 cells/ml, of which 50 to 60% were phagocytic as determined by neutral red staining. Fluids from four to five mice were pooled, 0.15% $NaHCO_3$ was added, and 3-ml samples were distributed into Falcon plastic tissue culture tubes (16 by 125 mm; for in vitro infection). After 12 to 18 h of incubation at 37 C in an atmosphere of 5% CO_2, nonadherent cells were removed by washing vigorously several times with 0.85% sterile saline. Cells were refed with maintenance medium. The remaining adherent cells were 95 to 99% phagocytic, as determined by neutral red staining.

"Stimulated" APEC were obtained by injecting 2 ml of thioglycolate medium by the intraperitoneal (i.p.) route 48 to 72 h prior to harvest of peritoneal cells; 70 to 80% of the 10^6 to 10^7 cells/ml obtained in this manner were phagocytic. Peritoneal fluids were processed as previously described, except 15-ml samples were dispensed in Falcon plastic tissue culture flasks (75 cm^2) along with 15 ml of maintenance medium (for transfer studies).

Splenocytes were suspended by forcing spleens and a small amount of medium through a wire mesh, diluted appropriately, and placed in plastic tissue culture flasks (75 cm^2). After 12 to 18 h of incubation, nonadherent cells were shaken into the medium which was then centrifuged lightly; pelleted cells were resuspended to desired volume. Adherent cells were washed several times and removed with a rubber policeman into saline, pelleted, and resuspended appropriately.

Cell transfer studies. Stimulated APEC obtained from 7-week-old male C57BL mice were suspended in cold saline, 10^6 viable cells per 0.05 ml (as determined by counting cells which excluded 0.025% trypan blue). Adherent cells cultured from the spleens of the same mice, and nonadherent cells from those spleens, were processed as previously described and resuspended at concentrations of 10^6 and 10^7 cells per 0.05 ml, respectively. Litters of suckling mice 4 to 5 days old were randomized and divided into groups which received APEC, adherent spleen cells, nonadherent spleen cells, or diluent. Twenty-four hours later all mice were challenged with 2,000 plaque-forming units of MCMV. Some litters were observed for morbidity

and mortality. Others were sacrificed for assay of virus titers in liver and spleen.

Determination of virus titers in various organs. In all virus assay experiments, organs from two mice were pooled, ground with sterile sand with mortar and pestle, and resuspended to 10% (wt/vol) in maintenance medium containing 10% Me_2SO. Extracts were stored at −70 C for subsequent virus assay of 0.5-ml samples on duplicate MECC monolayers as previously described (15).

Silica pretreatment studies. Mice were divided into three treatment groups (all injections were by the i.p. route) as follows: group 1 received 60 mg of silica and 2 h later received MCMV; group 2 received saline and 2 h later received MCMV; and group 3 received 60 mg of silica and 2 h later received diluent. Mice were observed for illness and death; at 3 and 5 days after infection, pairs of animals were sacrificed for virus assay of liver and spleen.

Infection of macrophages in vitro and subsequent assays for MCMV. APEC from 6-week-old adult CBA and C57BL mice were cultured in Falcon tubes and infected 24 h after harvest with 10^5 PFU of virulent or attenuated MCMV in 0.2 ml of maintenance medium. Virus was allowed to adsorb for 2 h, and then maintenance medium was added. At 3-day intervals, medium was changed, and spent medium was assayed for virus. Infectious center assays were also carried out on cultures from both strains infected with both types of virus. At 3-day intervals, cells were scraped from duplicate tubes into 1 ml of cold saline; viable cells were counted in the presence of trypan blue, diluted, and placed on duplicate MECC monolayers in 0.5 ml of maintenance medium. After allowing 1 h for cells to adhere, overlay was added and cells were incubated for 5 days at 37 C and then washed, fixed, and stained for enumeration of plaques representing infectious centers.

RESULTS

Relative susceptibility of various strains of mice to MCMV. Before considering how alterations in the macrophage population might affect the course of MCMV infection in mice, the susceptibility of several strains of mice to MCMV was tested. Two inbred strains (CBA and C57BL), the F_1 hybrid of these two strains, and one outbred Swiss strain were chosen for this purpose. Mice at various ages were infected by the i.p. route with various doses of MCMV and subsequently observed for mortality. Figure 1 shows the relative susceptibility of mice of various strains and ages by comparing the doses required to obtain 50% mortality (mean lethal dose) in each group. The F_1 hybrid resistance pattern resembled the CBA parent, whereas the outbred Swiss strain, like the C57BL strain, was more susceptible to virus. It should be stated that the dose range between 0 and 100% mortality was very narrow; i.e., the dose capable of killing 100% of the mice in a group was never more than four times that which killed none of the mice. At all ages tested, the dose which killed 100% of C57BL mice failed to kill any CBA animals. Figure 1 also shows that within a given strain resistance increased with age.

Groups of 3-week-old CBA and C57BL mice were also inoculated by the i.p. route with various doses of HSV. The mean lethal dose for CBA and C57BL mice using this virus were not measurably different: 5 and 8 PFU, respectively. This suggests that the factor(s) determining susceptibility of the two strains to MCMV is not a general property applicable to other herpesviruses.

Effects of silica treatment of MCMV infection. It has been demonstrated that silica provides selective toxicity for one cell type —macrophages (1, 16). Therefore, an experiment was designed in which silica was used to decrease macrophage activity, on the premise that this might enhance MCMV infection. Adult Swiss mice were injected i.p. with either 60 mg of silica in 1 ml of saline or with diluent. Two hours later, mice were challenged i.p. with MCMV. At 3 and 5 days after infection, two mice in each group were assayed for MCMV in liver and spleen extracts; the remaining mice were observed for mortality.

Table 1 shows data from such an experiment; the greatest difference in mortality between silica-treated mice and those receiving only virus occurred at a dose of 4×10^5 PFU of

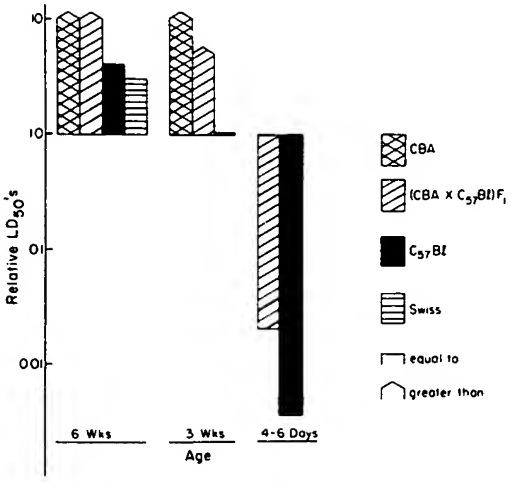

FIG. 1. *Relative susceptibility of various strains and ages of mice to MCMV infection. Mean lethal dose (LD_{50}) values are expressed as factors of a standard LD_{50} (2×10^5 PFU) which was obtained for C57BL weanling mice. Pointed tops indicate an LD_{50} greater than that indicated for instances in which the highest dose available did not kill 50% of the mice.*

TABLE 1. *Effects of silica treatment on the percent mortality in adult Swiss mice infected with MCMV*[a]

Dose (PFU) of virus	Mortality of 6-week-old mice (%)	
	Treated with silica, and virus	Treated with virus only
6×10^5	100	90
4×10^5	75	12
3×10^5	0	0

[a] Eight adult Swiss mice were injected by the i.p. route with 55 to 60 mg of silica 2 h prior to infection with MCMV. An equal number of controls received diluent 2 h prior to infection. Mice were then observed for mortality.

MCMV; the narrow range between lethal and nonlethal doses was again evident. At all doses of virus, titers of MCMV in liver extracts at 3 days after infection were 4- to 20-fold higher in mice that received silica than in animals that did not. Titers of virus in the liver dropped sharply by 5 days in mice that received virus only, whereas mice that had received silica still had levels of virus as high or higher than those observed 3 days after infection. In general, treatment with silica had little effect on the amount of virus detected in spleens of mice at either interval. In most cases, deaths occurred slightly earlier in silica-treated mice, although the difference was usually not greater than 24 h. Mice that received silica without virus remained healthy.

It was postulated that if the difference in susceptibility of CBA and C57BL mice were due to some difference in macrophage activity, treatment of CBA mice with silica might make these animals as susceptible to MCMV as C57BL mice. Therefore, 3-week-old CBA mice were inoculated i.p. with 60 mg of silica. Two hours later, these mice, as well as groups of untreated CBA and C57BL mice, received various doses of MCMV i.p. Although treatment with silica lowered the dose of virus necessary to produce 100, 50, and 0% mortality in CBA mice, these mice were still considerably more resistant than untreated C57BL mice (Table 2).

MCMV infection in suckling mice previously treated with syngeneic adult macrophages. The observed effects of silica suggested that decreasing macrophage activity had an enhancing effect on the course of MCMV multiplication and lethality. The greater lethality of MCMV for suckling mice relative to adults was also previously demonstrated (Fig. 1). To determine the effects of enhanced macrophage activity on the course of MCMV infection, 4- to 5-day-old C57BL mice were inoculated with approximately 10^6 adult, syngeneic macrophages 24 h prior to infection with MCMV. One group of control mice was inoculated with 10^7 to 10^8 adult, syngeneic lymphocytes (nonadherent cells) 24 h before infection; a second control group was not treated before infection. Mice were then observed for mortality. At 2, 4, 6, and 8 days after infection, two mice from each group were sacrificed for virus assay of spleen and liver.

Pretreatment of suckling mice with macrophages before MCMV infection resulted in a significant decrease in the number of deaths which occurred compared to mice which received only MCMV ($P < 0.025$) (Fig. 2); P values were calculated by the binomial test. Also, the time at which deaths occurred was slightly delayed in mice pretreated with macrophages. Pretreatment with lymphocytes conferred a significant degree of protection ($P < 0.05$); however, macrophages conferred a greater degree of protection than lymphocytes ($P < 0.05$) (Fig. 2). Unlike the silica experiments, there was no significant difference in titers of virus in either spleen or liver extracts, despite the significant differences in mortality.

In vitro infection of macrophages from adult CBA and C57BL mice with virulent and attenuated MCMV. Since previous experiments demonstrated that macrophage activity in vivo is an important component of the host defense mechanism against MCMV, attempts were made to assess differences in the ability of various macrophages to support the replication of virus. Macrophages from adult CBA and C57BL mice were infected with 10^5 PFU of virulent or attenuated MCMV in vitro. At 3-day intervals thereafter, extracellular fluids were assayed for virus, and cells were assayed for infectious centers. At 3 days after infection, in all groups only a small percent of infected

TABLE 2. *Effects of silica treatment of the percent mortality in CBA weanling mice*[a]

Mouse strain	Silica treatment	Doses (PFU) yielding:		
		90-100% mortality	50-60% mortality	0-10% mortality
CBA	0	8×10^5	4×10^5	2×10^5
CBA	55 to 60 mg	4×10^5	2×10^5	1×10^5
C57BL	0	8×10^4	5×10^4	3×10^4

[a] Three-week-old CBA mice were injected by the i.p. route with 55 to 60 mg of silica 2 h prior to infection with MCMV. Equal numbers of CBA and C57BL mice received diluent 2 h prior to infection. Mice were then observed for mortality.

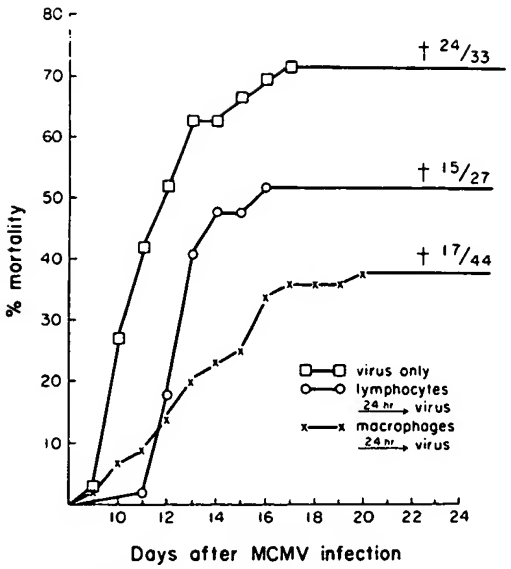

FIG. 2. *Effects of pretreatment with syngeneic adult macrophages or lymphocytes on the percent and distribution of mortality after MCMV infection in C57BL suckling mice. Four- to six-day-old mice were inoculated with 10^6 adult syngeneic macrophages 24 h prior to infection with 2,000 PFU of MCMV. Controls received either 10^7 to 10^8 adult, syngeneic lymphocytes, or were not treated prior to infection. Mice were observed for mortality. The data graphed is a composite of several experiments. Total number of deaths per total number of animals is represented for each group. The percentage of mortality in the macrophage-treated group is significantly different from that in the group which received virus only ($P < 0.025$). The percentage of mortality in the lymphocyte-treated group is significantly different from that in the other two groups ($P < 0.05$).*

macrophages could be detected (Fig. 3). The proportion of infected cells increased with time in culture so that by 9 days as many as 50% of the cells were infected. Results between experiments were quite variable, and there was no indication of more widespread infection with virulent virus or in C57BL cells, as one might have expected if pathogenicity were directly related to the ability of the host macrophage to support viral multiplication. Very little virus was detected in the extracellular fluid of any of the cultures studied; the yield was generally at least 10-fold lower than the initial inoculum.

Detection of histological changes in organs from MCMV infected CBA and C57BL mice. To further compare CBA and C57BL mice, 3-week-old animals from each strain were inoculated with a dose of virus calculated to produce 50% mortality in C57BL mice. Two animals from each group were sacrificed at daily intervals 1 to 6 days after infection; the spleens, livers, brains, lungs, and thymuses were removed, fixed in formalin, sectioned, and stained with hematoxylin and eosin. No pathological changes were observed in thymus or brain sections. In both strains, comparable interstitial inflammation was observed in sections of lung, and changes similar to those previously described (13, 18) were observed in spleen.

In contrast, livers from C57BL mice exhibited histological changes different from those seen in CBA livers. Intranuclear inclusions characteristic of cytomegalovirus were detectable in liver sections from both strains 1 day after infection (Fig. 4); but although inclusion-bearing cells seen in C57BL liver were surrounded by inflammatory cells, the same cytomegalic cells in CBA liver sections were not. Inclusion-bearing cells in the absence of inflammatory foci were ob-

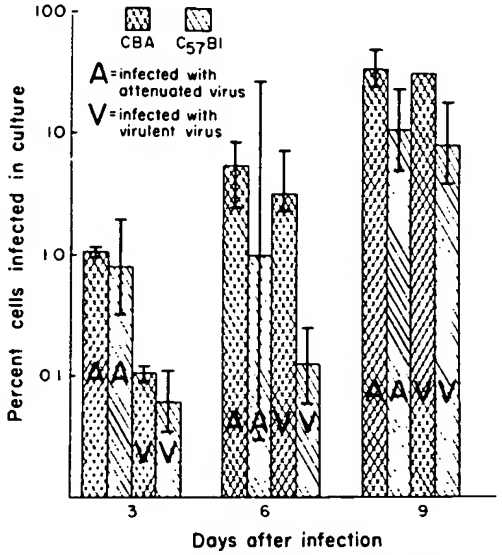

FIG. 3. *In vitro infection of macrophages from adult CBA and C57BL mice with virulent and attenuated MCMV: infectious center assay. Macrophage cultures were infected with 10^5 PFU of either 9th-passage attenuated MCMV or virulent MCMV. At 3, 6, and 9 days after infection, macrophages from two cultures were removed from their tubes, counted, diluted, and placed on duplicate MECC monolayers. Macrophage-monolayer preparations were incubated at 37 C for 1 h before overlay was added. Plaques were counted after 5 days of incubation at 37 C. Each plaque represented an infected macrophage in the initial culture. The average number of plaques, times the dilution factor, was divided by the total number of cells in the original culture to obtain the percent of cells infected (infectious centers). Averages and ranges of the number of infectious centers obtained from various experiments are plotted.*

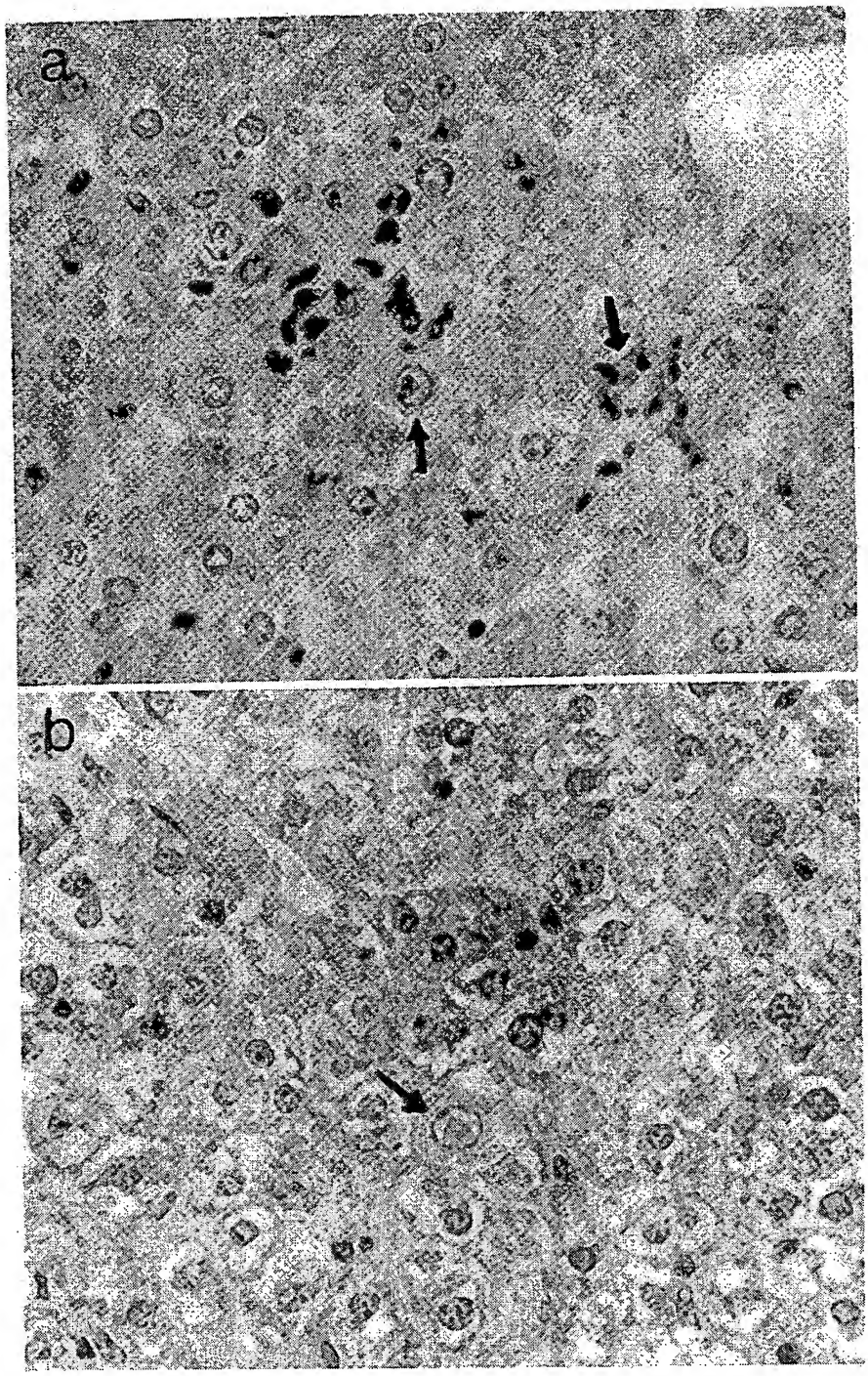

FIG. 4. *Hematoxylin and eosin stained sections of C57BL (a) and CBA (b) liver taken 1 day after MCMV infection. Three-week-old CBA and C57BL mice were inoculated with MCMV, and livers were removed from two mice in each group at 1 day post-infection, fixed in formalin, sectioned, and stained with hematoxylin and eosin. (a) C57BL liver section with an intranuclear inclusion characteristic of cytomegalovirus; and the inclusion-bearing cell is surrounded by inflammatory cells; (b) a similar inclusion in a section of CBA liver; however, there are no signs of inflammation* (×250).

served in liver sections from CBA mice throughout the 6-day period examined, whereas inclusions were always accompanied by inflammation in C57BL liver sections. Patterns of hepatic infiltration also differed, in that inflammatory foci tended to be scattered throughout the liver in both portal and parenchymal foci in C57BL mice; by contrast, inflammation in CBA mice was notably confined to portal areas and even in those areas was not as extensive as that seen in C57BL mice.

DISCUSSION

The data presented here demonstrated that CBA mice were more resistant to MCMV at all ages than were C57BL mice of comparable age, and that, as previously shown (9), susceptibility to MCMV is inversely proportional to age. Studies of resistant and susceptible strains of mice to both mouse hepatitis virus and several togaviruses—formerly group B arboviruses—demonstrated that susceptibility to these viruses is inherited by an autosomal dominant trait (8). In contrast, the present study of MCMV infections showed that the response of (CBA × C57BL)F_1 hybrid mice to MCMV resembled that of the resistant CBA parent, suggesting that the mechanisms responsible for resistance to mouse hepatitis virus and group B arboviruses are not the same as those responsible for resistance to MCMV infection. This finding contrasts with data presented by Diosi et al. (4), in which susceptibility to a wild strain of MCMV inoculated by the intracerebral route seemed to be inherited as an autosomal dominant trait. Probably the mechanisms of resistance necessary for prevention of infection initiated intracranially are different from those which mediate i.p. infection. The present data also show that there is no difference in the susceptibility of CBA and C57BL mice to HSV, suggesting that the defense mechanisms against HSV also differ from those against MCMV even though these two viruses are closely related.

Whereas the mechanisms of resistance of MCMV and HSV appear to be different, the macrophage seems to be important to both. Data from the present study yielded results similar to in vivo experiments with HSV (6, 23), in that prior treatment with silica—which is selectively toxic for macrophages (1, 16)—increased the susceptibility of adult Swiss mice to MCMV and increased titers of virus in the livers of these mice; transfer of syngeneic adult macrophages to C57BL suckling mice increased their resistance to MCMV infection.

Nachkov et al. (11) demonstrated that C57BL macrophages phagocytized a synthetic polypeptide more strongly than did CBA macrophages, suggesting that differences do exist between macrophages from these two strains. However, although treatment of weanling CBA mice with silica resulted in increased susceptibility to MCMV, even these treated mice were more resistant than untreated C57BL weanling animals. Therefore, it appears that, although differences in macrophage activity may be partially responsible for the difference in susceptibility of CBA and C57BL mice to MCMV, other factors must also be important.

A number of studies have demonstrated that macrophages from suckling mice are less active than adult macrophages in several respects, including (i) their ability to produce interferon in response to HSV (6) and antibody in response to sheep erythrocytes (2; W. Braun and L. H. Lasky, Fed. Proc. **26**:642, 1967); (ii) their ability to prevent growth and spread of several viruses (7, 23); and (iii) their ability to respond to proteose peptone stimulation (6). The increased resistance to MCMV of suckling mice pretreated with adult macrophages suggests that some activities of the mature macrophage are vital to host defenses against MCMV. The delay observed in the onset of deaths which did occur in macrophage-treated suckling mice relative to untreated animals resembles the delay in onset of deaths seen as a result of tissue-culture attenuation of virus relative to virulent virus (15). It is possible that transfer of macrophages curtails viral infection in some organs but diverts it to others in which lethal damage may eventually occur.

It is notable that transfer of nonimmune adult lymphocytes also provided some degree of protection to suckling mice, although not to the extent observed after transfer of macrophages. This is in contrast to experiments with HSV where adult lymphocytes had no protective effect for suckling mice (6), and suggests another difference in host response to these two closely related viruses.

Although results from the in vivo experiments in this study corresponded, for the most part, with studies using HSV instead of MCMV, results of in vitro experiments differed from Johnson's studies (7) which showed that HSV could replicate in and spread from macrophages derived from susceptible suckling mice, but not from resistant adult mice. In vitro infection of macrophages with MCMV demonstrated that macrophages from resistant CBA mice were at least as susceptible to infection as those from susceptible C57BL animals and that infection with attenuated virus was not less productive

than with virulent MCMV. In general, only a very small percentage of macrophages appeared to be productively infected initially. This was also the result of several attempts to infect suckling macrophages (unpublished data), and contrasts with results reported by Tegtmeyer and Craighead (20) in which extracellular MCMV was recovered from mouse macrophages infected in vitro at concentrations 10- to 100-fold higher than the inoculum. Reasons for this difference in findings are unclear.

The in vitro studies do not support the concept of a pivotal role for the macrophage per se in controlling viral replication and dissemination. Instead, comparison of the histological changes in livers of MCMV-infected CBA and C57BL mice suggests that the difference in susceptibility may be related to the type of cellular immune response which occurs, since the inflammatory response in C57BL livers was much greater than that observed in CBA livers. The importance of the macrophage in resistance to MCMV may be related to its role in the inductive phase of cellular immunity. In this regard, the macrophage may act to present and/or process antigen for recognition by thymus-derived lymphocytes (T cells) (21, 22). In the case of MCMV infection, a rapid response to the antigen might result in resolution of infection before enough antigen is produced to make a cellular immune response lethally destructive. Macrophages may also act to remove excess antigen which might be capable of eliminating isolated T cells, thus tolerizing the animal (21).

The results of this study show that, although the macrophage is important to host defenses against MCMV, this does not correlate with inability of virus to replicate and spread from these cells as is the case with HSV infection. Some other functions of the macrophage—possibly related to the inductive phase of cellular immunity—must be responsible for the importance of this cell to host defenses against MCMV.

ACKNOWLEDGMENTS

We acknowledge with gratitude the helpful advice of D. L. Walker and Oliver Smithies, and the valuable consultation of Enid Gilbert and Chirane Viseskul in interpretation of the histological preparations.

This study was supported by Public Health Srvice grants AI-09095 and AI-00451 from the National Institute of Allergy and Infectious Diseases.

LITERATURE CITED

1. Allison, A. C., S. S. Harington, and M. Berbeck. 1966. An examination of the cytotoxic effects of silica on macrophages. J. Exp. Med. 124:141-154.
2. Argyris, B. 1968. Role of macrophages in immunological maturation. J. Exp. Med. 128:459-467.
3. Bang, F. B., and A. Warwick. 1960. Mouse macrophages as host cells for mouse hepatitis virus and the genetic basis of their susceptibility. Proc. Nat. Acad. Sci. U.S.A. 46:1065-1069.
4. Diosi, P., P. Arcan, and L. Plavosin. 1974. Genetic control of resistance to mouse cytomegalovirus infection. Arch. Gesamte Virusforsch. 44:23-27.
5. Goodman, G. T., and H. Koprowski. 1962. Study of the mechanism of innate resistance to virus infection. J. Cell. Comp. Physiol. 59:333-373.
6. Hirsch, M. S., B. Zisman, and A. C. Allison. 1970. Macrophages and age-dependent resistance to *Herpes simplex* virus in mice. J. Immunol. 104:1160-1165.
7. Johnson, R. T. 1964. The pathogenesis of Herpes virus encephalitis: a cellular basis for the development of resistance with age. J. Exp. Med. 120:359-374.
8. Kantock, M., A. Warwick, and F. B. Bang. 1963. The cellular nature of genetic susceptibility to a virus. J. Exp. Med. 117:781-798.
9. Mannini, A., and D. N. Medearis, Jr. 1961. Mouse salivary gland virus infections. Amer. J. Hyg. 73:329-343.
10. Mirchamsy, H., and F. Rapp. 1968. A new overlay for plaquing animal viruses. Proc. Soc. Exp. Biol. Med. 129:13-17.
11. Nachkov, D., L. Dumanova, A. Dimitrova, and L. Christophorov. 1973. Phagocytic activity of macrophages from C57BL and CBA mice. B. Ist. Sier. 52:402-404.
12. Osborn, J. E., and D. N. Medearis, Jr. 1967. Suppression of interferon and antibody and multiplication of Newcastle disease virus in cytomegalovirus infected mice. Proc. Soc. Exp. Biol. Med. 124:347-353.
13. Osborn, J. E., and N. T. Shahidi. 1973. Thrombocytopenia in murine cytomegalovirus infection. J. Lab. Clin. Med. 81:53-63.
14. Osborn, J. E., and D. L. Walker. 1968. Enhancement of infectivity of murine cytomegalovirus *in vitro* by centrifugal inoculation. J. Virol. 2:853-858.
15. Osborn, J. E., and D. L. Walker. 1971. Virulence and attenuation of murine cytomegalovirus. Infect. Immunity 3:228-236.
16. Pearsall, N. N., and R. S. Weiser. 1968. The macrophage in allograft immunity. I. Effect of silica as a specific macrophage toxin. J. Reticuloendothel. Soc. 5:107-120.
17. Roberts, J. A. 1964. Growth of virulent and attenuated ectromelia virus in macrophages from normal and ectromelia immune mice. J. Immunol. 92:837-842.
18. Ruebner, B. H., T. Hirano, R. Slusser, J. Osborn, and D. N. Medearis, Jr. 1966. Cytomegalovirus infection: viral ultrastructure with particular reference to the relationship to lysosomes to cytoplasmic inclusions. Amer. J. Pathol. 48:971-989.
19. Sabin, F. R. 1923. Studies of living human blood-cells. Bull. Johns Hopkins Hosp. 34:277-288.
20. Tegtmeyer, P. J., and J. E. Craighead. 1968. Infection of adult mouse macrophages *in vitro* with cytomegalovirus. Proc. Soc. Exp. Biol. Med. 129:690-694.
21. Unanue, E. R. 1972. The role of the macrophage in antigenic stimulation. Advan. Immunol. 15:95-165.
22. Waldron, J. A., R. G. Horn, and A. S. Rosenthal. 1973. Antigen-induced proliferation of guinea pig lymphocytes *in vitro*. Obligatory role of macrophages in the recognition of antigen by immune T-lymphocytes. J. Immunol. 111:58-64.
23. Zisman, B., A. S. Hirsch, and A. C. Allison. 1970. Selective effects of anti-macrophage serum, silica and anti-lymphocyte serum on pathogenesis of Herpes virus infection of young mice. J. Immunol. 104:1155-1159.

THE JOURNAL

OF

IMMUNOLOGY

VOLUME 85

BALTIMORE, MD.

1960

BLOOD CLEARANCE OF P_{32}-LABELED VESICULAR STOMATITIS AND NEWCASTLE DISEASE VIRUSES BY THE RETICULOENDOTHELIAL SYSTEM IN MICE[1]

K. T. BRUNNER, D. HUREZ, R. T. McCLUSKEY AND B. BENACERRAF

From the Department of Pathology, New York University College of Medicine, New York, New York

Received for publication November 13, 1959

The phagocytic function of the reticuloendothelial cells of the liver and spleen has been extensively investigated with the help of colloidal suspensions injected intravenously (1, 2). The rate of clearance of particles of homogenous size follows an exponential function of the time, and most of the material phagocytized is recovered in the liver Kupffer cells (2). The efficiency of splanchnic clearance of such particles is very great, in the order of 80–90%, if the blood concentration is kept below a critical level (3, 4). For doses of particles above this critical concentration, the number of particles is in excess of the phagocytic capacity of the cells and the rate of clearance becomes inversely proportional to the injected dose illustrating the saturating effect of phagocytized particles on the reticuloendothelial system (RES) (2, 4).

The RES has been found also to phagocytize avidly denatured proteins (4) and antigen antibody complexes (5) according to the same criteria that govern phagocytosis of particulate suspensions.

Several studies have also been made of the blood clearance of bacteria by the RES (6, 7). Some Gram-positive bacteria appear to be phagocytized by liver Kupffer cells with a high degree of efficiency in the absence of specific antibody (8). The clearance of Gram-negative bacteria from the blood by the RES is a much more complex process than the clearance of colloidal particles, as the extent of opsonization by antibody and complement affects the efficiency of clearance by the liver and spleen (6, 7, 9).

Limited information is available concerning the phagocytosis of virus particles by the cells of RES. In view of their size and colloidal characteristics, virus particles might be expected to be efficiently cleared from the blood by the liver Kupffer cells. When tobacco mosaic virus (TMV) labeled with C_{14} (10, 11) or P_{32} (12) is injected intravenously in mice, it is found to be selectively concentrated in the liver Kupffer cells. Similarly, bacteriophage T_2 (13) is also selectively concentrated after intravenous injection in the liver and spleen of mice and dogs.

In this study the kinetics of blood clearance of two P_{32}-labeled viruses, vesicular stomatitis (VSV) and Newcastle disease virus (NDV), by the cells of the RES have been investigated in mice. These viruses were selected because of their small size and, in the case of NDV, because its hemagglutinating properties allowed an efficient purification of the labeled virus (14). It was found that these viruses are phagocytized by liver Kupffer cells with a high degree of efficiency. RES blockage slows down markedly this process whereas specific antibody accelerates significantly the clearance of viruses from the blood.

MATERIAL AND METHODS

Preparation of labeled virus suspensions

Vesicular stomatitis virus. The virus was grown on HeLa cells, which had been cultivated for 6 to 8 days in Eagle's medium containing 10% horse serum, which was replaced by a Tris buffered synthetic medium for the experiment. The P_{32} sodium phosphate (Squibb phosphotope) was added to the medium, either simultaneously with or 24 hr before virus inoculation. From 20 to 80 μc of P_{32}/ml of medium were used. Under these conditions, the cells were destroyed in 24 to 48 hr. The culture fluid was then harvested, centrifuged 20 min at 6000 rpm at 4°C to discard cellular debris. An equal volume of saturated ammonium sulfate solution was added in the cold to the supernatant and the pH adjusted to 7.5. A precipitate formed while standing 24 hr

[1] Supported by Research Grant No. E-2094 from the United States Public Health Service.

in the cold. The preparation was centrifuged, the supernatant discarded and the precipitate resuspended in phosphate buffered saline (PBS) in one tenth of the original volume. This preparation was dialyzed in the cold 48 hr against 0.9% saline. It was then centrifuged in the Spinco ultracentrifuge at 40,000 rpm for 1 hr. The pellet was resuspended in the same volume of PBS. This preparation was centrifuged at 6000 rpm for 20 min and the process repeated until the final product was completely clear. The amount of radioactivity which could be specifically attributed to VSV in the final preparation was determined by precipitation with rabbit antiserum prepared against VSV. This antiserum was prepared in rabbits immunized with VSV grown in embryonated eggs. The antiserum was used either undiluted or diluted 1:10, and normal rabbit serum was used as a control. Equal volumes of the purified VSV preparation and rabbit serum were mixed and incubated for 1 hr at 37°C, the mixture was then kept in the cold for 12 hr and centrifuged at 2500 rpm for 15 min. The radioactivity of the precipitates was measured with a Geiger Muller counter and compared to that of the supernatant in order to determine the amount of radioactivity specifically precipitable by the immune serum. This was corrected for the very small amount of activity which was precipitated by the normal, nonimmune rabbit serum under these experimental conditions. Ten preparations were made of P_{32}-labeled VSV. Their content of P_{32}-labeled virus varied from 25 to 66%. Most preparations contained around 40% P_{32}-labeled virus. Two preparations were selected for studies in mice—one unusually rich in labeled virus (containing 66%) and another, more representative of our usual experience with this technique, containing 37% of P_{32} specifically precipitable by the immune serum.

Newcastle disease virus. The NDV virus, strain Beaudette, heat stable variant, which had been kindly given us for these studies by Dr. Allan Granoff, Public Health Research Institute of the City of New York, was used in this study. The virus was cultured on chick embryo liver and lung cell monolayers grown in horse serum yeast extract lactalbumin medium. Preliminary titration, gave infective titers of approximately 10^{-7} for the virus preparations. P_{32} phosphate was added to the cell cultures after 24–48 hr incubation; 10 to 60 μc/ml of culture medium were used. After 24 hr incubation, the cells were inoculated with virus. Then, after 72 hr of further incubation at 37°C visible cellular destruction was about 50%. The culture fluid was harvested and centrifuged at 3500 rpm for 30 min to discard the cellular debris. The supernatant was then centrifuged in the Spinco ultracentrifuge at 30,000 rpm for 30 min. The pellet was resuspended in 10% of the original volume of PBS, pH 6, containing 0.2% gelatin. This preparation was then dialyzed for 24 hr in the cold against 0.9% saline. The radioactive virus suspension was purified according to the technique described by Franklin *et al.* (14), making use of the property of NDV of selective adsorption on and elution from chicken red cells. Fresh chicken erythrocytes were washed three times in PBS, pH 6, containing 0.2% gelatin. Packed red cells were added to the labeled virus suspension to make 10% red cells by volume. After mixing, the virus red cell suspensions were left for 20 min at 4°C for adsorption to take place; the erythrocytes were then centrifuged and washed three times in the cold in PBS at pH 6 (2000 rpm for 5 min). The red cells were then resuspended in the same volume of Tris saline gelatin pH 7.8 and incubated at 37°C in a water bath for 20 min to allow for the elution of the virus to take place. After elution, the red cells were discarded by centrifugation at 2000 rpm for 5 min and the supernatant was again centrifuged for 15 min at 4000 rpm to eliminate any ghost cells. The first supernatant of the red cell adsorption was again treated with chicken erythrocytes and the same process repeated to increase the yield of purified virus. After purification by this technique, the radioactivity of the preparation was considered to represent pure virus.

Animal experiments

White Swiss Webster male and female mice weighing 25–30 g were used. All mice were injected i.v. with 0.1 to 0.25 ml of a solution of heparin containing 1000 USP units/ml to avoid any intravascular clotting. Five minutes later, the virus preparations were injected in the tail veins in a maximal volume of 0.5 ml. A calibrated glass pipet was used to withdraw 0.05-ml blood samples from the retroorbital veinous plexus at various time intervals after injection. The blood

samples were spread on filter paper, cemented on glass slides and the radioactivity measured with a Geiger Muller counter, keeping the geometry constant. In the case of NDV, some animals were injected i.v. 5 hr previously with 0.25 ml of Thorotrast (thorium dioxide, 25% by volume, Testagar, Detroit). Other mice were injected with 0.5 ml of anti-NDV serum before the i.v. injection of the virus. (This serum was prepared by Dr. Granoff in sheep against NDV, C strain, and kindly given to us for this experiment.) The animals were sacrificed generally between 15 and 30 min after the injection of the labeled virus, and the liver, spleen, kidneys and lungs were analyzed for radioactivity. Their organs were digested in 10% NaOH in a boiling water bath. One-tenth milliliter of the digestion mixtures were then spread on filter papers cemented on glass slides and the radioactivity measured as above and related to the amount of radioactivity injected. Livers of mice injected with NDV were fixed in formalin and microautoradiographs were made using Kodak, Ltd. AR-10 film stripping.

RESULTS

The results of experiments performed on three mice injected with a P_{32}-labeled VSV preparation, which contained 66% of radioactivity specifically precipitable by immune serum, are presented in Figure. 1. The clearance curve represents the mean value of three experiments. The radioactivity disappeared from the blood at a very rapid rate. It decreased according to an exponential function of time, K = 0.380, for the first 3 min and until only 8% of the injected radioactivity remained in the blood. Then, a second phase of slower clearance was observed. Analysis of the organs revealed that around 70% of the radioactivity was concentrated in the liver and around 9% in the lungs. The speed of clearance of 90% of the preparation indicates that the efficiency of removal by the liver is of the same order of magnitude as that reported for efficiently cleared particles, such as chromium phosphate or denatured proteins, in mice (3, 4). In Figure 2, the results of experiments performed with a preparation containing only 37% precipitable radioactive virus are presented. One curve shows the kinetics of blood clearance of mice injected with such a preparation and another curve the results obtained when the supernatant from the precipitation of the labeled virus with antiserum is injected. The clearance of the purified virus again was quite rapid, but already began to lose its exponential character at the level of 25 to 30% of the initial blood concentration. Fifty-six per cent of the radioactivity was recovered in the liver. When the supernatant, which does not contain labeled virus, was injected, the clearance was much slower, and a considerably larger level of radioactivity remained in the circulation at the end of 20 min. The amount recovered in the liver also was much smaller, only 21%.

From this experiment, it can be seen that from a preparation poorer in virus content, VSV is

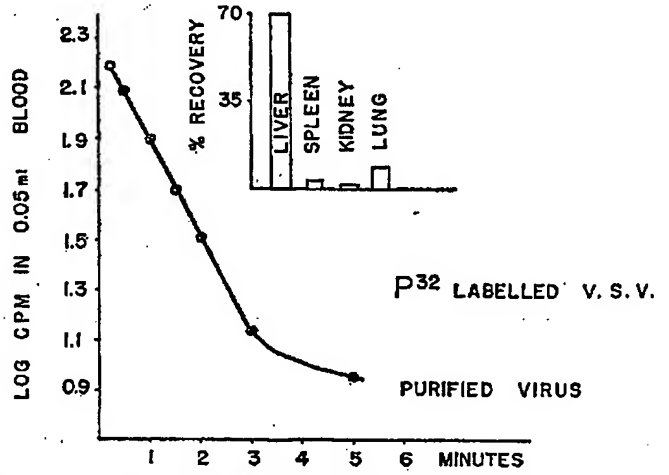

Figure 1. Kinetics of blood clearance of P_{32} labeled VSV injected intravenously in mice (66% precipitable by specific immune serum). Recovery of radioactivity in various organs 15 min after injection.

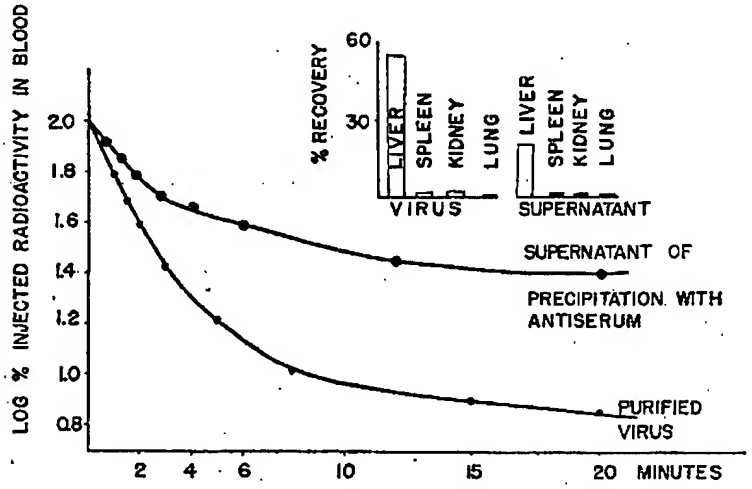

Figure 2. Kinetics of blood clearance of P_{32} labeled VSV injected intravenously in mice (37% precipitable by specific immune serum) and of the supernatant of precipitation with immune serum. Recovery of radioactivity in various organs 20 min after injection.

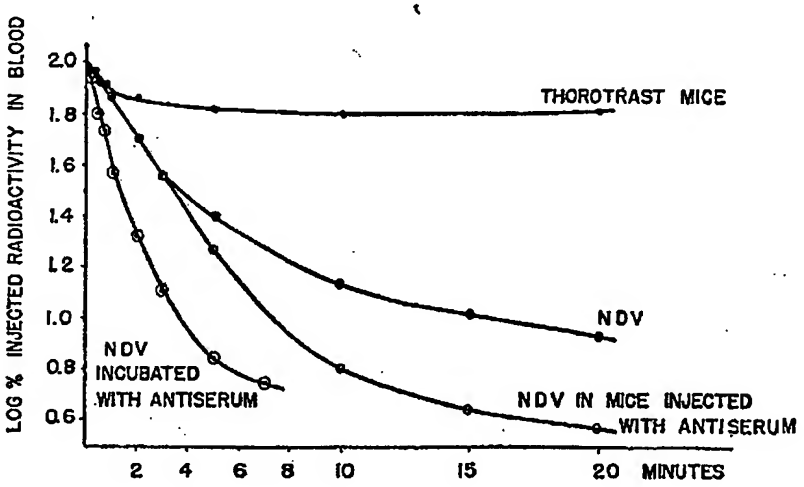

Figure 3. Kinetics of blood clearance of P_{32} labeled NDV injected intravenously in mice. Effect of Thorotrast blockade, of incubation with specific antiserum and of previous injection of specific antiserum before the virus injection.

still removed efficiently by the liver Kupffer cells. We can also conclude that some other cellular material from HeLa cells, which contained P_{32} and was isolated with the virus because of similar physicochemical characteristics, is also phagocytized by the RES.

The results of blood clearance of P_{32}-labeled NDV are presented in Figure 3. Each curve represents the average values of several mice: NDV alone, six mice; NDV in mice injected previously with antiserum, five mice; NDV in Thorotrast treated mice, two animals; NDV incubated with antiserum, two mice.

As in the case of VSV, the blood clearance of P_{32} labeled NDV was very rapid, but reveals an inhomogeneity in the material. The blood clearance was almost completely blocked in mice previously injected with Thorotrast. In mice previously injected with anti-NDV serum, the initial speed of clearance was not faster than that observed in mice injected with virus alone. However, the clearance remained rapid

TABLE I

*Distribution of radioactivity among various organs of mice injected intravenously with P_{32} labeled NDV and previously treated with Thorotrast or with specific antiserum**

Animals	Liver	Spleen	Kidney	Lungs
8 NDV alone	56 (47–65)	1.8	2.4	6.2
3 Thorotrast + NDV	26.3 (21–34)	4.2	3.8	19.7 (17–24)
3 NDV incubated with antibody	66 (60–72)	1.2	0.6	0.4
5 NDV in mice injected with antibody	58.6 (53–62)	2	1.1	1

* Values refer to percentage of injected radioactivity.

for a longer period of time and significantly lower blood concentrations were observed at 15 to 20 min. When NDV virus was incubated with antiserum for 30 min, the rate of clearance was much more rapid from the start and approached the maximal clearance rate that can be expected for material removed by the liver Kupffer cells with maximal efficiency (K = 0.35). After 5 min, the speed of clearance decreased in the case of this preparation also, showing that all the preparation was not treated in the same way by the phagocytic cells.

The results of analysis of the organs injected with P_{32} labeled NDV are presented in Table I. They agree with the results of the blood clearances. All animals receiving either NDV or NDV with antibody had more than 50% of the injected radioactivity in their livers when sacrificed; the highest values were observed in animals injected with NDV incubated with antibody. The mice which received Thorotrast and which had, when sacrificed, over 60% of the injected radioactivity in their circulation, showed a greatly decreased liver uptake and a high concentration of virus in the lung, part of it being accounted for by the blood these organs contained.

Figure 4 represents a microautoradiograph of the liver of a mouse injected with P_{32} labeled NDV, showing the concentration of the radioactivity in a Kupffer cell. Several such Kupffer cells could be seen in the section; however, many Kupffer cells did not show radioactivity indicating that although the amount of virus

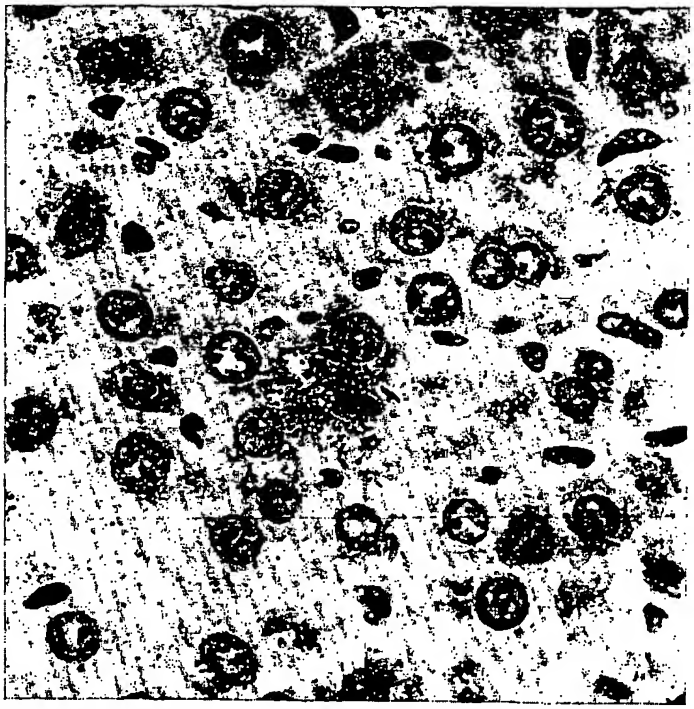

Figure 4. Microautoradiography of the liver of a mouse injected intravenously with P_{32} labeled NDV and sacrificed 30 min later. Magnification, × 800.

injected was high as far as infective dosage is concerned, it was very small in terms of the capacity of the clearance mechanism. This was also confirmed by the fact that identical clearance curves were observed when the amount of P_{32}-labeled virus injected into mice was decreased or increased by a factor of 2.

DISCUSSION

P_{32}-labeled VSV and NDV have been shown to be cleared very efficiently by the RES when injected into mice. The viruses were found to be highly concentrated in the liver and, in the case of NDV, it was demonstrated to be within Kupffer cells by autohistoradiography. Although the method of preparation and purification of P_{32} labeled VSV did not produce a preparation that was more than 66% pure virus, the amount recovered in the liver and the rapid clearance shows that the study of the radioactivity in the blood and in the organs is indeed a true indication of the fate of the virus particles. This problem did not present itself in the case of NDV which had been purified by adsorption-elution on chicken erythrocytes. With both virus preparations, whereas in the first stages the greatest part of the radioactivity disappeared with a first order rate, there was always a residual radioactivity which tended to circulate for a longer period of time. The reason for this persisting activity is not clear and may be due to smaller viral particles or less phagocytizable particles. Persisting circulating bacteria have also been observed during the clearance of bacterial suspensions from the blood by the RES. The efficiency with which most of the virus was removed from the blood by the liver Kupffer cells in the first stage was very high especially for VSV and NDV incubated with antiserum. The rate of clearance in both cases was of the order of magnitude observed for particles cleared with the maximum degree of efficiency by liver Kupffer cells (3, 4). As expected, a blockade of the phagocytic function of the RES by Thorotrast was very efficient in decreasing the rate of clearance of NDV in mice; only a small percentage of the injected radioactivity was then found in liver Kupffer cells. The effect of specific anti-NDV serum was, however, more difficult to interpret. Incubation of the virus suspension with the antiserum in vitro for ½ hr did not result in visible flocculation. Yet, the rate of clearance from the blood was significantly faster than that observed with NDV alone. It is possible that antibodies caused larger aggregates of viruses. Larger aggregates are known to be phagocytized more efficiently by the reticuloendothelial cells than smaller particles (4). When antibody is injected into the mice previous to the virus, the rate of clearance is not immediately increased, but ultimately NDV is cleared from the blood more efficiently than without antibody, since the level of blood radioactivity is significantly lower at 20 min.

Although VSV and NDV are noninfectious for mice, clearance of viruses from their blood was used as a model to study the behavior of virus particles of that size. The amount of virus injected, although very small compared to the clearance capacity of the RES, was very large in term of infective dose.

These experiments illustrate the role which the phagocytic system may play in viremia and a possible effect of antibodies in this defense mechanism.

Although adsorption onto and penetration of susceptible cells by animal viruses is a highly selective and presumably specific process, the virus particles are treated by the macrophages of the RES like other colloidal particles susceptible to be phagocytized.

SUMMARY

Vesicular stomatitis virus (VSV) and Newcastle disease virus (NDV) were grown with P_{32}-containing media. P_{32}-labeled VSV was purified by ammonium sulfate precipitation and differential centrifugation, and NDV by the adsorption-elution technique with erythrocytes. Both virus preparations were shown to be cleared from the blood by the reticuloendothelial cells of the liver when injected intravenously. In the case of NDV, it was observed that previous blockade with Thorotrast slowed the rate of clearance of the virus, whereas treatment with specific antiserum increased the rate of clearance significantly.

REFERENCES

1. BIOZZI, G., BENACERRAF, B. AND HALPERN, B. N., Brit. J. Exper. Path., 34: 441, 1953.
2. BENACERRAF, B., BIOZZI, G., HALPERN, B. N. AND STIFFEL, C., *The Physiology of the Reticulo-endothelial System*, p. 52, Oxford Blackwell Scientific Publications, 1957.

3. Dobson, E. L. and Jones, M. B., Acta med. scandinav., 144(Suppl.): 273, 1952.
4. Benacerraf, B., Biozzi, G., Halpern, B. N. and Mouton, D., Brit. J. Exper. Path., 38: 35, 1957.
5. Benacerraf, B., Sebestyen, M. and Cooper, N. S., J. Immunol., 82: 131, 1959.
6. Benacerraf, B., Sebestyen M. and Schlossman, S., J. Exper. Med., 110: 27, 1959.
7. Howard, G. J. and Wardlaw, A. C., Immunology, 1: 338, 1958.
8. Wardlaw, A. C. and Howard, J. G., Brit. J. Exper. Path., 40: 113, 1959.
9. Benacerraf, B. and Miescher, P., Unpublished data.
10. Gavosto, F. and Ficq, A., Nature, 172: 406, 1953.
11. Gavosto, F. and Ficq, A., Ann. Pasteur Inst., 86: 301, 1954.
12. Erickson, J. D., Hensley, T. J., Fields, M. and Libby, R. L., J. Immunol., 78: 94, 1957.
13. Keller, R. and Zatzman, M. L., J. Immunol., 83: 167, 1959.
14. Franklin, R., Rubin, H. and Davis, C. A., Virology, 3: 96, 1957.

ARTICLE doi:10.1016/j.ymthe.2004.09.012

Kupffer Cells and Not Liver Sinusoidal Endothelial Cells Prevent Lentiviral Transduction of Hepatocytes

Niek P. van Til,[1,*] David M. Markusic,[1] Roos van der Rijt,[1] Cindy Kunne,[1] Johan K. Hiralall,[1] Heleen Vreeling,[2] Wilma M. Frederiks,[2] Ronald P.J. Oude-Elferink,[1] and Jurgen Seppen[1]

[1]*AMC Liver Center, S1-172, Meibergdreef 69, 1105 BK Amsterdam, The Netherlands*
[2]*Department of Cell Biology and Histology, Academic Medical Center, Amsterdam, The Netherlands*

**To whom correspondence and reprint requests should be addressed. Fax: +31205669190. E-mail: n.p.vantil@amc.uva.nl.*

Available online 27 October 2004

Lentiviral vectors can stably transduce dividing and nondividing cells *in vivo* and are best suited to long-term correction of inherited liver diseases. Intraportal administration of lentiviral vectors expressing green fluorescent protein (Lenti-GFP) in mice resulted in a higher transduction of nonparenchymal cells than hepatocytes (7.32 ± 3.66% vs 0.22 ± 0.08%, respectively). Therefore, various treatments were explored to increase lentiviral transduction of hepatocytes. Lenti-GFP was injected into the common bile duct, which led to transduction of biliary epithelium and hepatocytes at low efficiency. Transient removal of the sinusoidal endothelial cell layer by cyclophosphamide to increase accessibility to hepatocytes did not improve hepatocyte transduction (0.42 ± 0.36%). Inhibition of Kupffer cell function by gadolinium chloride led to a significant decrease in GFP-positive nonparenchymal cells (2.15 ± 3.14%) and a sevenfold increase in GFP-positive hepatocytes compared to nonpretreated mice (1.48 ± 2.01%). These findings suggest that sinusoidal endothelial cells do not significantly limit lentiviral transduction of hepatocytes, while Kupffer cells sequester lentiviral particles thereby preventing hepatocyte transduction. Therefore, the use of agents that inhibit Kupffer cell function may be important for lentiviral vector treatment of liver disease.

Key Words: lentiviral vectors, gene transfer, GFP, liver, hepatocytes, Kupffer cells, sinusoidal endothelial cells

INTRODUCTION

Lentiviral vectors are able to deliver genes into a wide variety of both dividing and nondividing cell types *in vivo*, such as muscle, retina, neurons, pancreatic, and liver cells [1–5]. This property makes them an attractive tool for *in vivo* treatment of genetic liver disorders. Unfortunately, when lentiviral vectors are injected into the circulation, the majority of cells that are transduced in the liver are of nonparenchymal origin, notably endothelial cells and Kupffer cells [6–9]. Since many inherited liver diseases have an impaired hepatocyte function, improved lentiviral particle delivery to hepatocytes is a requirement.

Recently it has been shown that, *in vitro*, primary hepatocytes are efficiently transduced by lentiviral vectors [10–12]. However, *in vivo* transduction is much less efficient. We therefore investigated if there is a barrier that prevents efficient hepatocyte transduction *in vivo*. Several factors may cause preferential transduction of nonparenchymal cells.

The sinusoidal endothelium forms a barrier between the blood and the hepatocytes and may hamper passage of viral particles to the hepatocytes. Cyclophosphamide is an alkylating agent that has been used in cancer therapy [13] and also inhibits tumor growth by damaging the tumor vasculature [14]. Endothelial cells are relatively susceptible to cyclophosphamide-induced toxicity [15] and the drug has been shown to disrupt the endothelial cell layer in the sinusoids of the liver [16,17].

The liver is able to clear viruses such as vesicular stomatitis virus [18], simian immunodeficiency virus [19], and adenoviruses [20] efficiently from the bloodstream. In the liver, specialized macrophages called Kupffer cells are located inside the sinusoids and play

1525-0016/$30.00

an important role in the clearance of these viruses. Vesicular stomatitis virus G-protein (VSV-G)-pseudotyped lentiviral vectors may also be efficiently cleared from the circulation by Kupffer cells. It has been shown that agents such as gadolinium chloride ($GdCl_3$) can block phagocytosis and eliminate macrophages transiently [21] and can increase adenoviral transduction [22]. Selective depletion of these cells led to a higher and prolonged transgene expression after transduction with adenoviral vectors [23].

In addition to the ability of Kupffer cells to scavenge viral particles, Kupffer cells are also transduced themselves by VSV-G-pseudotyped lentiviral vectors [7,9].

The most common routes of administration to target lentiviral vectors to the liver are the portal vein and tail vein [9,24–27]. Adenoviral vector administration has been performed via the common bile duct in rats and resulted in efficient transgene expression in hepatocytes, but not in biliary epithelial cells [28]. In addition, it may be possible to administer lentiviral vectors via the common bile duct to avoid many of the above-mentioned barriers in sinusoids and to target viral particles exclusively to the liver. A drawback of this approach is the potential toxic effect of bile on the lipid-enveloped lentiviral particles.

The objective of this study was to improve lentiviral transduction of hepatocytes by exploring an alternate route of administration, by disruption of the sinusoidal endothelial cell layer, and by depletion of Kupffer cells. We show that by intraportal vein delivery of lentiviral vectors the majority of transduced liver cells are of nonparenchymal origin. Administration of lentiviral vectors via the common bile duct led to exclusive transduction of bile duct epithelium and some hepatocytes, but at low efficiency. Mild disruption of liver sinusoidal endothelial cells did not lead to an increase in hepatocyte transduction, while Kupffer cell depletion led to a significant increase in the transduction efficiency of hepatocytes.

RESULTS

Lentiviral Transduction of the Liver by Bile Duct Administration

We infused animals with 0.5×10^8 HeLa transducing units (HTU) into the bile duct, which led to GFP-positive epithelium throughout the biliary tract (Fig. 1A). The total number of GFP-positive cells in these livers (Fig. 1B) was much lower than in the animals injected intraportally. Only a small part of the GFP-positive cells were hepatocytes, most of them were localized in the periportal areas (Fig. 1B). No endothelial cells or Kupffer cells were transduced. No splenocytes were GFP positive (data not shown).

We found that incubation of bile with lentivirus resulted in decreased transduction of HeLa cells (data not shown). The relatively poor transduction of liver cells *in vivo* may be caused by inactivation of the lipid-enveloped lentiviral particles by the strong detergent action of bile, although we chose conditions to minimize the toxicity of bile, such as depletion of bile for 1 h and dissolving the lentiviral preparations in a relatively large volume (300 μl) to dilute residual bile in the biliary tract.

Lentiviral Transduction of Liver by Portal Vein Injection

In mice intraportally injected with 0.5×10^8 HTU, we observed transduction of hepatocytes and nonparenchymal cells (Fig. 2A). The total number of hepatocytes transduced in the liver was $3.16 \pm 1.11/mm^2$ ($n = 7$) 1 week after injection (Table 1). This represents about $0.22 \pm 0.08\%$ of the total hepatocyte population. The number of GFP-positive nonparenchymal cells was more than 20 times higher ($70.27 \pm 35.11/mm^2$, $n = 7$), which is comparable with other studies [6]. GFP-positive splenocytes were observed (data not shown).

Liver Sinusoidal Endothelial Cell Disruption

Animals treated with cyclophosphamide were analyzed for damage of sinusoidal endothelial cells with electron microscopy. Fig. 3 shows the variable degree of endothelial cell disruption in a cyclophosphamide-treated animal compared to a control animal. The endothelial lining is not intact at some places, whereas at other places the space of Disse (the area between the endothelial cells and hepatocytes) is dramatically enlarged. Other than the endothelial cell disruption, the morphology of the liver was normal.

Effect of Cyclophosphamide on Lentiviral Transduction *in Vitro*

Transduction of Hepa 1-6 mouse hepatoma cells was not affected by cyclophosphamide *in vitro* (data not shown). Cells incubated with cyclophosphamide for 24 h and subsequently incubated with lentivirus were transduced as efficiently as untreated cells. Therefore, cyclophosphamide did not seem to have a direct deleterious effect on lentiviral transduction.

Lentiviral Transduction of Liver by Portal Vein Injection after Cyclophosphamide Treatment

Upon treatment of mice with cyclophosphamide, the number of transduced hepatocytes and nonparenchymal cells did not change significantly (6.09 ± 5.19 and $95.12 \pm 71.76/mm^2$, respectively) compared to nonpretreated animals (Table 1). Additionally, there was no significant difference in the percentage of GFP-positive hepatocytes of the total number of GFP-positive cells in cyclophosphamide-treated animals ($5.19 \pm 2.73\%$) compared to nonpretreated animals ($5.27 \pm 2.78\%$, Table 1). GFP-positive splenocytes were observed (data not shown).

doi:10.1016/j.ymthe.2004.09.012

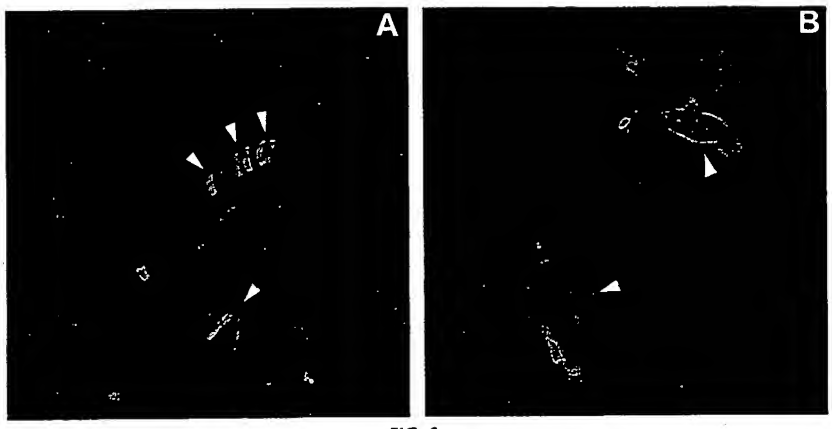

FIG. 1.

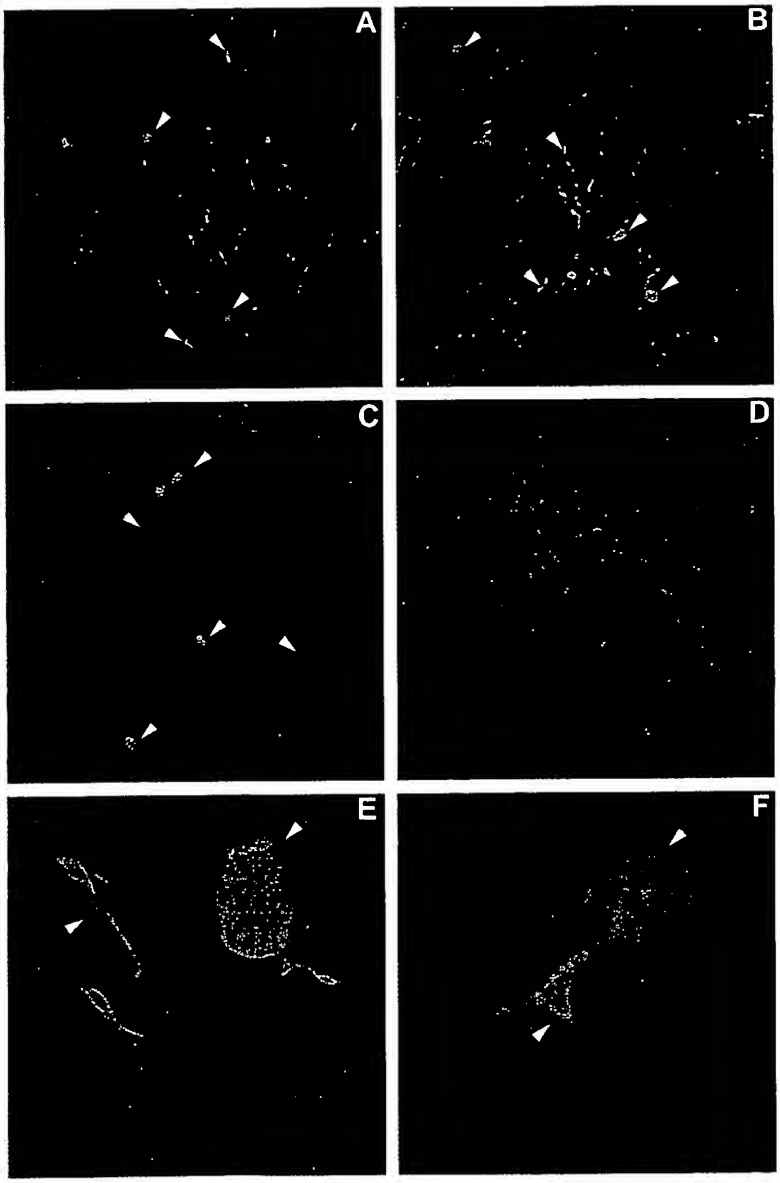

FIG. 2.

TABLE 1: GFP-positive cells in liver sections

	No pretreatment ($n = 7$)	Cyclophosphamide ($n = 5$)	$GdCl_3$ ($n = 7$)
GFP-positive hepatocytes[a]	3.16 ± 1.11	6.09 ± 5.18	21.43 ± 28.85*
GFP-positive nonparenchymal cells[a]	70.27 ± 35.11	95.12 ± 71.76	20.65 ± 30.13*
Percentage GFP-positive hepatocytes[b]	5.27 ± 2.78%	5.19 ± 2.73%	51.01 ± 16.12%**

GFP-positive cells were counted in liver sections of animals injected intraportally with Lenti-GFP. Mean values are presented ± SD.
[a] GFP-positive cells per mm^2.
[b] Percentage of GFP-positive hepatocytes of total number of GFP-positive cells in the liver.
* Significant difference compared to nonpretreated group: $P < 0.05$.
** Significant difference compared to nonpretreated group: $P \leq 0.001$.

Lentiviral Transduction of Liver by Portal Vein Injection after Kupffer Cell Blockage of Phagocytosis

It has been shown that the majority of lentivirally transduced cells in the liver may be Kupffer cells [7]. We also found that most of the GFP-positive nonparenchymal cells were positive for the Kupffer cell marker F4/80 (Fig. 4). Therefore we ablated Kupffer cells before lentiviral injection to determine the effect of this treatment on hepatocyte transduction. We performed transient ablation of Kupffer cells by two injections of $GdCl_3$ (10 mg/kg) at 30 and 6 h before transduction [21].

We assessed depletion of Kupffer cells by injection of India ink in a parallel group of mice that was treated identically. In control animals there was a clear accumulation of black pigment in the Kupffer cells localized in the sinusoids, while this was largely absent in $GdCl_3$-treated mice (Fig. 5).

Analysis of liver sections revealed that Kupffer cell depletion increased the number of GFP-positive hepatocytes approximately seven times (21.43 ± 28.85/mm^2, $n = 7$, $P < 0.05$) compared to animals with no pretreatment (3.16 ± 1.11/mm^2). Kupffer cell depletion reduced the number of nonparenchymal cell transduction by about 70% to 20.65 ± 30.13/mm^2 ($n = 7$, $P < 0.05$). The percentage of GFP-positive hepatocytes of the total number GFP-positive cells significantly increased from 5.27 ± 2.78% in nonpretreated animals to 51.01 ± 16.12% in $GdCl_3$-treated mice ($P \leq 0.001$, Table 1). We also observed GFP-positive splenocytes (data not shown).

Quantitative PCR of Lentiviral Integrations

We analyzed the total number of viral integrations in animals injected with lentivirus by quantitative PCR on genomic DNA isolated from the anterior right lobe of the liver (Table 2). The genomic integration percentage in nonpretreated animals was 10.54 ± 5.34% and there was no significant difference from cyclophosphamide-treated mice (6.22 ± 3.71%). The number of genomic integrations significantly decreased after $GdCl_3$ treatment (2.40 ± 1.80%, $P = 0.003$, Table 2). These data confirm our microscopic findings.

Alanine Aminotransferase Activity after Lentiviral Injections

Intraportal injection of lentivirus caused modest and transient increase in serum alanine aminotransferase (ALT) levels (Table 3) in nonpretreated, cyclophosphamide-treated, and $GdCl_3$-treated animals. However, the rise in ALT was not significant in $GdCl_3$-treated animals. At day 7 ALT levels returned almost back to normal.

DISCUSSION

The main aim of liver-directed gene therapy is to transduce sufficient numbers of hepatocytes, because in nearly all disorders this is the cell type that needs to be corrected. Thus far, in most studies that made use of lentiviral vectors, the route of administration was either the portal vein or the tail vein [9,24–26]. In the present study we wished to optimize hepatocyte transduction. For this purpose we used the third-generation lentiviral vector that we have previously described [10]. Given the fact that the percentage of hepatocytes transduced by this and other lentiviral vectors is low, we tested various treatments to increase targeting to the hepatocyte. We chose to use a dose of 0.5×10^8 HTU to demonstrate the mechanism without saturation of the reticuloendothelial system.

FIG. 1. GFP expression in the liver after bile duct infusion of lentiviral vectors. Fluorescence microscopy of tissue sections of mice injected with 0.5×10^8 HTU lentiviral vectors in the common bile duct. A small number of cells were transduced, consisting of bile duct epithelium (yellow arrowheads) and hepatocytes (white arrowheads). (A) Bile duct. (B) Liver. Both at 20× original magnification.

FIG. 2. GFP expression in the liver after portal vein injection of lentiviral vectors. Fluorescence microscopy of liver sections 1 week after intraportal injection of 0.5×10^8 HTU lentiviral vectors. Hepatocytes (white arrows) and nonparenchymal cells (yellow arrows) in the liver of mice were GFP positive. Nuclei were stained with DAPI. (A) No pretreatment. (B) Cyclophosphamide treatment. (C) $GdCl_3$ treatment. (D) Negative control (no lentivirus). All 10× original magnification. (E, F) No pretreatment, 40× original magnification.

doi:10.1016/j.ymthe.2004.09.012

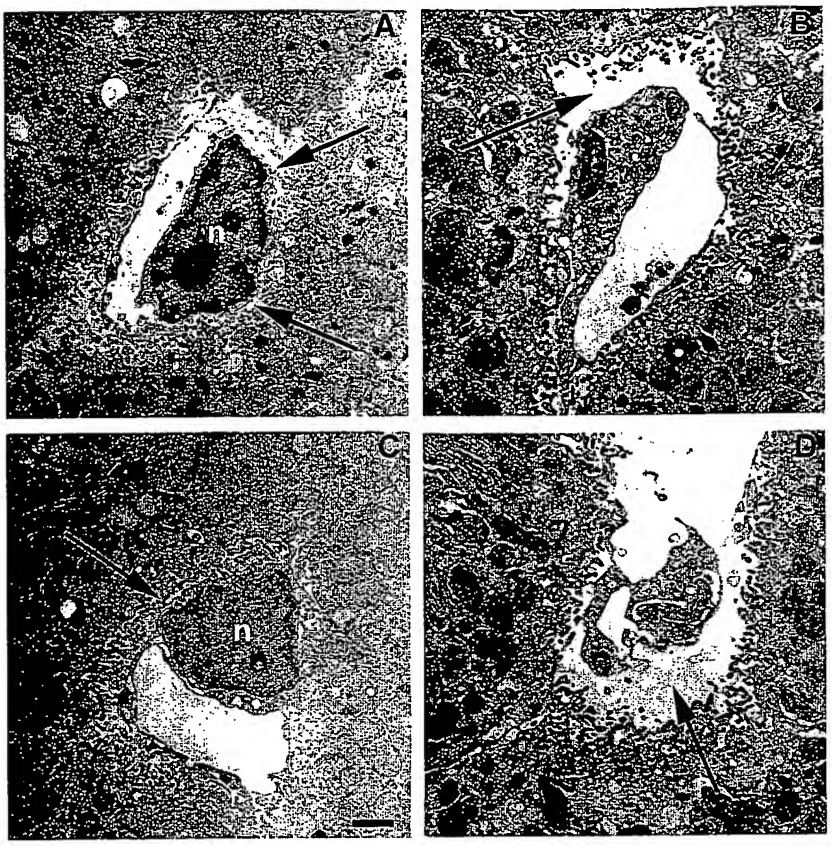

FIG. 3. Electron microscopy of livers of cyclophosphamide-injected animals. (A, C) Control animals. Normal liver morphology: hepatocytes and the fenestrated lining of the sinusoidal endothelial cells are intact. Arrows point to the space of Disse and microvilli of hepatocytes. (B, D) Animals treated with cyclophosphamide show variable degrees of disruption of the endothelial lining. Endothelial cells are detached from the hepatocytes, leading to a widening of the space of Disse. Bar denotes 1 μm.

To reduce Kupffer cell and endothelial cell transduction, we injected virus into the common bile duct, which led to transduction of hepatocytes and also of biliary epithelium. However, overall transduction efficiency by retrograde infusion of lentiviral vector into the biliary tract was low.

Inactivation of lentiviral vectors by bile (data not shown) might play a role in the low transduction efficiency. It could also indicate that the virus did not reach the bile canuliculi, because the majority of GFP-positive hepatocytes were located in portal tracts.

Hence, retrograde perfusion may reduce transduction of Kupffer cells and sinusoidal endothelial cells. In addition, extrahepatic transduction was reduced as well, which was determined by the disappearance of splenocyte transduction compared to animals injected into the portal vein (data not shown), but the efficiency of hepatocyte transduction is too low for therapeutic use.

Viral particles have to travel through the fenestrae of the liver sinusoidal endothelial cells to arrive in the space of Disse, before the particles can enter the hepatocytes. The size of the endothelial fenestrae is variable between 100 and 200 nm [29–32], which may form a physical barrier for HIV-derived lentiviral particles to pass through, because the size of HIV-1 particles has been estimated to be between 120 and 200 nm [33].

Disruption of sinusoidal endothelial cells by cyclophosphamide has been shown to improve grafting of transplanted liver cells [16]. We reasoned that it might similarly improve lentiviral transduction of hepatocytes. However, the effect of disruption of the sinusoidal endothelial lining on hepatocyte transduction was limited. The number of GFP-positive hepatocytes increased, but this was not significant (Table 1) and represented less than 0.5% of the total hepatocyte population. The total number of genomic integrations determined by quantitative PCR only decreased by approximately 30% compared to nonpretreated animals, which confirmed the cell counting (Tables 1 and 2). Our results therefore indicate that the endothelial layer is not a major obstacle to lentiviral hepatocyte transduction.

Kupffer cells are involved in the phagocytosis of foreign particles, such as viruses. $GdCl_3$ has been used in many studies to block Kupffer cell-mediated phagocytosis and deplete these cells transiently [20–22].

Kupffer cells may not only scavenge viruses, but are also highly prone to viral infection [7,9]. Indeed, we

doi:10.1016/j.ymthe.2004.09.012

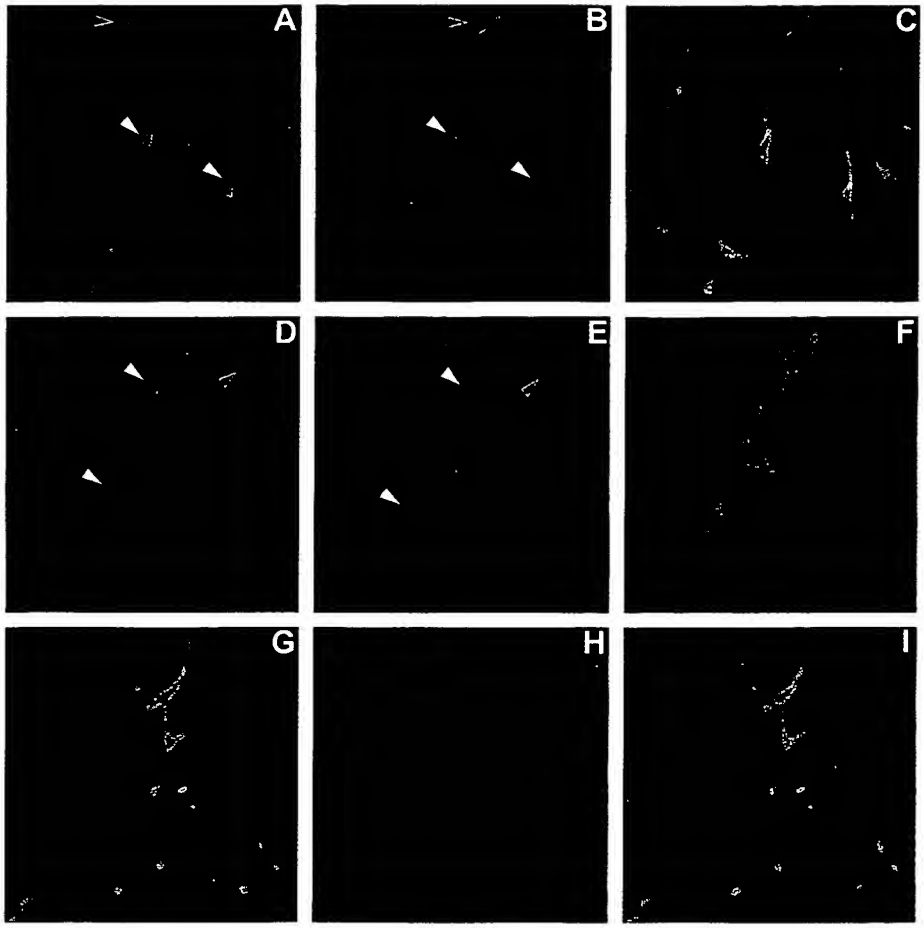

FIG. 4. Kupffer cells and viral transduction after portal vein injection of lentiviral vectors. Demonstration of GFP-positive Kupffer cells by colabeling with the Kupffer cell marker F4/80. Left (A, D, G): GFP expression. Middle (B, E): KC marker expression. (H) Negative control F4/80 staining, secondary antibody only. Right (C, F, I): merge. All 40× original magnification. The majority of GFP-positive cells costained for the KC marker. GFP-positive Kupffer cells (yellow arrowheads). GFP-negative/KC marker-positive cells (red arrowheads).

observed that the majority of GFP-positive nonparenchymal cells were positive for the Kupffer cell marker F4/80.

Injection of $GdCl_3$ led to inactivation of the function of Kupffer cells as shown by histochemical analysis (Fig. 5). Inactivation of Kupffer cells by $GdCl_3$ significantly decreased the transduction percentage of nonparenchymal cells from 7.32 ± 3.66% in nonpretreated mice to 2.15 ± 3.14%, indicating that the majority of nonparenchymal cell transduction was due to Kupffer cell transduction. Simultaneously, the number of transduced hepatocytes increased significantly by a factor of 7, which represents approximately 1.48 ± 2.01% of the total hepatocyte population.

The most straightforward interpretation of these results is that the Kupffer cells scavenge most viral particles before they reach the hepatocytes. Elimination of this scavenger function dramatically increases hepatocyte transduction.

Kupffer cell depletion led to 80% decrease in the number of viral integrations as assessed by quantitative

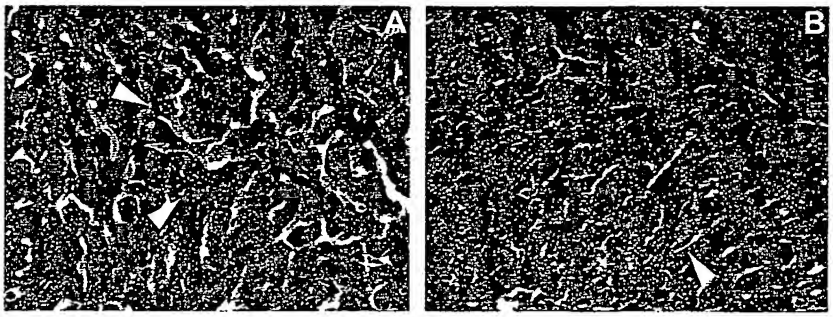

FIG. 5. Kupffer cell depletion by $GdCl_3$ treatment in mice. Histochemistry of ink-injected control and $GdCl_3$-treated mice. In animals treated with $GdCl_3$ the number of Kupffer cells is lower compared to animals without $GdCl_3$. Kupffer cells (white arrowheads). (A) Nonpretreated animal injected with ink. (B) Animal treated with $GdCl_3$ and ink. Both 40× original magnification.

doi:10.1016/j.ymthe.2004.09.012

TABLE 2: Quantitative PCR of genomic DNA

	No pretreatment (n = 8)	Cyclophosphamide (n = 5)	$GdCl_3$ (n = 6)
Proviral integrations	10.54 ± 5.34	6.22 ± 3.71	2.40 ± 1.80*

Number of proviral integrations per 100 genomes in the liver determined by quantitative PCR of genomic DNA.
* Significant difference compared to nonpretreated group: $P = 0.003$.

PCR (Table 2). However, the same treatment reduced the total number of GFP-positive cells by only 40%. Hence, in nonpretreated livers there were more viral integrations than in the Kupffer cell-depleted state. This observation is again in line with the scavenging function of the Kupffer cells. If Kupffer cells function to filter viral particles from blood, they are expected to take up more viral particles per cell and multiple integrations probably occur in these cells. Depletion of the Kupffer cells allows the viral particles to spread over the more numerous hepatocytes.

Kupffer cells are involved in the activation of the innate immune response against adenoviruses, which can lead to early phase hepatotoxicity [22]. The lentiviral vector administrations in our experiments induced mild but significant elevations of ALT in nonpretreated animals and cyclophosphamide-treated animals (Table 3). Our observation that lentivirus administration to Kupffer cell-depleted mice was relatively less toxic than in nonpretreated mice is in line with the reduced liver toxicity after adenovirus administration with $GdCl_3$ treatment [22].

Our results confirm earlier observations that *in vivo* administration of VSV-G-pseudotyped lentivirus can cause a modest but transient hepatotoxicity, with high variability between animals [34], which was also observed in all our treatment groups.

A drawback of the use of lentiviral vectors may be that these vectors could integrate in active cellular genes [35] and activate potential oncogenes. Because the proliferative activity of hepatocytes is approximately about 0.005 to 0.05% *in vivo* [36], the likelihood of tumorigenesis by a single integration is probably very low.

In conclusion, we have shown that Kupffer cells play an important role in limiting lentiviral hepatocyte transduction by sequestration of viral particles. To treat inherited liver diseases in the future, the inclusion of agents that block Kupffer cell activity or even eliminate these cells from the liver prior to gene transfer should be considered.

Materials and Methods

Lentiviral vector production. The lentiviral vector prrlcpptpgkgfppressin containing the hepatitis B virus posttranslational regulatory element, central polypurine tract, and phosphoglycerate kinase promoter driving GFP expression was used as described earlier [10].

Lentiviruses were produced as described by transient transfection of 293T cells using a calcium phosphate method, concentrated by ultracentrifugation, and titrated on HeLa cells [5,37]. Cell lines were grown in Dulbecco's modified Eagle's medium (DMEM) supplemented with 10% fetal bovine serum, 0.5 units/ml penicillin, 0.5 mg/ml streptomycin, and 2 mM L-glutamine.

Lentiviral inactivation by bile. Lentiviral particles were incubated with bile for 30 min at 37°C, followed by transduction of HeLa cells in 2 ml DMEM containing 10 μg/μl DEAE-dextran (Pharmacia). After 5 days, the number of transduced cells was determined by flow cytometry.

Animals, viral injections, and processing of tissues. Wild-type male FVB mice ages 8-12 weeks were used in all studies and fed *ad libitum*. All animal experiments were performed in accordance with the Animal Ethical Committee guidelines at the Academic Medical Center of Amsterdam.

Mice were anesthetized with an intraperitoneal injection of FFM mix (2.5 mg Fluanisone/0.105 mg Fentanyl citrate/1.25 mg Midozalam HCl/kg in H_2O, 7 ml/kg). Under deep anesthesia, the peritoneal cavity was opened and the mice were injected intraportally with a volume of 250 μl containing 0.5×10^8 HTU with a 30-gauge needle at day 0. The animals were sutured and received the analgesic Temgesic (20–30 μl, 0.03 mg/ml) subcutaneously following recovery from FFM.

After a period of 7 days, the mice were killed by *in vivo* fixation. Under deep anesthesia, the peritoneal cavity was opened, a ligature was applied around the anterior right lobe of the liver and tightened, and the lobe was removed and snap frozen in liquid nitrogen and stored at −80°C. Subsequently, the animals were perfused intracardially with 20 ml of phosphate-buffered saline (PBS) and 20 ml of 2% formaldehyde in PBS. After perfusion, the liver and spleen were removed and the liver lobes were fixed in a 4% formaldehyde solution in PBS for 4 h at room temperature.

TABLE 3: Analysis of liver toxicity by measurement of plasma ALT levels

		ALT	
	Normal level	Day 1	Day 7
No pretreatment	41.00 ± 1.73	179.86 ± 260.07*	68.00 ± 70.47
Cyclophosphamide	41.75 ± 7.04	188.25 ± 229.75*	85.25 ± 75.17
$GdCl_3$	39.71 ± 8.52	149.67 ± 195.72	106.71 ± 143.91

ALT levels (U/L) in mice intraportally injected with lentivirus with and without cyclophosphamide or $GdCl_3$ treatment. ALT levels were higher in nonpretreated, cyclophosphamide-treated, and $GdCl_3$-treated animals at day 1 after viral injections. The ALT levels were lower at day 7 compared to day 1. Mean values are presented with SD (n = 4–7).
* Significant difference compared to normal levels: $P < 0.05$.

The tissues were transferred to a 30% sucrose solution at 4°C overnight and subsequently snap frozen in liquid nitrogen and stored at −80°C.

Before cryosectioning, tissue was embedded in Tissue-Tek OCT medium (Bayer). Sections (6 μm) were laid on poly-L-lysine-coated glass slides and enclosed in mounting medium ((20 mg 1,4-diazabicyclo[2.2.2]octane (DABCO, Sigma), 0.1 M Tris/HCl, pH 8.0, in glycerol)/ml) containing 4′,6-diamidino-2-phenylindole (DAPI; Sigma).

Determination of plasma alanine aminotransferase activity. Serum ALT levels were taken as a measure of liver toxicity induced by various treatments [38,39]. Blood was collected by orbital puncture 3 days before lentiviral vector injection, 1 day after injection, and 30 min before the animals were killed at day 7. ALT was measured in plasma by routine clinical chemistry.

Mouse bile duct cannulation and lentiviral transduction. The animals were anesthetized as described above. After opening the peritoneal cavity, the common bile duct was clamped downstream of the gallbladder. Two sutures were placed around the gallbladder and an incision was made in the tip of the gallbladder. A catheter was placed in the common bile duct and one ligature was closed to keep the catheter in place. For 1 h bile was depleted and subsequently 300 μl of 0.5×10^8 HTU in PBS was injected in the catheter, which was then closed for 1 h. after viral transduction, the bile flow was restored by removal of the clamp. The catheter was removed and the gallbladder ligature placed at the start of the operation was closed. finally, the abdomen was closed. After 7 days, the animals were killed and organs were harvested.

Cell count and statistics. GFP-positive cells were counted in sections of the left lobe and median lobe with an inverse microscope (Leica DMRA2; Leica). An independent person randomly numbered the sections and all counting was performed in a blinded fashion. Per animal GFP-positive hepatocytes were counted in five sections of nonoverlapping cell layers. Images of the sections were captured and surface areas were measured by using Leica FW4000 software to determine the number of hepatocytes per square millimeter. The number of hepatocytes/mm^2 was determined in 80 times enlarged fields. This enabled us to determine the percentage of GFP-positive hepatocytes in the liver.

GFP-positive nonparenchymal cells were counted in a 20 times magnification field and were adjusted to nonparenchymal cells per square millimeter. The transduction percentage of nonparenchymal cells was determined by the assumption that hepatocytes represent 60% of the cells in the liver [40].

Statistical analyses were performed using SPSS10.0 software and significant difference was considered if $P < 0.05$ determined by Mann-Whitney U test.

Disruption of the sinusoidal endothelial cell layer. Disruption of sinusoidal endothelium was performed by injecting 200 mg/kg body weight cyclophosphamide in H_2O [16] (Endoxan, Baxter, Utrecht, The Netherlands) intraperitoneally 24 h before lentiviral vector injection.

Effect of cyclophosphamide on lentiviral transduction efficiency in vitro. To determine the effect of cyclophosphamide on lentiviral transduction efficiency Hepa 1–6 mouse hepatoma cells were transduced with lentivirus in a volume of 2 ml medium for 4 h in the presence or absence of cyclophosphamide. We assumed that 0.2 mg/g *in vivo* was equal to 0.2 mg/ml *in vitro*. Cells were incubated with serially diluted cyclophosphamide from 1 to 0 mg/ml. In addition, Hepa 1–6 mouse hepatoma cells were also cultured with cyclophosphamide for 28 h, with subsequent incubation of lentivirus for the last 4 h. Flow cytometry for gfp was performed 5 days later to determine the transduction efficiency.

Kupffer cell blockage of phagocytosis. For Kupffer cell blockage of phagocytosis and partial depletion from the liver, mice were injected intravenously with 10 mg/kg gadolinium chloride (5.65 mg/ml gadolinium chloride hexahydrate containing 4 mg/ml gadolinium chloride; Sigma) per body weight at 30 and 6 h [21] prior to lentiviral vector injection.

To determine Kupffer cell phagocytotic activity and distribution of Kupffer cells in the liver animals were injected intravenously via the tail vein with india ink (0.08 ml per 100 g body weight; Pelikan, Germany) [21]. Thirty minutes after injection, the animals were perfused with PBS and 2% formaldehyde in PBS; then, the liver was removed and incubated overnight in 4% formaldehyde in PBS and transferred to 70% ethanol. Liver tissue was dehydrated with ethanol and embedded in Paraplast Plus (Kendall). Sections (7 μm) were made and stained with hematoxylin and azophloxine.

Immunostaining. In vivo formaldehyde-fixed, sucrose-incubated, and subsequently snap-frozen material was used. Sections of 6 μm were made and kept at −20°C before use. Sections were washed in PBS for 15 min and blocked in PBS/Tween 20 (0.05%) with 10% mouse serum for 1 h. Subsequently, primary antibody was incubated for 1 h at room temperature. For Kupffer cell staining, sections were incubated with rat anti-mouse F4/80 antigen (1:10; Serotec). After primary incubation, sections were washed in PBS/Tween 0.05% for 15 min, followed by incubation with Texas red-conjugated goat anti-rat antibody (1:500; Rockland Immunochemicals) for another hour at room temperature. Then the sections were washed for another 15 min in PBS and embedded in mounting medium containing DAPI.

Electron microscopy. To determine the effect of cyclophosphamide on sinusoidal endothelial cells, liver tissue was prepared for electron microscopy as previously described [41]. In short, after treatment with cyclophosphamide as described above, the animal was perfused with PBS, followed by 2% paraformaldehyde in PBS. Small liver pieces (<1 mm^3) were made and fixed in a mixture of 1% (wt/vol) glutaraldehyde and 4% (wt/vol) formaldehyde in 100 mmol/L sodium cacodylate buffer (pH 7.4) and stored at 4°C for further use.

Genomic DNA isolation and quantitative PCR. Genomic DNA was isolated using the DNeasy tissue kit (Qiagen) according to the manufacturer's protocol. Quantitative PCR was performed in a Lightcycler apparatus (Roche) using Lightcycler Faststart DNA Master SYBR Green I (Roche) with 2 mM $MgCl_2$ according to the manufacturer's protocol. The following primer set was used to amplify a 274-bp product: HIV-U3 forward primer, 5′-CTGGAAGGGCTAATTCACTC-3′, and HIV PSI reverse primer, 5′-GGTTTCCCTTTCGCTTTCAG-3′. The primers amplify the integrated provirus only and not the transfer plasmid, thus reducing the risk of contamination. For every reaction 50 ng of genomic DNA was used. Three different PCRs were performed and averaged for every individual sample.

PCR conditions were 95°C for 10 min and then 40 cycles as follows: 95°C for 1 s, 62°C for 7 s, 72°C for 30 s, and 82°C for 1 s. Negative control sample was PCR amplification of animals not injected with lentivirus and amplification of PCR reagents without template. To determine the number of integrations per genome, Hepa 1–6 mouse hepatoma cells (ATCC, CRL-1830) were transduced at a low multiplicity of infection (14.8% GFP positive) to have approximately one integration per transduced cell. These cells were sorted to obtain a 100% GFP-positive population. DNA was extracted and diluted with negative DNA to make a standard curve ranging from 100 to 1% genomic integrations.

ACKNOWLEDGMENTS

We thank Didier Trono and Romain Zufferey (University of Geneva, Geneva, Switzerland) for providing us with the third-generation lentiviral vector system. We thank Jan Peeterse (Academic Medical Center, Amsterdam) for his assistance with editing of pictures. This research was made possible by a grant from NWO, 016.026.012, to J. Seppen.

RECEIVED FOR PUBLICATION AUGUST 5, 2004; ACCEPTED SEPTEMBER 17, 2004.

REFERENCES

1. Zufferey, R., Nagy, D., Mandel, R. J., Naldini, L., and Trono, D. (1997). Multiply attenuated lentiviral vector achieves efficient gene delivery in vivo. *Nat. Biotechnol.* 15: 871–875.
2. Zufferey, R., *et al.* (1998). Self-inactivating lentivirus vector for safe and efficient in vivo gene delivery. *J. Virol.* 72: 9873–9880.
3. Kafri, T., Blomer, U., Peterson, D. A., Gage, F. H., and Verma, I. M. (1997).

doi:10.1016/j.ymthe.2004.09.012

Sustained expression of genes delivered directly into liver and muscle by lentiviral vectors. *Nat. Genet.* 17: 314–317.
4. Naldini, L., *et al.* (1996). In vivo gene delivery and stable transduction of nondividing cells by a lentiviral vector. *Science* 272: 263–267.
5. Seppen, J., van der Rijt, R., Looije, N., van Til, N. P., Lamers, W. H., and Oude Elferink, R. P. (2003). Long-term correction of bilirubin UDPglucuronyltransferase deficiency in rats by in utero lentiviral gene transfer. *Mol. Ther.* 8: 593–599.
6. Pfeifer, A., *et al.* (2001). Transduction of liver cells by lentiviral vectors: analysis in living animals by fluorescence imaging. *Mol. Ther.* 3: 319–322.
7. Kang, Y., *et al.* (2002). In vivo gene transfer using a nonprimate lentiviral vector pseudotyped with Ross River virus glycoproteins. *J. Virol.* 76: 9378–9388.
8. De Palma, M., Venneri, M. A., and Naldini, L. (2003). In vivo targeting of tumor endothelial cells by systemic delivery of lentiviral vectors. *Hum. Gene Ther.* 14: 1193–1206.
9. Follenzi, A., Sabatino, G., Lombardo, A., Boccaccio, C., and Naldini, L. (2002). Efficient gene delivery and targeted expression to hepatocytes in vivo by improved lentiviral vectors. *Hum. Gene Ther.* 13: 243–260.
10. Seppen, J., Rijnberg, M., Cooreman, M. P., and Oude Elferink R. P. (2002). Lentiviral vectors for efficient transduction of isolated primary quiescent hepatocytes. *J. Hepatol.* 36: 459–465.
11. Nguyen, T. H., Oberholzer, J., Birraux, J., Majno, P., Morel, P., and Trono, D. (2002). Highly efficient lentiviral vector-mediated transduction of nondividing, fully reimplantable primary hepatocytes. *Mol. Ther.* 6: 199–209.
12. Giannini, C., *et al.* (2003). A highly efficient, stable, and rapid approach for ex vivo human liver gene therapy via a FLAP lentiviral vector. *Hepatology* 38: 114–122.
13. Colvin, D. M. (2000). Alkylating agents and platinum antitumor compounds. In *Cancer Medicine* (R. C. Bast, D. W. Kufe, R. E. Pollock, R. R. Weichselbaum, J. F. Holland, and E. Frei, Eds.), BC Decker, Hamilton, ON [Online publication].
14. Browder, T., *et al.* (2000). Antiangiogenic scheduling of chemotherapy improves efficacy against experimental drug-resistant cancer. *Cancer Res.* 60: 1878–1886.
15. DeLeve, L. D. (1996). Cellular target of cyclophosphamide toxicity in the murine liver: role of glutathione and site of metabolic activation. *Hepatology* 24: 830–837.
16. Malhi, H., *et al.* (2002). Cyclophosphamide disrupts hepatic sinusoidal endothelium and improves transplanted cell engraftment in rat liver. *Hepatology* 36: 112–121.
17. DeLeve, L. D. (2000). Liver function and hepatotoxicity in cancer. In *Cancer Medicine* (R. C. Bast, D. W. Kufe, R. E. Pollock, R. R. Weichselbaum, J. F. Holland, and E. Frei, Eds.), pp. 2346–2358. BC Decker, Hamilton, ON.
18. Brunner, K. T., Hurez, D., McCluskey, R. T., and Benacerraf, B. (1960). Blood clearance of ^{32}P-labeled vesicular stomatitis and Newcastle disease viruses by the reticuloendothelial system in mice. *J. Immunol.* 85: 99–105.
19. Zhang, L., Dailey, P. J., Gettie, A., Blanchard, J., and Ho, D. D. (2002). The liver is a major organ for clearing simian immunodeficiency virus in rhesus monkeys. *J. Virol.* 76: 5271–5273.
20. Alemany, R., Suzuki, K., and Curiel, D. T. (2000). Blood clearance rates of adenovirus type 5 in mice. *J. Gen. Virol.* 81: 2605–2609.
21. Hardonk, M. J., Dijkhuis, F. W., Hulstaert, C. E., and Koudstaal, J. (1992). Heterogeneity of rat liver and spleen macrophages in gadolinium chloride-induced elimination and repopulation. *J. Leukocyte Biol.* 52: 296–302.
22. Lieber, A., *et al.* (1997). The role of Kupffer cell activation and viral gene expression in early liver toxicity after infusion of recombinant adenovirus vectors. *J. Virol.* 71: 8798–8807.
23. Schiedner, G., Hertel, S., Johnston, M., Dries, V., van Rooijen, N., and Kochanek, S. (2003). Selective depletion or blockade of Kupffer cells leads to enhanced and prolonged hepatic transgene expression using high-capacity adenoviral vectors. *Mol. Ther.* 7: 35–43.
24. Schauber, C. A., Tuerk, M. J., Pacheco, C. D., Escarpe, P. A., and Veres, G. (2004). Lentiviral vectors pseudotyped with baculovirus gp64 efficiently transduce mouse cells in vivo and show tropism restriction against hematopoietic cell types in vitro. *Gene Ther.* 11: 266–275.
25. Peng, K. W., *et al.* (2001). Organ distribution of gene expression after intravenous infusion of targeted and untargeted lentiviral vectors. *Gene Ther.* 8: 1456–1463.
26. Park, F., Ohashi, K., and Kay, M. A. (2003). The effect of age on hepatic gene transfer with self-inactivating lentiviral vectors in vivo. *Mol. Ther.* 8: 314–323.
27. Pan, D., *et al.* (2002). Biodistribution and toxicity studies of VSVG-pseudotyped lentiviral vector after intravenous administration in mice with the observation of in vivo transduction of bone marrow. *Mol. Ther.* 6: 19–29.
28. Tominaga, K., *et al.* (2004). Repeated adenoviral administration into the biliary tract can induce repeated expression of the original gene construct in rat livers without immunosuppressive strategies. *Gut* 53: 1167–1173.
29. Wisse, E., *et al.* (1996). Structure and function of sinusoidal lining cells in the liver. *Toxicol. Pathol.* 24: 100–111.
30. Steffan, A. M., Gendrault, J. L., and Kim, A. (1987). Increase in the number of fenestrae in mouse endothelial liver cells by altering the cytoskeleton with cytochalasin B. *Hepatology* 7: 1230–1238.
31. Braet, F., and Wisse, E. (2002). Structural and functional aspects of liver sinusoidal endothelial cell fenestrae: a review. *Comp. Hepatol.* 1: 1.
32. Braet, F., Muller, M., Vekemans, K., Wisse, E., and Le Couteur, D. G. (2003). Antimycin A-induced defenestration in rat hepatic sinusoidal endothelial cells. *Hepatology* 38: 394–402.
33. Briggs, J. A., Wilk, T., Welker, R., Krausslich, H. G., and Fuller, S. D. (2003). Structural organization of authentic, mature HIV-1 virions and cores. *EMBO J.* 22: 1707–1715.
34. Park, F., Ohashi, K., and Kay, M. A. (2000). Therapeutic levels of human factor VIII and IX using HIV-1-based lentiviral vectors in mouse liver. *Blood* 96: 1173–1176.
35. Mitchell, R. S., *et al.* (2004). Retroviral DNA integration: ASLV, HIV, and MLV show distinct target site preferences. *PLoS. Biol.* 2: E234.
36. Leffert, H. L., Koch, K. S., Lad, P. J., Shapiro, I. P., Skelly, H., and de Hemptinne, B. (1988). Hepatocyte regeneration, replication, and differentiation. In *The Liver: Biology and Pathology* (I. M. Arias, W. B. J. Jakoby, H. Popper, D. Schachter, and D. A. Shafritz, Eds.), pp. 833–850. Raven Press, New York.
37. Seppen, J., *et al.* (2000). Apical gene transfer into quiescent human and canine polarized intestinal epithelial cells by lentivirus vectors. *J. Virol.* 74: 7642–7645.
38. Zhang, J., Huang, W., Chua, S. S., Wei, P., and Moore, D. D. (2002). Modulation of acetaminophen-induced hepatotoxicity by the xenobiotic receptor CAR. *Science* 298: 422–424.
39. Asamoto, M., Hokaiwado, N., Murasaki, T., and Shirai, T. (2004). Connexin 32 dominant-negative mutant transgenic rats are resistant to hepatic damage by chemicals. *Hepatology* 40: 205–210.
40. Arias, I. M., Jakoby, W. B. J., Popper, H., Schachter, D., and Shafritz, D. A. (1988). *The Liver: Biology and Pathobiology.* Raven Press, New York.
41. Mook, O. R., Van Marle, J., Vreeling-Sindelarova, H., Jonges, R., Frederiks, W. M., and Van Noorden, C. J. (2003). Visualization of early events in tumor formation of eGFP-transfected rat colon cancer cells in liver. *Hepatology* 38: 295–304.

Oncology Research, Vol. 9, pp. 313-325, 1997

Targeting Gene Therapy to Cancer: a Review.

Gabi U. Dachs[1*], Graeme J. Dougherty[2], Ian J. Stratford[3] and Dai J. Chaplin[1]

[1]Gray Laboratory, Mount Vernon Hospital, Northwood, HA6 2JR, UK
[2]Terry Fox Laboratory, British Columbia Cancer Agency, Vancouver, Canada
[3]Dept. Pharmacy, University of Manchester, Manchester, M13 9PL, UK.

(Submitted April 10, 1997; accepted April 28, 1997)

* Corresponding author:
Gabi U. Dachs; Gray Laboratory, Mount Vernon Hospital, Northwood, Middlesex HA6 2JR, UK.
tel: (44)-1923-828611, *fax*: (44)-1923-835210, *Email*: dachs@graylab.ac.uk

Abstract

In recent years the idea of using gene therapy as a modality in the treatment of diseases other than genetically inherited, monogenic disorders has taken root. This is particularly obvious in the field of oncology where currently more than 70 clinical trials have been approved world-wide. This report will summarise some of the exciting progress that has recently been made with respect to both targeting the delivery of potentially therapeutic genes to tumour sites and regulating their expression within the tumour microenvironment.

In order to specifically target malignant cells while at the same time sparing normal tissue, cancer gene therapy will need to combine highly selective gene delivery with highly specific gene expression, specific gene product activity and, possibly, specific drug activation. Although the efficient delivery of DNA to tumour sites remains a formidable task, progress has been made in recent years using both viral (retrovirus, adenovirus, adeno-associated virus) and non-viral (liposomes, gene gun, injection) methods. In this report emphasis will be placed on targeted rather than high efficiency delivery, although those would need to be combined in the future for effective therapy. To date delivery has been targeted to tumour specific and tissue specific antigens, such as epithelial growth factor receptor, c-kit receptor, folate receptor,and anaerobic bacteria, and these will be described in some detail.

To increase specificity and safety of gene therapy further, the expression of the therapeutic gene needs to be tightly controlled within the target tissue. Targeted gene expression has been analysed using tissue specific promoters (breast, prostate and melanoma specific promoters) and disease specific promoters (carcinoembryonic antigen, HER-2/neu, Myc-Max response elements, DF3/MUC). Alternatively, expression could be regulated externally with the use of radiation induced promoters or tetracycline responsive elements. Another novel possibility which will be discussed is the regulation of therapeutic gene products by tumour specific gene splicing. Gene expression could also be targeted at conditions specific to the tumour microenvironment, such as glucose deprivation and hypoxia.

We have concentrated on hypoxia targeted gene expression and this report will discuss our progress in detail. Chronic hypoxia occurs in tissue which is more than 100-200 μm away from a functional blood supply. In solid tumours hypoxia is widespread both because cancer cells are more prolific than the invading endothelial cells that make up the blood vessels and because the newly formed blood supply is disorganised. Measurements of oxygen partial pressure in patients' tumours showed a high percentage of severe hypoxia readings (less than 2.5mmHg); readings not seen in normal tissue. This is a major problem in the treatment of cancer, since hypoxic cells are resistant to radiotherapy and often to chemotherapy. However, severe hypoxia is also a physiological condition specific to tumours which makes it a potentially exploitable target. We have utilised hypoxia response elements (HRE) derived from the oxygen regulated phosphoglycerate kinase gene to control gene expression in human tumour cells *in vitro* and in experimental tumours.

The list of genes that have been considered for use in the treatment of cancer is extensive. It includes cytokines and co-stimulatory cell surface molecules intended to induce an effective systemic immune response against tumour antigens which would not otherwise develop. Other inventive strategies include the use of internally expressed antibodies to target oncogenic proteins (intrabodies) and the use of antisense technology (antisense oligonucleotides, antigenes and ribozymes). This report will concentrate more on novel genes encoding prodrug activating enzymes, so-called suicide genes (Herpes simplex virus thymidine kinase, *Escherichia coli* nitroreductase, *E. coli* cytosine deaminase, thymidine phosphorylase, cytochrome P450 isoforms, deoxycytidine kinase and our initial work on the *Clostridium acetobutylicum* hydrogenase and flavodoxin), and their prospective prodrugs. Details of our work on placing the gene encoding cytosine deaminase under hypoxia control will be discussed.

Key words: delivery, tissue specific, gene expression, regulation, enzyme-prodrug therapy

The original goal of gene therapy was to correct a genetic disorder by inserting a functional gene into an organism to replace a defective one. More recently the concept of using gene therapy in the treatment of diseases other than inherited, single gene disorders has emerged. Over 70 clinical trials for gene therapy of cancer have already started and early Phase 1 results have been published. Following initial cell-marking and feasibility studies, strategies currently under clinical investigation are the enhancement of tumour immunogenicity by insertion of cytokine or co-stimulatory molecule encoding genes, or direct tumour kill by insertion of tumoricidal genes, tumour suppressor genes, and genes encoding prodrug activating enzymes. The first gene therapy protocol for cancer treatment was approved in May 1989. Cancer patients with advanced melanoma were treated by reinfusion with their own tumour-infiltrating lymphocytes which were transduced with a marker gene *ex vivo* (Rosenberg et al., 1990). Treatment with these gene-modified lymphocytes was more effective than treatment with lymphokine-activated killer cells; effective tumour remission with gene therapy was achieved in 40% of melanoma patients.

The problem with cancer therapy is selectivity and specificity. It is relatively easy to design a cell cytotoxin which kills tumour cells *in vitro*. However, in order to only kill tumour cells *in vivo* and at the same time sparing normal tissue, a very selective strategy is necessary. The effective current therapies, such as ionising radiation, rely on spatial delivery and the increased proliferation rate of tumours in order to differentiate them from normal tissue. Some cancer gene therapy strategies rely on the same principle, but other means of selectively targeting tumour cells have also been developed which will add to tumour specificity. Cancer gene therapy can combine highly specific gene delivery with highly specific gene expression. Advances in gene delivery have been made using viral and non-viral methods, but effective and selective delivery of DNA to tumour cells remains a complex task due to a poor and disorganised bloodsupply, and high interstitial fluid pressure. In this report, we will concentrate on targeted rather than high efficiency delivery, e.g. tissue specific targeting or disease specific targeting.

Another level of specificity can be added to selective delivery by targeting gene expression. Transcriptional promoters that are specifically functional in single tissues, or are active in specific disease states, or are induced by tumour specific conditions have been identified during basic research into cancer progression and can be utilised for targeted expression.

Three basic approaches in the design of therapeutic genes for cancer have been undertaken: molecular chemotherapy, genetic immunopotentiation and mutation compensation. Molecular chemotherapy uses the delivery of a toxin gene (so-called suicide genes) to tumour cells for eradication, genetic immunopotentiation boosts the immune system to reject the tumour, and mutation compensation either ablates activated oncogenes or induces tumour suppressor gene expression. In this report we have chosen to concentrate on the first strategy. Two therapeutic genes derived from micro-organisms have been tested extensively *in vitro* and *in vivo*, and Phase 1 clinical trials using the herpes simplex virus thymidine kinase and cytosine deaminase encoding genes are under way. Other pro-drug activating enzymes are emerging in parallel to the development of new prodrugs for gene directed enzyme prodrug therapy, and we will discuss these promising new strategies.

1. TARGETED DELIVERY

Advances have been made in the transfer of foreign genetic material to human cells, and high efficiency delivery is now possible. However, targeted rather than highly efficient delivery is required for selective cancer gene therapy. Extracellular receptors and cell surface molecules specific to tumour cells have been identified which can be used to target delivery of therapeutic genes. Both viral and non-viral delivery vehicles have been developed for this purpose, including retro- and adenovirus, liposomes, polylysine constructs, T-cells and even bacteria.

One of the original delivery methods was based on retroviral transduction, as they only infect dividing cells and can therefore be targeted broadly to proliferating cancer cells. Retrovirus constructs containing cytokine encoding genes were shown to inhibit metastasis formation and thereby reduce the tumour burden in experimental animals (Hurford et al., 1995). Retroviral vectors have been developed further to achieve selective transfection.

To target only actively dividing cells a recombinant herpes simplex virus (HSV) vector was constructed which lacked the ribonucleotide reductase encoding gene (Carroll et al., 1996). Ribonucleotide reductase is only expressed in actively dividing cells and is essential for viral replication; the recombinant vector therefore has to rely on the host cell for the generation of deoxyribonucleotides for DNA synthesis. The recombinant HSV vector carrying the lacZ marker was shown to replicate in and kill only dividing cells *in vitro*. LacZ activity was observed only in tumour nodules in the liver following intrasplenic injection of the colon carcinoma cell line HT29 into nude mice, followed a week later by HSV vector intrasplenic injection. Only minimal lacZ activity was seen in normal liver.

1.1 Targeted delivery: retroviral vectors with modified envelope proteins

The transfer of genes by retroviral vectors is entirely dependent on the interaction between proteins in the viral envelope and suitable counter-receptors on the target cell surface (Luciw & Leung, 1992). The envelope (env) protein of the Moloney murine Leukaemia virus (Mo-MuLV), on which most retroviral vectors are based, is made up of two covalently linked peptides, termed SU and TM. The amino terminal SU peptide mediates binding of the virus to its cell surface receptor while the carboxy TM domain anchors the molecule to the viral membrane. Retrovirus can be targeted specifically to cells expressing a particular surface protein if the SU domain of the viral env protein is replaced by a single chain antigen binding protein (termed scFv) (Russel et al., 1993; Chu et al., 1994, Kasahara et al., 1994). scFv consists of the variable regions of both heavy and light chains of an antibody molecule. However, only a small subset of surface proteins can function as appropriate receptors for the uptake and expression of these genetically engineered retroviral vectors. Therefore, a means of rapidly identifying differentially expressed cell surface molecules which can function as receptors for these retroviral vectors was developed (Dougherty et al., 1996). Currently the vectors are being used to screen panels of monoclonal antibodies raised against vascular endothelial cells.

1.2 Targeted delivery: epidermal growth factor receptor to target lung cancer cells

The epidermal growth factor receptor (EGF-R) is overexpressed in the majority of lung cancer cells. Human heregulin is a ligand for EGF-R (and the related receptor

HER-2/neu) and was therefore used in the design of a retroviral vector to target delivery to lung cancer cells (Han et al., 1995). By replacing the moloney murine leukaemia virus envelope with heregulin encoding sequences the ecotropic virus was able to cross the species barrier and infect EGF-R overexpressing human cells. Human cells which showed low EGF-R expression were resistant to the viral infection.

Alternatively, recombinant human epithelial growth factor was incorporated into a polylysine vector to target cells rich in EGF-R (Cristiano & Roth, 1996). In the presence of replication defective adenovirus, which was required as an endosomal lysis agent, the EGF-DNA complex was able to transfect lung cancer cells at a high efficiency *in vitro*, whereas colon carcinoma cells showed little DNA uptake.

Another strategy targets cytotoxic T-cells (CTLs) to tumour cells which express EGF-R (Moritz and Groner, 1995). A recombinant T-cell receptor was constructed consisting of a single chain Fv (scFv) derivative of an anti-EGF-R monoclonal antibody, which serves as the extracellular antigen binding domain, and the zeta chain of the TCR/CD3 complex, which serves as a signal transduction domain. A hinge region between the binding and signal transduction domain appeared to be required for efficient binding. *In vitro* crosslinking of the recombinant receptor with externally added EGF-R in transfected T-cells showed that the signal transduction pathway was functional. Addition of these transfected CTLs to tumour cells in culture efficiently lysed EGF-R positive tumour cells.

1.3 Targeted delivery: folate receptor to target cancer cells

Folate receptors are overexpressed in the majority of tumours. Folate receptors are internalised through caveolae in a process termed potolysis, which is different from endocytosis. This process could be exploited for the targeted delivery of DNA by conjugating folate to poly-L-lysine (Gottschalk et al., 1994; Lee and Huang, 1996). Although marker gene expression was moderate, it was specific to tumour cells which highly overexpress the folate receptor and could be improved by the addition of replication defective adenovirus.

1.4 Targeted delivery: c-kit receptor to target hematopoietic cells and lung cancer

The proto-oncogene c-kit, a receptor tyrosine kinase, and its ligand, Steel factor, are required for melanogenesis, hematopoesis and gametogenesis, and also play a role in cell-matrix adhesion (Kinashi and Springer, 1995). c-kit is highly expressed on hematopoietic progenitor and small cell lung cancer cells. A delivery vehicle was constructed to target hematopoietic progenitor cells consisting of DNA condensed with polylysine covalently linked to streptavidin, the biotinylated ligand Steel factor (since streptavidin binds biotin), and polylysine coated adenovirus for endosomal lysis (Schwarzenberger et al., 1996). Only c-kit positive cells were transfected. The streptavidin/biotin system is versatile and could be changed by the addition of other biotinylated ligands.

1.5 Targeted delivery: anaerobic bacteria to target solid tumours

Intravenously injected clostridial spores specifically locate to solid tumours where they germinate in necrotic and hypoxic regions (Moese and Moese, 1964). In order to improve the efficacy of this unconventional treatment, the cytosine deaminase (an enzyme able to convert 5-fluorocytosine, 5-FC, to the toxic anti-cancer drug 5-fluorouracyl, discussed in detail later) encoding gene from *Escherichia coli* was transfected into the non-pathogenic anaerobe *Clostridium beijerinickii* (Fox et al., 1996). Supernatant containing active enzyme taken from the transformed bacteria could sensitise murine carcinoma cells 500 fold to 5-FC in air. As an alternative, the *E. coli* nitroreductase gene (which activates CB 1954 to a bifunctional alkylating agent, more later) was introduced into *C. beijerinickii* and the resultant spores injected into tumour bearing mice (Minton et al., 1995). Tumour lysates were tested and shown to contain the nitroreductase enzyme.

2. TARGETED EXPRESSION

Not only delivery can be targeted, but also gene expression to further improve selectivity of gene therapy of cancer. Therefore, even if therapeutic genes are delivered to normal tissue, the regulatory sequences should prevent them from being expressed. Based on extensive basic research, genes have been identified which are expressed in either a tissue specific or cancer specific way, or which are induced by conditions specific to tumours. The regulatory sequences required for the selected expression can lie within the basic promoter, or in the case of enhancer sequences, up to several hundred bases upstream or downstream. Isolated enhancer elements can function on their own or in combination with other regulatory sequences, and in both orientations and almost any location to the gene of interest.

2.1 Tissue targeted expression

2.1.1 Tissue targeted expression: alpha fetoprotein to target hepatocellular carcinoma

Although alpha-fetoprotein (AFP) is normally only expressed in foetal liver and not in adult tissue, it has been found to be abnormally activated in hepatocellular carcinoma. Transgenic mice carrying the SV40 large T-antigen develop hepatocellular carcinoma (Marci and Gordon, 1994). Crossing these mice with mice transgenic for HSV thymidine kinase (HSVtk activates the anti-viral agent ganciclovir (GCV) to a toxic drug, discussed in detail later) gene under the control of the AFP promoter delayed tumour progression significantly when treated with GCV.

Adenoviral delivery of the HSVtk encoding gene under the AFP promoter/enhancer control also sensitised specifically AFP expressing human hepatocellular carcinoma cells to GCV *in vitro* and *in vivo* (Wills et al., 1995; Kaneko et al., 1995). A short region (0.3 kb) of the human AFP gene promoter was found to be sufficient to direct expression of the HSVtk gene specifically to hepatoma cells (Ido et al., 1995). Gene expression could be modulated and toxicity increased further by treating the transfectants with dexamethasone due to a glucocorticoid response element in the AFP promoter. AFP regulated wt p53 expression was equally restricted to AFP producing cells and could inhibit cell growth *in vitro* and increase sensitivity to cisplatin (Xu et al., 1996).

However, disturbing results were reported when adenoviral delivery of a construct containing the AFP promoter and a marker gene was found to preferentially locate in normal liver of experimental animals, instead of the hepatoma (Arbuthnot et al., 1996). Another report also described extensive liver damage following adenoviral delivery of HSVtk, which questions the use of adenovirus as a delivery vehicle (Brand et al., 1997).

2.1.2 Tissue targeted expression: prostate specific antigen (PSA) to target prostate cancer

Prostate specific antigen (PSA) is a serine protease involved in the degradation of the major proteins in the seminal coagulum leading to semen liquefaction (for a review see Seregni et al., 1996). PSA is produced preferentially in the prostate and is often overexpressed in prostate cancer. However, PSA has also been found in accessory male sex glands, breast cancer and milk of lactating women.

The upstream region (620 bp) of the PSA encoding gene was used to specifically drive expression of a marker gene in PSA^+ prostate cell lines (Pang et al., 1995). Expression could not be detected in non-prostate and PSA^- cells, and could be stimulated further by dihydrotestosterone in PSA^+ cells. The transfected construct showed competitive inhibition of the endogenous genomic promoter indicating that prostate specific DNA binding proteins are required to activate the PSA promoter. By adding the strong non-specific cytomegalovirus (CMV) promoter to the PSA promoter to drive marker gene expression, tissue specificity could be retained and a further 4-5 fold increase in expression achieved. It therefore appears that the PSA promoter contains negative regulatory elements which can override the promiscuous expression of the CMV promoter to limit expression to PSA+ cells. Further analysis of the PSA promoter revealed both a proximal and a distant promoter which are required for enhanced expression (Pang et al., 1997). The distant 822 bp regulatory sequence increased the otherwise low expression of the proximal promoter, enhanced responsiveness to dihydrotestosterone and retained tissue specificity. The distant promoter on its own, however, showed only low activity.

The PSA promoter was also used to direct expression of antisense DNA to polymerase α and topoisomerase II α to prostate cancer cells (Lee et al., 1996). Varying levels of expression were detected in prostate cancer cells, but none in the non-prostate cells. Lipofection mediated transfer of either of the two antisense constructs reduced growth *in vitro*, which could be increased to 55% by co-transfection of both antisense constructs.

2.1.3 Tissue targeted expression: von Willebrand factor (vWf) to target endothelial cells

Angiogenesis, the sprouting of new bloodvessels from the pre-existing vessel bed, is an absolute requirement for the growth of tumours beyond the size of a mm^3. Tumour vasculature is an attractive target for therapy, since about 1000 tumour cells rely on every endothelial cell for the delivery of nutrients. Not all endothelial cells need to be damaged to achieve tumour response; effecting only a few can shut down the bloodsupply to the entire tumour. As a first step towards anti-angiogenic gene therapy, the von Willebrand factor (vWf) promoter was analysed to target the tumour vasculature (Ozaki et al., 1996). A region which encompasses most of the first non-coding exon showed strong promoter activity which appeared to be endothelial cell specific. Growth suppression *in vitro* was evident when the vWf promoter was used to drive expression of HSVtk followed by GCV treatment.

Endothelial cell specific genes have been identified using differential display (Hewett et al., 1996). A receptor tyrosine kinase, tie-2/tek, was identified which is only expressed in endothelial cells where it is upregulated during neovascularisation. The tie-2/tek promoter is currently being evaluated for vascular targeted gene therapy.

2.1.4 Tissue targeted expression: DF3 (MUC1) promoter to target breast cancer

DF3 (MUC1) is a high molecular weight mucin-like glycoprotein which is overexpressed in the majority of breast cancers. By fusing the DF3 promoter to the coding region of HSVtk it was possible to selectively sensitise DF3 positive breast tumour cells to GCV (Manome et al., 1994). It was further shown that i.p. injection of defective recombinant adenoviral vectors containing the DF3-HSVtk constructs into animals with breast cancer metastasis followed by GCV treatment inhibited tumour growth (Chen et al., 1995a).

2.1.5 Tissue targeted expression: albumin enhancer to target liver cancer

The albumin enhancer element and promoter were used to exclusively target expression of the marker gene β-galactosidase (β-gal) to hepatoma cells (Kuriyama et al., 1991). Delivery *in vivo* was performed by injection of an ecotropic retroviral vector containing the liver-specific expression system. Expression could only be detected in dividing hepatocytes following injection into the spleen or liver, not in other tissue or in non-dividing cells.

2.1.6 Tissue targeted expression: tyrosinase promoter to target melanoma cells

The tyrosinase enzyme is part of the pigment producing pathway in skin and melanoma cells. The 5' region of the tyrosinase encoding gene or the tyrosinase-related protein were used to direct expression of the marker gene β-gal specifically to human and murine melanoma cells and melanocytes *in vitro* (Vile and Hart, 1993). Injection of this construct into tumour bearing mice showed expression only in the melanoma cell line B16 derived tumours and in some normal melanocytes, but not in COLO26 tumours or other normal surrounding tissue. To develop the system further the genes encoding either IL2, IL4 or macrophage colony-stimulating factor (M-CSF) were placed under the control of the murine tyrosinase 5' region (Vile and Hart, 1994). Only IL2 expressing B16 transfectants were prohibited to grow in syngeneic mice. However injection of the DNA construct into established tumours did not effect tumour growth, even though expression of the cytokine genes could be detected. Expression of the HSVtk encoding gene under the tyrosinase promoter control following delivery by retrovirus and ganciclovir treatment could reduce lung metastasis of B16 cells in syngeneic mice (Vile et al., 1994). The magnitude of reduction indicated a significant bystander effect, which could not be detected in immunodeficient mice. It therefore appears that the bystander effect of the HSVtk system requires an immune component.

2.1.7 Tissue targeted expression: myelin basic protein promoter to target glioma cells

The marker gene β-gal was placed under the control of either the mouse glial fibrillary acidic protein promoter (GFAP), the myelin basic protein promoter (MBP) or the myelin proteolipid protein promoter (PLP) in order to target expression to glioma cells (Miyao et al., 1993). Expression *in vitro* was restricted to glioma cells, as transduced fibroblasts and myeloma cells did not show any β-gal activity. The MBP promoter region showed the strongest promoter activity and was therefore used to direct expression of the HSVtk encoding gene. Subsequent treatment of the transduced cells with ganciclovir specifically killed the glioma cells *in vitro*.

2.1.8 Tissue targeted expression: osteocalcin promoter to target osteosarcoma

The non-collagenous bone matrix protein osteocalcin is expressed at high levels in osteoblasts. The osteocalcin promoter could specifically drive expression in osteoblasts *in vitro*, and osteocalcin regulated HSVtk expression resulted in osteosarcoma tumour regression *in vivo* following nucleoside treatment (Ko et al., 1996).

2.2 Disease targeted expression

2.2.1 Disease targeted expression: carcinoembryonic antigen regulatory sequence

Human carcinoembryonic antigen (CEA) is a member of a family of membrane glycoproteins which are overexpressed in many carcinomas; in 40% of patients with gastric cancer CEA levels are increased. CEA functions as a homotypic intercellular adhesion molecule *in vitro* (Hauck and Stanner, 1995).

The promoter for CEA was used to control gene expression of the HSVtk encoding gene within CEA positive pancreatic carcinomas (Dimaio et al., 1994) or lung cancer cells (Osaki et al., 1994). Only CEA positive cells expressed the transgene, whereas negative ones did not. A reduction in tumour size of xenografts derived from the transfectants could be achieved by treating the mice with ganciclovir, even if only 10 % of the tumour cells contained the HSVtk gene.

Alternatively the CEA transcriptional regulatory sequence was fused to the cytosine deaminase encoding gene to selectively sensitise colorectal carcinoma cells to 5-FC (Huber et al., 1995). Following retroviral delivery the chimeric genes were expressed only in CEA positive cells. Studies using human tumour xenografts showed that the cytosine deaminase/5-FC combination in solid tumours could generate complete cures if only 4% of the solid tumour cell mass expressed this enzyme.

The sequences controlling CEA expression have been analysed. Four cis-acting elements were mapped to a positive regulatory region and one element to a silencing region (Hauck and Stanner, 1995). Several nuclear factors were identified that bind to the regulatory regions; USF, Sp1 and Sp1-like factor. Independently, sequences containing the promoter, sequences essential for basic expression, copy number regulation and selective expression were identified (Richards et al., 1995). The optimum combination of these regulatory sequences results in a 2-4 fold increase in expression over that induced by the strong SV40 promoter in CEA positive cells.

2.2.2 Disease targeted expression: HER-2/neu (erbB2)

The oncogene HER-2/neu is overexpressed in about one third of breast and pancreatic tumours, and is involved in the transformation of prostatic epithelial cells. Overexpression involves transcriptional upregulation with or without gene amplification. HER-2/neu is a transmembrane glycoprotein related to EGF-R which functions as a growth factor receptor to regulate cell growth and transformation. The HER-2/neu promoter was used to target expression of cytosine deaminase selectively to HER-2/neu$^+$ cells, whereas no enzyme could be detected in HER-2/neu$^-$ cells (Harris et al., 1994). Significant cell killing was observed in the HER-2/neu$^+$ transfectants when treated with 5-FC, whereas HER-2/neu$^-$ transfectants were resistant to the drug.

2.2.3 Disease targeted expression: Myc-Max response elements

The c-myc proto-oncogene has been implicated in the control of cell proliferation, differentiation and apoptosis. The Myc family of proteins, including c-myc, can form heterodimers with the Max protein which specifically binds to its recognition sequence to activate transcription (Kretzner et al., 1992). The binding sequences for the Myc-Max heterodimer can direct gene expression to cells which overexpress c-myc. Four repeats of the Myc-Max response element were ligated to the HSVtk encoding gene in order to target gene expression to a range of myc overexpressing cancer cells, including small cell lung cancer cells and colon carcinoma cells (Kumagai et al., 1996; Sugaya et al., 1996). Transfected tumour cells exhibited increased sensitivity to GCV *in vitro* and liposomal delivery to established tumours followed by drug treatment induced tumour regression *in vivo*.

2.3 Condition targeted expression

2.3.1 Condition targeted expression: Early growth response-1 gene regulated by ionising radiation

The early growth response gene (Egr-1) is a ubiquitous immediate early gene which encodes a zinc finger transcription factor. Egr-1 is induced by a wide variety of stimuli including ionising radiation and cytokines. However, it is expressed only at low levels in many human tumour cells (Huang et al., 1995). Still, the radiation controllability of Egr-1 has been exploited to regulate gene expression for cancer therapy. By linking the radiation inducible CArG elements of the Egr-1 promoter to the TNFα encoding gene, expression could be regulated by ionising radiation in a temporal and localised way (Weichselbaum et al., 1994). Injection of Egr-TNF transfected hematopoietic cells into xenografts grown from radiation resistant squamous cell carcinoma followed by radiation increased tumour cures compared to radiation alone. Alternatively, direct intratumoural injection of liposomes or adenoviral delivery of the Egr-1 controlled TNF construct into the radiation and TNF resistant tumours followed by 20 or 50 Gy of radiation could significantly reduce tumour size (Seung et al., 1995; Hallahan et al., 1995). The effect on tumour growth can be partly attributed to damage of the tumour vasculature following treatment (Mauceri et al., 1996). Adenoviral delivery of the Egr-TNF construct and radiation resulted in extensive intratumoural vascular thrombosis and necrosis. No thrombosis was detected in treated normal tissue, indicating that a tumour specific occlusion of microvessels was induced. The Egr-1 control element was also utilised to direct radiation controlled expression of HSVtk to glioma cell lines (Joki et al., 1995).

2.3.2 Condition targeted expression: tissue-type plasminogen activator regulated by radiation

Plasminogen activators have clinical significance as thrombolytic agents for management of stroke and myocardial infarction. Tissue-type plasminogen activator (t-PA) is induced over 50 fold after irradiation with X-rays in otherwise radioresistant human melanoma cells (Boothman et al., 1994). The t-PA protease might have a function equivalent to the SOS repair system in prokaryotes. A x-ray inducible element was identified in the t-PA promoter which might be useful for radiation inducible gene therapy.

2.3.3 Condition targeted expression: regulation by glucose regulated protein GRP78/BiP promoter

The expression of the glucose regulated protein GRP78/BiP is strongly upregulated by tumour specific conditions such as glucose deprivation, anoxia and acidity. Elevated levels of GRP proteins protect the cell against stress, as they function as chaperones and calcium binding proteins (Little et al., 1994). The promoter of the

GRP78/BiP encoding gene was therefore used to control expression of a marker gene in a murine fibrosarcoma model (Gazit et al., 1995). *In vitro* glucose deprivation of transduced fibrosarcoma cells showed an 8-fold induction over non-stressed cells. Comparison with the viral SV40 promoter showed a two fold lower basal level of expression. Tumours grown from transduced cells showed central pockets of enhanced expression of the marker gene, indicating that *in vivo* stress response could control the glucose regulated marker gene.

2.3.4 Condition targeted expression: hypoxia regulated gene expression

Our method is designed to take advantage of the abnormal physiology that exists in almost all solid tumours, regardless of their origin or location, and use this tumour-specific condition to control the expression of therapeutic genes (Dachs et al., 1997).

Aggressive tumours often have insufficient blood supply, partly because tumour cells grow faster than the endothelial cells that make up the blood vessels, and partly because the newly formed vascular supply is disorganised (Folkman, 1989). This results in areas of acidity and nutrient deprivation, as well as regions with reduced oxygen concentrations (hypoxia). Direct measurements taken in patients showed a median oxygen level in normal tissue of 24 to 66mmHg (3.1 to 8.7% O_2), whereas those in tumours ranged from 10 to 30mmHg (1.3 to 3.9%). More importantly tumours routinely posses microregions with pO_2 levels of less than 2.5 mmHg (0.3%), levels at which cells are three times more resistant to radiation than aerated cells (Vaupel, 1993). Such hypoxia is not necessarily chronic. Blood vessels can open and close, creating microregions with acute hypoxia. It is important to note that cells in this aberrant environment can remain viable and are often chemo- and radioresistant. Hence, hypoxia is considered a major hindrance to therapy. In fact, a recent study of patients with cervical cancer showed the oxygen status of a tumour to be the single most important prognostic factor, ahead of age of patient, menopausal status, clinical stage, and size and histology of tumour (Hoeckel et al., 1996). However, it is our aim to exploit the presence of this subpopulation of resistant cells.

Hypoxic conditions can modulate the expression of a number of genes including those encoding growth factors, transcription factors, and glycolytic and DNA repair enzymes (for a recent review Dachs and Stratford, 1996). Hypoxic expression is controlled by the binding of the transcription factor, hypoxia inducible factor-1 (HIF-1) to a short DNA sequence (hypoxia enhancer or hypoxia response element, HRE) which can be situated at any distance and both orientations from the coding region. We have utilised the mouse phosphoglycerate kinase-1 HRE (Firth et al., 1994) in this study to control expression of marker and therapeutic genes in response to low oxygen *in vitro* and *in vivo*.

The use of hypoxia responsive enhancer elements enables the regulation of the marker gene CD2 in response to low oxygen conditions (Dachs et al., 1997). These studies show that the *in vitro* response was time and oxygen concentration dependent, with no protein induction at oxygen levels similar to those observed in normal tissue. The level of hypoxia that was sufficient to induce the CD2 marker gene *in vitro* has been clinically observed (Hoeckel et al., 1996; Vaupel et al., 1989). Interestingly, not only hypoxia increased the levels of the marker gene, but subsequent reaeration increased it further. Although the reasons are not clear, it is possible that protein synthesis is restarted following growth arrest during reoxygenation, or that oxygen radicals similar to those found in reperfusion injury induced gene expression.

When the transfected tumour cells were grown as xenografts, expression of the marker gene was confined to areas adjacent to necrosis. Hypoxic induction in vivo of the HRE controlled CD2 was confirmed by combining CD2 staining with the comet assay. For the comet assay (Olive, 1995), tumour bearing mice are treated with radiation (which causes single strand breaks preferentially in oxic cells) and a bioreductive drug (which indices DNA crosslinks only in hypoxic cells). Single cell electrophoresis of single cells isolated from the treated tumours can differentiate the two populations. The hypoxic cells, according to the comet assay, stained positive for CD2, whereas the aerobic ones did not. These *in vitro* and *in vivo* results demonstrate the selectivity of the system and its potential for tumour specific targeting of gene expression.

A recent paper studied the possibility of delivering genes to hypoxic cells in rat hearts by injection or retroviral delivery (Prentice et al., 1996). It showed that not only could foreign genes be taken up in ischemic/reperfused tissue, but that the genes were transcribed and the protein synthesis machinery of the injured cells could produce recombinant proteins that retained enzymatic activity. Gene delivery to regions of chronic hypoxia in solid tumours will remain a formidable task, but the regions we aim to infect are those of transient hypoxia. These regions contain blood vessels that open and close, potentially allowing delivery of the therapeutic genes by repeated application.

2.4 Regulation by bacterial regulatory sequences

The luciferase reporter gene linked to a chimeric promoter containing binding sequences for the bacterial tetracycline repressor could be transactivated by cotransfection with genes encoding tTA (Maxwell et al., 1996). The addition of tetracycline could reduce luciferase expression of the tet repressor/tTA transfected cells in a graded manner. Enhanced tetracycline regulated expression of HSVtk was achieved by incorporating the tet repressor/tTA system in a retroviral construct (Hwang et al., 1996).

An interesting, though not targeted expression system, consists of the bacteriophage T7 promoter and T7 RNA polymerase encoding gene (Chen et al., 1995b). This T7 system can initiate and maintain itself, and requires no cellular factors for transcription, and is therefore inclined to function in any mammalian system. By co-transfecting constructs containing the promoter driving expression of a marker gene and its specific RNA polymerase, high cytoplasmic expression (up to 200 fold increase over nuclear gene expression) could be achieved in a wide variety of mammalian cells both *in vitro* and *in vivo*.

2.5 Alternative splicing

A critical step in eukaryotic gene expression involves the removal of intervening sequences encoded by introns from pre-mRNA transcripts prior to their transport to the cytoplasm where translation occurs (for a recent review see Dreyfuss et al., 1996). This process is termed "splicing". It is now appreciated that a large proportion of cellular genes encode primary transcripts in which exonic sequences can be spliced in different ways to generate multiple mRNA species that encode protein isoforms with unique structures and functions (Smith et al., 1989). This latter process, termed "alternative splicing", enhances the coding potential of the genome without the need to resort to gene duplication events. Alternative splicing is a highly regulated process

with distinct patterns of splicing occurring during cellular differentiation, in different tissues, or in response to extracellular signals.

In the last year or so, we have begun to investigate the possibility that differences in the ability of normal and malignant cells to alternatively splice pre-mRNA transcripts could perhaps be exploited as a means of targeting therapeutic genes to the malignant population. Specifically, we have made a series of vectors in which the cytosine deaminase gene is fused in frame to a cassette that contains two or more alternatively spliced exons derived from the gene encoding the adhesion protein CD44 such that expression of a functional CD44-cytosine deaminase chimera will only occur in cells that are capable of appropriately splicing out the intronic sequences that separate the CD44 exons (Asman et al., 1995). Although at an early stage of development, such vectors may allow the selective destruction of malignant and/or other rapidly proliferating cell types since these have been shown in numerous studies to differentially express certain alternatively spliced CD44 isoforms (East and Hart, 1993; Zoller, 1995; Sleeman et al., 1995).

3. THERAPEUTIC GENES: MOLECULAR CHEMOTHERAPY

The best choice for enzymes for gene directed enzyme prodrug therapy would be monomeric enzymes of viral or bacterial origin with a wide substrate specificity (Connors, 1995). It is therefore not surprising to see a viral (Herpes simplex virus thymidine kinase) and a bacterial (cytosine deaminase) gene as the first candidates of therapeutic genes in Phase 1 clinical trials.

Prodrugs are defined as chemicals which, even at high concentrations are non-toxic unless specifically activated by cellular conditions or enzymes to toxic metabolites. Using gene therapy it is possible to introduce a foreign enzyme encoding gene into human cells in order to sensitise them to an otherwise non-toxic prodrug. The ideal activated drug should be at least 100 fold more cytotoxic than the parent compound, should easily diffuse to kill non-transfected bystander cells and have a significant half-life to kill bystanders but not escape into the bloodstream to cause systemic toxicity.

3.1 Herpes simplex virus thymidine kinase (HSVtk)

Herpes simplex virus thymidine kinase (HSVtk) is the model for gene directed enzyme prodrug therapy and has been used extensively in pre-clinical studies. HSVtk converts non-toxic nucleoside analogues, such as ganciclovir, to phosphorylated compounds that can act as chain terminators and specifically kill dividing cells. Specific expression of the suicide gene in dividing cells can be further targeted by using retroviral gene transfer. Direct injection of packaging cells producing retrovirus containing the HSVtk encoding gene into established macroscopic liver metastasis in rats followed by ganciclovir treatment resulted in regression of tumour volume and reduction of mean cell mass by sixty fold (Caruso et al., 1993). HSVtk/GCV was also able to suppress metastasis in the short and long term in a mouse model of prostatic cancer, even after regrowth of the primary tumour (Hall et al., 1997).

Transgenic mice carrying the rat neu oncogene under the control of the mouse mammary tumour virus LTR develop breast cancers within 2-3 months of birth. Crossing these neu mice with mice transgenic for the HSVtk gene under the control of its own promoter and the polyoma enhancer resulted in double transgenic mice which still developed tumours at the same rate as the neu mice (Sacco et al., 1995). Intratumourally treatment with GCV reduced tumour growth in the double transgenics, but had no effect on the neu single transgenic mice. However, mammary tumours induced by the activated rat neu oncogene could not be eradicated by retroviral delivery of HSVtk followed by GCV treatment (Sacco et al., 1996). The lack of success could be attributed to the combination of low transduction efficiency by the retroviral vector and the lack of a bystander effect in the breast cancer cells due to the absence of functional gap junctions.

It has previously been shown that only a fraction of cells needed to contain the gene in order to activate the prodrug to its toxic product and kill untransfected bystanders. Gap junctions, which play a role in intercellular communications and require cell contact, had been implicated in this bystander effect. HeLa cells show very little ability to communicate via gap junctions, and also demonstrate little or no bystander effect when transfected with HSVtk and treated with ganciclovir (Mesnil et al., 1996). The bystander effect could however be restored to HeLa cells by transfection with the gene encoding the gap junction protein connexin 43. This strongly suggests that the bystander effect of the HSVtk/GCV system depends on gap junctions. However not all systems displaying a bystander effect rely on gap junctions.

Verapamil, a calcium channel antagonist which is also used to inhibit multidrug resistance, was shown to protect bystander cells from the HSVtk/GCV system (Marini et al., 1996). Verapamil inhibits the bystander effect both in co-culture *in vitro* and also in a tumour model, but is ineffective if given more than 2 days after GCV treatment. No difference in sensitivity of the transfectants was observed following verapamil and GCV treatment.

To address the effect of the immune system on treatment, rat mesothelioma cell lines transduced with HSVtk were grown in the flanks of either Fisher rats, nude rats or Fisher rats immunosuppressed with cyclosporin (Elshami et al., 1995). Adenoviral delivery of HSVtk followed by GCV treatment was significantly more effective in the nude or immunocompromised rats compared to the normal Fisher rats, indicating that the immune response against adenovirally transduced cells limited efficacy. Hence, it implied that immunosuppression might be a useful adjunct in this system.

However, the immunesystem is essential for an efficient bystander effect. Neighbouring untransfected tumour cells could be killed by inoculating syngeneic transfected cells and even irradiated xenogeneic transfected cells into tumour bearing mice (Freeman et al., 1995). Following GCV treatment upregulation of the cytokines IL-1α and IL-6 was evident as well as widespread necrosis, which resulted in prolonged animal survival.

Current work is under way to optimise the activity of HSVtk to reduce the amount of GCV necessary (Black et al., 1996). By random mutagenesis of the HSVtk encoding gene new mutants were identified which induced a 43-fold greater sensitivity to GCV in mammalian cells.

A phase 1 clinical trial is currently underway to test adenoviral delivery of HSVtk to patients (Eck et al., 1996). Patients with advanced brain tumours will receive stereotactic-guided injection of the vector construct at escalating doses followed by systemic GCV treatment. However, high toxicity has since been reported in mice after intravenous injection of adenovirus carrying the HSVtk followed by GCV treatment (Brand et al., 1997). HSVtk was found to accumulate in the liver causing extensive liver degradation. The toxicity was prevalent for at least 7 weeks after vector administration. A mechanism of toxicity of

phosphorylated GCV which is independent of cell division probably exists as the resting liver is non-proliferating.

3.2 Cytosine deaminase

Mammalian cells do not produce significant amounts of the enzyme cytosine deaminase. *E. coli* however possess the gene encoding cytosine deaminase and are capable of converting cytosine to uracil. The introduction of the bacterial gene to mammalian cells can sensitise them to the prodrug 5-fluorocytosine (5-FC), which is converted to the cytotoxic agent 5-fluorouracil (5-FU). 5-FU is currently the most effective single agent for the treatment of colorectal carcinoma. The human colorectal carcinoma cell line WiDr could be sensitised a thousand fold to 5-FC by the introduction of the cytosine deaminase encoding gene (Huber et al., 1993). *In vivo* experiments showed that the half-life of 5-FC is 40 minutes in nude mice. Daily treatment for 10 days of tumour bearing animals with 500 mg/kg 5-FC could reduce tumour size and thymidine incorporation of the transfected tumours. Interestingly however, 5-FU had little effect on these tumours.

Significant amounts of 5-FU were found in the supernatant of cytosine deaminase transfected cells treated with 5-FC, which would account for the bystander effect observed (Haberkorn et al., 1996). However, uptake studies with radiolabelled 5-FC indicated that moderate and unsaturatable amounts of the drug accumulated intracellular, possibly by diffusion only. 5-FC uptake is therefore a bottleneck in this treatment strategy.

5-FU is also used as a radiation enhancer. Cell kill *in vitro* could be enhanced by treating cytosine deaminase transfected cells with a combination of 5-FC and radiation (Khil et al., 1996). A bifunctional fusion protein consisting of cytosine deaminase and HSVtk was constructed (Rogulski et al., 1997). The fusion showed enzyme activity for both enzymes, increased radiosensitivity and a slight synergistic effect when the transfectants were treated with both 5-FC and GCV.

A comparison of HSVtk/GCV and cytosine deaminase/5-FC in a human colorectal xenograft showed that the HSVtk/GCV system required more than 10% of the cells to be transfected for an antitumour effect (Trinh et al., 1995). However less than 4% of transfected cells in the cytosine deaminase/5-FC system were sufficient to achieve 60% cure rate. The lack of a bystander effect in the HSVtk/GCV system could be explained by transmission electron microscope analysis of the tumour cells which showed that although they contained desmosomes, they lacked gap junctions. The reliance of the HSVtk/GCV system on functional gap junctions may limit its use in the clinic.

We have utilised the cytosine deaminase encoding gene in our hypoxia regulated system (Dachs et al., 1997). The gene was placed under the transcriptional control of the 9-27 gene promoter into which was inserted a triplet of HRE derived from the PGK gene. Human tumour HT1080 cells transfected with this DNA construct exhibited a seven fold increase in enzyme activity following hypoxia compared to normoxia. The increase in enzyme activity resulted in a 5.4-fold increase in sensitivity of the transfectants to 5-FC following hypoxia compared to normoxia. This suggested that 5-FC had been converted to the toxic 5-FU by cytosine deaminase following the hypoxic exposure.

3.3 Cytochrome P450 enzymes (CYP450 2B1)

Liver cytochrome P450 enzymes are able to convert cyclophosphamide (CPA) to a potent alkylating agent which has antitumour activity. However, the therapeutic effectiveness is limited by hematopoietic, renal and cardiac cytotoxicity. The transfer of these liver enzymes to tumour cells would reduce systemic toxicity and increase anti-tumour activity. The cytochrome P450 isomer, CYP2B1, converts CPA to a hydroxy intermediate which brakes down to form the DNA alkalyting toxin phosphoramide mustard. Gliosarcoma cells transfected with the gene encoding CYP2B1 showed increased sensitivity to cyclophosphamide (Chen and Waxman, 1995; Wei et al., 1995; Chen et al., 1996). The cells could be protected against the toxic effect by treatment with the CYP2B1 inhibitor metyrapone. Treatment with cyclophosphamide or ifosphamide of a mixed culture consisting of 10% transfected cells showed a bystander effect which did not require cell-cell contact. Fischer rats implanted with CYP2B1 expressing tumour cells showed an increased sensitivity to cyclophosphamide treatment; a significant growth inhibition was seen in the CYP2B1 positive tumours compared to a modest delay in CYP2B1 negative tumours following treatment.

3.4 Platelet-derived endothelial cell growth factor/thymidine phosphorylase

Platelet-derived endothelial cell growth factor functions as a chemotactic and angiogenic growth factor, and is used as a prognostic indicator in a range of tumour types. Expression of PD-ECGF is on average 27 fold increased in human breast tumours compared to normal breast (Patterson et al., 1995). The level of PD-ECGF in the tumour cell line MCF-7 is similar to that of the low expressers in human breast tumour biopsis. PD-ECGF is identical to the enzyme thymidine phosphorylase (dThdPase) which catalyses the phosphorolytic cleavage of 5'-deoxy-5-fluorouridine (5'-DFUR) to the anticancer agent 5-fluorouracil (5-FU). Transfection of MCF-7 cells with the PD-ECGF encoding gene increased the cells sensitivity to the prodrug 5'-DFUR by 165 fold, whereas no difference in the sensitivity to 5-FU was detected. A substantial bystander effect could be detected when transfectants were mixed with the parental MCF-7 cells *in vitro*.

3.5 Deoxycytidine kinase

Cytosine arabinoside (ara-C) is a cytidine analogue which, when incorporated into replicating DNA will cause lethal strand breaks. ara-C is an efficient anti-tumour agent for hematologic malignancies, but has only a limited effect against solid tumours. ara-C requires phosphorylation by deoxycytidine kinase (dCK) to be active. dCK phosphorolates deoxyribonucleosides and thereby provides an alternative to *de novo* synthesis of DNA precursors (see Arner and Erikkson, 1995 for a recent review). It is possible to sensitise glioma cells to ara-C by retro- or adenoviral delivery of the dCK encoding gene (Manome et al., 1996). dCK transduced glioma tumours implanted either intradermal or intracerebral showed a significant antitumour effect following ara-C treatment.

3.6 E. coli guanine phosphoribosyl transferase (gpt)

The *E. coli* guanine phosphoribosyl transferase (gpt) enzyme has been studied due to its unique dual sensitivity/resistance function. It confers resistance to mycophenolic acid and xanthine, but sensitivity to 6-thioxanthine (6TX) to transfected mammalian cells (Mroz and Moolten, 1993). Transfected sarcoma cells could be selected *in vitro* for their resistance to mycophenolic acid and xanthine, and treatment of tumours derived from gpt transfected cells with 6TX caused durable tumour regression. Further, retroviral delivery of the bacterial gene to rat glioma cells showed an increased sensitivity of the

transfectants and untransfected bystanders to 6TX (Tamiya et al. 1996). The bystander effect could be abolished by separating the cells with a microporous membrane, indicating that it was not due to diffusable metabolites. Subcutaneous and intracerebral tumours grown from the transfected cells could be controlled by 6TX treatment.

3.7 E. coli nitroreductase

The nitroreductase from *E. coli* B has been studied for its use in antibody directed enzyme prodrug therapy (ADEPT). The *E. coli* nitroreductase B, and to a lesser extend the Walker cell Dt-diaphorase, are able to activate CB 1954 (5(-aziridine-1-yl)-2,4-dinitrobenzamide) to a potent interstrand crosslinking agent (Knox et al., 1988). Nitroreductase is a flavoprotein which requires either NADH or NADPH cofactors which limits its use for ADEPT. Gene therapy approaches were therefore investigated and transfer of the bacterial gene to V79 hamster cells increased their sensitivity to CB 1954 by 770 fold compared to untransfected controls (Bailey et al., 1996).

3.8 Clostridium acetobutylicum electron transport enzymes

Metronidazole is the drug of choice for many serious anaerobic bacterial infections. Its use is based on the ability of most bacteria to convert metronidazole to a toxic species, whereas mammalian cells, even under anoxic conditions, lack this ability. Even among bacteria there is a substantial variation in sensitivity. For example, the obligate anaerobe *Clostridium acetobutylicum* is highly sensitive to metronidazole, whereas the facultative anaerobe *Escherichia coli* is up to 500-fold more resistant to the drug. In *C. acetobutylicum* metronidazole is reduced by enzymes of the electron transport system, including the flavodoxin and hydrogenase enzymes (Church *et al.*, 1988; Santangelo *et al.*, 1991; Santangelo et al., 1995). We are investigating whether the introduction of the bacterial genes encoding the flavodoxin and/or hydrogenase enzymes into human tumour cell lines could increase their sensitivity to metronidazole.

The introduction of the Clostridium genes encoding the enzymes flavodoxin or hydrogenase increased sensitivity to metronidazole in *E. coli* by up to 10-fold. Since nitrate reductase negative *E. coli* cells are already sensitive to metronidazole this is a significant increase in drug sensitivity. The minimal coding regions of the hydrogenase and flavodoxin encoding genes were then introduced into the two human tumour cell lines HT1080 (fibrosarcoma) and HT29 (colon carcinoma) under the control of the strong constitutive CMV promoter. RNA studies showed that the bacterial genes were transcribed in the transfected human tumour cells. However, only a modest increase in metronidazole sensitivity in the human cells was observed (2-3 fold). It is not yet known, if a functional enzyme or a protein is produced, but it appears that inefficient translation might be to blame. The regulatory sequence (Kozak sequence; Kozak, 1986) around the start codon differs greatly between the bacterial genes and mammalian genes. We have therefore used site directed mutagenesis to improve translation and are currently testing the transfectants.

4. CONCLUSION

By carefully choosing a strategy involving targeted delivery and expression of a therapeutic gene, selective and specific tumour kill in pre-clinical studies is possible. Gene therapy has the potential to have few side effects and a much lower systemic toxicity than current therapies. It can also selectively target micro-metastatic deposits, which are currently difficult to detect or treat. However, choosing only one criteria for selectivity, such as targeting delivery to proliferating cells or tissue specific expression, is not sufficient, as non-specific toxicity has been reported. Only by combining the most successful strategies in cancer gene therapy approaches, will a successful clinical treatment emerge.

References

Arbuthnot, P.B.; Bralet, M.P.; LeJossic, C.; Dedieu, J.F.; Perricaudet, M.; Brechot, C.; Ferry, N. In vitro and in vivo hepatoma cell-specific expression of a gene transferred with an adenoviral vector. Human Gene Therapy 7 (13): pp. 1503-1514; 1996.

Arner, E.S.J.; Eriksson, S. Mammalian deoxyribonucleoside kinases. Pharm. Therap. 67 (2): pp. 155-186; 1995.

Asman, D. C.; Dirks, J. F.; Ge, L.; Resnick, N. M.; Salvucci, L. A.; Gau, J-T.; Becich, M. J.; Cooper, D. L.; Dougherty, G. J. Gene therapeutic approach to primary and metastatic brain tumors: I. CD44 variant pre-mRNA alternative splicing as a CEPT control element. J. Neuro-Oncol 26: pp. 243-250; 1995.

Bailey, S.M.; Knox, R.J.; Hobbs, S.M.; Jenkins, T.C.; Mauger, A.B.; Melton, R.G.; Burke, P.J.; Connors, T.A.; Hart, I.R. Investigation of alternative prodrugs for use with Escherichia-coli nitroreductase in suicide gene approaches to cancer-therapy. Gene Therapy 3 (12): pp. 1143-1150; 1996.

Black, M.E.; Newcomb, T.G.; Wilson, H.M.P.; Loeb, L.A. Creation of drug-specific herpes-simplex virus type-1 thymidine kinase mutants for gene-therapy. Proc. Natl. Acad. Sci. USA 93 (8): pp. 3525-3529; 1996.

Boothman, D.A.; Lee, I.W.; Sahijdak, W.M. Isolation of an x-ray-responsive element in the promoter region of tissue-type plasminogen-activator - potential uses of x-ray-responsive elements for gene-therapy. Rad. Res. 138 (1): pp. s68-s71; 1994.

Brand, K.; Arnold, W.; Bartels, T.; Lieber, A.; Kay, M.A.; Strauss, M.; Dorken, B. Liver-associated toxicity of the HSV-tk/GCV approach and adenoviral vectors. Cancer Gene Therapy 4 (1): pp. 9-16; 1997.

Carroll, N.M.; Chiocca, E.A.; Takahashi, K.; Tanabe, K.K. Enhancement of gene-therapy specificity for diffuse colon-carcinoma liver metastases with recombinant herpes-simplex virus. Annals of Surgery 224 (3): pp. 323-329; 1996.

Caruso, M.; Panis, Y.; Gagandeep, S.; Houssin, D.; Salzmann, J.L.; Klatzmann, D. Regression of established macroscopic liver metastases after in-situ transduction of a suicide gene. Proc. Natl. Acad. Sci. USA 90 (15): pp. 7024-7028, 1993.

Chen, L.; Chen, D.S.; Manome, Y.; Dong, Y.H.; Fine, H.A.; Kufe, D.W. Breast cancer selective gene expression and therapy mediated by recombinant adenoviruses containing the DF3/MUC1 promoter. J. Clin. Invest. 96(6): pp.2775-2782; 1995a.

Chen, L.; Waxman, D.J. Intratumoral activation and enhanced chemotherapeutic effect of oxazaphosphorines following cytochrome-P450 gene-transfer - development of a combined chemotherapy cancer gene-therapy strategy. Cancer Res. 55 (3): pp. 581-589; 1995.

Chen, L.; Waxman, D.J.; Chen, D.S.; Kufe, D.W. Sensitization of human breast-cancer cells to cyclophosphamide and ifosfamide by transfer of a liver cytochrome-P450 gene. Cancer Res. 56 (6): pp. 1331-1340; 1996.

Chen, X.Z.; Li, Y.S.; Xiong, K.Y.; Xie, Y.F.; Aizicovici, S.; Snodgrass, R.; Wagner, T.E.; Platika, D. A novel nonviral cytoplasmic gene-expression system and its implications in cancer gene-therapy. Cancer Gene Therapy 2 (4): pp. 281-289; 1995b.

Chu, T.T.; Martinez, I.; Sheay, W.C.; Dornburg, R. Cell targeting with retroviral particles containing antibody-envelope fusion proteins. Gene Ther. 1:pp. 292-299; 1994.

Church, D.L.; Rabin, H.R.; Laishley, E.J. Role of hydrogenase 1 of *Clostridium pasteurianum* in the reduction of metronidazole. Biochem. Pharmacol. 37: pp. 1525-1534; 1988.

Connors, T.A. The choice of prodrugs for gene directed prodrug therapy of cancer. Gene Therapy 2: pp. 702-709; 1995.

Cooper, D.L.; Dougherty, G.J.; Dirks, J.F.; Asman, D.C. Gene-therapy advances - utilization of alternative splicing as a control element in the chimeric enzyme/prodrug therapy (CEPT) approach to primary and metastatic tumors. J. Clin. Ligand Assay 19 (1): pp. 80-84; 1996.

Cristiano, R.J.; Roth, J.A. Epidermal growth-factor mediated DNA delivery into lung-cancer cells via the epidermal growth-factor receptor. Cancer Gene Ther. 3 (1): pp. 4-10; 1996.

Dachs, G.U.; Patterson, A.V.; Firth, J.D.; Ratcliffe, P.J.; Townsend, K.M.S.; Stratford, I.J.; Harris, A.L. Targeting gene expression to hypoxic tumour cells. Nature Med. 3 (5); in press; 1997.

Dachs, G.U.; Stratford, I.J. The molecular response of mammalian cells to hypoxia and the potential for exploitation in cancer therapy. Brit. J. Cancer 74: pp. S126-132; 1996.

Dimaio, J.M.; Clary, B.M.; Via, D.F.; Coveney, E.; Pappas, T.N.; Lyerly, H.K. Directed enzyme pro-drug gene-therapy for pancreatic-cancer in-vivo. Surgery 116 (2): pp. 205-213; 1994.

Dougherty, G.J.; Peters, C.E.; Dougherty, S.T.; McBride, W.H.; Chaplin, D.J. Gene therapy-based approaches to the treatment of cancer. Development of targetable retroviral vectors. Transfus. Science 17: pp. 121-128; 1996.

Dreyfuss, G.; Hentze, M.; Lamond, A. I. From transcript to protein. Cell 85: pp. 963-972; 1996.

East, J. A.; Hart, I. R. CD44 and its role in tumour progression and metastasis. European J. Cancer 29A: pp. 1921-2; 1993.

Eck, S.L.; Alavi, J.B.; Alavi, A.; Davis, A.; Hackney, D.; Judy, K.; Mollman, J.; Phillips, P.C.; Wheeldon, E.B.; Wilson, J.M. Clinical protocol - Treatment of advanced CNS malignancies with the recombinant adenovirus H5.010RSVTK: A phase 1 trial. Human Gene Therapy 7 (12): pp. 1465-1482; 1996.

Elshami, A.A.; Kucharczuk, J.C.; Sterman, D.H.; Smythe, W.R.; Hwang, H.C.; Amin, K.M.; Litzky, L.A.; Albelda, S.M.; Kaiser, L.R. The role of immunosuppression in the efficacy of cancer gene-therapy using adenovirus transfer of the herpes-simplex thymidine kinase gene. Annals of Surgery 222 (3): pp. 298-310; 1995.

Folkman, J. What is the evidence that tumours are angiogenesis dependent? J. Natl. Cancer Inst. 82: pp. 4-6; 1989.

Fox, M.E.; Lemmon, M.J.; Mauchline, M.L.; Davis, T.O.; Giaccia, A.J.; Minton, N.P.; Brown, J.M. Anaerobic-bacteria as a delivery system for cancer gene-therapy- in-vitro activation of 5-fluorocytosine by genetically-engineered Clostridia. Gene Therapy 3 (2): pp. 173-178; 1996.

Freeman, S.M.; Ramesh, R.; Shastri, M.; Munshi, A.; Jensen, A.K.; Marrogi, A.J. The role of cytokines in mediating the bystander effect using HSV-TK xenogeneic cells. Cancer Letters 92 (2): pp. 167-174; 1995.

Gazit, G.; Kane, S.E.; Nichols, P.; Lee, A.S. Use of the stress-inducible GRP78/BiP promoter in targeting high-level gene-expression in fibrosarcoma in-vivo. Cancer Res. 55 (8): pp. 1660-1663; 1995.

Gottschalk, S.; Cristiano, R.J.; Smith, L.C.; Woo, S.L.C. Folate receptor-mediated DNA delivery into tumor-cells - potosomal disruption results in enhanced gene-expression. Gene Ther. 1 (3): pp. 185-191; 1994.

Haberkorn, U.; Oberdorfer, F.; Gebert, J.; Morr, I.; Haack, K.; Weber, K.; Lindauer, M.; Vankaick, G.; Schackert, H.K. Monitoring gene-therapy with cytosine deaminase - *in vitro* studies using tritiated 5-fluorocytosine. J. Nuc. Med. 37(1): pp.87-94; 1996.

Hall, S.J.; Mutchnik, S.E.; Chen, S.H.; Woo, S.L.C.; Thompson, T.C. Adenovirus-mediated herpes simplex virus thymidine kinase gene and ganciclovir therapy leads to systemic activity against spontaneous and induced metastasis in an orthotopic mouse model of prostate cancer. Int. J. Cancer 70 (2): pp. 183-187; 1997.

Hallahan, D.E.; Mauceri, H.J.; Seung, L.P.; Dunphy, E.J.; Wayne, J.D.; Hanna, N.N.; Toledano, A.; Hellman, S.; Kufe, D.W.; Weichselbaum, R.R. Spatial and temporal control of gene therapy using ionizing radiation. Nature Medicine 1 (8): 786-791; 1995.

Han, X.L.; Kasahara, N.; Kan, Y.W. Ligand-directed retroviral targeting of human breast-cancer cells. Proc. Natl. Acad. Sci. USA 92 (21): pp. 9747-9751; 1995.

Harris, J.D.; Gutierrez, A.A.; Hurst, H.C.; Sikora, K.; Lemoine, N.R. Gene-therapy for cancer using tumor-specific prodrug activation. Gene Ther. 1 (3): pp. 170-175; 1994.

Hauck, W.; Stanners, C.P. Transcriptional regulation of the carcinoembryonic antigen gene - identification of regulatory elements and multiple nuclear factors. J. Biol. Chem. 270 (8): pp. 3602-3610; 1995.

Hewett, P.W.; Siebert, P.D.; Murray, J.C. Cloning of the human endothelial cell specific tyrosine kinase receptor tek promoter. Br. J. Cancer S73: pp.67; 1996.

Hoeckel, M.; Schlenger, K.; Mitze, M.; Schaeffer, U.; Vaupel, P. Hypoxia and radiation response in human tumours. Sem. Rad. Onc. 6: pp. 1-8; 1996.

Huang, R.P.; Liu, C.T.; Fan, Y.; Mercola, D.; Adamson, E.D. Egr-1 negatively regulates human tumour cell growth via the DNA binding domain. Cancer Research 55 (21): pp. 5054-5062; 1995.

Huang; J.J.; Scuric, Z.; Anderson, W.F. Novel retroviral vector transferring a suicide gene and a selectable marker gene with enhanced gene expression by using a tetracyclin responsive expression system. J. Virology 70 (11): pp. 8138-8141; 1996.

Huber, B.E.; Austin, E.A.; Good, S.S.; Knick, V.C.; Tibbels, S.; Richards, C.A. In-vivo antitumor-activity of 5-fluorocytosine on human colorectal-carcinoma cells genetically-modified to express cytosine deaminase. Cancer Res. 53 (19): pp. 4619-4626; 1993.

Huber, B.E.; Richards, C.A.; Austin, E.A. VDEPT - an enzyme prodrug gene therapy approach for the treatment of metastatic colorectal cancer. Advanced Drug Delivery Reviews 17(3): pp.279-292; 1995.

Hurford, R.K.; Dranoff, G.; Mulligan, R.C.; Tepper, R.I. Gene-therapy of metastatic cancer by in-vivo retroviral gene targeting. Nature Genetics 10 (4): pp. 430-435; 1995.

Ido, A.; Nakata, K.; Kato, Y.; Nakao, K.; Murata, K.; Fujita, M.; Ishii, N.; Tamaoki, T.; Shiku, H.; Nagataki, S. Gene-therapy for hepatoma-cells using a retrovirus vector carrying herpes-simplex virus thymidine kinase gene under the control of human alpha-fetoprotein gene promoter. Cancer Res. 55 (14): pp. 3105-3109; 1995.

Joki, T.; Nakamura, M.; Ohno, T. Activation of the radiosensitive Egr-1 promoter induces expression of the herpes simplex virus thymidine kinase gene and sensitivity of glioma cells to ganciclovir. Human Gene Therapy 6 (12): pp. 1507-1513; 1995.

Kaneko, S.; Hallenbeck, P.; Kotani, T.; Nakabayashi, H.; McGarrity, G.; Tamaoki, T.; Anderson, W.F.; Chiang, Y.L. Adenovirus-mediated gene-therapy of hepatocellular-carcinoma using cancer specific gene-expression. Cancer Research 55 (22): pp. 5283-5287; 1995.

Kasahara, N.; Dozy, A.M.; Kan, Y.W. Tissue specific targeting of retroviral vectors through ligand-receptor interactions. Science 266: pp. 1373-1376; 1994.

Khil, M.S.; Kim, J.H.; Mullen, C.A.; Kim, S.H.; Freytag, S.O. Radiosensitization by 5-fluorocytosine of human colorectal carcinoma cells in culture transduced with cytosine deaminase gene. Clinical Cancer Res.2(1): pp.53-57; 1996.

Kinashi, T.; Springer, T.A. Regulation of cell-matrix adhesion by tyrosine kinases. Leuk. Lymphoma 18 (3-4): 203-208; 1995.

Knox, R.J.; Boland, M.P.; Friedlos, F.; Coles, B.; Southan, C.; Roberts, J.J. The nitroreductase enzyme in Walker cells that activates 5-(aziridin-1-yl)-2,4-dinitrobenzamide (CB1954) to 5-(aziridin-1-yl)-4-hydroxylamino-2-nitrobenzamide is a form of NAD(P)H dehydrogenase (quinone). Biochem. Pharmacol. 37: pp. 4671-4677; 1988.

Ko, S.C.; Cheon, J.; Kao, C.H.; Gotoh, A.; Shirakawa, T.; Sikes, R.A.; Karsenty, G.; Chung, L.W.K. Osteocalcin promoter-based toxic gene-therapy for the treatment of osteosarcoma in experimental-models. Cancer Research 56 (20): pp. 4614-4619; 1996.

Kozak, M. Influeneces of mRNA secondary structure on initiation by eukaryotic ribosomes. Proc. Natl. Acad. Sci. USA 83: pp. 2850-2854; 1986.

Kretzner, L.; Blackwood, E.M.; Eisenman, R.N. Myc and Max proteins possess distinct transcriptional activities. Nature 359: pp. 426-429; 1992.

Kumagai, T.; Tanio, Y.; Osaki, T.; Hosoe, S.; Tachibana, I.; Ueno, K.; Kijima, T.; Horai, T.; Kishimoto, T. Eradication of myc-overexpressing small cell lung cancer cells transfected with herpes simplex virus thymidine kinase gene containing myc-max response elements. Cancer Res. 56 (2): pp.354-358; 1996.

Kuriyama, S.; Yoshikawa, M.; Ishizaka, S.; Tsujii, T.; Ikenaka, K.; Kagawa, T.; Morita, N.; Mikoshiba, K. A potential approach for gene-therapy targeting hepatoma using a liver-specific promoter on a retroviral vector. Cell Struct. Funct., 16 (6): pp. 503-510; 1991.

Lee, C.H.; Liu, M.; Sie, K.L.; Lee, M.S. Prostate specific antigen promoter driven gene therapy targeting polymerase alpha and topoisomerase II alpha in prostate cancer. Anticancer Res. 16 (4A): pp. 1805-1811; 1996.

Lee, R.J.; Huang, L. Folate-targeted, anionic liposome-entrapped polylysine-condensed DNA for tumor cell-specific gene-transfer. J. Biol. Chem. 271 (14): pp. 8481-8487; 1996.

Little, E.; Ramakrishnan, M.; Roy, B.; Gazit, G.; Lee, A.S. The glucose regulated proteins (GRP78 and GRP94): functions, gene regulation, and applications. Crit. Rev. Eukaryotic Gene Expression 4: pp. 1-18; 1994.

Luciw, P.A.; Leung, N.J. Mechanisms of retroviral replication, in Levy JA (ed): The Retroviridae. New York, Plenum Press: pp. 159-298; 1992.

Macri, P.; Gordon, J.W. Delayed morbidity and mortality of albumin/SV40 T-antigen transgenic mice after insertion of an alpha-fetoprotein/herpes virus thymidine kinase transgene and treatment with ganciclovir. Human Gene Ther. 5 (2): pp. 175-182; 1994.

Manome, Y.; Abe, M.; Hagen, M.F.; Fine, H.A.; Kufe, D.W. Enhancer sequences of the DF3 gene regulate expression of the herpes-simplex virus thymidine kinase gene and confer sensitivity of human breast-cancer cells to ganciclovir. Cancer Res. 54 (20): pp. 5408-5413; 1994.

Manome, Y.; Wen, P.Y.; Dong, Y.H.; Tanaka, T.; Mitchell, B.S.; Kufe, D.W.; Fine, H.A. Viral vector transduction of the human deoxycytidine kinase cDNA sensitizes glioma-cells to the cytotoxic effects of cytosine-arabinoside in-vitro and in-vivo. Nature Medicine 2 (5): pp. 567-573; 1996.

Marini, F.C.; Pan, B.F.; Nelson, J.A.; Lapeyre, J.N. The drug verapamil inhibits bystander killing but not cell suicide in thymidine kinase ganciclovir prodrug-activated gene therapy. Cancer Gene Therapy 3 (6): pp. 405-412; 1996.

Mauceri, H.J.; Hanna, N.N.; Wayne, J.D.; Hallahan, D.E.; Hellman, S.; Weichselbaum, R.R. Tumour necrosis factor alpha (TNF-alpha) gene therapy targeted by ionizing radiation selectively damages the tumour vasculature. Cancer Research 56 (19): pp. 4311-4314; 1996.

Maxwell, I.H.; Spitzer, A.L.; Long, C.J.; Maxwell, F. Autonomous parvovirus transduction of a gene under control of tissue-specific or inducible promoters. Gene Therapy, 3 (1): pp. 28-36; 1996.

Mesnil, M.; Piccoli, C.; Tiraby, G.; Willecke, K.; Yamasaki, H. Bystander killing of cancer-cells by herpes-simplex virus

thymidine kinase gene is mediated by connexins. Proc. Natl. Acad. Sci. USA 93 (5): pp. 1831-1835; 1996.

Minton, N.P.; Mauchline, M.L.; Lemmon, M.J.; Brehm, J.K.; Fox, M.; Michael, N.P.; Giaccia, A.; Brown, J.M. Chemotherapeutic tumour targeting using Clostridial spores. FEMS Microbiology Reviews 17 (3): pp. 357-364; 1995.

Miyao, Y.; Shimizu, K.; Moriuchi, S.; Yamada, M.; Nakahira, K.; Nakajima, K.; Nakao, J.; Kuriyama, S.; Tsujii, T.; Mikoshiba, K.; Hayakawa, T.; Ikenaka, K. Selective expression of foreign genes in glioma-cells - use of the mouse myelin basic-protein gene promoter to direct toxic gene-expression. J. Neuroscience Res. 36 (4): pp. 472-479; 1993.

Moese, J.R.; Moese, G. Oncolysis by Clostridia. I. Activity of *Clostridium butyricum* (M-55) and other nonpathogenic Clostridia against the Ehrlich carcinoma. Cancer Res. 24: pp. 212-216; 1964.

Moritz, D.; Groner, B. A spacer region between the single-chain antibody-chain and the CD3 zeta-chain domain of chimeric T-cell receptor components is required for efficient ligand-binding and signaling activity. Gene Therapy 2 (8): pp. 539-546; 1995.

Mroz, P.J.; Moolten, F.L. Retrovirally transduced Escherichia-coli gpt genes combine selectability with chemosensitivity capable of mediating tumor-eradication. Human Gene Ther. 4 (5): pp. 589-595, 1993.

Olive, P.L. Detection of hypoxia by measurement of DNA damage in individual cells from spheroid and murine tumours exposed to bioreductive drugs II. RSU 1069. Brit. J. Cancer 71: pp. 537-542; 1995.

Osaki, T.; Tanio, Y.; Tachibana, I.; Hosoe, S.; Kumagai, T.; Kawase, I.; Oikawa, S.; Kishimoto, T. Gene-therapy for carcinoembryonic antigen-producing human lung-cancer cells by cell-type-specific expression of herpes-simplex virus thymidine kinase gene. Cancer Res. 54 (20): pp. 5258-5261; 1994.

Ozaki, K.; Yoshida, T.; Ide, H.; Saito, I.; Ikeda, Y.; Sugimura, T.; Terada, M. Use of von Willebrand factor promoter to transduce suicidal gene to human endothelial cells, HUVEC. Human Gene Therapy 7 (13): pp. 1483-1490; 1996.

Pang, S.; Dannull, J.; Kaboo, R.; Xie, Y.M.; Tso, C.L.; Michel, K.; deKernion, J.B.; Belldegrun, A.S. Identification of a positive regulatory element responsible for tissue-specific expression of prostate-specific antigen. Cancer Research 57 (3): pp. 495-499; 1997.

Pang, S.; Taneja, S.; Dardashiti, K.; Cohan, P.; Kaboo, R.; Sokoloff, M.; Tso, C.L.; Dekernion, J.B.; Belldegrun, A.S. Prostate tissue-specificity of the prostate-specific antigen promoter isolated from a patient with prostate-cancer. Human Gene Therapy 6 (11): pp. 1417-1426; 1995.

Patterson, A.V.; Zhang, H.; Moghaddam, A.; Bicknell, R.; Talbot, D.C.; Stratford, I.J.; Harris, A.L. Increased sensitivity to the prodrug 5'-deoxy-5-fluorouridine and modulation of 5-fluoro-2'-deoxyuridine sensitivity in MCF-7 cells transfected with thymidine phosphorylase. Brit. J. Cancer 72 (3): pp. 669-675; 1995.

Prentice, H.; Kloner, R.A.; Li, Y.W.; Newman, L.; Kedes, L. Ischemic /reperfused myocardium can express recombinant protein following direct DNA or retroviral injection. J. Mol. Cell. Cardiology 28: pp. 133-140; 1996.

Richards, C.A.; Austin, E.A.; Huber, B.E. Transcriptional regulatory sequences of carcinoembryonic antigen - identification and use with cytosine deaminase for tumor-specific gene-therapy. Human Gene Ther. 6 (7): pp. 881-893; 1995.

Rogulski, K.R.; Kim, J.H.; Kim, S.H.; Freytag, S.O. Glioma cells transduced with an Escherichia coli CD/HSV-1 TK fusion gene exhibit enhanced metabolic suicide and radiosensitivity. Human Gene Therapy 8 (1): pp. 73-85; 1997.

Rosenberg, S.A.; Aebersold, P.; Cornetta, K.; Kasid, A.; Morgan, R.A. Moen, R.; Karson, E.M.; Lotze, M.T.; Yang, J.C.; Topalian, S.L. Gene transfer into humans - immunotherapy of patients with advanced melanoma using tumour-infiltrating lymphocytes modified by retroviral transduction. N. Eng. J. Med. 323: pp. 570-578; 1990.

Russel, S.J.; Hawkins, R.E.; Winter, G. Retroviral vectors displaying functional antibody fragments. Nuc. Acids Res. 21: pp. 1081-1085; 1993.

Sacco, M.G.; Benedetti, S.; Duflotdancer, A.; Mesnil, M.; Bagnasco, L.; Strina, D.; Fasolo, V.; Villa, A.; Macchi, P.; Faranda, S.; Vezzoni, P.; Finocchiaro, G. Partial regression, yet incomplete eradication of mammary-tumors in transgenic mice by retrovirally mediated HSVtk transfer in-vivo. Gene Therapy 3 (12): pp. 1151-1156; 1996.

Sacco, M.G.; Mangiarini, L.; Villa, A.; Macchi, P.; Barbieri, O.; Sacchi, M.C.; Monteggia, E.; Fasolo, V.; Vezzoni, P.; Clerici, L. Local regression of breast-tumors following intramammary ganciclovir administration in double transgenic mice expressing neu oncogene and herpes-simplex virus thymidine kinase. Gene Ther. 2 (7): pp. 493-497; 1995.

Santangelo, J.D.; Duerre, P.; Woods, D.R. Characterization and expression of the hydrogenase-encoding gene from *Clostridium acetobutylicum* P262. Microbiology 141: pp. 1-10; 1995.

Santangelo, J.D.; Jones, D.T.; Woods, D.R. Metronidazole activation and isolation of *Clostridium acetobutylicum* electron transport genes. J. Bacteriol. 173 (3): pp. 1088-1095; 1991.

Schwarzenberger, P.; Spence, S.E.; Gooya, J.M.; Michiel, D.; Curiel, D.T.; Ruscetti, F.W.; Keller, J.R. Targeted gene-transfer to human hematopoietic progenitor cell lines through the c-kit receptor. Blood 87(2): pp.472-478; 1996.

Seregni, E.; Botti, C.; Ballabio, G.; Bombardieri, E. Biochemical characteristics and recent biological knowledge on prostate-specific antigen. Tumori 82 (1): 72-77; 1996.

Seung, L.P.; Mauceri, H.J.; Beckett, M.A.; Hallahan, D.E.; Hellman, S.; Weichselbaum, R.R. Genetic radiotherapy overcomes tumor resistance to cytotoxic agents. Cancer Res. 55 (23): pp. 5561-5565; 1995.

Sleeman, J.; Moll, J.; Sherman, L.; Dall, P.; Pals, S.T.; Ponta, H.; Herrlich, P. The role of CD44 splice variants in human metastatic cancer. Ciba Foundation Symposium 189, 142-151; 1995.

Smith, C. W.; Patton, J. G.; Nadal-Ginard, B. Alternative splicing in the control of gene expression. Annu Rev Genet 23: pp. 527-577; 1989.

Sugaya, S.; Fujita, K.; Kikuchi, A.; Ueda, H.; Takakuwa, K.; Kodama, S.; Tanaka, K. Inhibition of tumor-growth by direct intratumoral gene-transfer of herpes-simplex virus thymidine kinase gene with DNA-liposome complexes. Human Gene Therapy 7 (2): pp. 223-230; 1996.

Tamiya, T.; Ono, Y.; Wei, M.X.; Mroz, P.J.; Moolten, F.L.; Chiocca, E.A. Escherichia coli gene senitizes rat glioma cells to killing by 6-thioxanthine or 6-thioguanine. Cancer Gene Threapy 3 (3): pp. 155-162; 1996.

Trinh, Q.T.; Austin, E.A.; Murray, D.M.; Knick, V.C.; Huber, B.E. Enzyme/prodrug gene-therapy - comparison of cytosine deaminase/5-fluorocytosine versus thymidine kinase/ganciclovir enzyme/prodrug systems in a human colorectal-carcinoma cell-line. Cancer Research 55 (21): pp. 4808-4812; 1995.

Vaupel, P.; Kallinowski, F.; Okunieff, P. Bloodflow, oxygen and nutrient supply, and metabolic microenvironment of human tumours: a review. Cancer Res. 49: pp. 6449-6465; 1989.

Vaupel, P.W. Oxygenation of solid tumours. In: Drug Resistance in Oncology, Teicher BA, (ed.) Marcel Dekker: New York; pp. 53-85; 1993.

Vile, R.G.; Hart, I.R. In vitro and in vivo targeting of gene-expression to melanoma-cells. Cancer Res. 53 (5): pp. 962-967; 1993.

Vile, R.G.; Hart, I.R. Targeting of cytokine gene-expression to malignant-melanoma cells using tissue-specific promoter sequences. Annals Onc. 5 (s4): pp. s59-s65; 1994.

Vile, R.G.; Nelson, J.A.; Castleden, S.; Chong, H.; Hart, I.R. Systemic gene-therapy of murine melanoma using tissue-specific expression of the HSVtk gene involves an immune component. Cancer Res. 54 (23): pp. 6228-6234; 1994.

Wei, M.X.; Tamiya, T.; Rhee, R.J.; Breakefield, X.O.; Chiocca, E.A. Diffusible cytotoxic metabolites contribute to the in-vitro bystander effect associated with the cyclophosphamide cytochrome-P450 2B1 cancer gene-therapy paradigm. Clinical Cancer Res. 1(10): pp.1171-1177; 1995

Weichselbaum, R.R.; Hallahan, D.E.; Beckett, M.A.; Mauceri, H.J.; Lee, H.; Sukhatme, V.P.; Kufe, D.W. Gene-therapy targeted by radiation preferentially radiosensitizes tumor-cells. Cancer Res. 54 (16): pp. 4266-4269; 1994.

Wills, K.N.; Huang, W.M.; Harris, M.P.; Machemer, T.; Maneval, D.C.; Gregory, R.J. Gene-therapy for hepatocellular-carcinoma - chemosensitivity conferred by adenovirus-mediated transfer of the HSV-1 thymidine kinase gene. Cancer Gene Ther. 2 (3): pp. 191-197; 1995.

Xu, G.W.; Sun, Z.T.; Forrester, K.; Wang, X.W.; Coursen, J.; Harris, C.C. Tissue-specific growth suppression and chemosensitivity promotion in human hepatocellular-carcinoma cells by retroviral-mediated transfer of the wild-type p53 gene. Hepatology 24 (5): pp. 1264-1268; 1996.

Zoller, M. CD44: physiological expression of distinct isoforms as evidence for organ-specific metastasis formation. J. Mol. Med. 73: pp. 425-438; 1995.

Gene Therapy (2000) 7, 1940–1946

www.nature.com/gt

Recombinant adenovirus vectors with knobless fibers for targeted gene transfer

VW van Beusechem[1], ALCT van Rijswijk[1], HHG van Es[2], HJ Haisma[1], HM Pinedo[1] and WR Gerritsen[1]

[1]*Division of Gene Therapy, Department of Medical Oncology, University Hospital Vrije Universiteit, Amsterdam;* [2]*Galapagos Genomics, Leiden, The Netherlands*

Adenoviral vector systems for gene therapy can be much improved by targeting vectors to specific cell types. This requires both the complete ablation of native adenovirus tropism and the introduction of a novel binding affinity in the viral capsid. We reasoned that these requirements could be fulfilled by deleting the entire knob domain of the adenovirus fiber protein and replacing it with two distinct moieties that provide a trimerization function for the knobless fiber and specific binding to the target cell, respectively. To test this concept, we constructed adenoviral vectors carrying knobless fibers comprising the α-helix trimerization domain from MoMuLV envelope glycoprotein. Two mimic targeting ligands, a Myc-epitope and a 6His-tag, were attached via a flexible linker peptide. The targeted knobless fiber molecules were properly expressed and imported into the nucleus of adenovirus packaging cells, where they were incorporated as functional trimers into the adenovirus capsid. Both ligands were exposed on the surface of the virion and were available for specific binding to their target molecules. Moreover, the knobless fibers mediated gene delivery into cells displaying receptors for the coupled ligand. Hence, these knobless fibers are prototype substrates for versatile addition of targeting ligands to generate truly targeted adenoviruses. Gene Therapy (2000) **7**, 1940–1946.

Keywords: *gene therapy; targeting; adenovirus vector; fiber; trimerization*

Introduction

Recombinant adenoviral vectors are being used as gene delivery vectors in a variety of gene therapy strategies. While the efficient transduction of many different human tissues is on the one hand an important attribute of adenoviral vectors, this promiscuous tropism represents, on the other hand, a limiting feature for their use in gene therapy. *In vivo* delivery of adenoviral vectors yields efficient transduction of cells that may not be a target for the therapy, most notably liver cells.[1,2] Because of this vector sequestration by non-target cells, high vector doses are needed for effective gene delivery into target cells. This imposes an increased risk for unwanted side-effects of the gene therapy procedure, by direct toxicity or host immune responses against the vector. Therefore, adenoviral vectors could potentially be much improved if specific gene transfer into only the desired target cells is accomplished.

The primary high-affinity binding of adenovirus to the host cell surface is mediated by the knob domain of the fiber protein.[3,4] This knowledge has directed several strategies for adenoviral vector targeting by genetic modification of the viral capsid. Peptide motifs with receptor binding specificity have been incorporated into the fiber protein by extension of the carboxy terminus of the fiber[5–8] and by insertion into the flexible and accessible HI-loop of the fiber knob.[9,10] These studies have confirmed the feasibility of the two approaches to generate adenoviral vectors with altered binding specificities. Importantly, Roelvink *et al*[11] recently ablated the native receptor-binding domain by mutating the adenovirus type 5 (Ad5) fiber knob. By combining this mutation with the HI-loop insertion strategy, they developed a truly targeted adenovirus vector. However, it appears that incorporation of targeting ligands in the fiber knob is not always compatible with proper fiber folding, resulting in loss of fiber functions.[7,8] Deletions in the fiber knob as small as only two amino acids can result in loss of fiber trimerization, the second important function of this domain.[12,13] Since the trimeric fashion of the fiber is essential for its incorporation in the virus particle by binding to the penton base,[12,14] modifications that result in loss of trimerization function will prevent formation of viable viruses carrying the modified protein. Clearly, the development of chimeric fibers that impose few demands on the structure of the ligand while retaining their trimeric quaternary structure would extend the applicability of targeted adenoviruses in gene therapy.

Our approach to develop truly targeted adenoviruses is to delete the complete fiber knob and to replace it with two distinct protein moieties. The first moiety is a common oligomerization motif found in many proteins, the α-helical coiled-coil,[15] which serves to substitute for the fiber knob trimerization function. The second moiety is the target ligand that is coupled to the trimerization domain via a flexible linker peptide, such as to allow the

Correspondence: VW van Beusechem, Division of Gene Therapy, Department of Medical Oncology, University Hospital VU, PO Box 7057, 1007 MB Amsterdam, The Netherlands
Received 9 June 2000; accepted 17 August 2000

two moieties to adopt their functional conformations. To test this concept, we constructed a first set of knobless fiber mutants using the α-helix domain from the transmembrane subunit p15E of Moloney murine leukemia virus (MoMuLV) envelope glycoprotein[16] and two mimic targeting ligands, a Myc-epitope and 6His-tag. One of the chimeric proteins described here exhibited all the functions required for its use in targeted gene delivery. It was properly incorporated into the adenovirus capsid where its carboxy-terminal 6His- and Myc-epitopes were accessible for specific binding to nickel ions and immobilized anti-Myc antibodies, respectively. Moreover, these knobless fibers mediated gene transfer into cells displaying artificial receptors for His-tagged adenoviruses. Hence, the novel knobless fiber molecules described here are prototype substrates for incorporation of cell type-specific targeting ligands to generate truly targeted adenoviruses.

Results

Construction of knobless fiber genes

Two chimeric genes encoding the entire Ad5 fiber tail and shaft domains and a trimerization domain derived from the MoMuLV envelope glycoprotein were made and were designated TSC and TSFLC, respectively (Figure 1). In both molecules, Ad5 fiber sequences are included that encode Met-1 to Thr-403, where Thr-403 is the last residue of the highly conserved TLWT motif that delineates the start of the fiber knob. The trimerization domain in both genes covers the 33-residue trimeric coiled-coil from Asp-515 to Leu-547 in the MoMuLV envelope glycoprotein.[16] This domain has no known binding function of its own. In TSC, the fiber shaft and trimerization domains are separated by the sequence Gly-Ser-Gly, in TSFLC these domains are linked via a classical $(Gly_4Ser)_3$ linker commonly used in single-chain antibodies. Thus, TSC and TSFLC represent fusion proteins with a linkage between the fiber-shaft and α-helix domains that allows minimal or maximal folding freedom, respectively. TSC and TSFLC each have a carboxy-terminal $(Gly_4Ser)_2$ flexible linker extension with a unique *Bam*HI restriction site to allow targeting ligand addition. To test these knobless fibers for properties relevant to their use in genetically targeted adenovirus we added a carboxy-terminal Myc-epitope and 6His-tag via the *Bam*HI site, producing TSCmychis and TSFLCmychis, respectively.

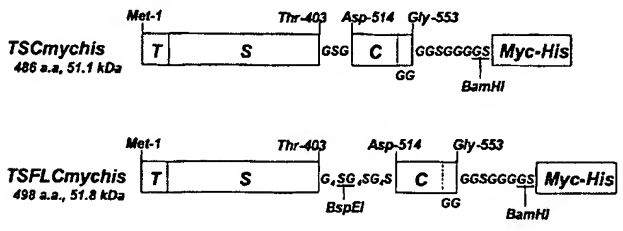

Figure 1 Structure of knobless fiber mutants TSCmychis and TSFLCmychis. T, Ad5 fiber tail-domain; S, Ad5 fiber shaft-domain; C, MoMuLV p15E coiled-coil domain; Myc-His, Myc/6His-tag from pcDNA3.1(–)mychis-A. The protein length is given in number of amino acids and the predicted molecular weight in kilodalton. Relevant amino acids and restriction sites are indicated. Numbers refer to the corresponding amino acids in the parental proteins.

Nuclear import of knobless fibers in mammalian cells

Expression of TSCmychis and TSFLCmychis knobless fiber proteins was initially evaluated by transient transfection of eukaryotic expression plasmids in 911 packaging cells.[17] This allowed the analysis of nuclear import in E1-complementing cells in the absence of a cytopathic effect (CPE). As a control, a vector expressing the bacterial *LacZ* gene with C-terminal Myc/6His-peptide was used. Twenty-four hours after transfection, Myc-epitope containing proteins could be detected by immunocytochemistry allowing analysis of the intracellular localization of the chimeric proteins (Figure 2). As was expected, the control protein LacZmychis was detected predominantly in the cytoplasm of transfected cells. In contrast, TSCmychis and TSFLCmychis proteins accumulated in the cell nuclei, where adenovirus capsids assemble. Thus, the nuclear localization signal in the Ad5 fiber tail is functionally intact and correctly targets the knobless fiber molecules with their carboxy-terminal peptide-ligands to the cell nucleus.

Trimerization of knobless fibers and accessibility of the C-terminal tag for specific binding

To produce knobless fiber-expressing adenovirus vectors on conventional 293 packaging cells[18] we cloned expression cassettes for TSCmychis and TSFLCmychis in the E1-region of an adenovirus vector also carrying an expression cassette for enhanced green fluorescent protein (GFP). The resulting vectors AdGFP-TSCmychis and AdGFP-TSFLCmychis co-express the knobless fiber variants with wild-type fibers. As a negative control, AdGFP virus with GFP as the only E1-insert was produced.

Protein lysates were prepared from adenovirus vector-infected 293 cells and subjected to Western analysis using anti-Myc and anti-fiber knob antibodies (Figure 3a). This showed that TSCmychis and TSFLCmychis knobless fibers were expressed, albeit at much lower levels than the wild-type fiber. The oligomeric structure of the knobless fiber molecules was assessed by comparing their electrophoretic mobility under semi-native *versus* denaturing conditions. As can be seen in Figure 3a, both TSCmychis and TSFLCmychis exhibited the expected molecular weight of approximately 50 kDa. Under semi-native con-

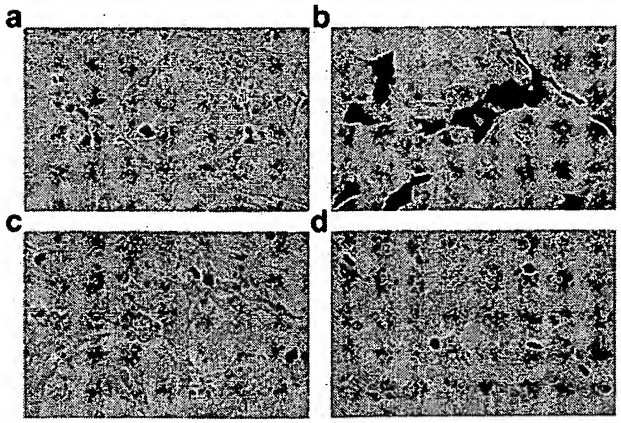

Figure 2 Nuclear import of knobless fiber proteins in 911 packaging cells. Cells transfected with CMV-driven expression constructs were stained with anti-Myc MoAb after 24 h. (a) mock transfection (empty pcDNA3.1(–)mychis-A vector); (b) pcDNA3.1(–)mychisLacZ; (c) pCMVtpl-TSCmychis; (d) pCMVtpl-TSFLCmychis.

ditions, approximately 5–10% was found as oligomers, as estimated by comparing band intensities of the high molecular weight and monomeric protein species. This shows that the MoMuLV trimerization domain is functional in both knobless fiber variants. The apparent molecular weight of the knobless fiber oligomers was larger than expected for homotrimers. However, analysis of the same samples with an antibody recognizing the trimeric wild-type fiber showed that most of this protein also migrated at a larger apparent molecular weight (Figure 3a). This is a well-described phenomenon that can be explained by partial unfolding of the fiber tail and shaft under laboratory conditions.[19]

We next investigated if the 6His-targeting ligand at the C-terminus of the knobless fiber molecules was accessible for binding. To this end, cell lysates were incubated with nickel-nitrilotriacetic acid (Ni-NTA) metal-affinity matrices. Unbound material was washed away and specifically bound 6His-containing proteins were eluted by competition with imidazol. Individual fractions were subjected to Western analysis. As can be seen in Figure 3b, TSCmychis and TSFLCmychis proteins bound to Ni-NTA matrices, confirming that their C-terminal ligand is accessible for binding.

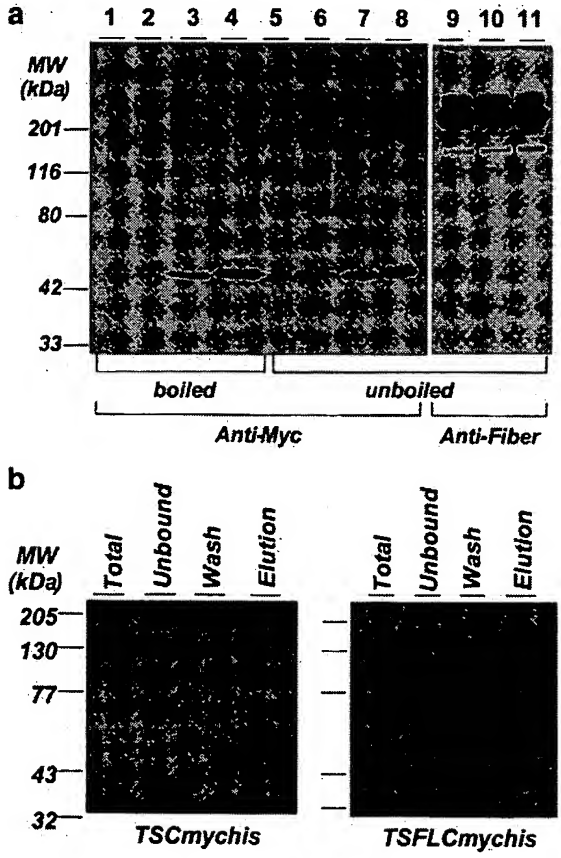

Figure 3 Analysis of knobless fiber proteins expressed in adenovirus vector-infected packaging cells. Cell lysates were subjected to Western analysis using an anti-Myc or anti-fiber knob antibody as indicated. Sizes of molecular weight markers are shown. (a) Knobless fiber protein oligomerization assessed by semi-native (unboiled) vs denaturing (boiled) SDS-PAGE. Lanes 1 and 5, uninfected 293 cells; lanes 2, 6 and 9, AdGFP infected; lanes 3, 7 and 10, AdGFP-TSCmychis infected; lanes 4, 8 and 11, AdGFP-TSFLCmychis infected. (b) Ni-NTA binding of knobless fiber proteins. Lysates (total) of 293 cells infected with AdGFP-TSCmychis (left panel) or AdGFP-TSFLCmychis (right panel) were loaded on to Ni-NTA beads, unbound material was collected and analyzed (unbound), as well as material eluted at low stringency (30 mM imidazol; wash) and at high stringency (300 mM imidazol; elution).

Incorporation of knobless fibers in adenovirus capsids

To investigate if the knobless fiber molecules are incorporated in complete adenovirus capsids, high-titer virus stocks of vectors AdGFP, AdGFP-TSCmychis and AdGFP-TSFLCmychis were purified by CsCl banding and subjected to Western analysis for wild-type and knobless fiber variants (Figure 4). As expected, wild-type fiber trimers were detected on the capsids of all three viruses and knobless fibers were not seen on AdGFP particles. TSCmychis molecules were only inefficiently co-purified with intact adenovirus particles. In contrast, the knobless fiber protein TSFLCmychis was reproducibly detected on AdGFP-TSFLCmychis particles.

To corroborate the capsid incorporation of TSFLCmychis molecules further, we investigated if functional AdGFP-TSFLCmychis viruses could bind with specificity to mimic receptors for the knobless fiber molecule. Accessibility of the 6His-tag on the virus capsid was tested by binding the virus to Ni-NTA beads. Elution of virus particles at increasing stringency of imidazol competition was quantified by measuring the functional GFP-vector titer (Figure 5a). The wild-type fiber-expressing AdGFP virus was gradually washed out upon subsequent incubation steps, indicating that as expected it did not bind to Ni-NTA with specificity. In contrast, approximately 9.5% and 1.3% of the total recovered AdGFP-TSFLCmychis virus was found in the 50 mM and 250 mM imidazol elution fractions, respectively. In addition, full-length viral DNA could be isolated from the 250 mM fraction and visualized on EtBr-stained agarose gel (not shown). Hence, intact infectious AdGFP-TSFLCmychis viral particles bound to Ni-NTA with high affinity via their 6His-tagged knobless fibers.

We also tested functional exposure of the Myc-tag on the virus capsid. To this end, AdGFP or AdGFP-TSFLCmychis virus was allowed to bind to immobilized anti-Myc antibody or to anti-fiber knob antibody as a control. Target cells were exposed to the bound virus and GFP-vector titers were measured (Figure 5b). Both viruses bound efficiently to the anti-fiber knob antibody

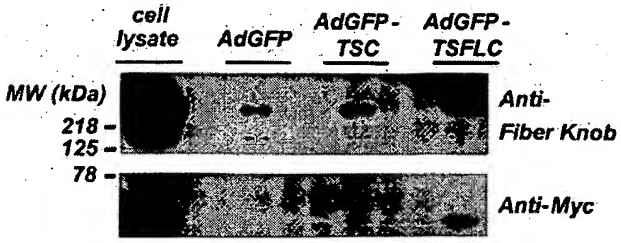

Figure 4 Protein analysis of purified adenovirus particles. Approximately 7×10^9 CsCl-purified virus particles were subjected to Western analysis for wild-type fiber using anti-fiber knob MoAb or for knobless fiber mutants using anti-Myc MoAb as indicated. A total protein lysate of 293 cells infected with AdGFP-TSCmychis virus was used as a control (cell lysate). Sizes of molecular weight markers are indicated. One of three Western analyses performed is shown. TSCmychis molecules were only detected in this experiment, TSFLCmychis molecules were found reproducibly.

(functional titers of 2.4×10^8 and 2.6×10^8 per 1×10^9 input virus particles, respectively). Background binding of the negative control AdGFP virus to the anti-Myc antibody was very low (ie only 0.2% of the anti-fiber knob binding). In contrast, approximately 2.3% functional AdGFP-TSFLCmychis viruses bound to the anti-Myc antibody, with 0.6% of these viruses adhering to the control plates.

Taken together, these findings explicitly demonstrate that the TSFLCmychis knobless fiber is incorporated in complete adenovirus vector capsids and exposes both the 6His-tag and the Myc-epitope for specific binding. The relative incorporation of knobless fibers compared with wild-type fibers was low. This is most probably a reflection of the relative abundance of the two fiber species in the packaging cells.

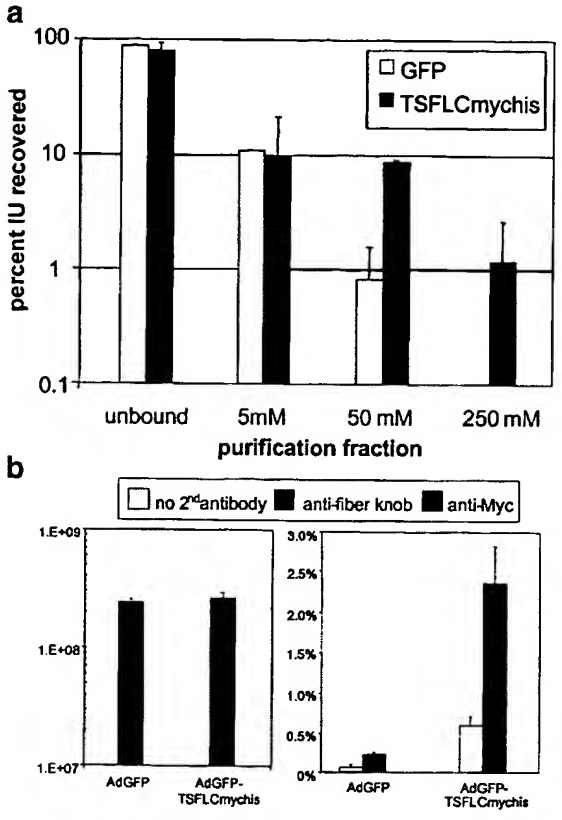

Figure 5 Accessibility of Myc and 6His-tags on knobless fiber carrying adenovirus particles. (a) Binding of adenovirus particles to Ni-NTA. 10^{12} virus particles were incubated with Ni-NTA beads and unbound particles, and particles eluting from the beads after competition with 5, 50, and 250 mM imidazol, respectively, were analyzed. Functional GFP virus titers were determined by limiting dilution titration. The bars depict the recovered virus in each individual Ni-NTA fraction as a percentage of the total recovered virus. The results shown are the average ± s.d. of two individual experiments each performed in duplicate. (b) Binding of adenoviruses to MoAbs. Left panel, binding of virus to anti-fiber knob MoAb per 10^9 input particles. Right panel, percentage virus bound to the anti-Myc MoAb, relative to the positive control binding to anti-fiber knob MoAb. The figure shows the result of a representative experiment performed in triplicate. Values given are average ± s.d. No second antibody, negative control plates coated with RbaMIgG only.

Targeted gene transfer by knobless fiber-carrying adenoviruses into cells displaying an artificial receptor

Knobless fiber-mediated gene transfer was demonstrated using 293.HissFv.rec cells.[20] 293.HissFv.rec cells display an anti-His single-chain antibody variant on their surface that functions as an artificial receptor for 6His-tagged adenoviruses.[20] Hence, these cells can be used to test the ability of 6His-tagged knobless fibers to function as primary binding molecules for CAR-independent adenovirus-mediated gene transfer.

293.HissFv.rec cells were infected with AdGFP or AdGFP-TSFLCmychis vectors at various MOI and GFP expression was measured the next day (Figure 6). To discriminate between wild-type and targeted infection, the alternative fiber–receptor interactions were blocked with neutralizing anti-fiber knob and anti-Myc antibodies, respectively. When the CAR-binding site on the wild-type fiber was blocked with anti-fiber knob antibody, gene transfer by AdGFP was efficiently inhibited to approximately 2% background infection. In contrast, depending on the MOI, AdGFP-TSFLCmychis virus exhibited 6–12% residual gene transfer in the presence of the anti-fiber knob antibody. Thus, part of the gene transfer by AdGFP-TSFLCmychis vector was wild-type fiber-independent. To confirm that this gene transfer was mediated by the TSFLCmychis knobless fiber, we added an anti-Myc antibody that binds to the carboxy terminus of the knobless fiber. This significantly reduced the gene delivery by AdGFP-TSFLCmychis vector, whereas it had no effect on the gene transfer by AdGFP. Hence, the TSFLCmychis knobless fibers on the AdGFP-TSFLCmychis capsid mediate targeted gene transfer through binding of their carboxy-terminal peptide to cell surface receptors.

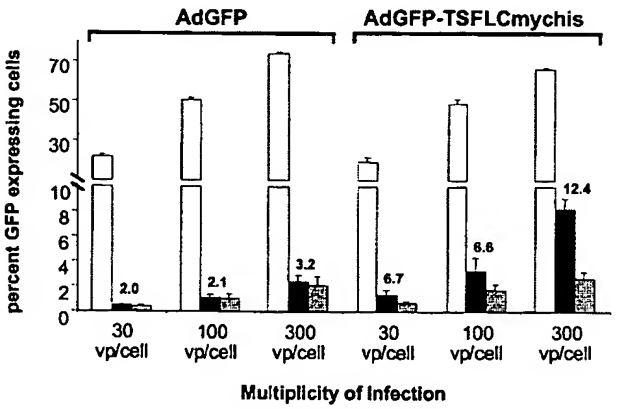

Figure 6 Knobless fiber-mediated gene transfer into cells displaying an artificial receptor. 293.HissFv.rec cells were subjected to infection with AdGFP or AdGFP-TSFLCmychis at MOI of 30, 100 or 300 particles per cell. Gene transfer was quantified by GFP fluorescence measurement. Wild-type fiber-dependent gene transfer was blocked with anti-fiber knob MoAb, knobless fiber-mediated gene transfer was blocked with anti-Myc MoAb. Results are given as average percent GFP expressing cells ± s.d. from a representative experiment performed in triplicate. Open bars, unblocked control infections; black bars, with anti-fiber knob MoAb; gray bars, with anti-fiber knob MoAb and anti-Myc MoAb. Relative percentage transduced cells in the presence of neutralizing anti-fiber knob MoAb compared with unblocked controls is indicated above the corresponding bars.

Discussion

Genetic modification of adenovirus capsid proteins to target new cell surface receptors is a potentially efficient way to overcome the promiscuous tropism of wild-type adenovirus vectors. The key role of the fiber knob in the adenovirus infection pathway makes this domain a rational target for such an endeavor. However, little is known about the structural requirements for successful ligand incorporation into the complex fiber knob domain.[21] The currently available data suggest that both the carboxy-terminal extension and the HI-loop insertion strategies allow inserts that are either very small or exhibit a high degree of protein flexibility. Here, we report on the generation of a new class of chimeric fibers in which the knob is replaced by a much less complex structure that complements for the trimerization function of the knob, but that is completely devoid of its wild-type binding property. To this end, we selected the trimeric α-helical coiled-coil that is found in the extraviral portion of the p15E envelope protein of MoMuLV[16] and made two knobless fiber variants that differed only in the nature of the peptide linkage between the fiber shaft and trimerization domain. Upon expression in adenovirus packaging cells, both knobless fibers with their peptide-tags properly accumulated in the cell nucleus. Furthermore, the two chimeric fibers formed oligomers. In different independent experiments performed, however, the efficiency of trimerization detected on semi-native gels varied considerably and was sometimes even undetectable. We attribute this to a rather weak stability of the molecules under laboratory conditions, which was not entirely unexpected, because p15E coiled-coils have a low thermostability.[22] In any event, the efficiency of trimerization was sufficient for incorporation of the chimeric fibers into the viral capsid. Several independent lines of evidence explicitly demonstrated that the TSFLCmychis knobless fiber variant was incorporated in complete and functional adenovirus vectors and exposed both its carboxy-terminal tags for specific binding. Capsid incorporation of TSCmychis molecules was much less efficient, suggesting that flexibility of the linkage between the fiber shaft and trimerization domain is important. This was a surprising observation, because trimerization and nuclear import efficiencies of the two variants seemed comparable. In addition, recent knowledge on the structure of the fiber shaft suggest that residues 393–398 that were included near to the linkage site in both knobless fiber variants already form a flexible linker.[23]

Importantly, TSFLCmychis knobless fibers mediated CAR-independent gene transfer into cells displaying an artificial receptor for His-tagged adenoviruses. Thus, TSFLCmychis molecules were functional in providing primary attachment to alternative cell surface receptors. The efficiency of targeted gene transfer reached approximately 10% of wild-type fiber-mediated transduction. Since the virus binding studies had indicated that AdGFP-TSFLCmychis particles carried only few TSFLCmychis molecules compared with wild-type fibers, we may conclude that TSFLCmychis knobless fiber-mediated gene delivery is very efficient.

In conclusion, the TSFLC knobless fiber variant exhibited all functions required for its use in truly targeted gene transfer. It is therefore a prototype substrate to derive targeted adenovirus vectors for a variety of cell types that are important targets for gene therapy. To determine the true value of this approach vectors lacking wild-type fibers will have to be made. For this purpose, it is of note that both carboxy-terminal peptide tags of the knobless fiber were accessible for functional binding. This will allow the incorporation of a cell type-specific binding ligand in place of the Myc-epitope, while the 6His-tag can be employed for vector propagation on 293.HissFv.rec cells. Such completely knobless virus particles may perhaps encounter similar limitations as have been observed with completely fiberless particles.[24,25] As yet unidentified domains of the fiber have been shown to play a role in particle maturation[24,26] and intracellular trafficking.[27] If either of these functions is mediated by the fiber knob, completely knobless fiber particles may exhibit reduced infectivity. Finally, the current generation of knobless fibers may be further improved by enhancing their thermostability. To this end, teachings on structural design of trimeric coiled-coils are at hand.[28,29] The stability of the current generation of chimeric fibers was shown to be sufficient for incorporation of peptide targeting-ligands, but a better stability could perhaps become important when more complex ligands, such as single-chain antibodies, are added.

Materials and methods

Construction of recombinant plasmids and adenoviral vectors

The knobless Ad5 fiber genes TSC and TSFLC were constructed using PCR techniques. To construct TSC, Ad5 sequences 31042–32250 were amplified using primers T-for (5′-CTAATACGACTCACTATAGGCTCGAgccaccATGAAGCGCGCAAGACCGTC-3′) and CS-rev (5′-CATC **TCCGGAACC**GGTCCACAAAGTTAGCTTATC-3′). T-for contains a *Xho*I site (underlined) and sequences fulfilling the Kozak consensus (small case) upstream of the Ad5 nt 31042–31061. CS-rev contains the antisense sequences of MoMuLV nt 7316–7319, three codons for Gly-Ser-Gly (bold), and Ad5 nt 32230–32250. The MoMuLV p15E helix was amplified using primers TC-for (5′-GTGGACC**GGTTCCGGA**GATGATCTCAGGGAGGT TGA-3′) and C-rev (5′-GCTA**GGATCCTCCACCTCC GGAACCTCCCCCTCCTTCTTTTAGAAATAAC**-3′). TC-for contains Ad5 nt 32244–32250, codons for Gly-Ser-Gly (bold) and MoMuLV nt 7316–7335. Antisense primer C-rev contains codons for $(Gly_4\text{-}Ser)_2$ (bold) including a restriction site for *Bam*HI (underlined) and MoMuLV nt 7414–7435 (the first two Gly residues of the flexible linker are from the MoMuLV envelope). Next, both PCR products were mixed and amplified in an assembly PCR with sense primer T-for and antisense primer XFL-rev (5′-GCTCTAGAGCTAGGATCCTCCACCTCC-3′), containing a *Xba*I site (underlined). To construct TSFLC, Ad5 nt 31042–32250 were amplified using primers T-for and FLS-rev(5′-GCTA**TCCTCCGGAACCGCCTCCACC**GGTCCAC AAAGTTAGCTTATC-3′). FLS-rev contains the antisense sequences of $Gly_4\text{-}Ser\text{-}Gly_2$ (bold) including a *Bsp*EI site (underlined), and Ad5 nt 32230–32250. The MoMuLV p15E helix was amplified using primers FLC-for (5′-**GGTTCCGGAGGAGGAGGATCAGGTGGTGGTGG ATCA**GATGATCTCAGGGAGGTTGA-3′) and C-rev. FLC-for contains codons for Gly-Ser-$(Gly_4Ser)_2$ (bold) including a *Bsp*EI site, and MoMuLV nt 7316–7335. Both

PCR products were (partially) digested with *Bsp*EI, mixed, ligated, and amplified using primers T-for and XFL-rev.

TSC and TSFLC were cloned into pcDNA3 vector (Invitrogen, San Diego, CA, USA) using the flanking *Xho*I and *Xba*I sites, yielding constructs pCMV-TSC and pCMV-TSFLC, respectively. Correct construction of the fusion genes was confirmed by sequencing. pCMV-TSCmychis and pCMV-TSFLCmychis were made by replacing the *Not*I–*Bam*HI fragment from pcDNA3.1 (–)/Myc-His/LacZ (Invitrogen) with the *Not*I–*Bam*HI fragment from pCMV-TSC or pCMV-TSFLC. In the ORF of pCMV-TSCmychis and pCMV-TSFLCmychis the C-terminal $(G_4S)_2$ linker is followed by the 29 amino acid sequence ELGTKLGPEQKLISEEDLNSAVDHHHHHH, where the Myc-epitope and 6His-tag are underlined.

The Ad2 tripartite leader (TPL) sequence was amplified from pMad5[30] using primers X-TPL (5′-TGCTCTAGACTCTCTTCCGCATCGCTG-3′), containing a *Xba*I site (underlined), and TPL-E (5′-CAGGAATTCTTGC GACTGTGACTGGTTAG-3′), with an *Eco*RI site (underlined). The *Xba*I and *Xho*I (TPL nt 172) digested PCR product was inserted into *Xba*I/*Xho*I digested pCMV-TSCmychis or pCMV-TSFLCmychis, creating pCMVtpl-TSCmychis and pCMVtpl-TSFLCmychis, respectively.

The Ad2 major late promoter (MLP) and TPL were amplified from pMad5 using primers N-MLP (5′-CTAAGAATGCGGCCGCGAGCGGTGTTCCGCGGTC-3′), containing a *Not*I site (underlined) and TPL-E. The PCR product was *Not*I/*Eco*RI (blunt) inserted into pBluescript II SK(–) (Stratagene, La Jolla, CA, USA) upstream of the *Xho*I (blunt)/*Pme*I fragment of pCMVtpl-TSCmychis or pCMVtpl-TSFLCmychis and the *Bam*HI (blunt)/*Hin*dIII SV40-pA fragment from pTet-Off (Clontech, Palo Alto, CA, USA). The correct sequence of the MLP-TPL PCR product was confirmed. The *Not*I–*Cla*I inserts were isolated and the *Cla*I sites were made blunt-end. These fragments were cloned into pAdTrack[31] digested with *Not*I/*Kpn*I (blunt), giving constructs pAdTrackMLP-TSCmychis and pAdTrackMLP-TSFLCmychis, respectively.

Adenovirus vector production

Recombinant adenoviruses were produced by homologous recombination in 293 cells.[18] Adenovirus backbone plasmid pAdEasy-1[31] was digested with *Pac*I and cotransfected together with *Pac*I/*Pme*I-digested pAdTrack, pAdTrackMLP-TSCmychis or pAdTrackMLP-TSFLCmychis by the Lipofectamine PLUS (Life Technologies, Paisley, UK) method according to the manufacturer's guidelines. Virus was prepared and further expanded on 293 cells using standard procedures.

Purified virus stocks were prepared by two rounds of CsCl banding and dialysis against 10 mM Hepes pH 7.4, 10% glycerol, 1 mM MgCl (storage buffer; SB) and were stored at –80°C until use. Virus identity was confirmed by PCR analysis. Virus particle titers were determined by OD260 measurement after lysis in PBS, 1% SDS, 1 mM EDTA at 55°C. Functional titers in infectious units were determined by end-point dilution infection on 293.HissFv.rec cells[20] and detecting GFP-expressing cells 6 days after infection. The absence of replication-competent adenovirus was confirmed by infection of A549 (ATCC No. CCL-185) cells.

Analysis of knobless fiber expression

Transfection on 911 cells[17] was performed using Lipofectamine PLUS reagent (Life Technologies) according to the manufacturer's instructions. Expression analysis by immunocytochemistry was performed at 24 h after transfection, using anti-Myc MoAb 9E10,[32] RbaMIgG-AP conjugate (Dako, Glostrup, Denmark) and BCIP/NBT substrate (Dako). Cells were counterstained with nuclear fast red.

For immunoblot analysis of adenovirus vector-infected 293 cells, cells in full CPE were harvested, washed in PBS, and lysed by four freeze–thaw cycles and three times 10 s sonification. Western samples were prepared by adding 2 volumes Laemmli loading buffer with 2% SDS, 5% β-mercaptoethanol and 5 min heating at 95°C (denaturing condition) or a modified loading buffer with 0.2% SDS and lacking β-mercaptoethanol, without heating (semi-native condition). Samples were separated by 7.5% SDS-PAGE and transferred to PVDF membrane (Sequiblot; Bio-Rad, Hercules, CA, USA). Immunoblots were processed according to standard procedures, using anti-Myc MoAb 9E10 or anti-fiber knob MoAb 1D6.14,[33] RbaMIgG-HRPO conjugate (Dako) and Lumilight^{PLUS} chemiluminescence detection reagent (Boehringer Mannheim, Mannheim, Germany). Fibers on adenovirus particles were analyzed under semi-native conditions as described above for cell lysates, starting from CsCl purified virus stocks in SB.

Ni-NTA purification of His-tagged proteins and viruses

Cell lysates were prepared from adenovirus vector-infected 293 cells as described above and cleared by centrifugation. Ni-NTA Superflow resin slurry (Qiagen, Hilden, Germany) equilibrated in PBS with 300 mM NaCl (PBS-300) and 5 mM imidazol was added to reach 10% v/v beads. After 1 h incubation at 4°C, Ni-NTA resin was spun down and the unbound material was harvested. The beads were washed twice with 3 volumes PBS-300/5 mM imidazol (discarded) and once with 3 volumes PBS-300/30 mM imidazol. Finally, specifically bound material was eluted by incubation with 3 volumes PBS-300/300 mM imidazol. The eluted proteins were concentrated using Ultrafree-0.5 centrifugal filters with Biomax-10 membrane (Millipore, Bedford, MA, USA) according to the manufacturer's instructions.

Virus particles (10^{12}) in SB were mixed with 0.1 volume Ni-NTA beads equilibrated in SB and incubated for 5 h at 4°C by end-over-end rotation. Beads were sedimented by gravity on ice and unbound material was aspirated. Beads were washed twice with 9 volumes SB/5 mM imidazol, twice with 9 volumes SB/50 mM imidazol and once with 9 volumes SB/250 mM imidazol. The unbound fraction and first-step elutions at 5 mM, 50 mM, and 250 mM imidazol were kept for analysis.

Antibody-mediated virus binding assay

Ninety-six-well Microlon 200 ELISA plates (Greiner, Frickenhausen, Germany) were coated with 10 μg/ml RbaMIgG MoAb (Dako) in PBS for 2 h at 37°C. After two washes with PBS, plates were incubated for 1.5 h at 37°C with PBS/1% BSA as a negative control or with 1 μg/ml anti-fiber knob MoAb 1D6.14 or anti-Myc MoAb 9E10 in PBS/1% BSA. After three washes with PBS, limiting dilution particle titrations of CsCl-purified virus were made in triplicate in DMEM/F12 medium (Life

Technologies) with 2% fetal bovine serum (FBS) and allowed to bind for 1 h at 37°C. Unbound virus was removed by five washes with PBS. Next, 293.HissFv.rec cells in DMEM/F12 medium with 10% FBS were seeded into the wells. After overnight culture at 37°C, cells were harvested, washed in PBS, fixated in PBS with 2.5% formaldehyde and analyzed for GFP fluorescence on a FACScan (Becton Dickinson, San Jose, CA, USA) according to standard procedures. Titer of functional virus bound was calculated according to the following equation: % GFP-expressing cells x number of cells seeded x virus dilution.

Targeted virus infection assay

293.HissFv.rec cells were seeded at 1×10^5 cells per well in 24-well tissue culture plates 24 h before infection. Virus was diluted in triplicate in DMEM/F12 with 1% FBS with or without 50 μg/ml 1D6.14 MoAb and/or 25 μg/ml 9E10 MoAb, and incubated at RT for 30 min. Next, the virus/antibody mixtures were added to the cells at MOI ranging from 30 to 300 particles per cell. The virus was allowed to bind for 30 min at RT, following which the medium was replaced by DMEM/F12 with 10% FBS. After 24 h incubation at 37°C, cells were harvested and analyzed for GFP expression on a FACScan according to standard procedures.

Acknowledgements

We thank David Curiel and Joanne Douglas, Gene Therapy Center UAB, Birmingham, Alabama for providing the 293.HissFv.rec cells and 1D6.14 MoAb; and Frits Fallaux, Leiden University Medical Center, The Netherlands for plasmid pMad5. This work was supported by the Netherlands Organization for Scientific Research (Spinoza Award 1997).

References

1 Herz J, Gerard RD. Adenovirus-mediated transfer of low density lipoprotein receptor gene acutely accelerates cholesterol clearance in normal mice. *Proc Natl Acad Sci USA* 1993; **90**: 2812–2816.
2 Huard J *et al*. The route of administration is a major determinant of the transduction efficiency of rat tissues by adenoviral recombinants. *Gene Therapy* 1995; **2**: 107–115.
3 Louis N *et al*. Cell-binding domain of adenovirus serotype 2 fiber. *J Virol* 1994; **68**: 4104–4106.
4 Henry LJ *et al*. Characterization of the knob domain of the adenovirus type 5 fiber protein expressed in Escherichia coli. *J Virol* 1994; **68**: 5239–5246.
5 Michael SI, Hong JS, Curiel DT, Engler JA. Addition of a short peptide ligand to the adenovirus fiber protein. *Gene Therapy* 1995; **2**: 660–668.
6 Wickham TJ, Roelvink PW, Brough DE, Kovesdi I. Adenovirus targeted to heparan-containing receptors increases its gene delivery efficiency to multiple cell types. *Nat Biotechnol* 1996; **14**: 1570–1573.
7 Wickham TJ *et al*. Increased *in vitro* and *in vivo* gene transfer by adenovirus vectors containing chimeric fiber proteins. *J Virol* 1997; **71**: 8221–8229.
8 Yoshida Y *et al*. Generation of fiber-mutant recombinant adenoviruses for gene therapy of malignant glioma. *Hum Gene Ther* 1998; **9**: 2503–2515.
9 Krasnykh V *et al*. Characterization of an adenovirus vector containing a heterologous peptide epitope in the HI loop of the fiber knob. *J Virol* 1998; **72**: 1844–1852.
10 Dmitriev I *et al*. An adenovirus vector with genetically modified fibers demonstrates expanded tropism via utilization of a coxsackievirus and adenovirus receptor-independent cell entry mechanism. *J Virol* 1998; **72**: 9706–9713.
11 Roelvink PW *et al*. Identification of a conserved receptor-binding site on the fiber proteins of CAR-recognizing adenoviridae. *Science* 1999; **286**: 1568–1571.
12 Novelli A, Boulanger PA. Deletion analysis of functional domains in baculovirus-expressed adenovirus type 2 fiber. *Virology* 1991; **185**: 365–376.
13 Hong JS, Engler JA. Domains required for assembly of adenovirus type 2 fiber trimers. *J Virol* 1996; **70**: 7071–7078.
14 Santis G *et al*. Molecular determinants of adenovirus serotype 5 fibre binding to its cellular receptor CAR. *J Gen Virol* 1999; **80**: 1519–1527.
15 Cohen C, Parry DAD. α-Helical coiled coils and bundles: how to design an a-helical protein. *Proteins Structure Function, Genetics* 1990; **7**: 1–15.
16 Fass D, Harrison SC, Kim PS. Retrovirus envelope domain at 1.7 angstrom resolution. *Nat Struct Biol* 1996; **3**: 465–469.
17 Fallaux FJ *et al*. Characterization of 911: a new helper cell line for the titration and propagation of early region 1-deleted adenoviral vectors. *Hum Gene Ther* 1996; **7**: 215–222.
18 Graham FL, Smiley J, Russell WC, Nairn R. Characteristics of a human cell line transformed by DNA from human adenovirus type 5. *J Gen Virol* 1977; **36**: 59–74.
19 Mitraki A *et al*. Unfolding studies of human adenovirus type 2 fibre trimers. Evidence for a stable domain. *Eur J Biochem* 1999; **264**: 599–606.
20 Douglas JT *et al*. A system for the propagation of adenoviral vectors with genetically modified receptor specificities. *Nat Biotechnol* 1999; **17**: 470–475.
21 Xia D, Henry LJ, Gerard RD, Deisenhofer J. Crystal structure of the receptor-binding domain of adenovirus type 5 fiber protein at 1.7 A resolution. *Structure* 1994; **2**: 1259–1270.
22 Fass D, Kim PS. Dissection of a retrovirus envelope protein reveals structural similarity to influenza hemagglutinin. *Curr Biol* 1995; **5**: 1377–1383.
23 van Raaij MJ, Mitraki A, Lavigne G, Cusack S. A triple beta-spiral in the adenovirus fibre shaft reveals a new structural motif for a fibrous protein. *Nature* 1999; **401**: 935–938.
24 Legrand V *et al*. Fiberless recombinant adenoviruses: virus maturation and infectivity in the absence of fiber. *J Virol* 1999; **73**: 907–919.
25 Von Seggern DJ, Kehler J, Endo RI, Nemerow GR. Complementation of a fibre mutant adenovirus by packaging cell lines stably expressing the adenovirus type 5 fibre protein. *J Gen Virol* 1998; **79**: 1461–1468.
26 Falgout B, Ketner G. Characterization of adenovirus particles made by deletion mutants lacking the fiber gene. *J Virol* 1988; **62**: 622–625.
27 Miyazawa N *et al*. Fiber swap between adenovirus subgroups B and C alters intracellular trafficking of adenovirus gene transfer vectors. *J Virol* 1999; **73**: 6056–6065.
28 Harbury PB, Zhang T, Kim PS, Alber T. A switch between two-, three-, and four-stranded coiled coils in GCN4 leucine zipper mutants. *Science* 1993; **262**: 1401–1407.
29 Harbury PB, Kim PS, Alber T. Crystal structure of an isoleucine-zipper trimer. *Nature* 1994; **371**: 80–83.
30 Toes RE *et al*. Protective anti-tumor immunity induced by vaccination with recombinant adenoviruses encoding multiple tumor-associated cytotoxic T lymphocyte epitopes in a string-of-beads fashion. *Proc Natl Acad Sci USA* 1997; **94**: 14660–14665.
31 He TC *et al*. A simplified system for generating recombinant adenoviruses. *Proc Natl Acad Sci USA* 1998; **95**: 2509–2514.
32 Chan S *et al*. A novel tumour marker related to the c-myc oncogene product. *Mol Cell Probes* 1987; **1**: 73–82.
33 Douglas JT et al. Targeted gene delivery by tropism-modified adenoviral vectors. *Nat Biotechnol* 1996; **14**: 1574–1578.

Uptake of Toxic Silica Particles by Isolated Rat Liver Macrophages (Kupffer Cells) Is Receptor Mediated and Can Be Blocked by Competition

Victoria Kolb-Bachofen
Institute for Immunobiology, Medical Faculty, Heinrich-Heine-Universität, D4000 Düsseldorf, Germany

Abstract

Silica particles (quartz dust) are toxic to macrophages after their uptake into these cells. These experiments describe the opsonization mechanism(s) and macrophage receptor(s) involved in silica uptake. Freshly isolated rat liver macrophages (Kupffer cells) were incubated at 37°C with silica particles in the presence or absence of autologous or heterologous plasma or purified plasma fibronectin and cell viability was assessed at various times. Within 60 min of coincubation, > 80% of macrophages were lysed in the presence of plasma or purified fibronectin but not in their absence (viability > 90%). Lysis was slower with defibronectinized plasma (28% in 60 min). Macrophages could be protected from lysis by addition of the monosaccharide *N*-acetyl-D-galactosamine but not by *N*-acetyl-D-glucosamine. Galactosylated serum albumin but not mannosylated albumin or native albumin exerted full protection from lysis. The pentapeptide GRGDS also prevented macrophage lysis in synergy with *N*-acetyl-galactosamine. Enzymatic deglycosylation of fibronectin reduced lysis significantly. These findings indicate an important opsonizing activity for fibronectin and dual recognition via the lectin-like galactose-specific binding activity of membrane-associated C-reactive protein and by integrin receptor(s). Binding experiments (at 4°C) revealed initial binding as primarily galactose-inhibitable, suggesting integrin-mediated binding as a later event necessary for effective uptake. (*J. Clin. Invest.* 1992. 90:1819–1824.) Key words: macrophages • rat • fibronectin • C-reactive protein • integrin • silica particles.

Introduction

Quartz dust particles are known to exert rapid and selective killing of macrophages (1) after their uptake into the phagocytes. Killing is dependent on uptake of the particles and leads to destruction of phagolysosomes as the earliest event (2, 3). Upon inhalation, silica dust is known to cause persistent inflammation, fibrosis, and granuloma in lung of humans and experimental animals (4, 5).

Upon injection into circulation, silica particles have been shown to effectively block various functions of the reticuloendothelial system (6–8), which are exerted mainly by the large population of resident liver macrophages, the Kupffer cells (9). A number of experimental studies on the role of macrophages in various diseases have used the macrophage-toxic effects of silica to impair in vivo phagocyte function in animals (6, 10, 11).

We now describe experiments where blockade of the toxic action of silica particles, i.e., blockade of their uptake, is used to elucidate the opsonic mechanism(s) and modes of recognition and uptake of silica particles by freshly isolated rat liver macrophages.

Methods

Chemicals. Silica particles (fraction DQ12) were kindly provided by Dr. Armbruster from the Rheinische Bergbau und Kohle Verein, Dortmund, Germany. The fraction DQ12 consists of medium sized (0.5–3.0 μm) quartz needles.

Collagenase H and *N*-glycanase F (*N*-glycosidase F, EC 3.2.2.18 and EC 3.5.1.52) were from Boehringer Mannheim GmBH (Mannheim, Germany), Eagle's Medium from Gibco BRL (Eggenstein, Germany), neoglycoproteins from Janssen Pharmaceutica (Beerse, Belgium), mono- and disaccharides from Fluka AG (Neu-Ulm, Germany). Gelatine-Sepharose 4B was from Pharmacia Fine Chemicals (Heidelberg, Germany). Antisera against the human proteins albumin, immunoglobulins; C-reactive protein (CRP),[1] serum amyloid protein, complement components C1q, C3, C4, and fibronectin were from Dakopatts (Hamburg, Germany) and Jackson ImmunoResearch Labs, Inc. (West-Grove, PA). All other chemicals were obtained from Sigma Chemical Co. (Tau f kirchen, Germany).

Isolation of rat liver macrophages. Rat liver macrophages were obtained by isolated liver perfusion with Collagenase H (180 mg in 100 ml perfusion buffer) and differential centrifugation of the resulting cell suspension, exactly as described previously (12). The resulting preparation routinely contained > 80% macrophages with ~ 10% contaminating hepatocytes and endothelial cells each. All experiments were performed with freshly isolated liver macrophages.

Plasma preparation. Blood was drawn from healthy volunteers or from rats without any chelating agent or with EDTA (10 mM). Care was taken to avoid air contact and cells were immediately removed by centrifugation. 0.5 ml of plasma or 0.5 ml of purified plasma fibronectin (~ 200 μg/ml, see below) in Tris-buffered saline ([TBS]: 50 mM Tris, 100 mM NaCl, pH 7.2] was incubated with 50 μl of silica suspension (5 mg/ml TBS) for 30 min at room temperature. This suspension was then used for macrophage incubations. For controls, 50 μl of silica was incubated with TBS in the absence of any protein but otherwise under identical conditions (sham incubation).

Plasma fibronectin (pFn) isolation. Fibronectin was isolated exactly as described (13): 20 ml of rat plasma (with 10 mM EDTA) was applied to a Gelatin-Sepharose column (20-ml bed size), washed with TBS buffer (20 mM Tris, 100 mM NaCl, 0.1 mM PMSF). A second wash with TBS plus 1 M urea was followed by elution of pFn with 4 M

Address correspondence to Prof. Dr. Victoria Kolb-Bachofen, Institute für Immunobiologie, Med. Einrichtungen der Heinrich-Heine-Universität, Moorenstrasse 5, D4000 Dusseldorf, Federal Republic of Germany.

Received for publication 4 November 1991 and in revised form 15 May 1992.

J. Clin. Invest.

0021-9738/92/11/1819/06 $2.00
Volume 90, November 1992, 1819–1824

1. *Abbreviations used in this paper:* CRP, C-reactive protein; GalNac, *N*-acetyl-galactosamine; GlcNAc, *N*-acetyl-glucosamine; GRDGS, Gly-Arg-Gly-Asp-Ser; mCRP, membrane-associated CRP; pFn, plasma fibronectin; pFn-Au, fibronectin-coated colloidal gold particles; TBS, Tris-buffered saline.

urea in TBS. Purity of each isolation was checked by SDS-PAGE and silver staining, only preparations with no contamination were used. Purified pFn was used after extensive dialysis against TBS.

Deglycosylation of pFn-coated silica. For experiments with deglycosylated fibronectin, enzymatic cleavage of glycans was performed on pFn immobilized (attached) to silica particles as described above. Enzymatic digestion with *N*-glycanase F was performed as recommended by the manufacturer: 100 μl of purified rat pFn-coated silica was centrifuged (10,000 *g*, 5 min), washed twice with Tris-buffer (50 mM Tris, pH 8.0) and resuspended in 50 mM Tris (pH 8.0), 20 mM EDTA, 0.1% Triton X-100, and 4 U *N*-glycanase F. After incubating at 37°C for 6 h, silica was again washed three times and finally resuspended in TBS. An aliquot of pFn-silica was sham incubated without *N*-glycanase F but otherwise identically. Particle aggregation by serial dilutions of ricin (RCA_{120}) and Con A was used to evaluate the success of deglycosylation as described previously (14), which showed a significant though not complete (~ 80%) reduction in agglutinability.

Cell incubation. 50 μl of isolated Kupffer cell suspension (2×10^6 cells/ml) in Eagle's medium was mixed with 25 μl of plasma-silica mixture or pFn-silica and $CaCl_2$ added to a final concentration of 2 mM. Cells plus silica were incubated at 37°C for the times indicated. For cell viability by trypan blue exclusion test aliquots were drawn from cell suspensions, mixed with an equal volume of 0.5% (wt/vol) trypan blue solution and immediately counted.

Electron microscopy. Adsorption of purified pFn onto colloidal gold particles with a mean diameter of 17 nm (pFn-Au) and cell-binding assays with pFn-Au were performed as described previously (14). Briefly, cells were mixed with pFn-Au in Eagle's medium plus $CaCl_2$ (2 mM) incubated for 10 min at 4°C. Binding was stopped by addition of an equal volume of ice-cold cacodylate-HCl-buffered 0.2% glutardialdehyde, immediately centrifuged, washed twice to remove unbound particles, and then processed for transmission electron microscopy. Ligand binding was quantified on electron micrographs of ultrathin sectioned specimens at a final magnification of 20,000×. Numbers of gold particles bound to the plasma membrane were counted and the length of plasma membranes determined using an HP 65 (Hewlett-Packard, Düsseldorf, Germany) equipped with a digitizing board and an area/distance program (HP-menu, Hewlett-Packard).

Results

Silica-mediated macrophage killing depends on opsonization by pFn. Isolated rat liver macrophages incubated at 37°C with silica particles in the absence of serum proteins can be maintained for 60 min and longer without loss of viability (Fig. 1). Addition of autologous plasma, obtained without coagulation inhibitors, leads to time dependent loss of viability as assessed by trypan blue exclusion and will lead to up to 80% dead cells within 60 min. Decrease of live cells is identical with addition of xenogeneic plasma of human origin (Fig. 1).

Electron microscopy of cells thus incubated confirms that lysis of macrophages was dependent on previous endocytosis of silica particles. Disruption of internal phagolysosomal membranes in the vicinity of silica needles was frequently found (Fig. 2). Micrographs also showed that in the absence of plasma absolutely no uptake was observed (not shown).

Agglutination of human plasma–opsonized silica particles with a series of antisera against human plasma proteins (albumin, immunoglobulins, serum amyloid protein, CRP, complement components C1q, C3, C4, fibronectin) showed that the particles were coated by fibronectin mostly, with little complement C3, traces of C1q, and none of the other proteins tested detectable.

To prove the dominant role of fibronectin in opsonization we repeated the macrophage toxicity assay described above by

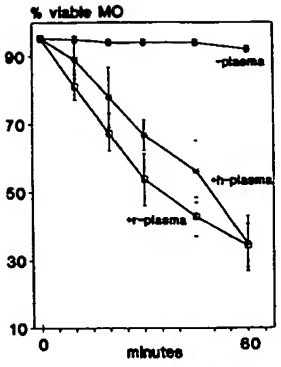

Figure 1. Viability of freshly isolated rat liver macrophages (*MO*) after coincubation with silica particles. 10^5 liver macrophages in 100 μl of TBS were incubated with silica particles (final concentration 125 μg/ml) at 37°C for the times indicated. Silica was either incubated with autologous rat plasma (*+r-plasma*, □), human plasma (*+h-plasma*, •), or was sham-incubated (*−plasma*, ×) as described in Methods. Cell viability was measured by trypan blue exclusion. Values are the mean±SD of three to eight individual experiments.

adding purified autologous rat plasma fibronectin. As shown in Fig. 3, results are identical. In confirmation of pFn as the most important opsonic signal, addition of pFn-free plasma led to a small decrease of macrophage viability only (statistically significant from plasma or purified pFn: $P < 0.005$).

Inhibition with monosaccharides or (neo)glycoproteins. We had previously shown that immobilized fibronectin is bound by liver macrophage membrane-associated CRP (mCRP), earlier termed galactose-particle receptor, in a galactose/*N*-acetylgalactosamine inhibitable way (14). Therefore incubation experiments with plasma- or pFn-opsonized silica and liver macrophages in the presence of various monosaccharides were performed. Whereas neither *N*-acetyl-glucosamine (GlcNAc) nor mannose addition had any effect on macrophage survival, *N*-acetyl-galactosamine (GlcNAc) blocked uptake of the opsonized particles (Fig. 4). The extent of blockade was the same with rat plasma or human plasma or purified fibronectin as opsonizing agents.

Inhibition experiments were also performed with glycoproteins and neoglycoproteins. As shown in Fig. 5, the two glycoproteins exposing terminal galactosyl groups completely prevented the toxic effect in a concentration-dependent way. Asialofetuin exposing a maximum of 12 terminal galactose residues per molecule exerted half-maximal inhibition at a concentration of $\sim 2 \times 10^{-5}$ mol/liter, galactose-BSA containing an average of 37–45 gal per molecule showed half-maximal inhibition at $\sim 5 \times 10^{-8}$ mol/liter. Neither mannose-BSA nor native BSA had significant protective effects, proving the galactose-specific recognition mode involved.

The relative inhibitory activity of the glycoproteins was measured with rat plasma, purified rat pFn, or purified human pFn. Comparison of the data obtained showed no difference, neither in the various carbohydrate compounds nor in their relative concentrations needed for inhibition.

Role of Arg-Gly-Asp (RGD)-recognizing integrin receptors. The experiments described confirm a major role of fibronectin as opsonizing signal and a galactose-specific recognition by mCRP. Fibronectin, however, is known to be bound to many cell surfaces, including macrophages, via recognition of the RGD sequence by integrin receptors.

Whether the pentapeptide Gly-Arg-Gly-Asp-Ser (GRGDS) would have a protective effect in macrophage-silica incubation experiments was therefore tested. Surprisingly the pentapeptide also prevents lysis in a concentration dependent way with full protection achieved at 2 mg/ml. Again results were identi-

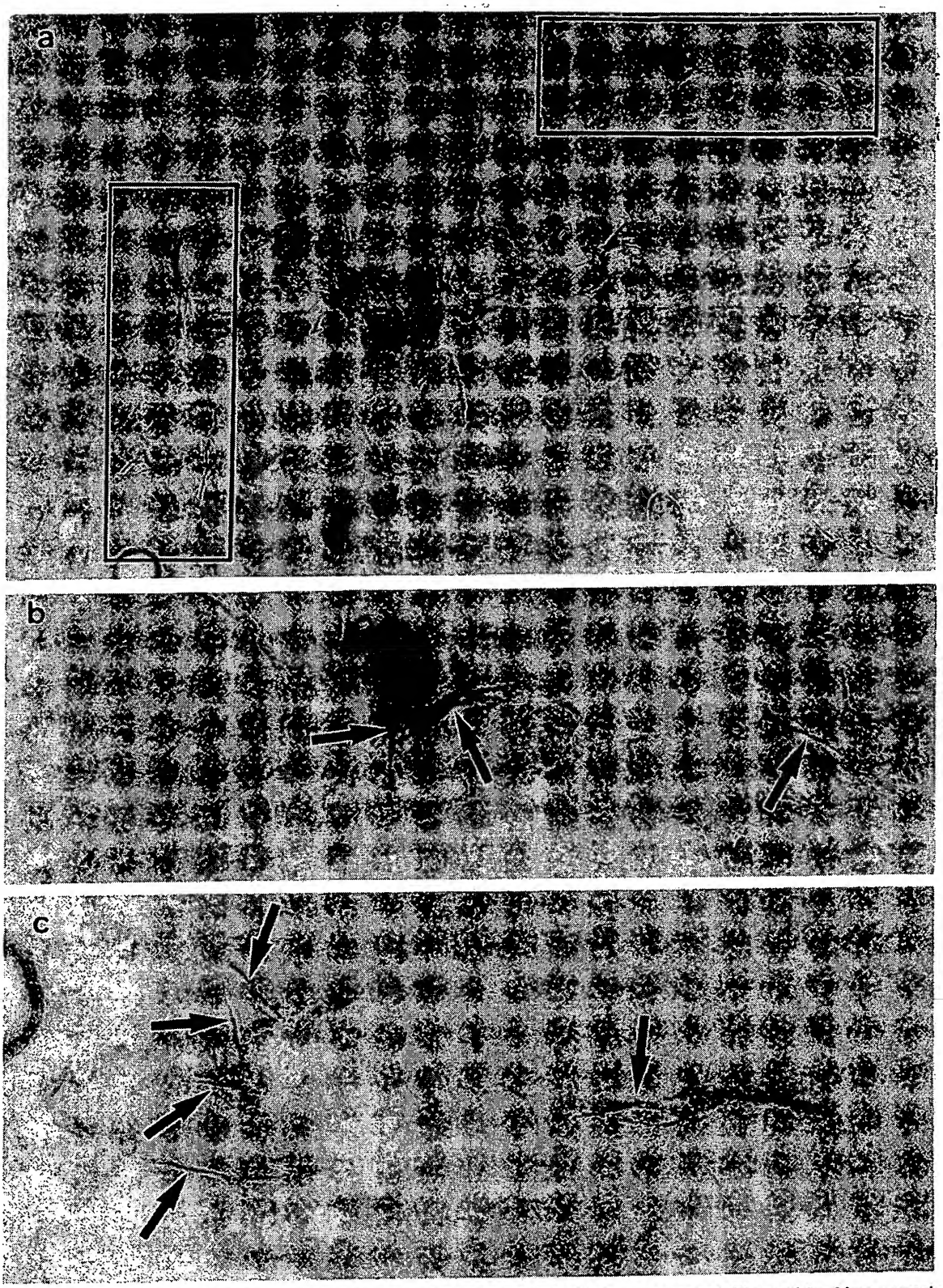

Figure 2. Electron micrographs of freshly isolated liver macrophages incubated with plasma-opsonized silica particles. Liver macrophages were incubated as in Fig. 1 (*+r-plasma*). After incubation for 10 min at 37°C, cells were fixed and processed for transmission electron microscopy. Shown are details from a macrophage not yet lysed. (*a*) Part of a digestive vacuole with ingested silica particles aggregated to bundles. The framed areas are shown at higher magnification in (*b*) and (*c*). (*b* and *c*) Silica particles are found outside the vacuoles and rupture of vacuolar lining membrane is evident.

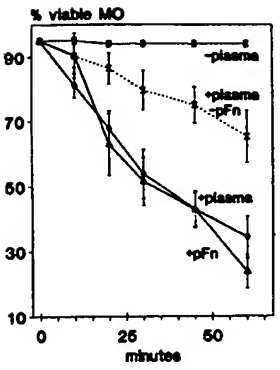

Figure 3. Isolated liver macrophages (*MO*) were incubated as in Fig. 1. Silica particles were previously incubated either with autologous plasma (+*plasma*, ◇), with fibronectin purified from autologous plasma (+*pFn*, △), with rat plasma after removal of fibronectin by gelatin-Sepharose (+plasma-pFn, ⧖) or was sham incubated (−*plasma*, ×). Comparison of the opsonizing agents show no difference in activity of whole plasma or purified fibronectin whereas removal of fibronectin from plasma diminishes toxic action significantly ($P < 0.005$ to plasma at 60 min). Values are the mean±SD of three to seven individual experiments.

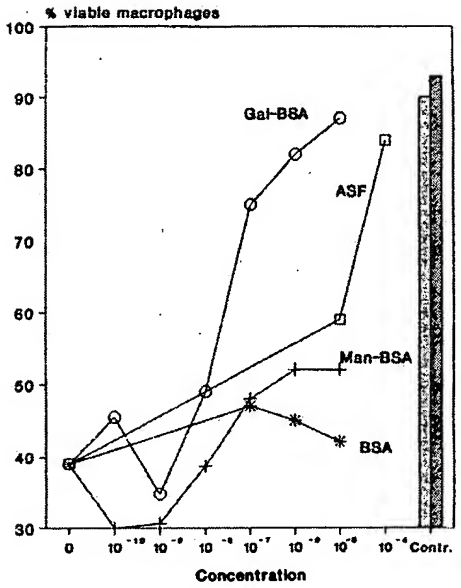

Figure 5. Concentration-dependent inhibition of toxic action by glycoconjugates. Isolated liver macrophages were incubated with rat fibronectin-opsonized silica particles for 60 min at 37°C in the presence of various concentrations of galactosylated bovine serum albumin (*Gal-BSA*), asialofetuin (*ASF*), mannosylated BSA (*Man-BSA*), or native BSA. Controls were macrophages incubated in the absence of silica (*hatched bar*) or with unopsonized silica (*gray bar*).

cal with rat or human plasma or purified pFn as opsonizing source (Fig. 6). Combination of low concentrations of competing monosaccharide GalNAc and pentapeptide showed synergistic increase in protection from killing (Fig. 7).

Deglycosylation of rat pFn-opsonized silica particles. Silica particles opsonized with purified rat fibronectin were treated with *N*-glycanase F for 6 h before cell incubation to determine the role of the glycan portion(s). The enzymatic removal of *N*-glycans resulted in significant reduction of silica toxicity (Fig. 8) compared with sham-treated particles. The small reduction in cell viability during the 60-min incubation period could be blocked to control values by addition of GRGDS (Fig. 8 *B*).

Binding experiments with pFn adsorbed onto colloidal gold. Since the toxic effect of silica particles depends on their uptake by the cells, binding experiments and quantitative electron microscopy to elucidate the role of the two receptor activities in initial recognition (binding) and/or uptake of opsonized particles were performed. Quartz dust needles contain little electron scattering elements and thus are barely visible as single particles in transmission electron microscopy. The silica visible in Fig. 2 is aggregated to bundles and is thus recognizable. These conditions, however, allow no quantitative measurement of binding. Therefore fibronectin-coated collodidal gold particles (pFn-Au) were used in these experiments. Macrophages were incubated with pFn-Au at 4°C with or without monosaccharides, pentapeptide, or the mixture. The amount of particles bound per micrometer of plasma membrane was determined on electron micrographs of the fixed and processed specimen. As shown in Fig. 9, binding of pFn-Au was completely inhibited by GalNAc (significantly different from binding in Fig. 9 *A*: $P < 0.001$) but not by GlcNAc (no significant difference to Fig. 9 *A*). In contrast, addition of GRGDS at highest concentration (2 mg/ml) did not lead to complete inhibition of surface binding (significantly different from GalNAc-inhibition: $P < 0.001$), although uptake at 37°C was com-

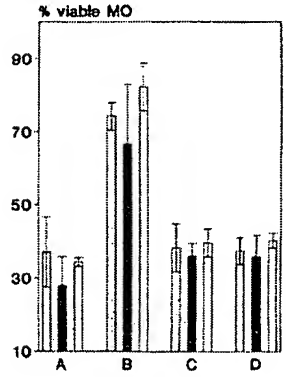

Figure 4. Inhibition of macrophage (*MO*) lysis by monosaccharides. Liver macrophages were incubated as in Fig. 1 for 60 min at 37°C before viability tests. Cells were incubated with: (*A*) pFn- or plasma-opsonized silica particles only; (*B*) as in (*A*), plus 80 mM *N*-acetyl-D-galactosamine; (*C*) as in (*A*), plus 80 mM GlcNAc; (*D*) as in (*A*), plus 80 mM mannose. Particles were opsonized either with rat plasma (*gray bars*) or with rat fibronectin (*hatched bars*) or with human plasma (*open bars*). *N*-acetyl-D-galactosamine significantly protected cells from toxic action ($P \ll 0.0001$ between values in *B* and *C*). Values are the mean±SD of three to five individual experiments.

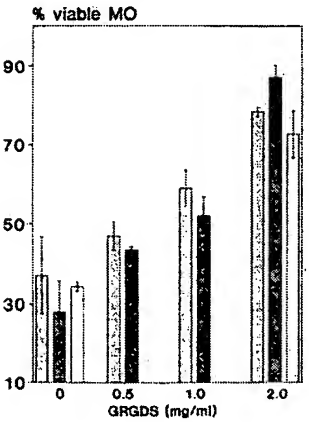

Figure 6. Inhibition of silica-mediated toxicity by the pentapeptide GRGDS. Isolated liver macrophages were coincubated with silica particles opsonized with rat plasma (*gray bars*), with rat fibronectin (*hatched bars*), or with human plasma (*open bars*). After 60 min at 37°C in the presence of the pentapeptide GRGDS at concentrations indicated, viability of macrophages (*MO*) was assessed by trypan blue exclusion. Values at 2.0 mg/ml GRGDF are significantly different from 0: $P \ll 0.0001$. Values are the mean±SD of three to four individual experiments.

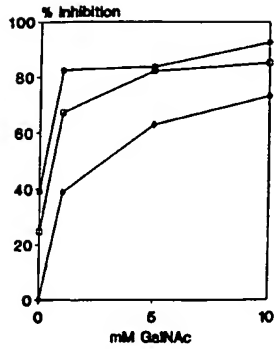

Figure 7. Synergistic action of GalNAc and pentapeptide-mediated inhibition. Isolated macrophages were incubated with rat pFn-opsonized silica for 60 min at 37°C in the presence of GalNAc concentrations indicated plus or minus pentapeptide. Viability of macrophages was 27% without inhibitors and 93% with sham-treated silica. (◇) no peptide present, (□) plus 0.5 mg/ml pentapeptide, (•) plus 1.0 mg/ml pentapeptide. Values are the mean of two to four individual experiments.

pletely blocked (not shown). The combination of 10 mM GalNAc and 1.0 mg/ml pentapeptide leads to total inhibition.

Discussion

Fibronectin is a multifunctional protein (for reviews see references 15–17) supporting, for instance, cell attachment and spreading of eucaryotes, bacterial cell adhesion, binding to a large number of substrates, and triggering a variety of cellular responses, including phagocytosis.

All but one of the functions listed above are now mapped to specific areas of the fibronectin molecule, only the phagocytosis-mediating or -enhancing activity is not yet clearly ascribable to a specific part of the molecule.

The experiments described here strongly support a dominant role for fibronectin as the prime opsonizing signal rendering silica particles recognizable for liver macrophages: comparison of all uptake and inhibition experiments did not show any difference whether whole plasma or purified pFn was used,

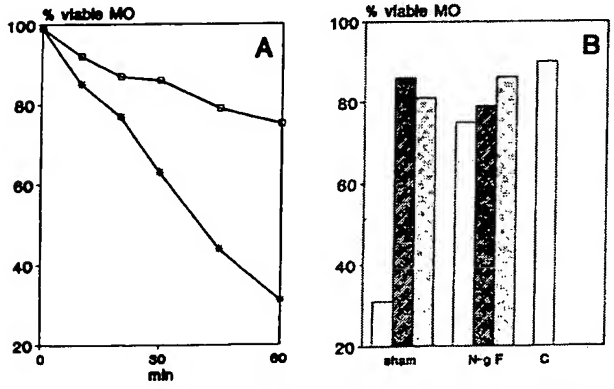

Figure 8. *N*-glycanase F treatment of rat pFN-opsonized silica reduces its macrophage toxicity. Rat pFn-opsonized silica particles were incubated with *N*-glycanase F or sham incubated as described in Methods before addition to isolated macrophages. (*A*) Time dependence of silica-mediated macrophage (*MO*) killing (□) *N*-glycanase F-treated particles, (•) sham-treated particles. (*B*) Inhibition of killing during an incubation of 60 min at 37°C with sham-treated pFn-silica (*sham*) or with *N*-glycanase-treated pFn-silica (*N-g-F*). Control (*C*) was with sham-incubated silica (as *–plasma* in Fig. 1). (*Open bars*) no inhibitor added; (*dark bars*) in the presence of GalNAc (80 mM); (*gray bars*) in the presence of GRGDS (2 mg/ml).

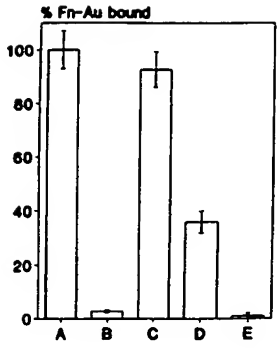

Figure 9. Competitive inhibition of binding of fibronectin-opsonized particles to liver macrophages. Colloidal gold particles were coated with purified rat fibronectin (*Fn-Au*), isolated liver macrophages were coincubated for 10 min at 4°C, and cells were processed for transmission electron microscopy. The number of particles bound to cells was measured on electron micrographs. *A*, no additives; *B*, plus GalNAc (80 mM); *C*, plus GlcNAc (80 mM); *D*, plus GRGDS (2 mg/ml); *E*, plus GalNAc (10 mM) and GRGDS (1 mg/ml). Data are the mean±SD from 35 to 45 individual cells micrographed from two different experiments. 100% binding equals 11.3±5.8 Fn-Au particles/10 μm plasma membrane.

suggesting that in the presence of pFn this appears to be the dominant opsonizing molecule. In the presence of pFn-free plasma, silica-mediated macrophage killing is slowed down significantly. This finding is in agreement with the description of high affinity fibronectin receptors on isolated rat liver Kupffer cells (18).

The immobilized fibronectin is recognized by two different receptor activities present on the rat phagocyte and both binding activities have to act in synergy to mediate effective uptake: interference with either one of the two modes of recognition will lead to uptake blockade as visualized by the protective effect for cell viability. This double recognition mode may also explain the relatively high affinity of binding measured for fibronectin-opsonized particles on rat Kupffer cells (18), which was found to be one to two orders of magnitude higher than those measured for RGD recognition by integrins.

A number of very different observations suggest synergism of RGD-recognizing integrins with other binding activities. On T lymphocytes (19) and melanoma cells (20), a second integrin ($\alpha_4\beta_1$) recognizes a peptide sequence (Leu-Asp-Val) in the IIICS domain of the fibronectin molecule. Immobilized but not soluble fibronectin in synergy with anti-CD3 antibodies supports activation and proliferation of naive T lymphocytes, whereas no effect is found with either of the two factors alone (21). Experimental data on adhesion of microvascular endothelial cells (22) and of fibroblasts (23) on fibronectin-coated surfaces as well as uptake of fibronectin-coated beads by gingival fibroblasts (24) also suggest involvement of additional recognition modes.

The interaction of immobilized but not soluble fibronectin with immobilized CRP has been observed (25–27) and recently we could show that the interaction of a membrane-associated form of CRP (mCRP) on rat liver macrophages (28) with immobilized fibronectin occurs via a low-affinity galactose-specific binding (14).

I therefore now propose that the opsonic activity of the glycoprotein fibronectin partly resides in the peptide sequence of the central cell binding domain of this molecule and partly within its glycan portions, which so far have not been associated with any function besides protection from proteolysis (29).

On the other hand evidence is increasing that low-affinity carbohydrate-specific interactions synergize with attachment

signals as has been recently shown very elegantly for the low-affinity binding (rolling) via the selectin PADGEM as a prerequisite for the leucocyte adhesion through integrins LFA-1, Mac-1 (30). In direct analogy to these results, I propose that the low-affinity interaction of mCRP with fibronectin-coated particles leads to a slowdown of these particles within the circulation, analogous to the leucocyte rolling, as a prerequisite for the development of stable integrin-mediated binding. This proposal is supported by the binding inhibition experiments.

The competition data are of potential interest in prevention of pulmonary diseases associated with toxic and/or excessive dust burden. Both fibronectin as well as CRP are known constituents of broncho-alveolar lavage fluid and were recently described to increase in acute inflammatory processes (31, 32). Work is now in progress to examine silica uptake and receptor expression in rat alveolar macrophages.

Acknowledgments

I thank Andrea Schlömer, Marija Lovrencic, and Ulla Lammersen for excellent technical assistance; Sabine Wenzel-Unger for photographic assistance; and Ingeburg Werner for typing the manuscript.

This work was supported by a grant from the Deutsche Forschungsgemeinschaft (Ko 806/3-1).

References

1. O'Rourke, E. J., S. B. Halstead, A. C. Allison, and T. A. E. Plattes-Mills. 1978. Specific lethality of silica for human peripheral blood mononuclear phagocytes, in vitro. *J. Immunol. Methods.* 19:137–151.

2. Allison, A. C., J. S. Harington, and M. Birbeck. 1966. An examination of the cytotoxic effects of silica on macrophages. *J. Exp. Med.* 124:141–154.

3. Heppleston, A. G., and J. A. Styles. 1967. Activity of a macrophage factor in collagen formation by silica. *Nature (Lond.).* 214:521–522.

4. Davis, G. S. 1986. Pathogenesis of silicosis: current concepts and hypotheses. *Lung.* 164:139–154.

5. Ziskind, M., R. N. Jones, and H. Weill. 1976. Silicosis. *Am. Rev. Respir. Dis.* 113:643–665.

6. Zisman, B., E. F. Wheelock, and A. C. Allison. 1971. Role of macrophages and antibody in resistance of mice against yellow fever virus. *J. Immunol.* 107:236–243.

7. Levy, M. H., and E. F. Wheelock. 1975. Effects of intravenous silica on immune and nonimmune functions of the murine host. *J. Immunol.* 115:41–48.

8. Chaouat, G., and J. G. Howard. 1976. Influence of reticuloendothelial blockade on the induction of tolerance and immunity by polysaccharides. *Immunology.* 30:221–227.

9. Saba, T. M. 1970. Physiology and physiopathology of the reticuloendothelial system. *Arch. Intern. Med.* 129:1031–1052.

10. Brosnan, C. F., M. B. Bornstein, and B. R. Bloom. 1981. The effects of macrophage depletion on the clinical and pathologic expression of experimental allergic encephalomyelitis. *J. Immunol.* 126:614–620.

11. Oschilewski, M., E. Schwab, U. Kiesel, U. Opitz, K. Stünkel, V. Kolb-Bachofen, and H. Kolb. 1986. Administration of silica or monoclonal antibody to Thy-1 prevents low-dose streptozotocin-induced diabetes in mice. *Immunol. Lett.* 12:289–294.

12. Schlepper-Schäfer, J., and V. Kolb-Bachofen. 1988. Red cell aging results in a change of cell surface carbohydrate epitopes allowing for recognition by galactose-specific receptors of rat liver macrophages. *Blood Cells. (NY).* 14:259–269.

13. Engvall, E., and E. Ruoslahti. 1977. Binding of soluble form of fibroblast surface protein fibronectin, to collagen. *Int. J. Cancer* 20:1–5.

14. Kolb-Bachofen, V., and F. Abel. 1991. Participation of D-galactose-specific receptors on liver macrophages in recognition of fibronectin-opsonized particles. *Carbohydr. Res.* 214:201–213.

15. Rouslahti, E. 1988. Fibronectin and its receptors. *Annu. Rev. Biochem.* 57:375–413.

16. Saba, T. M. 1989. Trends in shock research. Fibronectin: relevance to phagocytic host response to injuri. *Circ. Shock.* 29:257–278.

17. D'Souza, S. E., M. H. Ginsberg, and E. F. Plow. 1991. Arginyl-glycyl-aspartic acid (RGD): a cell adhesion motif. *Trends Biochem. Sci.* 16:246–250.

18. Cardarelli, P. M., F. A. Blumenstock, P. J. McKeown-Longo, T. M. Saba, J. E. Mazurkiewicz, and J. A. Dias. 1990. High-affinity binding of fibronectin to cultured Kupffer cells. *J. Leukocyte Biol.* 48:426–437.

19. Wayner, E. A., A. Garcia-Pardo, M. J. Humphries, J. A. McDonald, and W. G. Carter. 1989. Identification and characterization of the T lymphocyte adhesion receptor for an alternative cell attachment domain (CS-1) in plasma fibronectin. *J. Cell Biol.* 109:1321–1330.

20. Mould, A. P., A. Komoriya, K. M. Yamada, and M. J. Humphries. 1991. The CS5 peptide is a second site in the IIICS region of fibronection recognized by the integrin $\alpha_4\beta_1$. *J. Biol. Chem.* 266:3579–3585.

21. Cardarelli, P. M., S. Yamagata, W. Scholz, M. A. Moscinski, and E. L. Morgan. 1991. Fibronectin augments anti-CD3-mediated IL-2 receptor (CD25) expression on human peripheral blood lymphocytes. *Cell. Immunol.* 135:105–117.

22. Cheng, Y.-F., R. I. Clyman, J. Enenstein, N. Waleh, R. Pytela, and R. H. Kramer. 1991. The integrin complex $\alpha_v\beta_3$ participates in the adhesion of microvascular endothelial cells to fibronectin. *Exp. Cell Res.* 194:69–77.

23. Ylänne, J. 1990. RGD peptides may only temporarily inhibit cell adhesion to fibronectin. *FEBS (Fed. Eur. Biochem. Soc.) Lett.* 267:43–45.

24. McKeown, M., G. Knowles, and C. A. G. McCulloch. 1990. Role of the cellular attachment domain of fibronectin in the phagocytosis of beads by human gingival fibroblasts in vitro. *Cell Tissue Res.* 262:523–530.

25. Salonen, E. M., T. Vartio, K. Hedman, and A. Vaheri. 1984. Binding of fibronectin by the acute phase reactant C-reactive protein. *J. Biol. Chem.* 259:1496–1501.

26. Du Clos, T. W. 1989. C-reactive protein reacts with the U1 small nuclear ribonucleoprotein. *J. Immunol.* 143:2553–2559.

27. Swanson, S. J., M. M. McPeek, and R. F. Mortensen. 1989. Characteristics of the binding of human C-reactive protein (CRP) to laminin. *J. Cell. Biochem.* 40:121–132.

28. Kempka, G., P. H. Roos, and V. Kolb-Bachofen. 1990. A membrane-associated form of C-reactive protein is the galactose-specific particle receptor on rat liver macrophages. *J. Immunol.* 144:1004–1009.

29. Olden, K., R. M. Pratt, and K. M. Yamada. 1978. Role of carbohydrates in protein secretion and turnover: effects of tunicamycin on the major cell surface glycoprotein of chick embryo fibroblasts. *Cell.* 13:461–473.

30. Lawrence, M. B., and T. A. Springer. 1991. Leukocytes roll on a selectin at physiologic flow rates: distinction from and prerequisite for adhesion through integrins. *Cell.* 65:859–873.

31. Nagy, B., É. Katona, J. Erdei, L. Karmazsin, and J. Fachet. 1991. Fibronectin in bronchoalveolar lavage fluid and plasma of dogs with acute inflammation of the lungs. *APMIS (Acta Pathol. Microbiol. Immunol. Scand.)* 99:387–390.

32. Li, J. J., R. L. Sanders, K. P. McAdam, C. A. Hales, B. T. Thompson, J. A. Gelfand, and J. F. Burke. 1989. Impact of C-reactive protein (CRP) on surfactant function. *J. Trauma.* 29:1690–1697.

JOURNAL OF SURGICAL RESEARCH 45, 82–89 (1988)

Use of Ricin A-Chain to Selectively Deplete Kupffer Cells

MICHAEL E. ZENILMAN, M.D.,* MARIA FIANI, PH.D.,† PHILIP STAHL, PH.D.,† ELIZABETH BRUNT, M.D.,‡ AND M. WAYNE FLYE, M.D., PH.D.*

*Departments of *Surgery, †Physiology and Cell Biology, and ‡Pathology, Washington University School of Medicine, St. Louis, Missouri 63110*

Presented at the Annual Meeting of the Association for Academic Surgery, Orlando, Florida, November 1–4, 1987

We used the A-chain of the toxin ricin (RTA) as a toxin specific to Kupffer cells in mice. RTA is specifically taken up by the mannose receptor present exclusively in macrophages. Kupffer cells were quantitated by shifts in β-glucuronidase clearance and microscopic counts of cells which phagocytosed India ink. When compared to saline controls, 20 mg/kg of RTA intraperitoneally (divided over 4 days) or intraportally (single doses) significantly prolonged the $t_{1/2}$ half-life of β-glucuronidase by 270 ± 37 and 210 ± 8%, respectively. Kupffer cell numbers were significantly decreased by 27 ± 8 and 33 ± 16%. This effect persisted for at least 3 days after toxin administration. Despite effects on Kupffer cell number, minimal histological damage to liver, spleen, lung, and heart was noted. Higher doses of RTA or doses potentiated by ureteral ligation to prevent renal clearance resulted in prohibitive mortalities and histologic liver damage. Doses of *Hura crepitans* inhibitor, a toxin similar to RTA but not mannose-receptor specific, did not affect Kupffer cell numbers. We conclude that RTA given both intraperitoneally and intraportally at low doses is toxic specifically to Kupffer cells. Kupffer cell numbers can be indirectly measured by β-glucuronidase clearance.

INTRODUCTION

Ribosomal inactivating proteins (RIPs) are toxins which are able to kill cells in a 1:1 ratio by enzymatically inhibiting the 60 S subunit of the ribosome [1, 2]. The A-chain of the toxin ricin (RTA) is such a protein, 30,000 Da in size and containing mannose residues [1]. Recently, Simmons *et al.* [3] demonstrated that RTA is specifically taken up by rat bone marrow macrophages through mannose-receptor-mediated endocytosis. Similarly, Skilleter and Foxwell [4] have shown RTA to be taken up by rat hepatic nonparenchymal cells in a manner which is inhibited by D-mannose, while liver parenchymal cells showed only minimal nonspecific uptake of RTA. Since the mannose receptor is found exclusively on macrophages [5–8], the possibility was raised of using RTA as a toxin specific to Kupffer cells (liver specific macrophages).

As a toxin specific for Kupffer cells in mice, RTA was administered by three routes —intraperitoneal, intraperitoneal in the presence of ureteral obstruction, and intraportal injection. Kupffer cell function was measured by clearance of a mannose terminal glycoprotein, β-glucuronidase, which is cleared via mannose-receptor-mediated endocytosis [6]. Kupffer cell number was quantitated by microscopic counts of cells which phagocytosed carbon particles after an intravenous injection of India ink.

MATERIAL AND METHODS

Protocol

Female Balb/c mice weighing 20 g were used (Sasco, Indianapolis, IN) and were grouped into control and treated groups. Since initial single doses of ricin A-chain (RTA) intraperitoneally (ip) had no effect on Kupffer cell function or number ($n = 15$), the toxin was subsequently administered as (1) daily intraperitoneal doses for 4 days using 10 mg/kg RTA ($n = 4$), 20 mg/kg RTA ($n = 18$), and 30 mg/kg RTA ($n = 4$); (2) single

0022-4804/88 $1.50

ip doses of 15 mg/kg RTA in the presence of ureteral obstruction (administered 24 hr after bilateral ureteral ligation, $n = 8$); or (3) as a single intraportal (ipv) injection of 10 mg/kg RTA ($n = 4$), 20 mg/kg RTA ($n = 6$), or 30 mg/kg RTA ($n = 4$). For the last two groups, operations were performed under 50 mg/kg Nembutal anesthesia using clean technique. Control animals for each group received normal saline ($n = 4$). Ureters were ligated with 4-O silk ligatures 24 hr prior to toxin administration in Group 2. Doses of toxins are expressed as the *total* dose given to each animal. Mortalities are expressed as percentages for each treatment group. The Kupffer cell population was assessed 24 hr after the last dose of toxin.

Toxins

Ricin was purified from castor beans (*Ricinus communis*) purchased from Hummert's Seed Company (St. Louis), by the previously described protocol [9]. Briefly, after binding 70 mg of intact ricin to a 1 × 30-cm galactose–Sepharose column, ricin A-chain was separated from B-chain by eluting with 250 cc of 1 *M* 2-mercaptoethanol in 0.2 *M* Tris, pH 6.6. The eluate was passed through a second 1-cc galactose–Sepharose column (to bind any residual ricin and free B-chain), concentrated by Amicon PM-10 ultrafiltration, and dialyzed against multiple volumes of Tris-buffered saline 24 hr prior to the experiments. The A-chain thus purified was contaminated with <0.02% intact ricin.

A toxin similar to RTA, *Hura crepitans* inhibitor (HCI), also a member of the ribosomal-inactivating protein family, was isolated as described in [10] from the sap of the *Hura crepitans* plant, kindly provided by Fairchild Botanical Gardens (Miami, FL). Sap (10 cc) was diluted with 10 vol of phosphate-buffered saline, pH 7.2, and dialyzed against multiple volumes of the same buffer for 24 hr at 4°C. The suspension was then centrifuged at 28,000*g* for 30 min and the supernatant was chromatographed through acid-treated Sepharose 6B. The eluate was then dialyzed against a 5 m*M* phosphate buffer, pH 6.5, overnight, centrifuged at 28,000*g* for 30 min, and then applied to a CM52 column. Elution of the column was performed with a 500-cc zero to 0.3 *M* NaCl gradient in the same buffer, 2-cc fractions were analyzed at 280 nm, and peak No. 5 was pooled.

The presence of toxin in each batch isolated was confirmed by 10% polyacrylamide gel electrophoresis (each toxin is 28,000–32,000 Da in size). Concentration was determined by absorbance at 280 nm. Activity was established by ability to inhibit protein synthesis ([^{35}S]methionine incorporation after a 4-hr pulse of 5 μCi) in cultured rabbit alveolar macrophages [3]. Typically, the ID_{50} of RTA, i.e., the concentration needed to inhibit 50% of [^{35}S]methionine incorporation in cultured macrophages (5×10^5 cells/cc RPMI media) was 0.1 μg/ml.

Assay of Kupffer Cell Population

The integrity of the Kupffer cell population at 24 hr (and at 3 and 7 days for two groups of animals receiving 20 mg/kg RTA intraperitoneally) after treatment with toxins was assessed by two methods:

(a) Clearance of the lysosomal enzyme β-glucuronidase. With a depleted population of cells, the ability of intact animals to clear this enzyme specifically through the mannose receptor [8] should be impaired, the clearance curve should shift to the right and the calculated half-life ($t_{1/2}$) should increase. β-glucuronidase was isolated by methods described in [11] from female rat preputial glands purchased from Harlan (Omaha, NE). After anesthesia with 50 mg/kg Nembutal, 0.1 cc of a 1.0 μg/ml solution of β-glucuronidase was injected intravenously and 100-μl venous samples (from the tail) were taken at 0, 1, 2.5, 5, 10, and 15 min and stored at 4°C. Serum β-glucuronidase activity was determined by incubation of 5 μl of serum diluted in 95 μl water with 100 μl of 4 m*M* 4-methyl-

umbelliferone glucuronide (Sigma, St. Louis) dissolved in 0.1 *M* acetate buffer, pH 4.5, at 37°C for 1 hr. The reaction was then stopped with 1.8 cc of 67 m*M* NaCl, 130 m*M* glycine, 83 m*M* $NaCO_3$, pH 10, and the level of free 4-methylumbelliferone determined in a Forand fluorometer with Corning filters (primary No. 5860, secondary No. 3387 and No. 5583). Enzyme activity was expressed as a percentage of the level observed 1 min after completion of the β-glucuronidase infusion, and a clearance curve was generated. The half-life ($t_{1/2}$) of β-glucuronidase was estimated by fitting the clearance curve to a linear line in a semi-log plot.

(b) Kupffer cell numbers were determined by phagocytosis of intravenously injected carbon particles. After completion of the clearance test, 0.1 cc of India ink (Higgins Ink, Faber–Castell Corp., Newark, NJ), previously filtered through a 20-μ*M* Millipore filter and diluted 1/10 in normal saline, was injected intravenously into treated and control mice. Thirty minutes later, the animals were sacrificed. Animals not surviving 30 min were excluded from the study. The tissues were fixed in formalin, and standard H and E stains were prepared. Cells containing carbon were counted in 16 high power fields (HPF, 100×) in a blinded fashion. Values were expressed as number of cells per high power field. Control specimens of kidney, heart, lung, and spleen were also examined for each animal.

Statistics. All values are expressed as means ± SEM. Comparisons between treated and matched control groups were analyzed by unpaired student's *t* tests, and statistical significance was defined at the $P < 0.05$ level.

RESULTS

Normal Saline Groups

Mice treated with normal saline intraperitoneally ($n = 5$) or intraportally ($n = 4$) had $t_{1/2}$ of β-glucuronidase of 7.4 ± 0.3 and 6.9 ± 3.5 min, respectively. Clearance was completely inhibited by the presence of 50 mg/ml yeast mannan ($t_{1/2} > 100$ min, $n = 2$), confirming mannose-receptor-mediated uptake. Kupffer cell counts for both groups were also similar, with respective values of 14.1 ± 2.3 and 12.6 ± 0.8 cells per HPF (Fig. 6A). All animals treated with saline showed no sign of illness while most animals treated with RTA did show anorexia, weight loss, lethargy, and piloerection.

Histology

Samples of liver, spleen, lung, heart, and kidney were examined histologically in each group of animals. In general, all groups showed no structural damage (necrosis, ischemia, or thrombosis) to the liver, heart, lung, or spleen. In the ureteral obstruction group, evidence of hydronephrosis was present in the kidneys, while the kidneys were normal in all other groups.

Kupffer Cell Counts and β-Glucuronidase Clearance

Intraperitoneal ricin A-chain. Single doses of RTA (1 to 40 mg/kg, $n = 15$) had no effect on β-glucuronidase clearance or Kupffer cell counts (data not shown). Doses divided over 4 days, however, showed a dose-related response (Figs. 1 and 2). A total dose of 10 mg/kg caused a slight increase in β-glucuronidase half-life (8.6 ± 2.5 min, P = NS) and a slight decrease in Kupffer cell counts (11.6 ± 1.1 cells/HPF, P = NS) with no mortality within the group ($n = 4$). RTA, 20 mg/kg, ip, divided over 4 days, increased the $t_{1/2}$ to 20 ± 7.3 min ($P < 0.05$ compared to saline control values) and decreased Kupffer cell counts to 10.3 ± 0.8 cells/HPF ($P < 0.05$ compared to saline controls), but had a mortality rate of 28% ($n = 7$). Divided doses of 30 and 40 mg/kg RTA had mortality rates of over 50% ($n = 8$). Although surviving animals had depressed Kupffer cell counts, all specimens showed histologic evidence of hepatic sinusoidal congestion and diffuse mild vacuolization of hepatocytes.

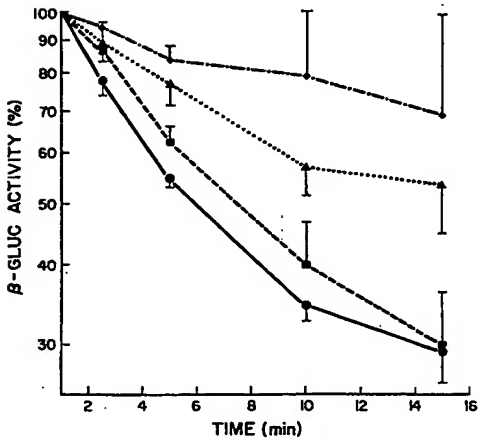

FIG. 1. Clearance of intravenously injected β-glucuronidase in mice 24 hr after completion of intraperitoneal administration of RTA. (●) Normal saline control, (■) 10 mg/kg RTA divided over 4 days, (▲) 20 mg/kg RTA divided over 4 days, (♦) 15 mg/kg RTA given as one dose 24 hr after bilateral ureteral ligation. Values are expressed as means ± SEM.

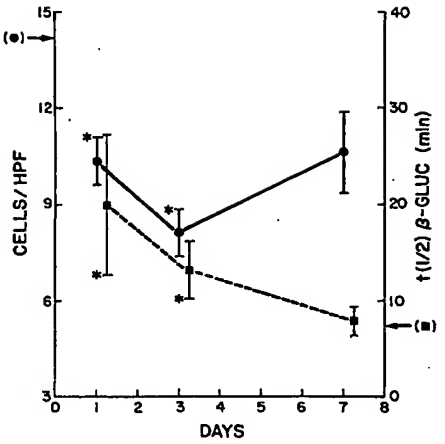

FIG. 3. Recovery of Kupffer cell counts (●) and β-glucuronidase clearance (■) 1, 3, and 7 days after intraperitoneal RTA (20 mg/kg divided over 4 days). Control values for cell counts and β-glucuronidase half-lives ($t_{1/2}$) are shown on y axis. Kupffer cell counts remain depressed for 3 days after drug administration and approach original values by 7 days. Half-lives start to return to normal by 3 days and at 7 days are back to baseline. *$P < 0.05$ compared to saline control.

In order to determine the duration of Kupffer cell depletion by RTA, 11 additional animals were treated with RTA and were studied at 3 days ($n = 4$) or 7 days ($n = 4$) after receiving 20 mg/kg RTA ip (mortality = 27%). At 3 days Kupffer cell counts remain depressed (8.13 ± 0.74 cells/HPF, $P < 0.05$ compared to control), while the half-life of β-glucuronidase had apparently begun to recover (13.2 ± 3 min, $P < 0.05$ to control) (Fig. 3). At 7 days, both Kupffer cell counts (10.63 ± 1.25 cells/HPF) and β-glucuronidase half-life (7.89 ± 1.5 min) had recovered such that they were not statistically significantly different when compared to saline controls.

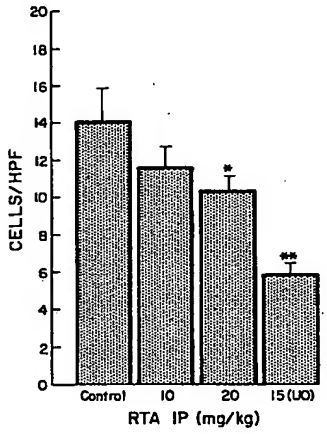

FIG. 2. Kupffer cell counts (cells/HPF; 16 fields averaged; magnification, 100×) in mice 24 hr after intraperitoneal RTA. The control, 10 and 20 mg/kg, doses were administered as divided doses over 4 days, and the 15 mg/kg (uo) dose was administered as a single dose 24 hr after bilateral ureteral ligation (uo). *$P < 0.05$ compared to control. **$P < 0.05$ compared to control and 20 mg/kg RTA.

Since RTA has a molecular weight of 30,000 Da, and has been shown to be present in the kidney after an intravenous dose (up to 12% of the injected dose [12]), a group of mice were given ip injections 24 hr after bilateral ureteral obstruction. A single ip dose of 15 mg/kg RTA in the presence of ureteral obstruction (Figs. 1 and 2) increased the $t_{1/2}$ of β-glucuronidase to over 20 min ($n = 3$) and depressed Kupffer cell counts to 5.9 ± 0.42 (significant when compared to both

saline controls and to 20 mg/kg RTA divided over 4 days) (Fig. 6C). Unfortunately, this group of eight animals showed a mortality rate of 63%, and histologic specimens of the liver showed pronounced portal venous and sinusoidal congestion in addition to the Kupffer cell depletion.

Intraportal ricin A-chain. Single doses of ricin A-chain intraportally had more pronounced effects on the Kupffer cells than intraperitoneal doses, with less mortality. Ten milligrams per kilogram ipv ($n = 4$) and 20 mg/kg ipv ($n = 6$) caused only slight increases in the $t_{1/2}$ of β-glucuronidase, 7.3 ± 2.5 min (P = NS) and 14.7 ± 1.2 min ($P < 0.05$ compared to saline controls), respectively (Fig. 4), while significantly reducing KC counts to 9.31 ± 1.4 and 8.38 ± 2.3 cells/HPF ($P < 0.05$ compared to controls, Figs. 5 and 6B). No mortalities occurred in either group, while doses of 30 mg/kg and above were associated with mortalities of 100% ($n = 4$).

β-Glucuronidase clearance. β-Glucuronidase clearance seemed to be a fairly accurate measure of absolute Kupffer cell counts. Overall, the β-glucuronidase $t_{1/2}$ correlated well with KC counts, with a correlation coefficient of $r^2 = 0.44$, $P < 0.05$. This indicates that this test is a good indirect measure of cell number.

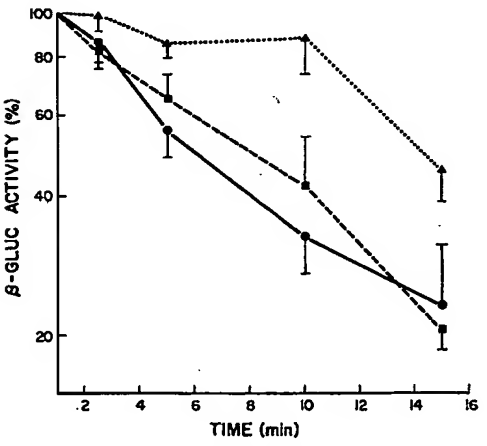

FIG. 4. Clearance of intravenously injected β-glucuronidase in mice 24 hr after a single intraportal injection of RTA. (●) Saline control, (■) 10 mg/kg ipv, (▲) 20 mg/kg ipv. Values are expressed as means ± SEM.

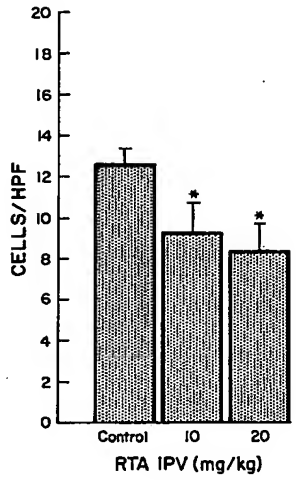

FIG. 5. Kupffer cells counts (cells/HPF; 16 fields averaged; magnification, 100×) in mice 24 hr after intraportal RTA (10 or 20 mg/kg) given as a single dose. *$P < 0.05$ compared to saline control.

Hura crepitans inhibitor. Rabbit alveolar macrophages (5×10^5 cells/ml) when cultured *in vitro* for 18 hr with increasing doses of HCI showed a dose-dependent inhibition of protein synthesis (data not shown). The ID_{50} was 5 μg/ml compared to 0.1 μg/ml for RTA. Unlike RTA, HCI showed no inhibition of activity in the presence of yeast mannan, indicating a non-mannose-receptor-mediated event. We therefore used HCI *in vivo* as a toxin for non-mannose-receptor-mediated uptake. Animals exposed to 20 mg/kg intraperitoneally divided over 4 days had mortalities of 100% ($n = 4$). When 10 mg/kg was given divided over 2 days, mice showed 12.2 ± 2 ($n = 4$) Kupffer cells/HPF (Fig. 6D). Histology of the liver in three animals showed numerous scattered acidophilic bodies; two animals showed pancreatitis. Although more toxic *in vivo* than RTA, HCI did not affect the mannose-receptor-bearing Kupffer cells by histologic criteria. β-Glucuronidase clearance tests in these animals were not performed.

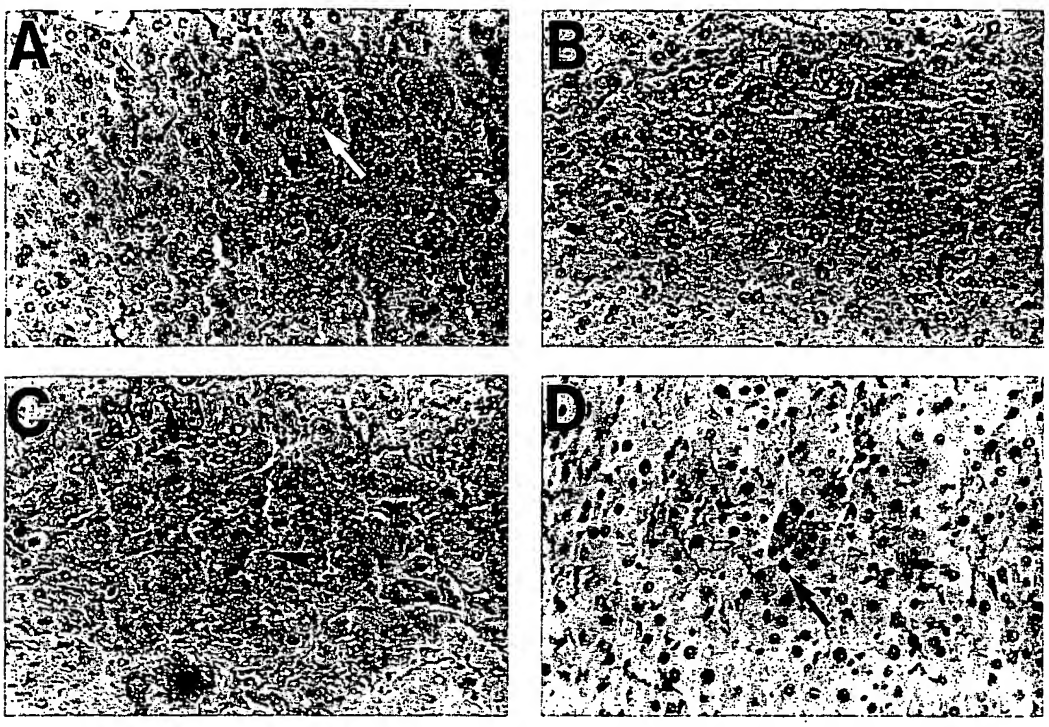

FIG. 6. Typical histologic specimens of liver tissue from experimental animals. All animals were pretreated with India ink 30 min prior to sacrifice, highlighting the Kupffer cells (white arrow in (A)). (A) Normal saline control; (B) 20 mg/kg RTA ipv 24 hr prior to sacrifice; (C) 15 mg/kg RTA ip in the presence of ureteral obstruction, arrowhead denotes hepatic congestion; (D) HCl 20 mg/kg ip in two divided doses with final dose 24 hr prior to sacrifice, black arrow denotes acidophilic body. Magnification, 90×.

DISCUSSION

We used the A-chain of the toxin ricin (RTA) as a toxin specific to Kupffer cells *in vivo*. The toxin is apparently specific to Kupffer cells; the most effective dose (i.e., most depletion with least mortality) was 20 mg/kg ipv or ip. At this dose, Kupffer cells were depleted by 33 and 27%, respectively. No histologic evidence of injury to the liver, spleen, kidney, heart, or lung was seen. This effect appeared to last for at least 3 days, and by 1 week evidence of Kupffer cell repopulation was found.

This *in vivo* data parallels previous work performed with RTA. Skilleter and Foxwell [4] and Simmons *et al.* [3] showed that RTA is specifically toxic *in vitro* to rat macrophages and liver nonparenchymal cells by mannose-receptor-mediated endocytosis. Bourrie *et al.* [12] showed that immunotoxins formed by linking the antibody T101 (specific for the T1 antigen) to RTA are preferentially cleared *in vivo* by the liver in a manner inhibited by yeast mannan (i.e., probably through the mannose-receptor-bearing Kupffer cells). We postulate that in our model, mouse Kupffer cells are affected via the mannose receptor. In animals depleted of Kupffer cells, decreases in the clearance of the mannosylated glycoprotein β-glucuronidase were observed. Also, in experiments using HCl, a toxin similar to RTA but which is not mannose receptor specific, Kupffer cell numbers were unaffected and evidence of damage to liver and pancreatic parenchyma was noted. This was probably due to specific uptake of the toxin through a

different receptor or by a nonspecific mechanism.

Doses of RTA greater than 20 mg/kg ip or ipv resulted in prohibitive mortality rates. Attempts to potentiate the effects of the drug through bilateral ureteral obstruction, thereby blocking renal clearance of RTA, similarly resulted in lower KC counts, but yielded mortalities greater than 50% with histologic evidence of hepatic sinusoidal congestion. The increased mortality in these groups may be secondary to either nonspecific toxicity or to disruption of hepatic sinusoidal tissue after elimination of the Kupffer cells. Derenzini *et al.* [13] in one of the only studies on mechanism of toxicity of intact ricin to a host, showed that after injection of rats with ricin the liver was primarily affected. Electron microscopic examination revealed that severe sinusoidal destruction occurred first, after which thrombosis and necrosis of hepatocytes became evident. Our findings of hepatic congestion may therefore be secondary to this effect in the sinusoids. In addition, greater than 30–40% depletion of Kupffer cells may not be compatible with life.

If, however, the cause of the higher mortality is nonspecific toxicity, we may obtain a higher specific toxicity by using RTA linked to an anti-macrophage antibody or by altering RTA to enhance its receptor specificity. Alternatively, one may use intact ricin, either linked to an antibody or even alone at sublethal doses as a specific toxin. Recent evidence has shown that hepatic nonparenchymal cells are 100 times more sensitive to intact ricin than are parenchymal cells [14].

Selective depletion of Kupffer cells may be a useful tool in hepatic transplantation. Kupffer cells, endothelial cells, and, in certain conditions, bile duct cells have been shown to express the class II (Ia) antigen of the major histocompatability complex [15], while hepatocytes do not. Cells expressing Ia, particularly macrophages, mediate the presentation of foreign antigen to T cells (thereby stimulating the immune response). Engemann *et al.* [16] have shown that in rat liver allografts, Ia expression increased in Kupffer cells during periods of rejection and cells became Ia negative when transplantation tolerance occurred (e.g., after cyclosporin A administration, survival >100 days). Kupffer cells may be considered to act as an important mediator of liver allograft rejection. Selectively depleting the Kupffer cell population in donor hepatic tissue by using specific toxins may decrease the immunogenicity of the liver and modulate the development of subsequent rejection.

Our observed close correlation of Kupffer cell counts and β-glucuronidase clearance indicates that clearance can be used as an indirect, noninvasive measure of Kupffer cell numbers in mice (and rats [6]). Theoretically, one could pretreat a donor animal with a toxin specific to Kupffer cells until a predetermined shift occurs in the β-glucuronidase clearance. The subsequently transplanted Kupffer cell-depleted liver would then be suitable for study of development of rejection.

REFERENCES

1. Barbieri, L., and Stirpe, F. Ribosome inactivating proteins from plants: Properties and possible uses. *Cancer Surveys* 1:489, 1982.
2. Stirpe, F., and Barbieri, L. Ribosome inactivating proteins up to date. *FEBS Lett.* **195**: 1, 1986.
3. Simmons, B. M., Stahl, P. T., and Russell, J. H. Mannose receptor mediated uptake of ricin toxin and ricin A chain by macrophages. *J. Biol. Chem.* **261**: 7912, 1986.
4. Skilleter, D. N., and Foxwell, B. M. J. Selective uptake of ricin A chain by hepatic nonparenchymal cells *in vitro*. *FEBS Lett.* **196**: 344, 1986.
5. Ashwell, G., and Harford, J. Carbohydrate specific receptors of the liver. *Ann. Rev. Biochem.* **51**: 531, 1982.
6. Schlesinger, P., Rodman, J. S., Frey, M., Lang, S., and Stahl, P. Clearance of lysosomal hydrolases following intravenous infusion. *Arch. Biochem. Biophys.* **177**: 606, 1976.
7. Stahl, P. D., Rodman, J. S., Miller, M. J., and Schlesinger, P. H. Evidence for receptor mediated binding of glycoproteins, glycoconjugates, and lysosomal glycosidases by alveolar macrophages. *Proc. Nat. Acad. Sci. USA* **75**: 1399, 1978.

8. Stahl, P. D., Rodman, J. S., and Schlesinger, P. H. Clearance of lysosomal hydrolases following intravenous infusion: Kinetic competition experiments for the β-glucuronidase and *N*-acetyl-*b*-D-glucosaminidase. *Arch. Biochem. Biophys.* 177: 594, 1976.
9. Simmons, B. M., and Russell, J. H. A single affinity column step method for the purification of ricin toxin from castor beans (Ricinus communis). *Anal. Biochem.* **146:** 206, 1985.
10. Stirpe, F., Campani, A. G., Barbieri, L., Falasca, A., Abbondanza, A., and Stevens, W. A. Ribosomal inactivating proteins from the seeds of *Saponaria officinalis,* of *Agrostemma githago,* and *Asparagus officinales* and from the latex of *Hura crepitans* (sandbox tree). *Biochem. J.* 215: 617, 1983.
11. Keller, R. K., and Touster, O. Physical and chemical properties of β-glucuronidase from the preputial glands of the female rat. *J. Biol. Chem.* **250:** 40,765, 1975.
12. Bourrie, B., Casselas, P., Blythmun, H., and Jansen, F. Study of the plasma clearance of antibody-ricin-A-chain immunotoxin. *Eur. J. Biochem.* **155:** 1, 1986.
13. Derenzini, M., Bonetti, E., Marinozzi, V., and Stirpe, F. Toxic effects of ricin: Studies on the pathogenesis of liver lesions. *Virchows Arch. (Cell Pathol.)* **20:** 15, 1976.
14. Skilleter, D. N., Paine, A. J., and Stirpe, F. A comparison of the accumulation of ricin by hepatic parenchymal and non-parenchymal cells and its inhibition of protein synthesis. *Biochem. Biophys. Acta* **677:** 495, 1981.
15. Rubinstein, D., Roska, A. K., and Lipsky, P. E. Liver sinusoidal lining cells express class II major histocompatibility antigens but are poor stimulators of fresh allogenic T lymphocytes. *J. Immunol.* **137:** 1803, 1986.
16. Engemann, R., Gassel, H. J., Schumeder, U., Thiede, H., and Hamelmann, H. The expression of class II antigens in liver allografts after orthotopic liver transplantation spontaneously occurring in cyclosporin-induced tolerance. *Transplant. Proc.* **18:** 1353, 1986.

Available online at www.sciencedirect.com
SCIENCE DIRECT®
ELSEVIER
Toxicology 210 (2005) 197–204
TOXICOLOGY
www.elsevier.com/locate/toxicol

Methyl palmitate: Inhibitor of phagocytosis in primary rat Kupffer cells

P. Cai, B.S. Kaphalia, G.A.S. Ansari*

Department of pathology, University of Texas Medical Branch, Galveston, TX 77555, USA

Received 18 November 2004; received in revised form 2 February 2005; accepted 5 February 2005
Available online 20 March 2005

Abstract

Kupffer cells are involved in phagocytosis and known to release biologically active mediators during early events of liver injury. Such functional properties of Kupffer cells can be modulated by methyl palmitate (MP). Therefore, efficacy of MP to modulate Kupffer cell function was evaluated in cultured primary Kupffer cells from rat liver. Phagocytic activity of Kupffer cells was measured by their capacity to phagocytize latex beads and the release of TNF-α, IL-10, IL-6, nitric oxide, and PGE2 was determined in cell culture medium after incubating the cells with various concentrations of MP for 24 h followed stimulation with lipopolysaccharide (LPS) for 6 h. To understand the mechanism of phagocytosis, we investigated the hydrolysis of MP, and determine ATP levels and activity of NF-κB in MP-inhibited Kupffer cells. A significant decrease was observed in phagocytosis. Phagocytosis evaluated at 0.5 mM MP was found to be time-dependent with a maximum decrease of 49% at 6 h. Exposure of Kupffer cells to MP followed by LPS stimulation showed a dose-dependent decrease in phagocytosis and reduced the release of TNF-α, IL-10, nitric oxide, and PGE2 but not of IL-6 levels in the supernatant as compared to the control. While ATP levels were unchanged, the nuclear factor NF-κB (p65) activity was inhibited in Kupffer cells treated with MP after LPS stimulation (35.6 RLU versus 49.6 RLU in control). Hydrolysis of MP was found to be time-dependent; maximum concentration of MP and palmitic acid (hydrolysis products) in the cell being at 3 and 6 h, respectively. In general, MP appears to reduce phagocytosis and levels of TNF-α, IL-10, nitric oxide, and PGE2 without affecting ATP levels and is probably mediated by NF-κB. This in vitro model is useful for detailed mechanistic studies of inhibition of phagocytosis by MP and other fatty acid esters.

Keywords: Kupffer cell; Methyl palmitate; Phagocytosis; NF-κB

1. Introduction

Methyl palmitate (MP, methyl ester of palmitic acid) and other fatty acid methyl esters (FAMEs) are endogenous compounds (Lough et al., 1962; Leikola et al., 1965; Fisher et al., 1966; Lough and Garton, 1968; Kaphalia et al., 1995). Concentration of FAMEs can be increased after exposure to methanol in rats and human hepatocellular carcinoma (HepG2) cell line following methanol exposure (Kaphalia et al., 1995, 1999; Mericle et al., 2004). In general, FAMEs can pen-

* Corresponding author. Tel.: +1 409 772 3655; fax: +1 409 747 1763.
E-mail address: sansari@utmb.edu (G.A.S. Ansari).

0300-483X/$ – see front matter © 2005 Elsevier Ireland Ltd. All rights reserved.
doi:10.1016/j.tox.2005.02.001

etrate mouse epidermis and alter microviscosity in vitro of synaptosomal membrane from rat and monkey brain cortex (Wertz and Downing, 1990; Lazar and Medzihradsky, 1992) and, in particular, MP is shown to inhibit Kupffer cell functions (Diluzio and Wooles, 1964) and affect hepatocyte proliferation through modulation of TNF-α (Rusyn et al., 2000).

Kupffer cells are bone marrow derived hepatic macrophages, reside in sinusoids and are highly populated in periportal area. Kupffer cells offer a first line of defense from noxious xenobiotic substances to avert toxicological consequences. However, in certain situations activated Kupffer cells can also cause deleterious effects.

MP has been shown to reduce/inhibit the hepatotoxicity induced by several chemicals (Sipes et al., 1991; Gunawardhana et al., 1993; Rose et al., 1997, 2000) and imparts protection against sepsis (Villa et al., 1996; Meng et al., 1992). Pretreatment with MP increases survival of skin semi-allografts (Sebestik et al., 1977) and orthotopic liver transplantation (Marzi et al., 1991). However, the later claim has been disputed (Rentsch et al., 2002). These therapeutic effects are based upon the premise that MP inhibits Kupffer cell functions, yet no attempt has been made to elucidate the mechanism of such inhibition. In this study, we show that MP reduces phagocytosis and alters the release of various mediators, a protective mechanism probably mediated through MP-induced inhibition of NF-κB. Since cytokines, PGE2, and nitric oxide can also be altered individually by fatty acids and/or alcohol (Barton et al., 1991; Bradford et al., 1999; Wallace et al., 2000), a time-dependent metabolism of MP was also investigated.

2. Materials and methods

2.1. Chemicals and reagent

The RPMI 1640 and DMEM cell culture medium from Gibco (Grand Island, NY) and Diff-Quik stain set from Dade Behring AG (CH-3186 Dudingen, Switzerland) was used. Methyl palmitate (MP, purity >99%) was purchased from Sigma–Aldrich (St. Louis, MO). Radioactive [9,10-^{3}H]-MP (specific activity 60 μCi/mmol, purity 99%) was purchased from American Radiolabeled Chemicals Inc. (St. Louis, MO).

2.2. Animals

Male Sprague–Dawley rats (~175 g) obtained from Harlan Sprague–Dawley Inc. (Indianapolis, IN) were acclimatized and maintained in humidity and temperature controlled animal care facility for one week.

2.3. Kupffer cell isolation

Kupffer cells were isolated according to the standard procedures (Smedsrod and Pertoft, 1985; Pertoft and Smederod, 1987; Friedman and Roll, 1987). Briefly, rats were anesthetized with pentabarbital and abdominal cavity were opened, liver perfused with 200 ml complete Ca^{2+}- and Mg^{2+}-free Hanks balanced salt buffer through the portal vein at a flow rate of 12 ml/min at 37 °C. Subsequent perfusion was done with 100 ml DMEM containing 0.025% collagenase IV and 0.01% DNase at 37 °C for 5 min. Liver was removed and perfused until the hepatic parenchyma beneath the capsule appeared liquefied. After complete digestion, the liver cells were dispersed in collagenase buffer. The resulting cells were filtered (mesh 40) and centrifuged ($50 \times g$) for 3 min at 4 °C. The supernatant was removed and the pellet was dispersed with RPMI 1640 and centrifuged again. The pooled supernatant, which contains nonparenchymal cells, was washed twice with RPMI 1640 to remove the dead cells and debris. Nonparenchymal cells were then centrifuged on a Percoll density cushion at $1000 \times g$ for 15 min, and the Kupffer cell fraction was collected and washed. Cells were seeded onto tissue culture plates (6 cm diameter) at a density of 5×10^6 cells/2 ml/plate. The cells were cultured in RPMI 1640 medium without fetal bovine serum at 37 °C, with 5% CO_2. Non-adherent (endothelial) cells were removed after 20 min by washing the plated cells and replenished with RPMI 1640 in 10% fetal bovine serum, 100 U/ml penicillin G and 100 μg/ml streptomycin and the cells cultured for 48 h before treatment. The Kupffer cell enrichment was more than 90% as determined by the cell morphology.

2.4. Preparation of MP

Two-hundred mM MP was dissolved in 0.5% ethanol. The working solution was made by dilution with fetal bovine serum, 3 min sonication and further dilution with RPMI 1640 medium to obtain 0.25, 0.5,

and 1 mM working solutions of MP in 10% fetal bovine serum.

2.5. MTT cytotoxicity assay

The Kupffer cells were treated with MP 0.5, 1, and 2 mM for 24 h followed by with 20 μl MTT (0.5% in PBS) for 4.5 h. Hundred microliters 10% SDS–0.01 M HCl was added and left for over night. The absorbance was measured at 570 nm.

2.6. Phagocytic activity of Kupffer cells

For time-dependent studies, Kupffer cells were treated with 0.5 mM MP for 0.5, 1, 2, 4, and 6 h. For dose-dependent studies, the Kupffer cells were treated with MP (0.25, 0.5, and 1 mM) for 24 h followed by LPS (500 ng/ml) stimulation for 6 h. The latex beads were added (14 μl/plate, 10%, 3 μm size) and incubated for additional 2 h. The supernatant was decanted and the cells were carefully washed. Diff–Quik stain set was used to stain the cells per manufacturer's instructions. More than 40 Kupffer cells were counted for internalized latex beads under the microscope (400×) in minimum of four fields. Photographs were taken using a Nikon FE2 camera.

2.7. Measurement of cytokine in cell culture medium

TNF-α, IL-6, and IL-10 cytokine production by Kupffer cells were determined in the supernatant after treatment with MP at different concentration (0.25, 0.5, and 1 mM) for 24 h, followed by with or without LPS (500 ng/ml) stimulation for 6 h. The supernatant was collected and TNF-α, IL-6, and IL-10 were measured using kits (KRC3011, KRC0061, and KRC0101) from Biosource (Camarillo, CA).

2.8. Measurement of nitrite and prostaglandinE2

The concentration of nitrite, a stable oxidized product of nitric oxide, was determined in cell culture supernatant by Griess reagent. Briefly, 100 μl culture supernatant was combined with 200 μl Griess reagent 100 μl 1% sulfanilamide in 5% H_3PO_4 and 100 μl 0.1% *N*-(1-naphthyl) ethylenediamine dihydrochloride in water in a 96-well plate, followed by spectrophotometric measurement at 570 s nm. Nitrite concentration in the supernatants was determined using sodium nitrite as standard. ProstaglandinE2 (PGE2) was measured using the kit (RPN22) from Amershan Biosciences (Buckinghamshire, UK).

2.9. Hydrolysis of MP by Kupffer cells

Kupffer cells were treated with 0.5 mM [9,10-^{3}H]-MP (5×10^6 DPM/μmol/dish) for different times. The cells were washed with PBS thrice before extraction. The supernatant and cells were extracted thrice with 10 ml chloroform: methanol (2:1, v/v). The extracts were pooled, concentrated to 100 μl and subjected to thin layer chromatography (TLC) using petroleum ether: diethyl ether: acetic acid (75:5:1, v/v/v), as solvent, for the separation of palmitic acid (PA) and MP. Silica gel corresponding to the relative flow of MP and PA was scraped, desorbed with methanol:water (6:1, v/v), mixed with 15 ml scintillation cocktail, and the radioactivity measured by Packard 1900CA Liquid Scintillation Analyzer.

2.10. ATP levels

ATP levels were measured in cell lysates using ATP Bioluminescence assay kit HS II (Roche Diagnostics Gmbh, Mannheim, Germany) on Fluoroskan Ascent FL (Thermo Labsystems, Franklin, MA) per manufacturer's instructions and data expressed as 10^{-6} mol/10^6 cells.

2.11. NF-κB assay

The NF-κB p65 binding activity (RLU) was quantified using NF-κB p65 Chemi transcription factor assay kit (Active Motif, Carlsbad, CA) on Fluoroskan Ascent FL. The nuclear extract was prepared using nuclear extract kit from Active Motif and 1.5 μg protein/well was used to determine NF-κB binding activity.

2.12. Statistical analysis

All data are presented as mean ± standard error of the mean (S.E.M.). Analysis of variance (ANOVA) followed by Student–Newman–Keuls post hoc test was used to analyze the data. Values with $p < 0.05$ were considered statistically significant.

3. Results

Fig. 1 shows the effect of MP on Kupffer cell viability and phagocytic activity. Cell viability, as determined by MTT assay, decreased significantly ($p < 0.01$) at 2 mM MP while changes at 0.5 and 0.1 mM MP were insignificant (Fig. 1A). Fig. 1B shows a time-dependent decrease in phagocytic activity of the Kupffer cells at 0.5 mM MP, which was significant at 4 and 6 h ($p < 0.05$). The phagocytic activity of Kupffer cells decreased significantly at all the MP concentration tested (Fig. 2), when cells were incubated with MP for 24 h followed by LPS treatment for 6 h ($p < .05$).

The concentration-dependent release of cytokine TNF-α, IL-6, and IL-10 from the Kupffer cells after exposure to MP is shown in Fig. 3. TNF-α released from the Kupffer cells after exposure to 1 mM MP for 24 h following LPS stimulation for 6 h was significantly lower than control ($p < .01$) (1567 pg/ml versus 2532 pg/ml in control) (Fig. 3A). As shown in Fig. 3B, IL-10 decreased by seven-fold in the 1 mM MP treated cells (76 pg/ml versus 555 pg/ml in control). The cells not stimulated with LPS did not show any decrease in the levels of either TNF-α or IL-10. However, release of IL-6 in the supernatant at 0.5 mM MP without LPS stimulation was significantly higher than control ($p < 0.05$) (166 pg/ml versus 128 pg/ml in control) and also with LPS stimulation than that of control, but statistically not significant (Fig. 3C).

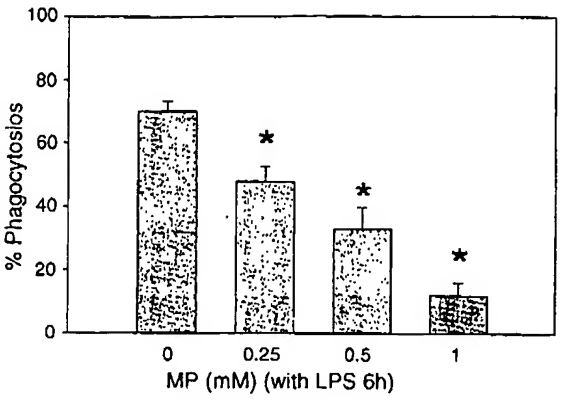

Fig. 2. Phagocytic activity of Kupffer cells as determined by latex bead uptake after exposing to various concentrations of MP for 24 h followed by LPS stimulation for 6 h. Values are mean ± S.E. of four determinations (*$p < 0.05$ vs. control).

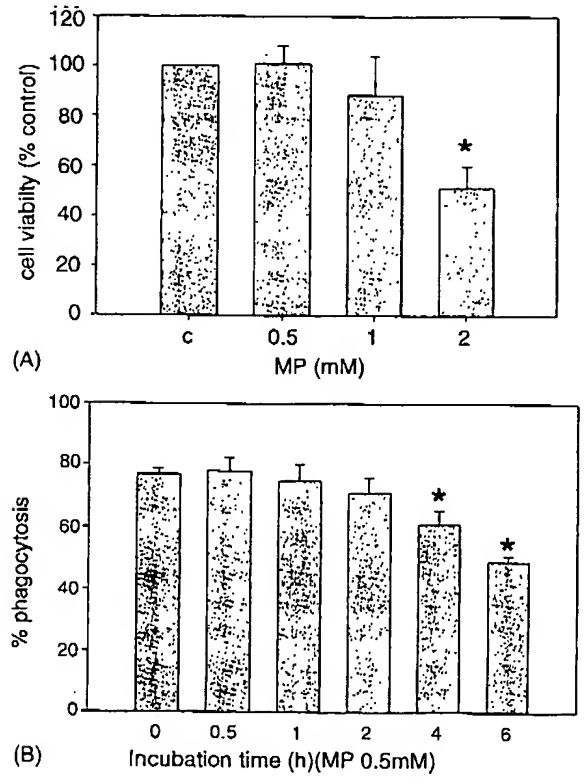

Fig. 1. Effects of MP on primary rat Kupffer cell viability and phagocytic activity. Kupffer cells were incubated with various concentrations of MP for 24 h. Cell viability was determined by MTT assay (A), and time-dependence of phagocytosis was determined by latex bead uptake at 0.5 mM MP (B).

The nitrite production, as shown in Fig. 4A, was significantly inhibited (0.35, 0.33, and 0.30 μM, as compared to 0.53 μM in control) after exposure of Kupffer cells to MP (0.25, 0.5, and 1 mM, respectively) for 24 h ($p < 0.05$). No change in nitrite production was observed in cells stimulated with LPS. The PGE2 (Fig. 4B) was also decreased ($p < 0.05$) at 1 mM with (13.0 ng/ml versus 19.6 ng/ml in control) or without (23.7 ng/ml versus 38.9 ng/ml in control) LPS stimulation.

The hydrolysis of MP in Kupffer cells treated with 0.5 mM [^{3}H]-MP is shown in Fig. 5. The hydrolysis of MP was determined by measuring [^{3}H]-MP and [^{3}H]-PA in the supernatant and cells, which was found to be time-dependent in the supernatant; the lowest level of MP and highest level of PA were found at 12 h (0.09 mM and 0.37 mM, respectively) (Fig. 5A). The maximum concentration of MP in the

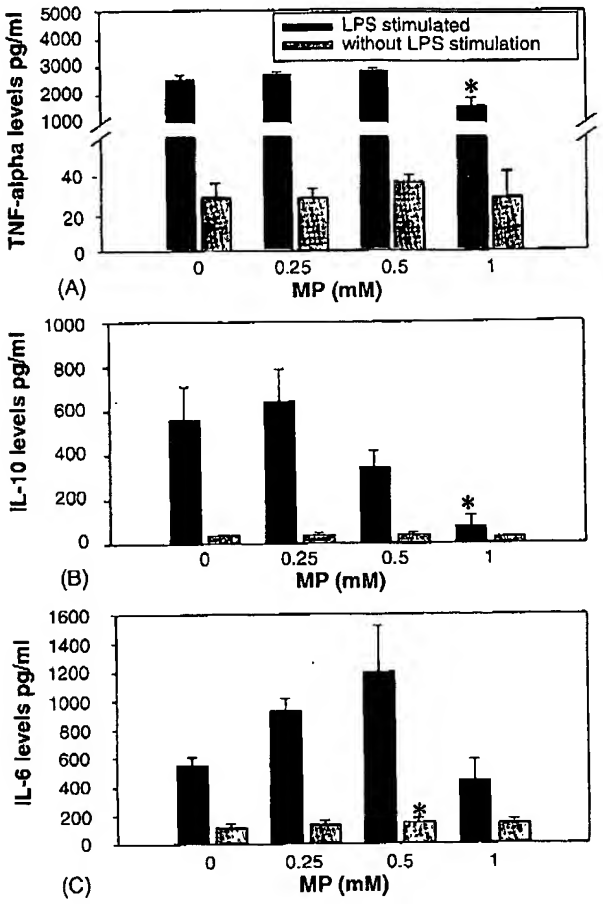

Fig. 3. The effect of MP on the release of TNF-α (A), IL-10 (B), and IL-6 (C) from rat liver Kupffer cell incubated with MP for 24 h and stimulated with LPS (500 ng/ml) for 6 h. TNF-α (A), IL-10 (B), and IL-6 (C) were measured in the supernatant. Each bar graph represents the mean ± S.E. of four determinations ($^{*}p < .05$ vs. controls).

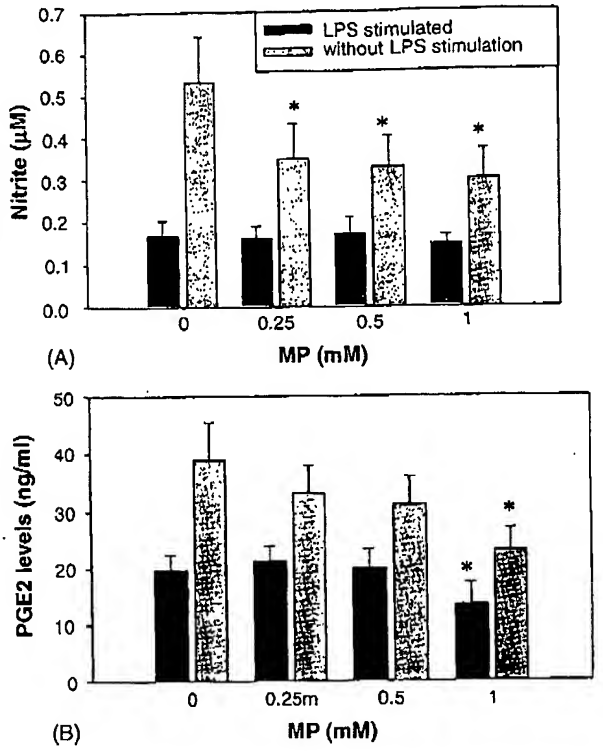

Fig. 4. Nitrite (A) and PGE2 (B) contents in the supernatant of rat liver Kupffer cells treated with different concentrations of MP for 24 h and stimulated with LPS (500 ng/ml) for 6 h. Each bar graph represents mean ± S.E. of four determinations ($^{*}p < 0.05$ vs. controls).

cell was at 3 h (5.4 nmol/10^6 cells) and of PA at 6 h (21.1 nmol/10^6 cells) (Fig. 5B). The total recovery of [^{3}H] radioactivity was ~80% at all the time points studied. Overall, the concentration of MP was low in the cells as compared to PA, and the concentrations of both were inversely proportional.

No significant change in levels of ATP was observed after treatment of the cells with 0.5 mM MP for 24 h (Fig. 6). As shown in Fig. 7, the NF-κB p65 binding activity in the nuclear extract of Kupffer cells to oligonucleotide containing an NF-κB consensus binding site, treated with 0.5 mM MP for 24 h and stimulated with LPS for 6 h, was significantly lower than that of control (35.6 RLU versus 49.6 RLU in control). No change occurred without LPS stimulation.

4. Discussion

Kupffer cells, the resident macrophages of the liver, contribute to various protective roles after activation. However, in some cases this protective role becomes detrimental and needs to be suppressed. Several chemicals such as gadolinium chloride, glycine and MP are commonly used to suppress Kupffer cell function. MP suppresses the activation of Kupffer cells by ~70% (Cowper et al., 1990). Although MP was used to suppress Kupffer cell functions in several investigations (Sipes et al., 1991; Gunawardhana et al., 1993; Rose et al., 1997, 2000), the mechanism of such a suppression is not clear. Therefore, in the present study efficacy of MP to inhibit phagocytosis and release of various bi-

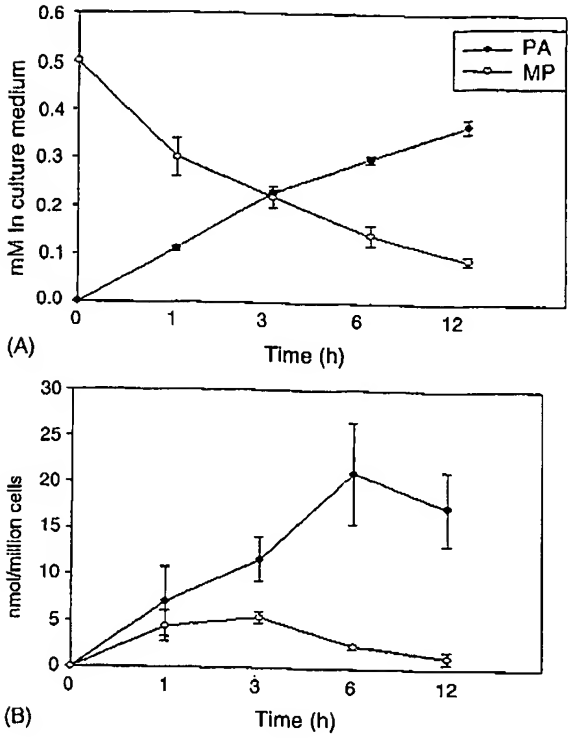

Fig. 5. The Hydrolysis of MP in Kupffer cells treated with 0.5 mM [9.10-^{3}H]-MP (5×10^6 DPM/μmol) at different time intervals. The cells were harvested after centrifugation. The supernatant (A) and cells (B) were extracted with chloroform: methanol (2:1, v/v). The extract was subjected to TLC and the radioactivity corresponding to relative flow of MP and PA was measured.

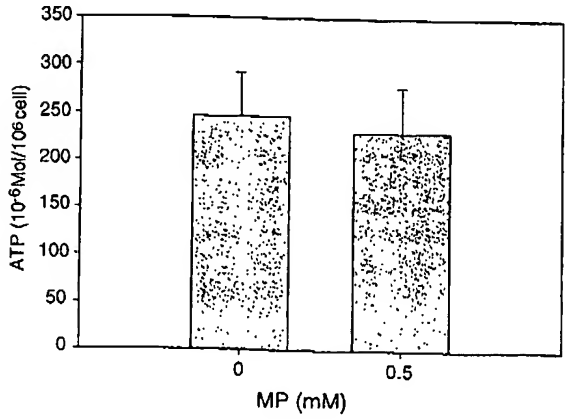

Fig. 6. ATP levels in Kupffer cells treated with 0.5 mM MP for 24 h. ATP was determined in the cell lysates using Bioluminescence assay kit. Values are mean ± S.E. of four determinations.

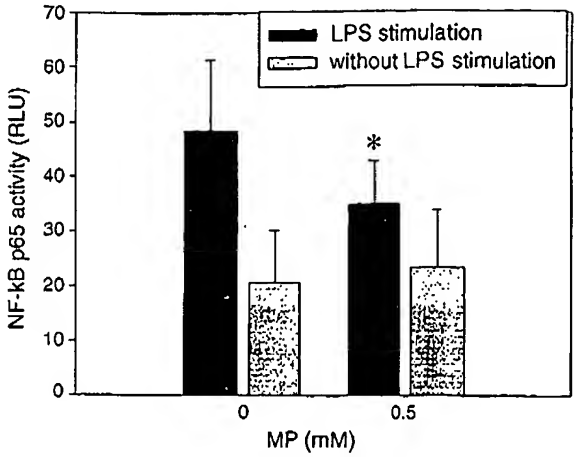

Fig. 7. NF-κB activation of Kupffer cell treated with 0.5 mM MP for 24 h and stimulated with LPS (500 ng/ml) for 6 h. The nuclear protein of Kupffer cells was extracted by nuclear extract kit (Active Motif). The NF-κB p65 activation was measured by NF-κB p65 Chemi transcription factor assay kit (Active Motif). Each bar graph represents mean ± S.E. of six determinations ($^*p < .05$ vs. controls).

ological mediators was evaluated in cultured primary Kupffer cells.

MP is a persistent endogenous compound (Leikola et al., 1965; Fisher et al., 1966; Lough and Garton, 1968; Kaphalia et al., 1995) and its concentration can be modulated by methanol treatment and inhibitors of fatty acid ethyl ester synthase (Kaphalia et al., 1995; Mericle et al., 2004). The pool of the FAMEs can also be increased by S-adenosylmethionine-associated methylation of free fatty acids (Zatz et al., 1981).

First set of experiments was conducted to establish the model. Indeed, the cultured isolated Kupffer cells were viable and MP was able to inhibit their phagocytic function in a time- and concentration- dependent manner as evident by the reduced uptake of latex beads. Inhibition of cytokine secretion of TNF-α and IL-10, nitric oxide and PGE2, indicate that MP also inhibits functional competency of Kupffer cells. These experiments validate inhibition of Kupffer cell functions by a fatty acid methyl ester (MP). Although inhibition of NF-κB activity was expected to suppress the secretion of IL-6 (Luckey et al., 2002), increased levels of IL-6 after exposure to MP, as found in the present study, could not be explained. However, such a response is possible in an attempt of the cells to recover from the injury caused by MP, since IL-6 production is fundamental to liver regeneration (Streetz et al., 2000).

Kupffer cells play a key role in activation of catalase pathway of alcohol metabolism by increasing the availability of fatty acids for oxidation (Bradford et al., 1999). Present study clearly demonstrates that MP is hydrolyzed (metabolized) and is not 'non-metabolizable' as claimed earlier (Rose et al., 2000). With increasing incubation time, concentration of palmitic acid (PA) increases both in the medium and cells. This increased concentration of PA in the cells and/or cell culture media may be a causative factor for the decreased levels of TNF-α, nitric oxide and probably other mediators such as PGE2. It is currently not known whether such a biological response observed in Kupffer cells following treatment with MP is associated with its hydrolysis products, palmitic acid and/or methanol. Both metabolic products may directly inhibit phagocytosis and release of mediators which needs to be investigated.

The low concentration of MP in the cells is supported by the ubiquitous presence of esterases (Mentlein et al., 1980; Satoh and Hosokawa, 1998) and short half-life of MP formed in vivo (Kaphalia et al., 1995). Furthermore, FAME hydrolase activity has been described in the liver (Spector and Soboroff, 1972). Fatty acid formed by hydrolysis can be incorporated in various lipids (Marks et al., 1996), undergo β-oxidation to generate ATP (Ghisla, 2004) or incorporated into proteins (James and Olson, 1990). A decrease in recovery of fatty acid ester/acid in a time-dependent manner can be explained by these possibilities. We first postulated that incubation of Kupffer cells with MP increases the concentration of palmatic acid/ester in the cell and their uptake by the mitochondria increases the pool of palmatic acid/ester which inhibits ATP generation via β-oxidation. Inhibition of ATP production may suppress Kupffer cell function. Since no change in ATP levels was observed following exposure to MP, we then speculated that observed inhibition could be associated with inhibition of NF-κB activity, which is supported by our finding (Fig. 7). However, a detailed investigation needs to be conducted to elucidate the mechanism of inhibition of phagocytosis by MP. Elucidation of such a mechanism will open new avenues to develop better inhibitors to suppress activation of Kupffer cells (macrophages), which could lead to the development of a new class of drugs against sepsis and perhaps tissue rejection.

Acknowledgment

This publication was made possible by grants ES04815 (G.A.S.A.) from the National Institute of Environment Health Sciences (NIEHS) and AA13171 (B.S.K.) from the National Institute of Alcohol Abuse and Alcoholism (NIAAA), and its contents are solely the responsibility of the authors and do not necessarily represent the views of the NIH, NIEHS or NIAAA.

References

Barton, R.G., Wells, C.L., Carlson, A., Singh, R., Sullivan, J.J., Cerra, F.B., 1991. Dietary omega-3 fatty acids decrease mortality and Kupffer cell prostaglandinE2 production in a rat model of chronic sepsis. J. Trauma-Injury Inf. Crit. Care 31, 768–773.

Bradford, B.U., Enomoto, N., Ikijima, K., Rose, M.L., Bojes, H.K., Forman, D.T., Thurman, R.G., 1999. Peroxisomes are involved in swift increase in alcohol metabolism. J. Pharmacol. Exp. Therap. 288, 254–259.

Cowper, K.B., Currin, R.T., Dawson, L., Lindert, K.A., Lemasters, J.J., Thurman, R.G., 1990. A new method to monitor Kupffer-cell function continuously in the perfused rat liver dissociation of glycogenolysis from particle phagocytosis. Biochem. J. 266, 141–147.

Diluzio, N.R., Wooles, W.R., 1964. Depression of phagocytic activity and immune response by methyl palmitate. Am. J. Physiol. 206, 939–943.

Fisher, G.A., Sauk, J.J., Kabara, J.J., 1966. The occurrence of natural and artificial methyl esters in lipid extracts. Microchem. J. 11, 461–468.

Friedman, S.L., Roll, F.J., 1987. Isolation and culture of hepatic lipocytes, Kupffer cells, and sinusoidal endothelial cells by density gradient centrifugation with Stractan. Anal. Biochem. 161, 207–218.

Ghisla, S., 2004. Beta-oxidation of fatty acids. A century of discovery. Eur. J. Biochem. 271, 459–461.

Gunawardhana, L., Mobley, S.A., Sipes, I.G., 1993. Modulation of 1,2-dichlorobenzene hepatotoxicity in the Fischer 344 rat by a scavenger of superoxide anions and an inhibitor of Kupffer cells. Toxicol. Appl. Pharmacol. 119, 205–213.

James, G., Olson, E.N., 1990. Fatty acylated proteins as components of intracellular signaling pathways. Biochemistry 29, 2623–2634.

Kaphalia, B.S., Carr, J.B., Ansari, G.A.S., 1995. Increased endobiotic fatty acid methyl esters following exposure to methanol. Fundam. Appl. Toxicol. 28, 264–273.

Kaphalia, B.S., Green, S.M., Ansari, G.A.S., 1999. Fatty acid ethyl and methyl ester synthases and fatty acid anilide synthase in HepG2 and AR42J cells: interrelationships and inhibition by tri-o-tolyl phosphate. Toxicol. Appl. Pharmacol. 159, 34–141.

Lazar, D.F., Medzihradsky, F., 1992. Altered microviscisity at brain membrane surface induce distinct and reversible inhibition of opioid receptor binding. J. Neurochem. 59, 1233–1240.

Leikola, R., Nieminen, E., Salomaa, E., 1965. Occurrence of methyl esters in the pancreas. J. Lipid Res. 6, 490–493.

Lough, A.K., Felinski, L., Garton, G.A., 1962. The production of methyl esters of fatty acids as artifacts during the extraction of storage of tissue lipids in the presence of methanol. J. Lipid Res. 3, 478–479.

Lough, A.K., Garton, G.A., 1968. The lipids of human pancreas with special reference to the presence of fatty acid methyl esters. Lipids 3, 321–323.

Luckey, S.W., Taylor, M., Sampey, B.P., 2002. 4-Hydroxynonenal decreases interleukin-6 expression and protein in primary rat Kupffer cells by inhibiting nuclear factor-κB activation. J. Pharmacol. Exp. Therap. 302, 296–303.

Marks, D.B., Marks, A.D., Smith, C.M., 1996. Basic Medical Biochemistry: A Clinical Approach. Section IV. Lipid Metabolism. Williams and Wilkins Publisher.

Marzi, I., Cowper, K., Takei, Y., Lindert, K., Lemasters, J.J., Thurman, R.G., 1991. Methyl palmitate prevents Kupffer cell activation and improves survival after orthopic liver transplantation in the rat. Transplant. Int. 4, 215–220.

Meng, X., Qiu, B., Li, X., Song, X., 1992. The role of Kupffer cells in the development of hepatic dysfunction during sepsis. Chin. Med. J. 105, 34–38.

Mentlein, R., Heiland, S., Heymann, E., 1980. Simultaneous purification and characterization of six serine hydrolases from rat liver microsomes. Arch. Biochim. Biophys. 200, 547–559.

Mericle, K.A., Kaphalis, B.S., Ansari, G.A.S., 2004. Modulation of fatty acid ethyl esters in rats pre-treated with tri-o-tolyl phosphate. J. Toxicol. Environ. Health 67, 583–593.

Pertoft, H., Smederod, B., 1987. Separation and characterization of liver cells. Cell Sep.: Methods Selected Appl. 4, 1–23.

Rentsch, M., Beham, A., Sirek, S., Iesalnieks, I., Geissler, E.K., Anthuber, M., Jauch, K.-W., 2002. Glycine but not gadolinium chloride or methyl palmitate reduces postischemic white blood cell accumulation and early graft nonfunction after liver transplantation in the rat. Transplant. Proc. 34, 2389–2390.

Rose, M.L., Germolec, D.R., Schoonhoven, R., Thurman, R.G., 1997. Kupffer cells are casually responsible for the mitogenic effect of peroxisome proliferators. Carcinogenesis 18, 1453–1456.

Rose, M.L., Rusyn, I., Bojes, H.K., Belyea, J., Cattley, R.C., Thurman, R.G., 2000. Role of Kupffer cells and oxidants in signaling peroxisome proliferator-induced hepatocyte proliferation. Mut. Res. 448, 179–192.

Rusyn, I., Rose, M.L., Bojes, H.K., Thurman, R.G., 2000. Novel role of oxidants in the molecular mechanism of action of peroxisome proliferators. Antioxid. Redox Signal 2, 607–621.

Satoh, T., Hosokawa, M., 1998. The mammalian carboxylesterase; from molecules to functions. Annu. Rev. Pharmacol. Toxicol. 38, 257–288.

Sebestik, V., Paluska, E., Potmesilova, I., Nezvalova, J., 1977. Effect of methyl palmitate on the survival of skin semi-allografts in rats. Experientia 33, 391–392.

Sipes, I.G., Sisi, A.E., Sim, W.W., Mobley, S.A., Earnest, D.L., 1991. Reactive oxygen species in the progression of CCl_4-induced liver injury. Adv. Exp. Med. Biol. 283, 489–497.

Smedsrod, B., Pertoft, H., 1985. Preparation of pure hepatocyes and reticuloendothelial cells in high yield from a single rat liver by means of Percoll centrifugation and selective adherence. J. Leukoc. Biol. 38, 213–230.

Spector, A.A., Soboroff, J.M., 1972. Long chain fatty acid methyl ester hydrolase activity in mammalian cells. Lipids 7, 186–190.

Strectz, K.L., Luedde, T., Manns, M.P., Trautwein, C., 2000. Interleukin 6 and liver regeneration. Gut 47, 309–312.

Villa, P., Demitri, M.T., Meazza, C., Sironi, M., Gnocchi, I., Ghezzi, P., 1996. Effect of methyl palmitate on cytokine release, liver injury and survival in mice with spsis. Eur. Cytokine Networks 7, 765–769.

Wallace, F.A., Neely, S.J., Miles, E.A., Calder, P.C., 2000. Dietary fat effects macrophage-mediated cytotoxicity towards tumor cells. Immunol. Cell Biol. 78, 40–48.

Wertz, P.W., Downing, D.T., 1990. Metabolism of topically applied fatty acid methyl esters in BALB/C mouse epidermis. J. Dermatol. Sci. 1, 33–37.

Zatz, M., Dudley, P.A., Kloog, Y., Marley, S.P., 1981. Nonpolar lipid methylation. Biosynthesis of fatty acid methyl esters by rat lung membranes using S-adenosylmethionine. J. Biol. Chem. 256, 10028–10032.

Transplant International ISSN 0934-0874

ORIGINAL ARTICLE

Benefit of Kupffer cell modulation with glycine versus Kupffer cell depletion after liver transplantation in the rat: effects on postischemic reperfusion injury, apoptotic cell death graft regeneration and survival*

Markus Rentsch,[1] Kerstin Puellmann,[2] Slawo Sirek,[2] Igors Iesalnieks,[2] Klaus Kienle,[2] Thomas Mueller,[2] Ulrich Bolder,[2] Edward Geissler,[2] Karl-Walter Jauch[1] and Alexander Beham[2]

1 Department of Surgery, Ludwig-Maximilians University of Munich, Klinikum Grosshadern, Munich, Germany
2 Department of Surgery, University of Regensburg, Regensburg, Germany

Keywords
apoptosis, early graft dysfunction, ischemia-reperfusion, microcirculation, rat liver transplantation.

Correspondence
Markus Rentsch MD, Department of Surgery, Klinikum Grosshadern, Ludwig-Maximilians University of Munich, Marchioninistrasse 15, 81377 Munich, Germany. Tel.: +49 89 7095 1; fax: 49 89 7095 5464; e-mail: markus.rentsch@med.uni-muenchen.de

*Parts of this study were presented at the meeting of the ILTS, Berlin, Germany, 2001 and at the Congress of the Transplantation Society, Miami, FL, USA, 2002. This work was supported by grants of the Deutsche Forschungsgemeinschaft, grant no. RE 1560/1-1.

Received: 5 August 2004
Revision requested: 3 January 2005
Accepted: 17 May 2005

doi:10.1111/j.1432-2277.2005.00185.x

Summary

Inhibition or destruction of Kupffer cells (KC) may protect against ischemia-reperfusion (IR) induced primary graft nonfunction (PNF) in liver transplantation. Besides KC activation, PNF is characterized by microvascular perfusion failure, intrahepatic leukocyte accumulation, cell death and hepatocellular dysfunction. KCs can be inactivated by different agents including gadolinium chloride ($GdCl_3$), methyl palmitate (MP) and glycine. The effects of three KC inactivators on IR-injury after rat liver transplantation were compared in the present study. Lewis liver donors were treated with $GdCl_3$, MP, glycine or saline (control). Liver grafts were transplanted following 24 h storage (UW solution). KC populations and IR damage were assessed by histologic analysis, quantitative real-time polymerase chain reaction (RT-PCR) and intravital microscopy. The number of hepatic ED-1 positive macrophages was diminished after $GdCl_3$ ($114.8 \pm 4.4/mm^2$ liver tissue) and MP treatment (176.0 ± 5.0), versus the glycine (263.9 ± 5.5) and control (272.1 ± 5.6) groups. All three treatment modalities downregulated phagocytic activity for latex particles, paralleled by reduced microvascular injury (acinar perfusion index, $GdCl_3$: 0.75 ± 0.03; MP: $0.83 \pm .03$; glycine: 0.84 ± 0.03; 0.63 ± 0.03). Quantitative RT-PCR revealed elevated myeloperoxidase mRNA after glycine versus $GdCl_3$ and MP pretreatment (3.2- and 3.4-fold, $P = 0.011$, respectively), without difference to controls (2.9-fold of glycine). TNFα-mRNA was reduced after glycine- (5.2-fold), $GdCl_3$- (19.7-fold), MP-treatment (39.5-fold) compared with controls. However, profound prevention of intrahepatic cell death and liver graft failure was solely achieved with glycine preconditioning. Different than $GdCl_3$ and MP, glycine modulates rather than destroys KCs. Glycine appears to preserve cell viability and to TNFα/leukocyte dependent organ regeneration capacity, which is related to increase graft survival following liver transplantation.

Introduction

Liver graft injury because of cold ischemia and reperfusion represents one of the major obstacles in liver transplantation protocols [1]. Ischemia-reperfusion (IR) injury is known to severely compromise early graft function, potentially contributing to graft loss and requirement of re-transplantation. Furthermore, it predicts long-term success after transplantation related to early induction of immune processes [2,3], becoming apparent as ischemic

type biliary lesions or graft rejection. Despite intense research on the development of new therapeutic strategies to counteract IR-dependent mechanisms [4], only a small fraction of the concepts have been introduced into clinical practice.

The IR-injury in liver grafts is characterized by a sequence of morphologic changes. These include disturbances of microvascular perfusion secondary to injury of the sinusoidal lining signified by endothelial cells and Kupffer cell (KC) disturbances [5,6], intrahepatic accumulation of white blood cells (WBCs) [7], and impaired hepatocellular function [8,9]. In addition, apoptotic cell death has been acknowledged as an important mechanism related to cellular IR injury [5,10]. Nonetheless, activation of KCs has been identified as a key event in the initiation and perpetuation of the IR injury. Indeed, activated KCs represent a major intrahepatic source of potent mediators such as reactive oxygen species, tumor necrosis factor (TNF)α, cytokines [interleukin (IL)-6], eicosanoids and chemokines. However, the detrimental or protective function of some mediators remains to be identified. For these reasons substances have been characterized to control KCs, either by destruction or by modulation. Among these substances are gadolinium chloride ($GdCl_3$), methyl palmitate (MP) and glycine. $GdCl_3$ is a rare earth metal salt with high similarity in crystal radii to calcium. $GdCl_3$ can replace calcium ions, potentially interfering with calcium uptake and calcium-dependent cellular processes [11] including phagocytosis and proteolysis activation. $GdCl_3$ causes KC elimination, without described effects on other hepatic cell populations [12]. MP, a non-hydrolyzable fatty acid ester, exerts its effects by inhibiting KC phagocytic activity, and by reducing the immunologic response to foreign antigens [13–15]. Although the underlying mechanisms remain somewhat speculative, MP integration into cell membranes seems to change membrane characteristics to provide a protective effect. The third substance of importance in the present study is glycine, which inhibits calcium influx into cells by binding to a glycine-gated chloride channel [16,17]. Activation of this channel by glycine leads to hyperpolarization of the cell membrane by permitting chloride influx into the cell. This blunts calcium-influx into the cell by limiting the opening of voltage-gated channels [16], which decreases KC activity and protects liver grafts [18,19]. However, although there is clear evidence for the detrimental effect of KCs after warm ischemia *in vivo*, increasing evidence in recent publications strongly challenge this pathologic concept in the context of cold ischemia and reperfusion in liver transplantation [20,21].

Although KC inhibition by $GdCl_3$, MP and glycine have been evaluated in several experimental models in the past, direct comparisons after liver transplantation are rare, and existing studies were performed in highly specialized *in vitro* models or with short preservation times [19,22]. The purpose of the present study was to evaluate these three KC inhibitors on early graft IR injury, intrahepatic cellular apoptosis, regeneration stimuli and survival after liver transplantation in the rat.

Material and methods

Experimental groups

Four experimental groups were compared. Each group was divided into two sets of studies, consisting of one set of intravital microscopy experiments, and a second set of survival experiments. Separation of these study sets permitted the exclusion of influences of the intravital microscopy on animal survival following transplantation. In one treatment group donor animals were pretreated with a single intravenous injection of $GdCl_3$ (10 mg/kg, 1 ml; Sigma Chemicals, Deisenhofen, Germany) 24 h before graft harvesting. In a second treatment group organ donors were treated in the same way with a bolus intravenous injection of MP (300 mg/kg; Sigma Chemicals). MP was prepared as a stock emulsion by sonification of 100 mg MP/ml Ringers solution containing 0.2% Tween-20 and 5% dextrose. In the third treatment group donors were pretreated with glycine (300 mM, 1 ml; Merck, Darmstadt, Germany) as a 1 h i.v. infusion preceding the graft UW perfusion. All treatment regimen were reproduced with minor modifications from previous publications [15,22]. The fourth group, pretreated with an equal volume of physiologic saline 24 h prior to reperfusion, served as the control group.

Additional experiments with glycine treatment 24 h before, and $GdCl_3$ and MP treatment 1 h before graft harvest were performed to exclude specific effects of timing of donor pretreatment. The determination of survival for 7 days showed no differences between the groups. Results were excluded from further analyses.

Surgical procedure

Syngeneic orthotopic liver transplantation, including sequential arterial reconstruction, was performed in male Lewis rats weighing 170–190 g (Charles River Wiga, Sulzfeld, Germany). Details of the surgical technique have been described in detail previously [23,24]. The cold ischemia time was 24 h in UW solution (4 °C; Du Pont de Nemours, Bad Homburg, Germany). Bile flow was monitored after insertion of a polyethylene tube (PE-50, 0.58 mm inside diameter; Portex, Hythe, UK) into the common bile duct. Liver tissue specimens were collected after a 90 min interval of intravital microscopy (see below) or at 360 and 540 min after graft reperfusion. In

experiments, determining animal survival, the bile duct was reconstructed. Animals were given free access to food and water after the surgical procedure. According to previous studies in syngeneic rat liver transplantation experiments [23], and our own observations, surgery related technical complications and early graft failure as causes of death can be excluded within 7 days postreperfusion. Therefore, all recipients surviving 7 days were assumed to be long-term survivors. All experiments were carried out in accordance with the German legislation on animal protection (permission no 621-2531.1-13/99, Government of Oberpfalz, Germany) and with the 'Principles of Laboratory Animal Care' (NIH publication no. 86–23, revised 1985).

Intravital fluorescence microscopy and video analysis

After complete graft revascularization and recovery of the animals from the anhepatic period, *in vivo* epi-illumination microscopy was performed from 30 to 90 min after portal graft reperfusion, as described previously in detail [24]. Hepatic acinar and sinusoidal perfusion was assessed after injection of sodium fluorescein (1 μmol/kg; Merck). Eighty minutes after reperfusion, phagocytic activity was quantified after an intra-arterial bolus injection of fluorescent latex particles (3×10^8 yellow-green 1.1 μm diameter particles/kg; Polysciences Inc., Warrington, PA, USA). Video-registered microscopy sequences were assessed off-line by frame-to-frame analysis. Estimation of acinar perfusion was performed in lower magnification (240×; 50–100 acini) classifying acini as completely perfused, irregularly perfused, or nonperfused, depending on the distribution of sodium fluorescein. In accordance with previous studies [24], the acinar perfusion index was calculated as (well-perfused acini + *0.5* × irregularly-perfused acini)/total number of acini.

In addition, sinusoidal perfusion and KC phagocytic activity were assessed (600× magnification) in randomly selected individual acini at 35 until 80 min after graft reperfusion. Sinusoidal perfusion was expressed as the percentage of nonperfused of all observed sinusoids in each subacinar zone (periportal, midzonal, pericentral). Of note, distribution characteristics of fluorescent compounds permit the quantification of sinusoidal perfusion exclusively within perfused acini.

Kupffer cell phagocytic activity was analyzed continuously from 80 to 90 min after reperfusion in 15–20 randomly selected microscopic fields (405 × 540 μm). The percentage of moving latex-particles per field (8–12 s of observation) was determined. The measurements started in each experiment with appearance of the first particle within the sinusoids. Latex particles in postsinusoidal venules were not quantified.

Graft excretory function

For evaluation of graft excretory function, the total volume of bile secreted during the initial 90-min reperfusion interval was measured. Bile production was standardized to milliliter per 100 g liver tissue, per 90 min. Bile acid content (μmol/100 g/90 min) was assessed using the 3-α-dehydrogenase test [25].

Immunohistochemistry

To assess KC numbers, paraffin-embedded liver tissue sections were stained for ED-1 (CD68) with a CD68-specific antibody (BMA, Basel, Switzerland). Visualization was achieved with the DAKO streptavidin–biotin complex staining method (DAKO, Hamburg, Germany), and the chromogen 3,3′-diaminobenzidin-tetrahydrochloride. Sections were counterstained with hematoxylin (Merck). Cells were counted in 10 randomly chosen high-power fields in each tissue section, with one sections of the large left and right liver lobe per animal, and expressed as positive cells per square millimeter liver tissue.

Terminal UDP nick end labeling assay

The number of apoptotic cells was determined by standard terminal UDP nick end labeling (TUNEL) staining (Boehringer, Mannheim, Germany) of liver tissue sections, according to the manufacturers instructions. TUNEL was visualized using 3,3′-diaminobenzidin-tetrahydrochloride. TUNEL positive cells were counted in 10 randomly chosen high-power fields in each tissue section, with one sections of each, the large left and right, liver lobe per animal, and expressed as positive cells per square millimeter liver tissue.

Western blotting

Detection of caspase 3 (CPP32) and its active cleavage product (p20 subunit) in hepatic tissue was performed by Western blot analysis. Tissue was minced in buffer containing 1% nonylphenoxypolyethoxyethanol, 0.5% sodium deoxycholate and 0.1% SDS in PBS supplemented with a protease-inhibitor mixture containing aprotinin (100 U/ml), sodium orthovanadate (184 mg/ml) and phenylmethylsulfonyl fluoride (100 mg/ml). The protein concentrations were determined using a 'BC assay: protein quantitation kit' (Uptima, Interchim, Montlucon, France). Similar protein quantities in electrophoresis gels were controlled by actin determinations. SDS gel-electrophoresis and protein transfer onto nitrocellulose membranes was followed by incubation with caspase 3 (p20) and actin specific antibodies (24 h/4 °C). For

visualization horseradish peroxidase (HRP) conjungated secondary antibodies were used (all antibodies from Santa Cruz Biotechnology, Santa Cruz, CA, USA).

Quantitative real-time polymerase chain reaction

Quantitative real-time polymerase chain reaction (RT-PCR) was used to measure intrahepatic messenger RNA (mRNA) expression of CD163 (specific for mononuclear cell), myeloperoxidase (specific for granulocytes), and of TNF-α. Tissue samples were homogenized in TRIzol reagent (Invitrogen, Karlsruhe, Germany) and total RNA was extracted. To exclude potential genomic DNA contamination the samples were treated with DNAseI (DNAfree, Ambion, Huntingdon, UK). Reverse transcription was performed with the first strand cDNA Synthesis Kit (Roche Diagnostics, Penzberg, Germany) using oligo-dT primers. PCR primers were designed from the corresponding cDNA sequences from the GeneBank (numbers: CD163: XM_232342; MPO: XM_220830; TNFa: NM_012675). RT-PCR was performed using a Light Cycler and the Fast Start cDNA SYBR Green Kit (Roche Diagnostics) with 0.5 μM of primers and 2 μl cDNA template. Detection temperature and $MgCl_2$ concentration were optimized for each primer. Gene expression was normalized to glyceraldehyde 3-phosphate dehydrogenase (GAPDH). The specificity of the PCR was confirmed by sequencing the products of each primer pair, the absence of nonspecific amplification was confirmed by agarose gel electrophoresis. PCR levels are presented as relations of arbitary units.

Statistical analysis

Data are presented as mean ± SEM. Non-normally distributed data was calculated after rank transformation. Depending on the number of measurements per experiment one-way ANOVA or univariate ANOVA was used for calculations, and Tukey-HSD test was used for *post hoc* comparisons between the groups. $P < 0.05$ was considered significant. Survival was estimated using Kaplan–Meier/log-rank analysis. As previously described [26], kinetic of latex particle adherence was calculated using a general-linear model with log-transformed percentages of moving latex particles as the dependent variable. All calculations were performed by use of the SPSS procedures UNIVARIATE and GLM (SPSS® Inc, Chicago, IL, USA).

Results

Effect of KC inhibitor pretreatment on KC numbers and function

Immunohistological ED-1 staining of liver grafts revealed clear differences in the number of positive cells between the groups (Fig. 1). $GdCl_3$ pretreatment of the grafts resulted in a marked decrease in the total number of ED-1 positive cells versus controls ($P < 0.001$). MP treatment caused a less pronounced decrease in ED-1 positive cells ($P < 0.001$ versus controls and versus $GdCl_3$,), however, glycine had no significant effect compared with controls. These results was furthermore supported by measurements of the monocyte-specific epitope CD163 with quantitative RT-PCR, which showed a highly significant decrease (440-fold, $P < 0.001$) after $GdCl_3$ and MP-pretreatment of liver grafts in contrast to controls, which was not evident after glycine treatment (7-fold decrease, $P = 0.07$). Together, these data indicated a decrease in the number of KCs is after $GdCl_3$ or MP treatment, and minor effects of glycine on the KC population.

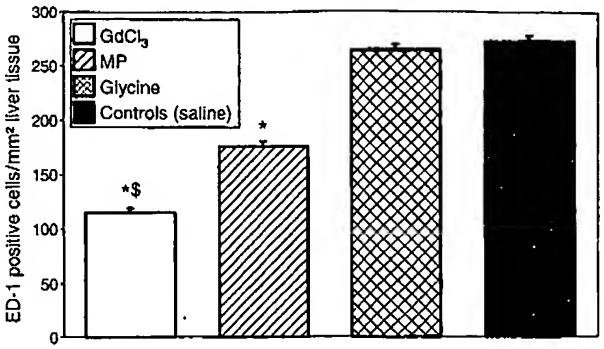

Figure 1 Immunohistological staining of ED-1 at 90 min after reperfusion as assessed with light microscopy. Pretreatment of organ donors with $GdCl_3$ or MP resulted in a significant decrease in intrahepatic ED-1 positive cells, compared with glycine pretreatment or controls. Data are presented as the mean ± SEM. *$P < 0.05$ vs. controls.

Live analysis of injected latex particles revealed a progressive decrease in their movement in all groups within the transplanted liver (Fig. 2). This decrease in particle movement reflects phagocytic activity in the liver, which is primarily because of KCs [24,26]. When making a closer comparison of the mean kinetic curves and 95% confidence intervals of the different groups, particle movement decreased faster in the control group versus groups pretreated with $GdCl_3$, MP and glycine. Therefore, these data suggest that KC phagocytic activity is lowered by each of the KC-inhibitors used in our experiments, most pronounced after profound destruction of KCs with $GdCl_3$.

Effects of KC-inhibitor pretreatment on macrohemodynamics and early hepatocellular bile excretion

Parameters which fundamentally affect early graft function and microhemodynamics, such of donor and recipient weight, liver graft weight and anhepatic period showed no statistical differences between the different groups and between the two sets of experiments (intravital microscopy

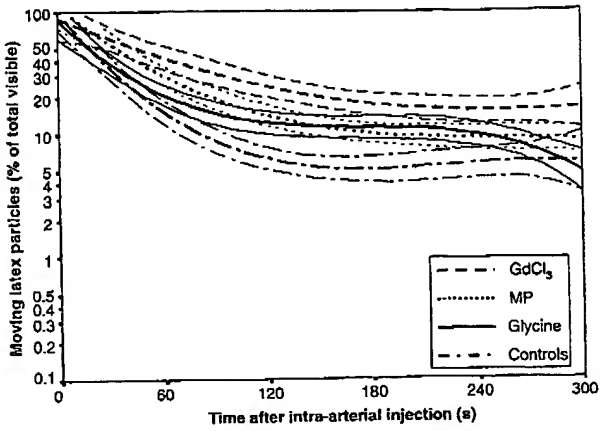

Figure 2 Phagocytosis of latex particles after a single bolus intra-arterial injection at 80 min after graft reperfusion in IVM experiments. Curves represent mean percentages of moving particles relative to all visible particles ± 95% confidence interval. Analysis reveal a faster decline in particle movement in controls, compared with glycine, MP or $GdCl_3$ pretreatment. As the decelerated velocity in particle movement is an indicator of increased phagocytic activity, these results suggest reduced phagocytic activity in all groups pretreated with KC inactivators, most pronounced after profound depletion of KCs with $GdCl_3$.

and survival experiments) (Table 1). However, mean arterial pressure during the intravital microscopy varied between 58.4 and 64.9 mmHg in the different groups and thus reflected depressed macrohemodynamic stability after liver transplantation. This effect was similar in all groups independent of the treatment modalities ($GdCl_3$, MP, glycine and controls). Together, from these data, any influence on early graft excretory function and microvascular graft injury in the different groups can be excluded.

Bile flow and bile acid excretion, however, is a highly sensitive indicator of early graft function in human liver transplantation [8,9], which may depend on the activation state of KCs [24]. Therefore, by inhibition of KCs changes in hepatocellular function could be expected. However, no significant difference was detectable in comparison to recipients after treatment with $GdCl_3$ (2.2 ± 0.5 ml/100 g liver tissue/90 min), MP (3.2 ± 0.6), glycine (2.8 ± 0.5), versus controls (2.8 ± 0.7). Bile acid excretion showed a tendency to higher levels after glycine pretreatment (122 ± 27.4 μmol/100 g/90 min), as compared with the $GdCl_3$ (93.5 ± 25.2), MP (101.1 ± 18.7), and control groups (91.1 ± 21.6), but this difference was not statistically different.

Effects of KC-inhibitor pretreatment microvascular graft injury

As expected, a certain percentage of hepatic acini showed complete perfusion failure. Nonetheless, the relative number of nonperfused acini in this analysis ranged between 1.6 ± 1.1% (glycine) and 14.0 ± 4.3% (controls). Calculation of the acinar perfusion-index showed that perfusion was most homogenous with glycine (0.84 ± 0.03) and MP (0.83 ± 0.03) donor organ pretreatment, versus a markedly lower index with $GdCl_3$ (0.75 ± 0.03; $P = 0.019$). However, in comparison to controls (0.63 ± 0.03), all three KC modulating substances produced more homogeneous acinar perfusion ($P < 0.007$).

Furthermore, by means of intravital microscopy the percentage of nonperfused sinusoids was determined. In the present analysis, the glycine group revealed the highest number of nonperfused sinusoids (13.2 ± 1.1%), as compared with the groups after $GdCl_3$- (10.8 ± 1.1%) and MP pretreatment (10.9 ± 1.1%) and controls (12.9 ± 0.9%), however this difference was not significant. The surprisingly high percentage of sinusoidal perfusion failure after glycine pretreatment was due to perfusion disturbances in the periportal subacinar region (18.6 ± 1.7%), when analyzing the number of nonperfused sinusoids separately for in each subacinar region.

Effects of KC- inhibitor pretreatment on cell death, organ regeneration and graft survival

The effects of KC-inhibitors on the survival of sinusoidal lining and parenchymal cells in liver grafts was determined by TUNEL staining. At 90 min after graft reperfusion, all three KC-inhibitors reduced the number of nonviable sinusoidal lining and parenchymal cells to the same extent, compared with controls (Fig. 3a,b).

These results led us to test for caspase 3 activity in these tissues at 90 min after graft reperfusion, in order to confirm the process of apoptosis. Activation of caspase 3 (CPP32) represents the terminal step in the caspase cascade, and a decisive executive step of apoptotic cell death. Once activated, caspase 3-dependent processes leading to apoptosis, such as inactivation of PARP (poly-ADP-ribose polymerase; a repair enzyme for DNA strand-breaks) cannot be reversed. Importantly, caspase 3 cleavage precedes morphological signs of apoptosis in affected cells.

Western blotting KC-inhibitor pretreated liver grafts showed reduced levels of the caspase 3 cleavage product p20 after glycine treatment, when compared with $GdCl_3$, MP at 90 min after graft reperfusion (Fig. 4). As a consequence, morphological signs of apoptosis should be different after $GdCl_3$, MP and glycine pretreatment when compared after complete execution of apoptosis. We therefore analyzed the number of TUNEL positive cells after 360 and 540 min following graft reperfusion, and indeed found significant higher levels of TUNEL positive sinusoidal lining cells (Fig. 3a) and hepatocytes (Fig. 3b)

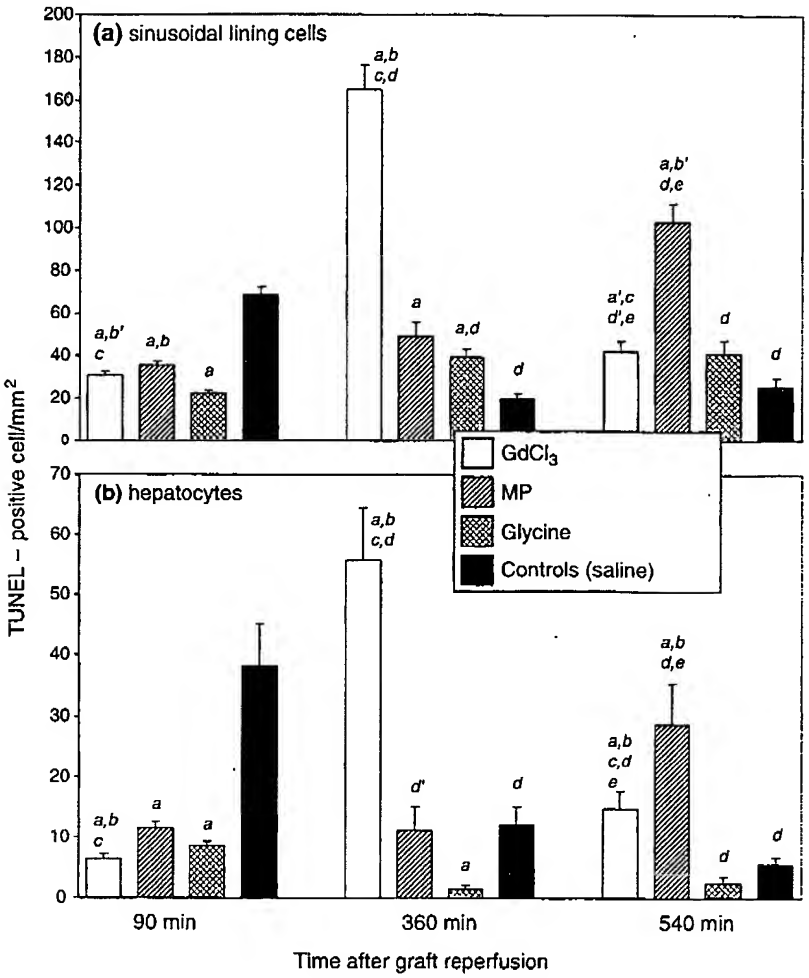

Figure 3 Quantification of apoptosis by TUNEL assay, expressed as TUNEL positive cells per mm^2. Whereas the number of TUNEL positive sinusoidal lining cells (a) and hepatocytes (b) is lowered at 360 and 540 as compared with 90 min after reperfusion in controls, positive cell counts are elevated after $GdCl_3$ and MP treatment at corresponding time points. In contrast, glycine pretreated grafts revealed stable low levels of TUNEL positive cells at 90, 360 and 540 min after reperfusion. Differences are calculated as follows: $^{a}P < 0.0001$ vs. controls; $^{a'}P < 0.05$ vs. controls; $^{b}P < 0.0001$ vs. glycine; $^{b'}P < 0.05$ vs. glycine; $^{c}P < 0.0001$ vs. MP; $^{c'}P < 0.05$ vs. MP; $^{d}P < 0.0001$ vs. 90 min level within the same group; $^{d'}P < 0.05$ vs. 90 min level within the same group; $^{e}P < 0.0001$ vs. 360 min level within the same group; $^{e'}P < 0.05$ vs. 360 min level within the same group.

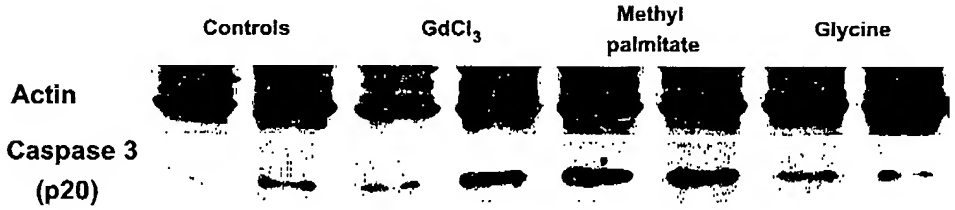

Figure 4 Caspase 3 cleavage. Representative Western blot analyses show decreased activity of cleaved caspase 3, the key enzyme for irreversible execution of apoptosis after $GdCl_3$ and MP pretreatment, compared with controls and the glycine group. The difference in activity of cleaved caspase 3 might explain the differences in the number of apoptotic cells at 360 and 540 min after portal reperfusion.

following $GdCl_3$- or MP-pretreatment numbers at 360 or 540 min after graft reperfusion as compared with 90 min levels in the same group and as compared with the control and the glycine group at corresponding time points. This effect was also observed after glycine pretreatment, but was restricted to sinusoidal lining cells and not evident for hepatocytes. This indicates a prevention of apoptosis execution by glycine in comparison to GdCl3 and MP after extended cold liver graft ischemia and reperfusion. In control animals, however, the number of apoptotic cells at time points later than 90 min was found to be lower as compared with the 90 min-value. This may indicate, that the process of apoptosis execution in the control group peaked very early after reperfusion, and apoptotic cells are not found in the liver after 6 h postreperfusion.

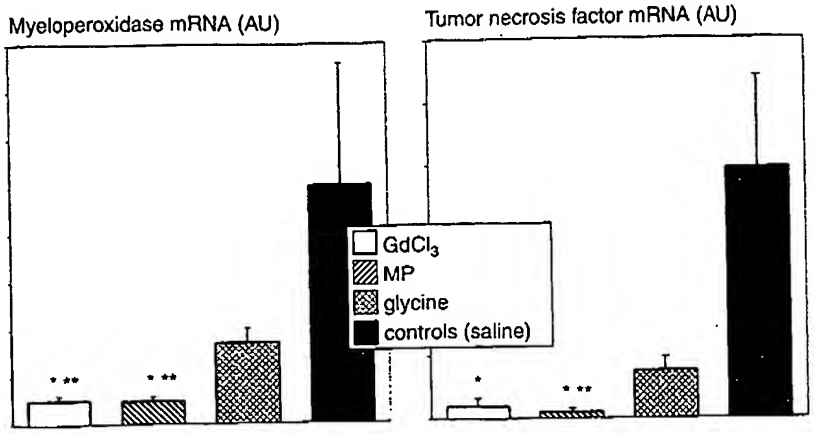

Figure 5 Intrahepatic WBC accumulation indicated by expression of myeoloperoxidase as well as TNFα expression verified by quantitative RT-PCR. Treatment with KC depleting substances ($GdCl_3$ and MP) are associated with reduced myeloperoxidase activity compared with the glycine group and controls, indicating reduced WBC accumulation following $GdCl_3$ and MP pretreatment. In parallel, TNFα expression is reduced after KC depletion. Together these data may represent a reduced potential of regenerative response of the liver grafts. Data are presented as the mean ± SEM. $*P < 0.05$ vs. controls, $**P < 0.05$ vs. glycine.

Effects of KC-inhibitor pretreatment on TNFα expression and intrahepatic granulocyte accumulation

Intrahepatic TNFα-dependent leukocyte accumulation appears to be mandatory for the regeneration capacity of hepatic tissue after cold ischemia in (partial) liver transplantation. In order to further test the cyto- and graft-protective potential of glycine in contrast to $GdCl_3$ and MP, quantitative RT-PCR was performed in hepatic tissue for detection of intragraft TNF expression. As indicator for the presence of granulocytes, relative intrahepatic MPO was in addition quantified by RT-PCR (Fig. 5). Quantitative RT-PCR revealed elevated myeloperoxidase expression after glycine compared with $GdCl_3$ (3.2-fold, $P = 0.011$) and MP pretreatment (3.4-fold, $P = 0.011$). In control grafts MPO levels were found higher than in the glycine group (2.9-fold elevation), however with no statistical difference ($P = 0.58$). In accordance with the hypothesis that TNF-expression is associated with liver graft infiltration with leukocytes we detected strongly reduced levels of TNF reduced after glycine- (5.2-fold), $GdCl_3$- (19.7-fold), MP-treatment (39.5-fold) compared with controls. Although markedly distinct differences of glycine- versus $GdCl_3$- and MP-pretreated grafts were evident, TNF was found to be significantly lower solely in the MP compared the glycine group ($P = 0.01$).

Graft recipient survival

Because survival of the transplant recipient is the primary goal of any organ pretreatment strategy, we examined survival after KC-inhibitor use. Although direct graft function indicators, such as bile flow did not differ between the groups at 90 min after graft reperfusion, log-rank statistics on Kaplan Meier survival plots (Fig. 6) revealed a critical advantage of survival in animals receiving grafts pretreated with glycine, as compared with animals receiving grafts pretreated with $GdCl_3$ ($P = 0.045$), MP ($P = 0.014$) or saline ($P = 0.036$). Therefore, our direct comparison of the various KC-inhibitors indicates that glycine is most effective at preserving critical liver graft functions determining long-term survival.

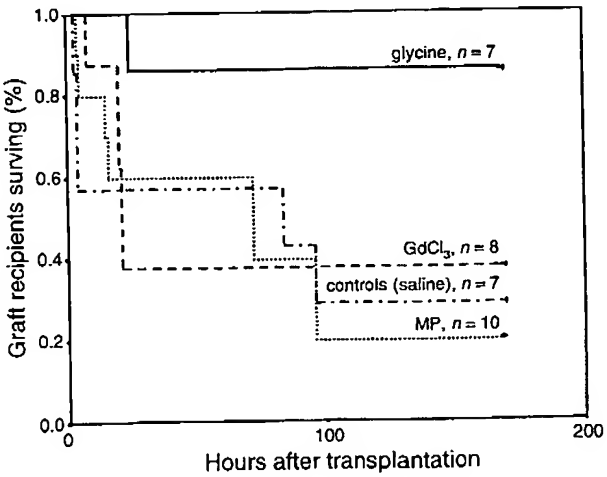

Figure 6 Glycine pretreatment was accompanied by significantly improved recipient survival, as compared with all the other groups. Kaplan–Meier estimations and log-rank comparisons, significance level 0.05.

Table 1. General data.

	$GdCl_3$ ($n = 9$)	MP ($n = 9$)	Glycine ($n = 7$)	Controls ($n = 7$)
IVM experiments				
Donor weight (g)	179.4 ± 9.6	186.6 ± 5.5	195.5 ± 7.8	196.8 ± 7.7
Recipient weight (g)	213.8 ± 16.5	215.6 ± 10.1	205.5 ± 5.5	212.6 ± 4.2
Graft weight (g)	6.9 ± 0.4	7.7 ± 0.3	7.8 ± 0.3	8.4 ± 0.2
Anhepatic time (min)	14.8 ± 0.4	14.7 ± 0.6	13.3 ± 0.4	14.9 ± 0.6
Arterialization delay (min)	5.5 ± 0.8	3.4 ± 0.5	3.5 ± 0.3	4.4 ± 0.6
Mean arterial pressure (mmHg)	64.6 ± 2.1	61.5 ± 2.6	58.4 ± 5.4	64.9 ± 3.3
Survival experiments	($n = 10$)	($n = 9$)	($n = 10$)	($n = 8$)
Donor weight (g)	175.0 ± 9.8	188.2 ± 6.3	188.8 ± 3.7	192.4 ± 13.0
Recipient weight (g)	201.2 ± 9.4	207.8 ± 6.9	214.7 ± 7.3	197.8 ± 8.6
Graft weight (g)	7.0 ± 0.4	9.2 ± 0.3	7.8 ± 0.2	8.0 ± 0.6
Anhepatic time (min)	13.7 ± 0.4	14.8 ± 0.7	13.9 ± 0.5	12.7 ± 0.9
Arterialization delay (min)	6.1 ± 1.5	3.7 ± 0.6	6.1 ± 1.0	3.1 ± 0.5

Data presented as mean ± SEM. No significant differences between all groups. n = numbers of individuals in each group.

Discussion

Recent evidence suggests that inactivation or destruction of KCs could serve as an effective regimen to overcome hepatic organ dysfunction or failure [17,19,22,27]. The present study is the first to directly compare the effects of $GdCl_3$, MP, or glycine pretreatment on post-transplant liver functions. We demonstrate that microvascular graft injury is reduced by KC inactivation early after liver transplantation following 24 h of graft storage. However, survival after liver transplantation is solely improved significantly in glycine pretreated recipients, which might be due to different effects of $GdCl_3$, MP, or glycine on apoptosis of sinusoidal lining cells and hepatocytes, as well as on the potential of graft regeneration after severe ischemia and reperfusion induced injury. These results strongly support the use of glycine as a protective drugs in liver transplantation. Furthermore, it sustains studies on warm ischemia and reperfusion and acetaminophen-induced liver injury [20,21,28] which query previous observations of beneficial effects of KC destroying agents.

Our side-by-side comparison of these three KC inhibitors revealed important differences in their effects on KCs. One difference is that the number of KC was only reduced after $GdCl_3$ and MP treatment, although phagocytic activity for fluorescent latex particles was found to be reduced in all three $GdCl_3$, MP, or glycine pretreated groups.

Therefore, our results suggest that glycine downregulates KC activity, but does not alter the number of KCs in liver grafts. Interestingly, glycine pretreatment of grafts was the only KC inhibitor strategy that significantly prolonged recipient survival.

Our finding of improved animal survival only with glycine is in contrast with previous investigations showing similar effects of $GdCl_3$ and glycine [22]. It is notable, however, that in the other investigations, liver grafts received gentle manipulation and were only held in storage short-term (1 h), or were examined under isolated perfusion conditions. Therefore, previous experiments did not apply as much stress to the explanted liver before and after transplantation. It is likely, therefore, that longer-term storage conditions in our experiments increase the sensitivity of the model system to possible differences between KC inhibitor treatment regimens. In fact, macrohemodynamic conditions, recipient age, body weight, liver graft weight, and time for graft revascularization showed no statistical difference between the groups which ensures comparability of the results. Also, to avoid practical variations, the KC inhibitors used were prepared and applied as previously described [15,22].

Analysis of liver microcirculation in our study revealed some subtle differences between the different KC inhibitors. Indeed, it has already been shown that KC inactivation with $GdCl_3$ significantly reduces microvascular perfusion failure in hepatic sinusoids using the same rat model [27], and homogenization of microvascular perfusion in gently manipulated livers has been demonstrated with $GdCl_3$ or glycine [22]. Consistent with these studies, we observed a reduced number of nonperfused acini after pretreatment with $GdCl_3$ and MP, but this effect was most impressive with glycine. However, this effect was not reproducible with any of the 3 KC inhibitors when we analyzed sinusoidal graft perfusion in our experiments. This observation may be due to the fact, that distribution of fluorescent components sinusoidal perfusion allows the quantification exclusively in perfused acini, when intravital microscopy is applied. As a consequence sinusoidal perfusion measurements in intravital microscopy experi-

ments can only be interpreted in the context of acinar perfusion failure. Nonetheless, hepatic acini containing multiple single hepatic sinusoids (in our experiments 3–12, mean: 7 sinusoids) represent a much larger microvascular unit than do sinusoids. Microvascular perfusion failure of complete acini may affect a much larger volume of hepatic tissue than do individual sinusoids. Indeed, our observation that glycine pretreated animals showed the best survival after 7 days supports this conclusion.

Leukocyte adherence and accumulation in liver grafts early after reperfusion has been postulated as a likely contributor to ischemia reperfusion injury by being a source of potentially toxic mediators [4,7,24]. The significance of leukocyte adherence has been questioned although [29], and intravital microscopy studies of transplanted livers after prolonged cold ischemia failed to document beneficial effects of blocking leukocyte adherence on early graft function [30]. In addition, liver regeneration after 70% partial hepatectomy has been shown to be dependent on an intact recruitment sequence of leukocyte adherence [31]. In this model, KCs may play a fundamental role in the recruitment of leukocytes via release of cytokines, in particular TNF-α and IL-6 [31]. Furthermore, this mechanism appears to be mandatory for regeneration of reduced size rat liver grafts as well as severely injured livers after CCl_4 exposition [32,33]. However, the effect of KC depletion or modulation on cell survival and capacity of regeneration on liver grafts severely injured by cold ischemia is yet unknown. This led us to examine in particular leukocyte infiltration and TNF-α expression in liver grafts of the present experiments. As assessment of leukocyte adherence by means of intravital microscopy may provide information only on intravascular flow and adherence behavior of leukocytes, myeloperoxidase activity in hepatic tissue was quantified by real time polymerase chain reaction (quantitative RT-PCR). In paralleled examinations, TNF-α expression was analyzed. Interestingly, in complete accordance with the mentioned studies, [32,33] MPO as well as TNF-α expression was higher after glycine treated liver grafts as after depletion of KCs with $GdCl_3$ or MP, probably indicating the preserved ability for regeneration via TNF-α dependent leukocyte recruitment following glycine pretreatment. Previous observations with examining the potential of hepatic regeneration after elimination of KCs with $GdCl_3$ [31] and MP [34] clearly demonstrate the detrimental effect of KC depletion, and our data on TNF-α levels und leukocyte infiltration together with the results of animal survival measured 7 days after transplantation would favor this assumption.

Nonetheless, differences of cellular graft function or intrahepatic cell death after transplantation could be expected, if the difference in graft survival was determined by variations in the potential of liver regeneration after transplantation in dependence on KC depletion or modulation. We monitored early liver graft function by hepatocellular excretion, which, in contrast to serum levels of hepatocellular enzymes or hepatic mediators, indicates graft function independent of perfusion irregularities [8]. Bile flow over 90 min, was not affected by any of the three treatment regimens. A slightly, but not significant, improved bile salt excretion after glycine pretreatment might indicate some degree of hepatocellular protection in the glycine-, as compared with the MP- or $GdCl_3$-group. However, the striking differences in survival between the groups may not be explained by effects on graft excretory function.

Interestingly, although all three KC-inhibiting agents reduced apoptotic cell death as early as 90 min after graft reperfusion, $GdCl_3$ and MP treatment only delayed the development of cell death. Analysis of TUNEL-sections of liver grafts retrieved at 6 and 9 h following reperfusion further suggest, that KC inactivation plus direct cellular protection by glycine might result in a profounder protection of liver grafts, than depletion of KCs by $GdCl_3$ and MP. This finding is substantiated by our results on caspase activation showing a strong signal for cleaved (activated) caspase 3 after $GdCl_3$ and MP treatment, but not after glycine treatment. In untreated controls however, induction of cell death leading to graft loss of 70% of recipients, may either be strongly accelerated or, more likely, independent of caspase 3 cleavage. This latter mechanism would be supported by the necrapoptosis hypothesis [35], presuming mixed modes of cell death (apoptosis and necrosis) after cold ischemia and reperfusion of liver grafts. Cell death via necrosis occurs rapidly after graft reperfusion [6], whereas apoptosis takes several hours to develop [5]. This could explain the high numbers of TUNEL positive cells in the control group without elevation of cleaved caspase 3. On the other hand, apoptosis is a dynamic process, and caspase 3 cleavage was found strongly augmented early after reperfusion of liver grafts following 24 h of cold storage as compared with solely cold stored livers [36]. Thus, detection of TUNEL positive cells at 90, 360 and 540 min after liver graft reperfusion may simply represent morphologic expression of preceding molecular mechanisms. The elevation of TNF-α in control and glycine pretreated liver grafts compared with KC-depleted grafts not necessarily contradicts the findings of apoptotic cell death. Overwhelming TNF-α levels indeed strongly induce apoptosis and necrosis [35,37]. However, TNF-α stimulation may exert multiple distinct effects, including the induction of NF-κB, which is related to a cellular regenerative response after several types of injury [33,38]. Thus, again, glycine pretreatment may preserve the potential for

TNF-α dependent regeneration processes superior to $GdCl_3$ or MP. Together, the present data emphasize the previously assumed beneficial effects of glycine-preconditioning of liver grafts [17,19] and as the first outline substantial advantages in contrast to KC depleting agents. The glycine-effects are most likely linked to prevention microvascular injury and preserved cellular regeneration potential and reduced apoptotic and necrotic cell death, resulting in increased liver graft survival.

In summary, glycine is a highly effective substance for preventing ischemia and reperfusion-related liver graft injury. As protective effects on kidney, heart, intestine beside of the hepatoprotective [17], and no adverse effects with its use are reported, glycine may therefore have multiple advantages for clinical use and should be broadly considered to reduce the incidence of early liver graft dysfunction.

Acknowledgement

We thank Mrs. A. Schwendt, Mrs V. Kidder and Mrs. N. Engelhard, Department of Surgery, University of Regensburg, for excellent technical support.

References

1. Ploeg RJ, D'Alessandro AM, Knechtle SJ, *et al.* Risk factors for primary dysfunction after liver transplantation – a multivariate analysis. *Transplantation* 1993; 55: 807.
2. Pirenne J, Gunson B, Khaleef H, *et al.* Influence of ischemia-reperfusion injury on rejection after liver transplantation. *Transplant Proc* 1997; 29: 366.
3. Land W, Schneeberger H, Schleibner S, *et al.* The beneficial effect of human recombinant superoxide dismutase on acute and chronic rejection events in recipients of cadaveric renal transplants. *Transplantation* 1994; 57: 211.
4. Clavien PA, Harvey PR, Strasberg SM. Preservation and reperfusion injuries in liver allografts. An overview and synthesis of current studies. *Transplantation* 1992; 53: 957.
5. Natori S, Selzner M, Valentino KL, *et al.* Apoptosis of sinusoidal endothelial cells occurs during liver preservation injury by a caspase-depedent mechanism. *Transplantation* 1999; 68: 89.
6. Caldwell Kenkel JC, Currin RT, Tanaka Y, Thurman RG, Lemasters JJ. Kupffer cell activation and endothelial cell damage after storage of rat livers: effects of reperfusion. *Hepatology* 1991; 13: 83.
7. Jaeschke H. Preservation injury: mechanisms, prevention and consequences. *J Hepatol* 1996; 25: 774.
8. Sankary HN, Foster P, Brown E, Hart M, Williams JW. A comparison of Collins and UW solutions for cold ischemic preservation of the rat liver. *J Surg Res* 1991; 51: 87.
9. Sumimoto K, Inagaki K, Yamada K, Kawasaki T, Dohi K. Reliable indices for the determination of viability of grafted liver immediately after orthotopic transplantation. Bile flow rate and cellular adenosine triphosphate level. *Transplantation* 1988; 46: 506.
10. Borghi-Scoazec G, Scoazec J, Durand F, *et al.* Apoptosis after ischemia-reperfusion in human liver allografts. *Liver Transpl Surg* 1997; 3: 407.
11. Weiss GB, Goodman FR. Effects of Lanthanum on contraction, calcium distribution and Ca[45] movement in intestinal smooth muscle. *J Pharmacol Exp Ther* 1969; 160: 46.
12. Hardonk MJ, Dijkhuis FWJ, Hulstaert CE, Koudstaal J. Heterogeneity of rat liver and spleen macrophages in gadolinium chloride-induced elimination and repopulation. *J Leukoc Biol* 1992; 52: 296.
13. Di Luzio NR, Wooles WR. Depression of phagocytic activity and immune response by methyl palmitate. *Am J Physiol* 1964; 206: 939.
14. Al Tuwaijri A, Akdamar K, Di Luzio NR. Modification of galactosamine-induced liver injury in rats by reticuloendothelial system stimulation or depression. *Hepatology* 1981; 1: 107.
15. Marzi I, Cowper K, Takei Y, Lindert K, Lemasters JJ, Thurman RG. Methyl palmitate prevents Kupffer cell activation and improves survival after orthotopic liver transplantation in the rat. *Transpl Int* 1991; 4: 215.
16. Ikejima K, Qu W, Stachlewitz RF, Thurman RG. Kupffer cells contain a glycine gated chloride channel. *Am J Physiol* 1997; 272: G1581.
17. Zhong Z, Wheeler MD, Li X, *et al.* L-Glycine: a novel antiinflammatory, immunomodulatory, and cytoprotective agent. *Curr Opin Clin Nutr Metab Care* 2003; 6: 229.
18. den Butter G, Lindell SL, Sumimoto R, Schilling MK, Southard JH, Belzer FO. Effect of glycine in dog and rat liver transplantation. *Transplantation* 1993; 56: 817.
19. Schemmer P, Bradford BJ, Rose ML, *et al.* Intravenous glycine improves survival in rat liver transplantation. *Am J Physiol* 1999; 276: G924.
20. Imamura H, Sutto F, Brault A, Huet PM. Role of Kupffer cells in cold ischemia and reperfusion injury of rat liver. *Gastroenterology* 1995; 109: 189.
21. Kobayashi T, Hirano KI, Yamamoto T, *et al.* The protective role of Kupffer cells in the ischemia-reperfused rat liver. *Acta Histol cytol* 2002; 65: 251.
22. Schemmer P, Connor HD, Arteel GE, *et al.* Reperfusion injury in livers due to gentle in situ manipulation during harvest involves hypoxia and free radicals. *J Pharmacol Exp Ther* 1999; 290: 235.
23. Kamada N, Calne RY. Orthotopic liver transplantation in the rat. Technique using cuff for portal vein anastomosis and biliary drainage. *Transplantation* 1979; 28: 47.
24. Post S, Palma P, Rentsch M, Gonzalez AP, Menger MD. Differential impact of Carolina rinse and University of Wisconsin solutions on microcirculation, leukocyte adhesion, Kupffer cell activity and biliary excretion after liver transplantation. *Hepatology* 1993; 18: 1490.

25. Turley SD, Dietschy JM. Re-evaluation of the 3 alpha-hydroxysteroid dehydrogenase assay for total bile acids in bile. *J Lipid Res* 1978; 19: 924.
26. Dan C, Wake K. Modes of endocytosis of latex particles in sinusoidal endothelial and Kupffer cells of normal and perfused rat liver. *Exp Cell Res* 1985; 158: 75.
27. Schauer RJ, Bilzer M, Kalmuk S, *et al.* Microcirculatory failure after rat liver transplantation is related to Kupffer cell-derived oxidant stress but not involved in early graft dysfunction. *Transplantation* 2001; 72: 1692.
28. Ju C, Reilly TP, Bourdi M, *et al.* Protective role of Kupffer cellsin acetaminophen-induced hepatic injury in mice. *Chem Res Toxicol* 2002; 15: 1504.
29. Otto G, Hofheinz H, Hofmann WJ, Manner M. Questionable role of leukocyte sticking in the pathogenesis of preservation damage. *Transplant Proc* 1991; 23: 2385.
30. Rentsch M, Post S, Palma P, Lang G, Menger MD, Messmer K. Anti-ICAM-1 blockade reduces WBC adherence following ischemia and reperfusion but does not improve early grafts functioning rat liver transplantation. *J Hepatol* 2000; 32: 821.
31. Selzner N, Selzner M, Odermatt B, Tian Y, van Rooijen N, Clavien PA. ICAM-1 triggers liver regeneration through leukocyte recruitment and Kupffer cell-dependent release of TNF-alpha/IL-6 in mice. *Gastroenterology* 2003; 124: 692.
32. Selzner N, Selzner M, Tian Y, Kadry Z, Clavien PA. Cold ischemia decreases liver regeneration after partial liver transplantation in the rat: A TNF-alpha/IL-6-dependent mechanism. *Hepatology* 2002; 36(4 Pt 1): 812.
33. Yamada Y, Fausto N. Deficient liver regeneration after carbon tetrachloride injury in mice lacking type 1 but not type 2 tumor necrosis factor receptor. *Am J Pathol* 1998; 152: 1577.
34. Kato K, Kazuhiko O, Kato J, Kasai S, Mito M. The immuno-stimulant OK-432 enhances liver regeneration after 70% hepatectomy. *J Hepatol* 1995; 23: 87.
35. Jaeschke H, Lemasters JJ. Apoptosis versus oncotic necrosis in hepatic ischemia/reperfusion injury. *Gastroenterology* 2003; 125: 1246.
36. Rentsch M, Beham A, Iesalnieks I, Mirwald T, Anthuber M, Jauch KW. Impact of prolonged cold ischemia and reperfusion on apoptosis, activation of caspase 3, and expression of bax after liver transplantation in the rat. *Transplant Proc* 2001; 33: 850.
37. Brock RW, Lawlor DK, Harris KA, Potter RF. Initiation of remote hepatic injury in the rat: interactions between Kupffer cells, tumor necrosis factor-alpha, and microvascular perfusion. *Hepatology* 1999; 30: 137.
38. Liu ZG, Hsu H, Goeddel DV, Karin M. Dissection of TNF receptor 1 effector functions: JNK activation is not linked to apoptosis while NF-kappa B activation prevents cell death. *Cell* 1996; 87: 565.